JPL Contract 953311

(NASA-CR-128336) OUTER PLANET ENTRY PROBE SYSTEM STUDY. VOLUME 1: SUMMARY Final Report (Martin Marietta Corp.) Aug. 1972 167 p CSCL 22A
N72-33826
Unclas
G3/30 43906

Outer Pla[illegible] En[illegible] Probe System Study

Final Report

Volume I
Summary

August 1972

JPL Contract 953311

Volume I | Summary | August 1972

OUTER PLANET ENTRY PROBE SYSTEM STUDY

FINAL REPORT

R. S. Wiltshire

R. S. Wiltshire
Program Manager

MARTIN MARIETTA CORPORATION
P. O. Box 179
Denver, Colorado 80201

Survivable Saturn Atmosphere Probe

FOREWORD

This final report has been prepared in accordance with requirements of Contract JPL-953311 to present data and conclusions from a six-month study for the Jet Propulsion Laboratory by Martin Marietta Aerospace, Denver Division. The report is divided into the following volumes:

Volume I - Summary

Volume II - Supporting Technical Studies

Volume III - Appendixes

ACKNOWLEDGEMENTS

The following Martin Marietta Corporation, Denver Division, personnel participated in this study, and their efforts are greatly appreciated:

Raymond S. Wiltshire	Study Leader, Program Manager
Allen R. Barger	Science Integration
Eugene A. Berkery	Telecommunications, Data Handling, Power, and ACS, Lead
Dennis V. Byrnes	Navigation
Philip C. Carney	Mission Analysis
Patrick C. Carroll	Systems
Revis E. Compton, Jr.	Telecommunications
Robert G. Cook	Mechanical Design
Douglas B. Cross	Mission Analysis
Ralph F. Fearn	Propulsion
Robert B. Fischer	Mission Analysis
Thomas C. Hendricks	Mission Analysis
John W. Hungate	Systems, Lead
Carl L. Jensen	Thermal Analysis
Melvin W. Kuethe/ Rufus O. Moses	Mechanical/Structural/Probe Integration, Lead
Kenneth W. Ledbetter	Science, Lead
Paula S. Lewis	Mission Analysis
John R. Mellin	Structures
Jack D. Pettus	Data Link Analysis
Robert J. Richardson	Receiver Systems
Arlen I. Reichert	Propulsion
E. Doyle Vogt	Mission Analysis, Lead
Donald E. Wainwright	Systems
Clifford M. Webb	Thermal Analysis
Charles E. Wilkerson	Data Handling

CONTENTS

Table

I. INTRODUCTION

The material in this report summarizes the results of a six-month study of scientific probes to explore the atmospheres of Jupiter, Saturn, Uranus, and Neptune to a pressure depth of between 2 and 30 bars. Included are study constraints, science and mission objectives, parametric analyses to define requirements, and definitions of four different probe systems.

The study consisted of five major tasks, shown in Figure I-1 with their relationship to each other. These tasks are (1) define a nominal Jupiter probe system using nominal constraints of a 1979 Type I mission, -20° entry angle, 5° latitude, 2 R_J flyby periapsis, etc; (2) evaluate the subsystems defined by reviewing NASA and Air Force programs for component availability, cost impact, and sensitivity to the environment; (3) use the nominal Jupiter probe as a "reference" for a program parametric analysis in which the constraints are varied incrementally as shown by 3a in the figure to define a reasonable set of alternative Jupiter probe constraints. Use these new constraints to define two alternative Jupiter probe systems as shown by 3b in the figure; (4) use data from the Jupiter probe definition to conduct parametric activity to determine requirements for Saturn, Uranus, and Neptune atmospheric entry as shown by 4a, 4b, and 4c in the figure; and (5) define a Saturn probe with inputs from Tasks 1 and 3 and assess the changes necessary to use it at Uranus as shown by 5a and 5b in the figure.

To ensure that study results would be as objective as possible, many outside contacts were made with interested scientists. Martin Marietta has retained a group of consultant scientists for assistance in the planetary program studies, and they provided many helpful suggestions and advice for this study. These consultants include Dr. Richard Goody, Dr. Donald Hunten, Dr. Michael McElroy, Dr. Robert Vogt, Mr. Harvey Allen. Dr. George Wetherill and Dr. Alan Barrett. In addition, outside engineering consultation was obtained in the areas of propulsion, thermal control, telecommunications, and power subsystems to determine component availability and state-of-the-art technology.

REPRODUCIBILITY OF THE ORIGINAL PAGE IS POOR.

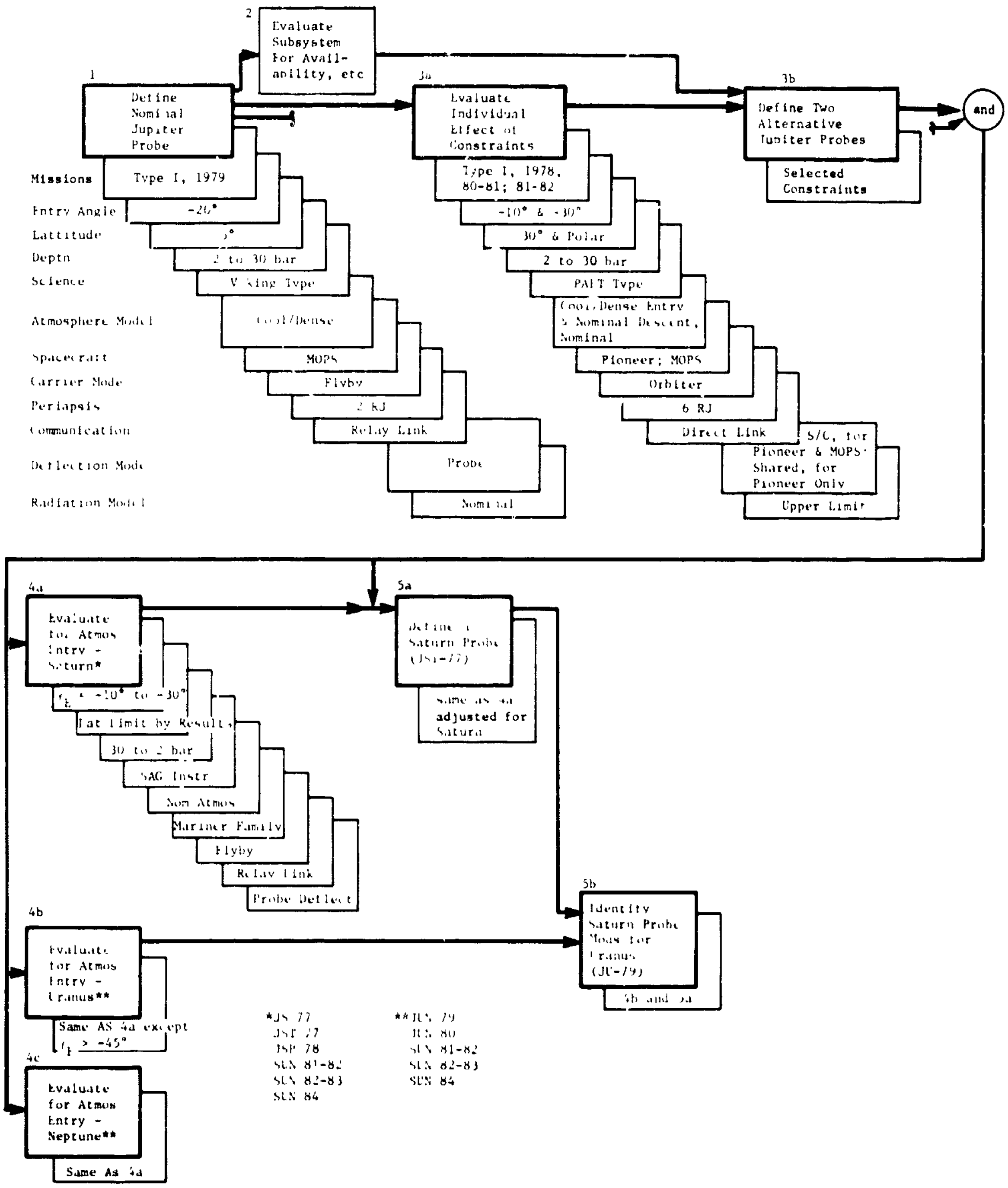

Figure 1-1 Study Task Definition and Flow Diagram

II. SUMMARY

The study showed that a Type I Jupiter dedicated mission in 1979 with a nominal set of mission constraints such as a -20° entry angle, 5° latitude and periapsis radius of $2R_J$ implies a probe with an ejected weight of approximately 156 kg (344 lb), an entry ballistic coefficient of 102 kg/m^2 and a two-step descent ballistic coefficient of 18.9 kg/m^2 and 213.6 kg/m^2 to meet the science measurement criteria. In addition, a Jupiter probe-dedicated mission in which the spacecraft performs the deflection maneuver for a -15° entry angle, 30° latitude, and a flyby periapsis radius of $2R_J$, implies a less complex probe than the one above and has an ejected weight of approximately 127 kg (2.80 lb) and satisfies the science measurement requirements with only 13 bars depth of penetration into a cool/dense atmosphere. Compared with this probe-dedicated configuration, the study also showed that a Jupiter spacecraft-radiation-compatible mission in which the probe performs the deflection maneuver, a -15° entry angle, 5° latitude, and a flyby periapsis radius of $6R_J$ implies a probe of approximately 166 kg (365 lb) to meet the science measurement requirements.

The study also showed that a Saturn probe for a high inclination JS 77 mission for Titan encounter with -25° entry angle and a flyby periapsis radius of 2.33 R_S implies a probe with an ejected weight of approximately 115 kg (253 lb) and satisfies the science measurement requirements at a maximum depth of 7 bars with a descent ballistic coefficient of 100 kg/m^2. In addition, a common probe for use at Saturn or Uranus was feasible with a weight penalty of approximately 2 kg to the Saturn probe.

The study is summarized in this chapter which is organized to present first the general mission considerations and science prospectus, which are of a general nature that applies to several or all planetary applications. These two major topics are followed by the five probe system definitions: (1) nominal Jupiter probe system, (2) Jupiter probe-dedicated alternative probe system, (3) Jupiter spacecraft radiation-compatible alternative probe system, (4) Saturn probe system, and (5) Saturn probe applicability for Uranus. These definitions are followed by the parametric analysis summary for mission analysis of a general nature, then cover specific parametric analysis for Jupiter, Saturn, Uranus and Neptune. Finally, this summary discusses the program from the hardware availability viewpoint and then from the aspect of commonality.

A. MISSION DESIGN CONSIDERATIONS

The purpose of this section is to describe the implementation of the science goals and requirements through the design of the mission from launch to probe entry and descent. It consists of two main topics: (1) the general profile of a typical probe mission to demonstrate the relationships between the various phases of the mission; (2) an overview of the different missions and constraints considered in the study.

1. Mission Profile

a. Launch - The probe mission begins with a launch from the Eastern Test Range at Cape Kennedy. The prime launch vehicle is the Titan IIIE/5-Segment Centaur with Burner II. Spacecraft include the pioneer spacecraft or a Mariner class spacecraft. The Pioneer is spin-stabilized and weighs 248 kg. The Mariner vehicle is three-axis stabilized and weighs 500 kg. The spacecraft is launched into a 185 km parking orbit and after a short coast is injected on the interplanetary trajectory.

b. Planetary Approach - After the interplanetary cruise, which may include a swingby of an intermediate planet or a phase under solar electric power, the spacecraft approaches the target planet. Before the end of this cruise phase, tracking is initiated for a final midcourse maneuver that refines the approach trajectory toward its desired value. The midcourse maneuver is assumed to occur 13 days before the deflection maneuver. It is assumed that the execution errors of this midcourse are small and therefore are dominated by tracking uncertainties at the time of the maneuver. The control errors of the spacecraft following the midcourse are therefore modeled as resulting solely from those tracking uncertainties. Tracking uncertainties at the various planets have been investigated for combined Doppler/range tracking, QVLBI (Quasi-Very Long Baseline Interferometry) and optical tracking.

c. Deflection - The deflection maneuver is performed at a range of from about 5 to 50 million km from arrival at the target planet. The deflection maneuver consists of three critical tasks: (1) The probe is separated from the spacecraft and placed on a trajectory intersecting the target entry site; (2) the probe must be oriented for zero relative angle of attack at entry, (3) the relative geometry between the probe and spacecraft must be established for an effective communication link. These entry conditions are illustrated in Figure 11-1 below.

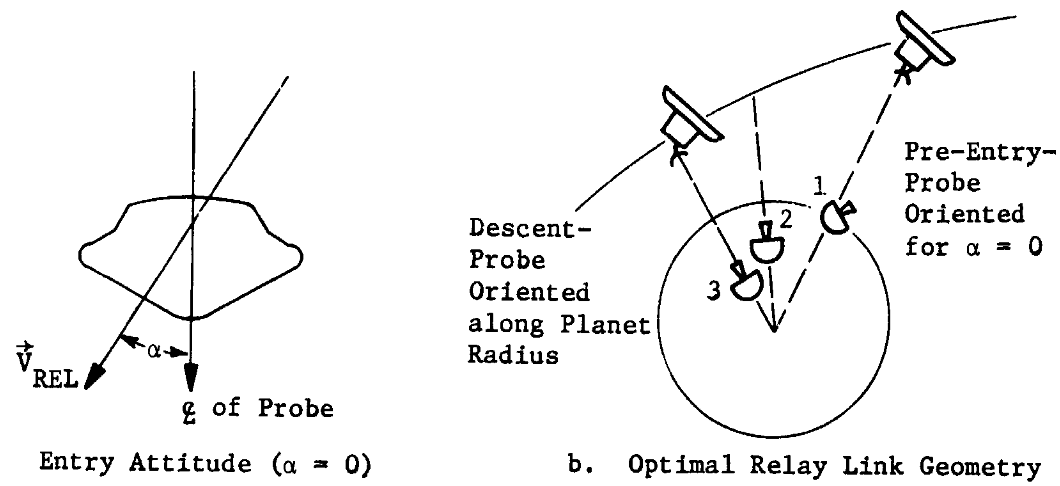

a. Zero Relative Angle of Attack

Figure II-1 Definition of Entry Conditions

As indicated, the optimal relay link geometry has the spacecraft directly above the probe during the probe descent (on the parachute).

Three distinct modes or operational sequences identified to perform this deflection maneuver are shown in Figure II-2 and summarized in the following paragraphs

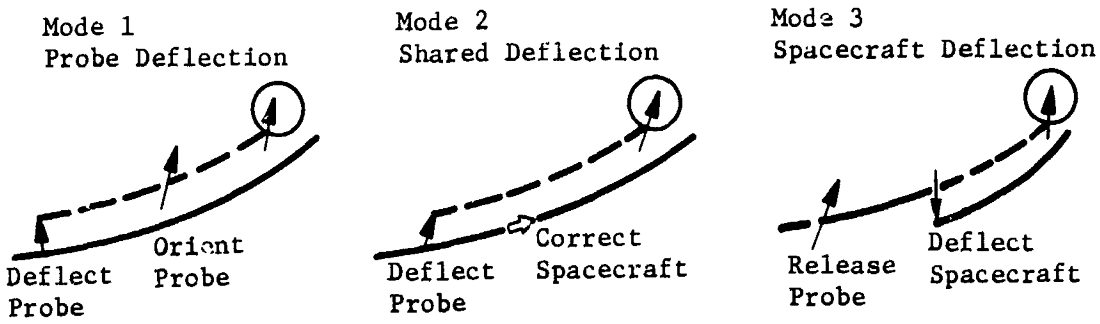

Figure II-2 Comparison of Deflection Modes

1) Mode 1 (Probe Deflection) - The spacecraft releases the probe in the attitude required for deflection ΔV. After applying the ΔV the probe reorients itself to the attitude required for zero angle of attack at entry.

2) Mode 2 (Shared Deflection) - The spacecraft releases the probe in the proper attitude for zero angle of attack at entry. The probe fires a ΔV in that direction so it is deflected to the entry site. The spacecraft then accelerates to achieve required communications geometry at entry.

3) Mode 3 (Spacecraft Deflection) - The spacecraft trajectory is targeted to impact the entry site. The spacecraft releases the probe in the proper attitude for zero angle of attack. The spacecraft then orients itself and fires a ΔV to establish desired flyby trajectory and communications geometry,

Thus, the first mode requires the most complicated probe. It must be capable of providing the deflection ΔV as well as the precession and ACS maneuvers. The requirements for probe precession and ACS maneuvers are removed in the second mode, The third mode results in the simplest probe because nominally all three requirements are removed and the full capability of the spacecraft is exploited. However, some attitude refinement may be required in the second and third modes because of tip-off and spin-up errors.

d. Entry and Descent - After deflection the probe remains dormant for a coast period of 5 to 50 days; then about an hour from entry, a timer is set off in the probe. The entry batteries are activated, science instrument warmup is initiated, and spacecraft acquisition is achieved. Engineering data on the status of the probe and instruments is then transmitted. Shortly thereafter the probe enters the planetary atmosphere. The nominal Jupiter probe pre-entry transmission is terminated at the sensing of 0.1 g. The peak deceleration and maximum dynamic pressure is reached in less than half a minute after entry. Staging of the aeroshell at Mach number 0.7 occurs less than a minute and a half after entry.

Following a timed interval from 0.1 g, the descent antenna is activated. As the probe descends through the atmosphere, measurements are taken and transmitted to the spacecraft for relay to the Earth. The mission ends at pressures of about 10 to 30 bars and descent times of about half an hour.

Mission Constraints

The general mission constraints, mentioned earlier, are summarized in Tables II-1 and II-2. Both tables show the launch vehicle to be the Titan IIIE with Centaur and Burner II upper stages. Although the 5-segment Titan IIIE is emphasized throughout the study due to the fact that it is being developed for Viking, the 7-segment vehicle has been considered for comparison purposes. The payload capability for these vehicles is shown in Figure II-3.

Many missions have been analyzed during the course of this study. Table II-3 lists the missions most often referred to in subsequent discussions. Missions A, B, C, I and J are the system design missions described fully in Chapter II, Sections C through G. Missions D, E, and F are Jupiter probe-dedicated missions, similar to Mission A, but launched in different years, studied to determine the impact of launch year. Mission G is an "optimal" Jupiter orbiter mission, analyzed for the problems introduced by including a probe on an orbiter mission. Mission H is a low inclination approach trajectory consistent with a JS 77 mission. All of the data listed in Table II-3 refers to the nominal design of the specific mission. In many cases, parametric studies were made about this nominal design; thus, in certain sections, mission parameters will differ from those given in the table.

A detailed discussion of general mission considerations is found in Volume II, Chapter IV and includes mission profiles, launch and interplanetary trajectories, approach orbit determination, planetary encounter, dispersion analysis, planetary entry, and missions to other planets.

Table II-1 Jupiter Study Constraints

Constraint	Nominal	Alternative
Mission	Type I, 1979	Type I, 78, 80-81. 81-82
Periapsis Radius	2 R_J	6 to 7 R_J
Deflection Mode	Probe	Bus for Pioneer and MOPS; shared for Pioneer only
Communciation Mode	Relay	Direct
Entry Flight Path Angle	-20°	-10°; -30°
Entry Latitude	5°	30°; Polar
Atmosphere	Cool/Dense	Cool/Dense entry and nominal descent; nominal entry and nominal descent
Deceleration Criteria	to M $\leq$ 1 above 100 mb	
Descent Depth	2 to 30 bars	2 to 30 bars
Spacecraft	MOPS	Pioneer; Mariner Family
CARRIER operational Mode	Flyby	Orbiter
Launch Vehicle	Titan IIIE with Centaur and Burner II	

Table II-2 Saturn, Uranus, and Neptune Study Constraints

Constraint	Saturn	Uranus	Neptune
Mission	Type I, JS 77, JST 77, JSP 78, SUN 81-82, SUN 82-83, SUN 84	Type I, JUN 79 JU 79, SUN 80 SUN 81-82 SUN 82-83 SUN 84	Type I, JUN 79 SUN 80 SUN 81-82 SUN 82-83 SUN 84
Deflection Mode	Probe	Probe	Probe
Communication Mode	Relay	Relay	Relay
Entry Flight Path Angle	-10° to -30°	<-45°	-10° to -30°
Atmosphere	Nominal	Nominal	Nominal
Deceleration Criteria	To Mach $\leq$ 1 above 100 mb		
Depth of Descent	2 to 30 bars	2 to 30 bars	2 to 30 bars
Spacecraft	Mariner	Mariner	Mariner
Carrier Operational Mode	Flyby	Flyby	Flyby
Launch Vehicle	Titan IIIE with Centaur and Burner II		

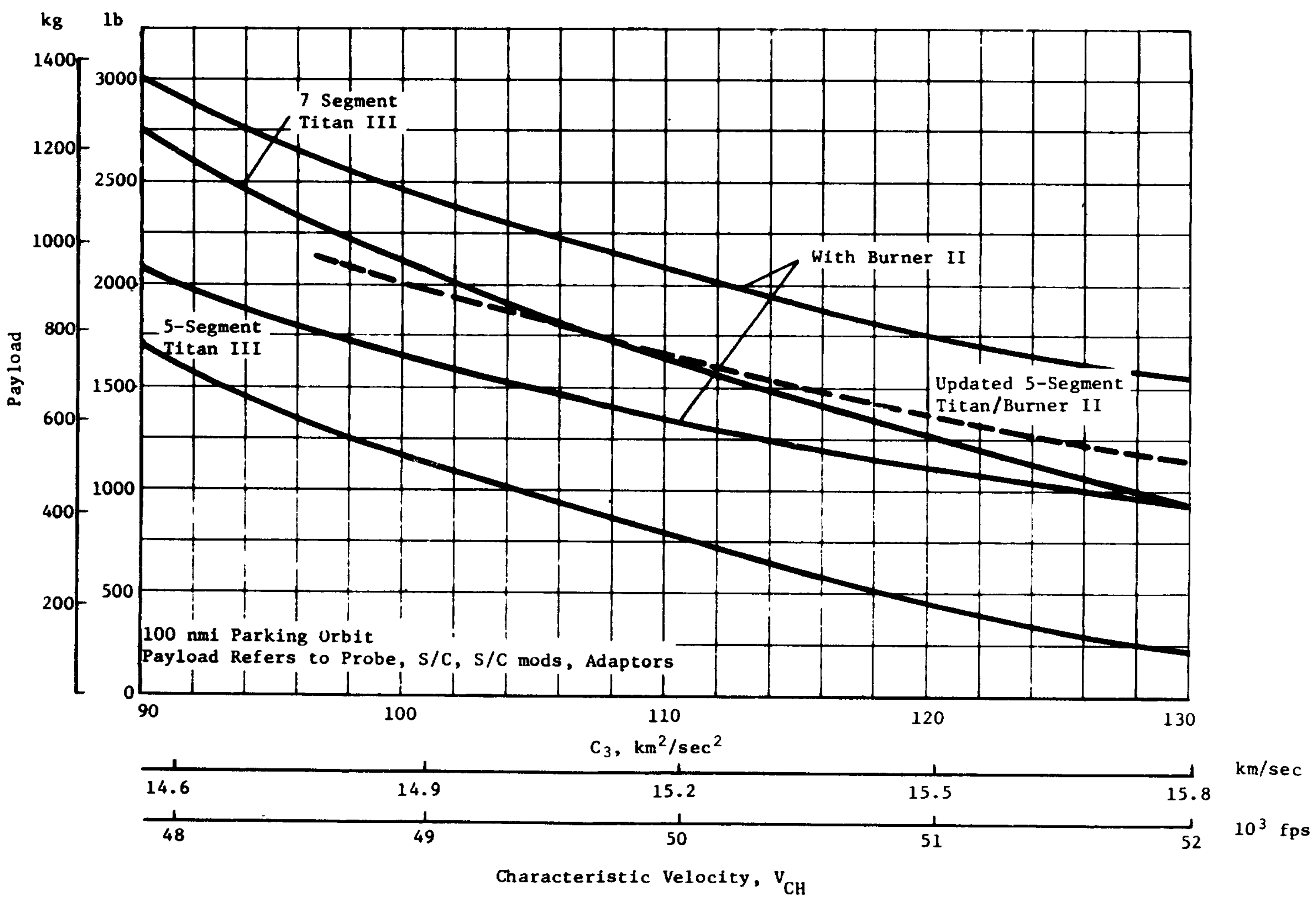

Figure II-3 Titan III/Centaur Performance Data

Table II-3 *Summary of Reference Missions*

Mission Index	Mission Title	Launch Date	Jupiter Arrival	Planetary Arrival	C_3 km^2/sec^2	Total Trip Time, day	VHP, km/sec	Periapsis, Planet Radii	Entry Angle, deg	Deflection Radius, $\times 10^6$ km	ΔV, m/sec
A.	Jupiter Nominal[1]	11/7/79	9/17/81	9/17/81	105	680	8.47	2.00	-20	10	221
B.	Jupiter Probe-Dedicated[1]	11/7/79	9/17/81	9/17/81	105	680	8.47	2.00	-15	30	71
C.	Jupiter Radiation-Compatible[1]	11/7/79	9/17/81	9/17/81	105	680	8.47	6.00	-15	30	256
D.	Jupiter 1978	10/10/78	8/10/80	8/10/80	122	670	8.33	2.00	-20	10	221
E.	Jupiter 1980	12/5/80	10.12/82	10/12/82	98	676	8.69	2.00	-20	10	221
F.	Jupiter 1982	1/4/82	11/10/83	11/10/83	95	675	8.63	2.00	-20	10	221
G.	Jupiter Probe/Orbiter	10/29/79	12/1/81	12/8/81	105[2]	764	7.27	2.00	-20	10	221
H.	Saturn/Fast JS 77	9/5/77	3/16/79	12/8/80	111	1190	14.87	2.02	-20	10	141
I.	Saturn/JST 77[1]	9/4/77	4/16/79	2/16/81	107	1261	13.66	2.33	-25	10.15	170
J.	Uranus/JU 79[1]	11/6/79	6/19/81	5/19/86	113	2386	13.62	2.42	-60	9.75	170
K.	Nepturn/JUN 79[1]	11/6/79	6/19/81	3/12/90	113	3779	15.46	3.00	-20	10	95

[1]Missions used for systems designs

[2]DLA < 36° constraint ignored

B. SCIENCE PROSPECTUS

The basic science questions that the nominal probe mission will attempt to answer were taken from the previous study (Ref 2) which referenced a JPL document (Ref 3), and are:

1) What are the relative abundances of hydrogen, deuterium, helium, neon, and other elements, and what are their isotopic compositions?

2) What are the present-day atmospheric composition and altitude profiles of pressure, temperature, and density, and what effect do they have on the radiation balance?

3) What are the chemical composition and vertical distribution of the clouds?

4) What is the level of turbulence in the atmosphere?

From these questions, measurements to provide answers can be defined, and are given in Table II-4.

Table II-4 Measurements Relevant to Objectives

1.	Determine the relative abundances of H and He in the lower atmosphere (below the turbopause)
2.	Determine the isotopic ratios H/D, He^3/He^4, Ne^{20}/Ne^{22}, C^{12}/C^{13}, A^{36}/A^{40} and others in the lower atmosphere.
3.	Determine the concentration profiles of the minor atmospheric constituents, particularly Ne, A, CH_3, CH_4, NH_3, and H_2O, down to the design limit.
4.	Determine the temperature versus pressure and time profiles from above the cloud tops down to the design limit with precision sufficient to ascertain whether the lapse rate is adiabatic.
5.	Determine the atmospheric mean molecular weight and identify the major contributing gasses.
6.	Obtain an indication of the vertical distribution and structure of the cloud layers with respect to pressure and temperature, and the chemical composition of each layer.
7.	Obtain an indication of the magnitude and frequency of any atmospheric turbulence from above the cloud tops down to the design limit.

In general, there is no exact one-to-one correspondence between the questions and observable measurements. Some questions require many kinds of measurements, while a single measurement may contribute to several questions. The questions themselves are strongly interrelated and an answer to one requires at least a partial answer to others. The first four measurements listed in the table are those that determine the bulk composition and general atmospheric properties. Each of these can be measured by one of the SAG Exploratory instruments without additional data reduction, and thus are the primary measurements. The fifth measurement, that of determining the mean molecular weight of the bulk atmosphere, can be accomplished primarily from mass spectrometer data with assistance from the other instruments, and is also a primary measurement. The last two measurements cannot be directly made by any of the Exploratory pay-load instruments, but indications can be obtained by all the instruments; thus these are considered secondary.

The science instrument payload was specified at the beginning of the study to be the SAG Exploratory payload consisting of four instrument types; a neutral mass spectrometer, temperature gage, pressure gage, and accelerometer triad (Ref 1). The primary science activities during the course of the study were (1) to establish measurements and performance criteria consistent with this payload, based upon data from the previous study (Ref 2) and discussions with consulting scientists; (2) to provide specific instrument characteristics to subsystem areas and to establish the word content of each instrument measurement and interface with the data handling system; (3) to determine the descent profiles and instrument sequencing and evaluate the measurement performance with respect to the criteria.

For the relevant measurements to be useful for mission design and evaluation, criteria must be established with which the instrument performance can be compared to assure that the particular design will satisfy the objectives. Both depth of penetration (pressure) and number of measurements are important. Table II-5 presents the established criteria for each measurement. These criteria were influenced by the previous study (Ref 2), the JPL Assessment Report (Ref 4), and discussions with a panel of science consultants which included Dr. Richard Goody, Dr. Donald Hunten, Dr. Michael McElroy, Dr. Robert Vogt, Mr. Harvey Allen, Dr. George Wetherill and Dr. Alan Barrett.

Table II-5 Performance Criteria

Measurement	Pressure Depth	Minimum Sampling Required
H/He Ratio	1 bar Minimum	4 Measurements at Different Pressures
Isotopic Ratios	1 bar Minimum	4 Measurements at Different Pressures
Minor Constituents	To Design Limit	2 per Scale Height below Cloud Tops
Temperature	To Design Limit	1 per °K
Pressure	To Design Limit	2 per Kilometer below Cloud Tops
Mean Molecular Weight	5 bars Minimum	4 Measurements at Different Pressures
Cloud Layering	To Design Limit	2 Measurements Inside Each Cloud
Turbulence	To Design Limit	1 per Kilometer below Cloud Tops

The entry site on the planet should be selected so that it is both relevant to the desired objectives and typical of the planet as a whole, in order to permit extrapolation of the results to other locations. The lack of optical or ionospheric instruments simplifies the landing site selection considerations for all of the outer planets, making lightside or darkside entries essentially equivalent, with the exception of Uranus, which has its pole pointing toward the Sun so that all solar energy is input into one hemisphere. It is desirable to enter at least 20° into the Sun side of the planet from the terminator. It would also be unacceptable, for any planet, to enter close to the terminator because the processes occuring here may cause atmospheric variations that the instruments could not separate from normal conditions. Thus, a corridor 6° wide centered on the terminator should be avoided. Note that this restriction is overruled for Uranus by the 20° mask angle, because there is a large differential in atmospheric conditions between the light and dark side which is not curtailed by planetary rotation. Also, for Jupiter, it would be desirable to avoid shear layers and very high velocity turbulence by entering at a quiescent site.

Table II-6 shows the relationship of the SAG Exploratory instruments to the measurements they are required to make, indicating whether the measurement is indirect or direct.

Table II-6 Instruments Related to Measurements

Measurement	Instrument			
	Accelerometer Triad	Pressure Gage	Temperature Gage	Mass Spectrometer
H/He Ratio	R	R	R	D
Isotopic Ratios	N	N	N	D
Minor Constituents	N	R	R	D
Temperature/Pressure	R	D	D	R
Mean Molecular Weight	R	R	R	R
Cloud Layering	N	R	R	R
Turbulence	R	R	R	N

D = Direct Measurement

R = Related Measurement

N = Little or No Relation

The accelerometers function both during entry and descent. That used on both Viking and PAET is the Bell Aerospace Model IX System which consists of one longitudinal and two cross-axis pendulous, force rebalance acceleration transducers accompanied by an analog-to-digital converter. To obtain a range of 10^{-2} g to 1600 g requires only a small modification in the flexure of the pendulous proof mass and with new uses of hybrid microelectronics, the package will be no larger than that being used for Viking. The digital accelerometer system used in this study consists of four parts: the analog accelerometer, pulse rate converter, onboard processor, and an entry g sensor, all packaged in two separate components.

During the entry phase of the mission, the accelerometers must measure the entry g-load with sufficient accuracy to enable reconstruction of the g-load versus time curve especially at the peak g point. From this, the atmospheric structure can be determined. The axial accelerometer is sampling at a rate of between 5 and 10 samples/sec while the lateral accelerometers are sampling at a rate exactly half of each of these.

After the parachute is deployed, a signal is sent to the accelerometer processor to instruct it to switch the measurement mode to descent, simultaneously with the deployment of the temperature gage. During the descent phase, the objective of the accelerometer is to determine the magnitude and frequency of the probe response to turbulence variations. This is done by making an analog sweep of 8 to 15 sec duration and using onboard processing to determine the average value of turbulence, the peak value of turbulence, and the number of average crossings. This is schematically pictured in Figure II-4. This technique is used for the axial accelerometer and a combination of the two lateral accelerometers so that the result is a separate measurement of vertical and horizontal turbulence.

Both the Viking pressure gage and the PAET pressure gage were considered for use as a source that could be modified for the entry probe. The PAET instrument is slightly lighter in weight but significantly smaller in volume, which translates into a savings in supporting system weight. Two PAET-type vibrating diaphragm instruments are required to cover the pressure range under consideration; one has a range from a few millibars to about 1 bar and the second covers the range from this point down to the design pressure limit. The inlets are short and exit the probe body perpendicular to the body and approximately perpendicular to the flow streamline.

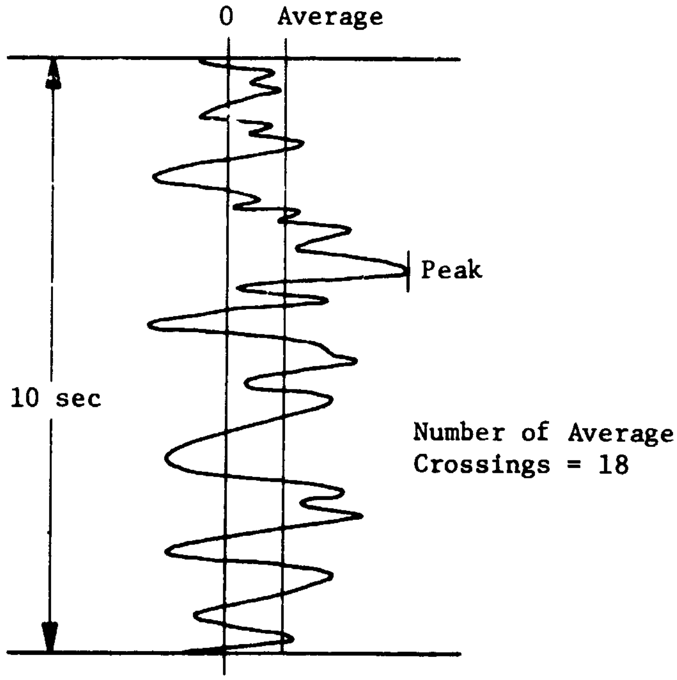

Figure II-4 Turbulence Accelerometer Measurements

A comparison of the sensor and deployment mechanism between the Viking and PAET Temperature gages showed that they are very similar. Only one gage is required for outer planet application. The Viking temperature gage has a range of 100 to 400°K, and thus is applicable without modification to Jupiter entries, although minor modifications must be made for the remainder of the planets. Figure II-5 shows the deployment mechanism for the temperature gage used. In the deployed position, the temperature sensor protrudes 1-in. from the probe body. The instrument will begin sampling with the other descent instruments as soon as the aeroshell is released and the sensor deployed.

The neutral mass spectrometer is the primary instrument in the SAG Exploratory payload making direct composition measurements of the planetary atmosphere. The mass range is from 1 to 40 amu. This is sufficient to measure the constituents that compose greater than 99.9% of the expected Jovian atmospheres. The design used here, while similar to both Viking and PAET, most closely resembles one being proposed for the Pioneer Venus which must descend to 100 atmospheres of pressure. The analyzer, however, can be either the Viking magnetic sector or the PAET quadrupole.

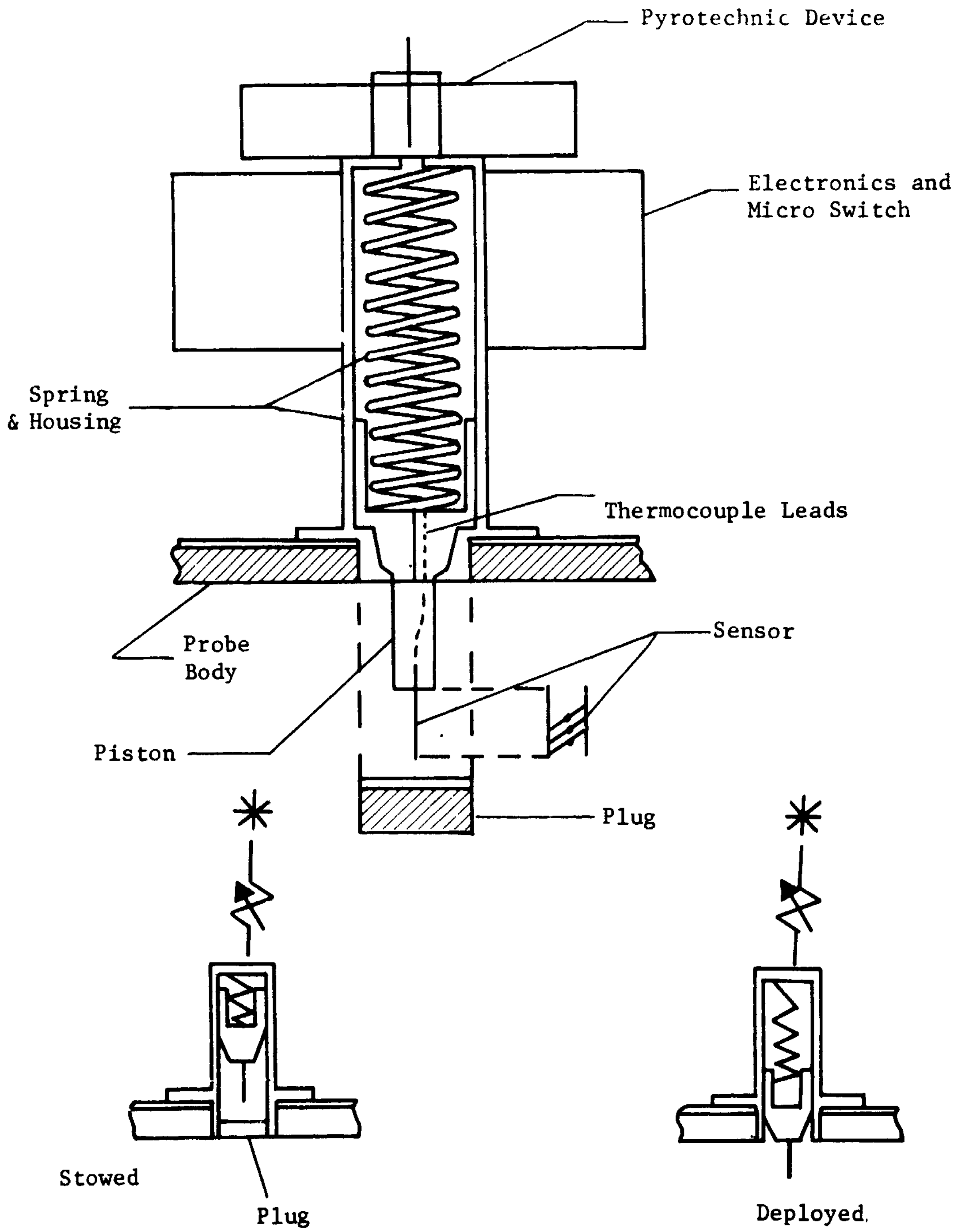

Figure II-5 Viking Temperature Gage

The inlet system is of the remote sampling design, which uses three porous sintered leaks and an evacuated ballast volume (Fig, II-6) to control the pressure of the sample volume and consequently, the flow into the analyzer. The magnetic sector instrument is a double focusing type with an electrostatic analyzer that provides both energy filtering and spatial focusing. The mass separation is brought about by the magnetic field as in a conventional mass spectrometer. The quadrupole analyzer consists of four parallel cylindrically hyperbolic electrodes upon which a dc voltage and RF field are superimposed. Mass scanning is accomplished by varying the field applied to the rods. The analyzer section of either mass spectrometer is state of the art and available, The inlet system requires further test and evaluation to verify the design, The response time between gas entering the first leak from the ambient atmosphere and the analyzer is about 30 sec, with good possibility of obtaining < 10, sec. by reducing the sample volume to the order of 0.1 cm^3. However, a problem exists because of the masses of the primary constituents existing in two different groups, specifically 1-4 amu and 15-18 amu. The leak rates through the sintered plug could be appreciably different, distorting the measurements.

A laboratory model of this proposed inlet system has been built and tested at Martin Marietta in Earth atmosphere under pressure, and will soon undergo tests in a simulated Venus atmosphere. Several laboratory experiments have been identified by this study which need to be performed to aid in understanding the application of this system to the Jovian atmospheres. In particular, they are: (1) determination of the extent of mass discrimination by the molecular inlet leak through the analysis of known amounts of two gases with widely separated masses, (e.g. H_2 and N_2) with consideration of the effect of variations in inlet system temperature; (2) understanding of the condensation problem in the inlet system by analysis of a gas with high concentrations of ammonia and/or water at different temperatures; (3) investigation of the pumping problems associated with the high concentration of inert helium in the Jovian atmospheres; (4) complete analysis of a simulated Jovian atmosphere containing H_2, He, NH_3, CH_4, and H_2O.

The sequence of science events for all of the entry probe missions is approximately the same, with the times and pressures for occurences varying. The instruments are turned on at least 5 min before entry for warmup, with time increments due to trajectory uncertainties added to this. The accelerometers immediately begin sampling data but will not begin storing the deceleration data from all three axes until a g sensor associated with the accelerometer processor senses the beginning of entry.

On the missions investigated, entry varies from 19 to 79 seconds, terminating when the probe reaches Mach 0.7. This occurs at a pressure level of from 33 to 92 millibars in the design missions. At this point the main parachute is deployed to slow the vehicle to terminal velocity. After a 12-sec delay during which the aeroshell is released, the descent measurements begin as the pyrotechnics deploy the temperature gage, first ejecting the plug, uncovering the mass spectrometer inlet aperture releasing the vacuum. The accelerometers are switched from the entry to the turbulence measurement mode and the full set of descent measurements begins, at a pressure range from about 40 to 120 millibars. These events are preprogrammed and science data is stored because the spacecraft has not yet acquired the probe.

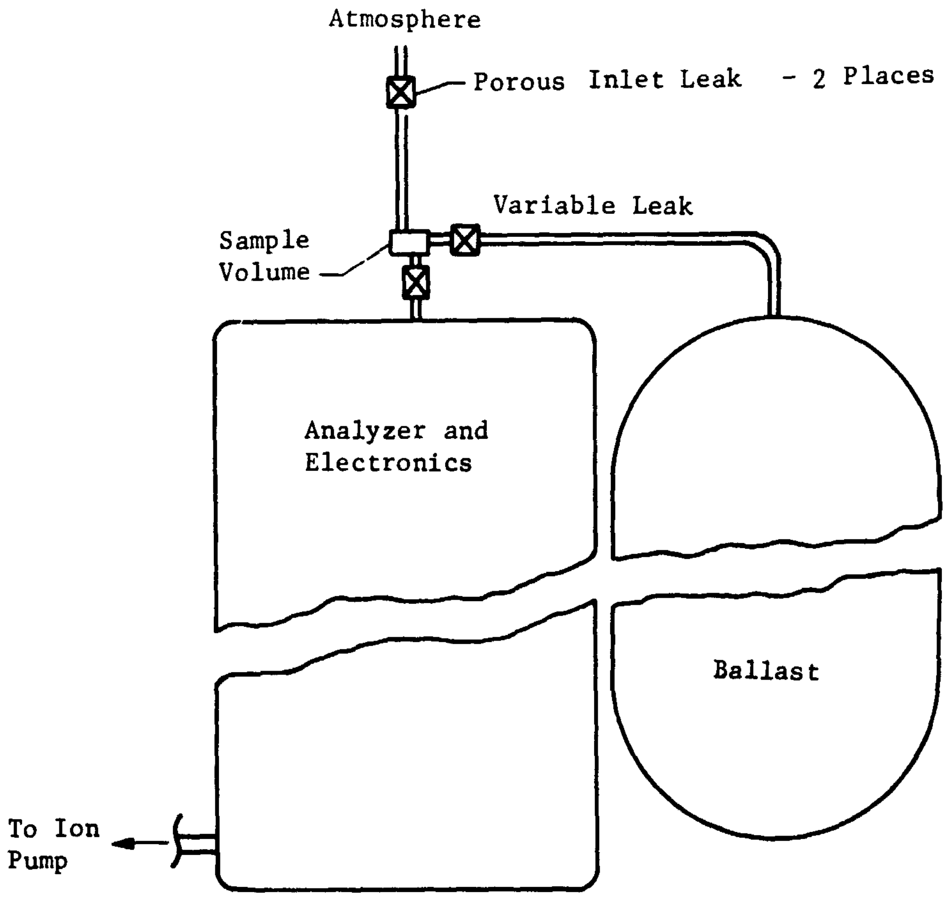

Figure II-6 Mass Spectrometer Inlet System

For descents into Saturn, Uranus, and Neptune, much higher ballistic coefficients are required than for Jupiter. For these missions, after a delay of about an additional 3 sec, the main parachute is released and a secondary parachute is deployed. All four instruments for all missions collect data in the descent mode and store it with the entry accelerometer data. After approximately 90 sec, the spacecraft acquires the probe and data transmission begins, sending all the data subsequently collected back in real time and interleaving the stored data.

The descent parametrics for each planet, including selection of ballistic coefficients and instruments sampling times are detailed in subsequent chapters. To meet the instrument performance criteria , three distinct points in the descent are critical.

1) Descent where the temperature begins to increase, generally 2 to 4 min after chute deployment;

2) the first encounter of clouds, which varies from 2 to 8 min after deployment;

3) immediately after drogue chute deployment, when this occurs.

The design limit pressure is that point in a descent profile where all of the requirements, within an overall set of constraints, have been met by the actual performance. In this study, this overall constraint was to descend to 2 to 30 bars depending upon the "risk and cost effect" of the higher pressures. Actual end of mission varies from 7 to 30 bars.

The measurement that controls the depth is that of determining the composition of the lowest (above 30 bars) cloud in the given atmosphere with the mass spectrometer. The specific requirement is to obtain two full mass spectrometer sweeps inside the cloud. The design limit pressures that were determined in this study are shown in Table II-7.

Table II-7 Design Limit Pressures

Atmospher	Cloud	Pressure, bars
Jupiter, C/D	H_2O	13
Jupiter, Nom	H_2O	7.5
Saturn, Nom	H_2O	7
Uranus, Nom	NH_3	7
Nepture, Nom	NH_3	20

C. NOMINAL JUPITER PROBE SYSTEM DEFINITION SUMMARY

The constraints for this configuration follow.

Mission	Type I, in 1979
Entry Angle	-20°
Entry Latitude	5°
Depth of Descent and Atmosphere	30 bars in a cool/dense atmosphere
Science	SAG Exploratory playload (Viking)
Spacecraft	TOPS
Carrier Mode	Flyby
Periapsis Radius	2 R_J
Communication Mode	Relay
Deflection Mode	Probe
Ejection Radius	10×10^6 km
Entry Ballistic Coefficient	0.65 slug/ft^2(102 kg/m^2)
Descent Ballistic Coefficient	0.12 slug/ft^2(19 kg/m^2) and 1.5 slug/ft^2(236 kg/m^2)

1. Mission Definition

The Nominal Jupiter Probe Mission is described in Figure II-7 and detailed in Table II-8. Important mission design results are summarized in this section.

a. *Interplanetary Trajectory Selection* - The interplanetary trajectory is pictured in Figure II-7(a) with 100-day intervals noted. The launch date of November 7, 1979 and arrival date of September 17, 1981 (trip time of 680 days) result in a maximization of the payload weight as discussed in Volume II, Chapter IV, Section A. As indicated in the figure, the spacecraft arrives at Jupiter shortly before the view to Jupiter is obstructed by the Sun.

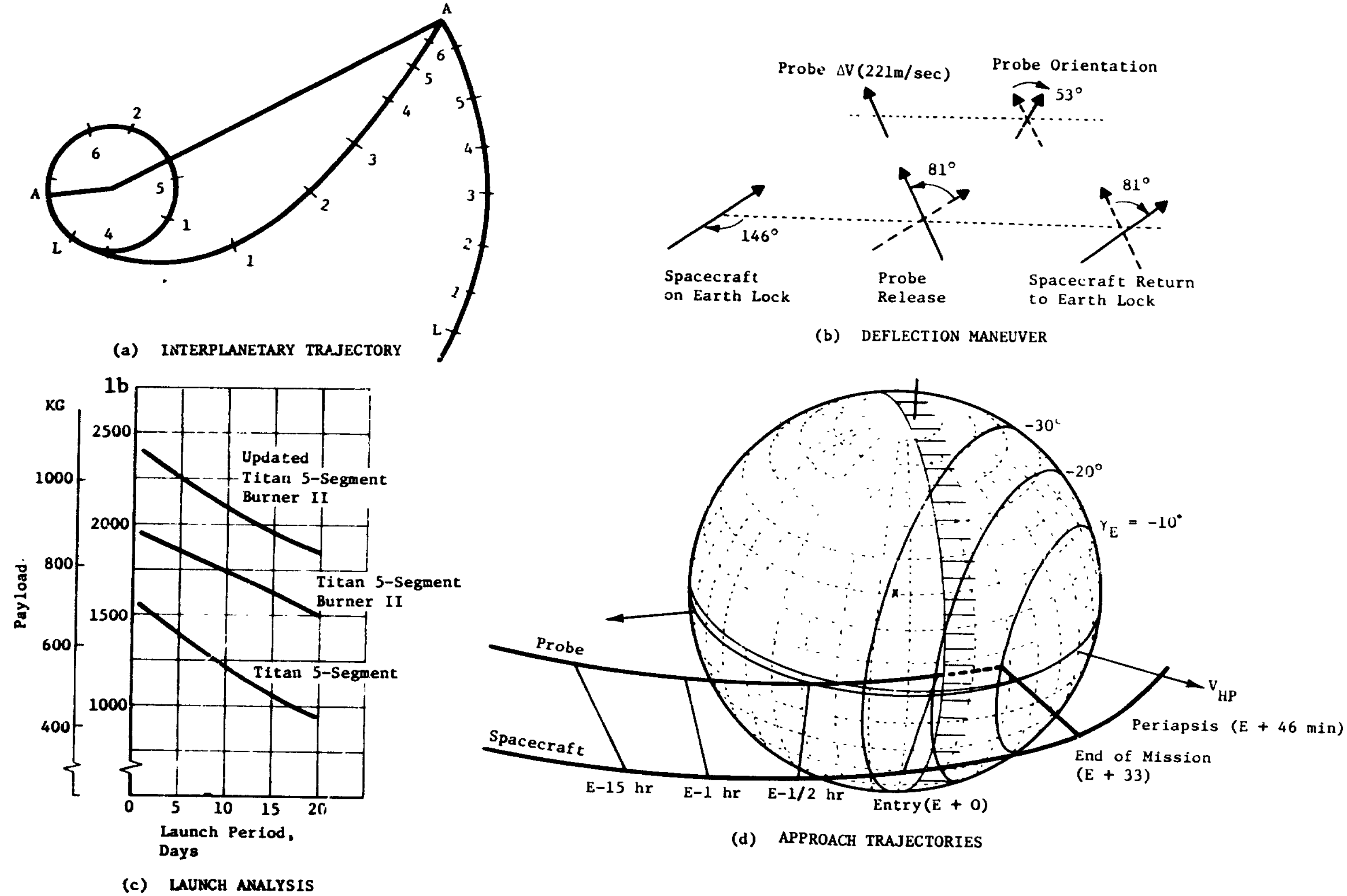

Figure II-7 Nominal Jupiter Probe Mission Description

Table II-8 Nominal Jupiter Probe Mission Summary

a. Conic Trajectory Data

Interplanetary Trajectory	Launch Trajectory	Arrival Trajectory
Launch Date: 11/7/79 Arrival Date: 9/17/81 Flight Time: 680 days Central Angle: 155°	Nominal C_3: 93.6 km^2/sec^2 Nominal DLA: 30.5° Launch Window: 1.17 hr Parking Orbit Coast: 36 min C_3 (10 day): 97.5 km^2/sec^2 C_3 (20 day): 105 km^2/sec^2 Azimuth Range: 101.7° - 115°	VHP: 8.474 km/sec RA: 161.3° DEC: 6.81° ZAE: 145.2° ZAP: 141.4° RP: 2 R_J INC: 10°

b. Deflection Maneuver and Probe Conic

Deflection Maneuver	Probe Conic Definition
Deflection Mode: Probe Deflection Radius: 10 x 10^6 km Coast Time: 9.75 days ΔV: 221 m/sec Application Angle: 116° Out-of-Plane Angle: 0° Rotation for Probe Release: 81° Probe Reorientation Angle: -53° Spacecraft ΔV from Earth: NA	Entry Angle: -20° Entry Latitude: 5.0 Entry Longitude: 88.9 Lead Time: 45.8 min Lead Angle: -12.05° Probe-Spacecraft Range (Entry): 96,742 km Probe Aspect Angle (Entry): 43.9° Probe Aspect Angle (Descent): 21.0° Probe Aspect Angle (EOM): 4.7°

c. Dispersion Analysis Summary

Naviation Uncertainties	Execution Errors (3σ)	Dispersions (3σ)
Type: Range-Doppler 167-day arc SMAA: 1482 km SMIA: 139 km β: 88° TOF: 54 sec	ΔV Proportionality: 1% ΔV Pointing: 2° Probe Orientation Pointing: 2°	Entry Angle: 1.1° Angle of Attack: 2.5° Down Range: 2.02° Cross Range: 0.80° Lead Angle: 4.4° Lead Time: 7.4 min Entry Time: 8.0 min

d. Entry and Descent Trajectory Summary

Entry Parameters	Descent Parameters	Critical Events: Time from Entry	Critical Events: Altitudes above 1 atm
Entry Velocity, km/sec: 60 Entry Altitude, km: 304.6 Entry B, $slug/ft^2$: 0.65 kg/m^2: 102.1 Entry Atmosphere: Cool/Dense Max Deceleration, g: 1500 Max Dynamic Pressure, lb/ft^2: 2.1 x 10^4 kg/m^2: 1.0 x 10^6	Descent Atmosphere: Cool/Dense EOM Pressure, bar: 30 Descent B, $slug/ft^2$: $slug/ft^2$: 0.12 kg/m^2: 18.84	g = 0.1, sec: 6.0 Max g, sec: 12 M = 0.7, sec: 34 Descent Time, min: 33.3 EOM, min: 33.8	km: 182 km: 65 km: 32 km: -85

b. Launch Analysis - The launch analysis is provided in Figure II-7(c). Available payload is plotted against launch period for three sets of launch vehicle performance data: standard data for the Titan 5-Segment vehicle with and without Burner II plus updated data for the Burner II. For reference, the payload weight (probe, spacecraft, spacecraft modifications, and spacecraft-launch vehicle adaptor) is about 454 kg (1000 lb) for a Pioneer mission and 680 kg (1500 lb) for a MOPS mission. Thus, the Burner II option is necessary for a MOPS-type mission to obtain a 20-day launch period. The nominal launch trajectory summarized in Table II-8(a) indicates that the daily launch window and parking orbit coast time are satisfactory.

c. Approach Trajectory - The approach trajectory is pictured in Figure II-7(d) and summarized in Table II-8(a). The spacecraft trajectory was selected with a periapsis radius of 2 R_J to obtain a good communication geometry between the probe and spacecraft during the probe descent phase. The inclination of 10°, with respect to the orbital plane of Jupiter, was chosen so that the probe entry site defined by a latitude of 5° and an entry angle of -20° could be achieved with an in-plane deflection. The communication geometry chosen has a lead angle of -12.05°, probe leading spacecraft at entry, so that the probe aspect angle at the start of descent is 21°, passes through zero during descent, and is 5° at the end of the mission (EOM).

d. Deflection Maneuver - The probe deflection mode was used for the deflection maneuver for this mission. The deflection maneuver is illustrated in Figure II-7(c) and summarized in Table II-8(b). The deflection radius of 10 million km resulted in a ΔV of 221 m/sec and a coast time (time from deflection to probe entry) of 9.8 days. The ΔV is applied at an angle of 116° to the approach asymptote and is in the plane of the spacecraft trajectory. The spacecraft must rotate 81° from its Earth-lock attitude to release the probe. After firing the ΔV, the probe must precess 53° to obtain the attitude required for zero relative angle of attack.

e. Dispersion Analysis - The navigation and dispersion analysis results are summarized in Table II-8(c). The navigation uncertainties have little impact on dispersions at entry, even assuming only a standard range and Doppler tracking arc. All the entry parameter dispersions are within satisfactory tolerances. The communication parameter dispersions are discussed in the telecommunication subsection.

f. Entry and Descent Trajectories - Table II-8(d) summarizes the entry and descent phases of the mission. The cool/dense atmosphere model is used for both phases of this mission. The entry phase starts at 304.6 km above the 1 atm pressure level (0 km alt - 71,726 km) and ends at the staging of the aeroshell 34 sec later. During this phase, the peak deceleration of 1500 g is attained. The descent phase starts after staging and lasts until the end of the mission at 30 bars. The total mission time (entry and descent) is 33.8 min.

2. Science

Many of the mission characteristics of the nominal Jupiter probe were specified by the statement of work. The science instruments were specified to be Viking-derived wherever possible. The temperature gage is the Viking parachute phase instrument; its range of operation is sufficient for the Jupiter probe. Two pressure transducers are necessary to cover the pressure range required. One can have a range similar to that of the Viking instrument (0-300 mb) and the other must have a larger range. The accelerometer triad is the Bell Model IX 3-axis system with pulse rate convertor, with a modification to scale up the flexure for 1500 g peak load. The proposed neutral mass spectrometer deviates from Viking, but is considered to be a magnetic sector analyzed with a porous leak remote inlet system. The characteristics are compatible with Viking derivations.

The nominal Jupiter probe analysis considered only the cool/dense atmosphere and the descent profile (Fig. II-8) was chosen with this assumption. Also, this initial task was to determine what was necessary for descent to 30 bars. The resulting parameters that were chosen to be consistent with the criteria are:

Design pressure limit - 30 bars

Main parachute ballistic coefficient - 0.12 slug/ft^2 (18.84 kg/m^2)

Drogue parachute ballistic coefficient - 1.50 slug/ft^2 (235.5 kg/m^2)

Separation Pressure - 10 bars

Parachute deployment pressure = 92 millibars

Pressure at first measurement = 111 millibars

Entry Time = 34 sec

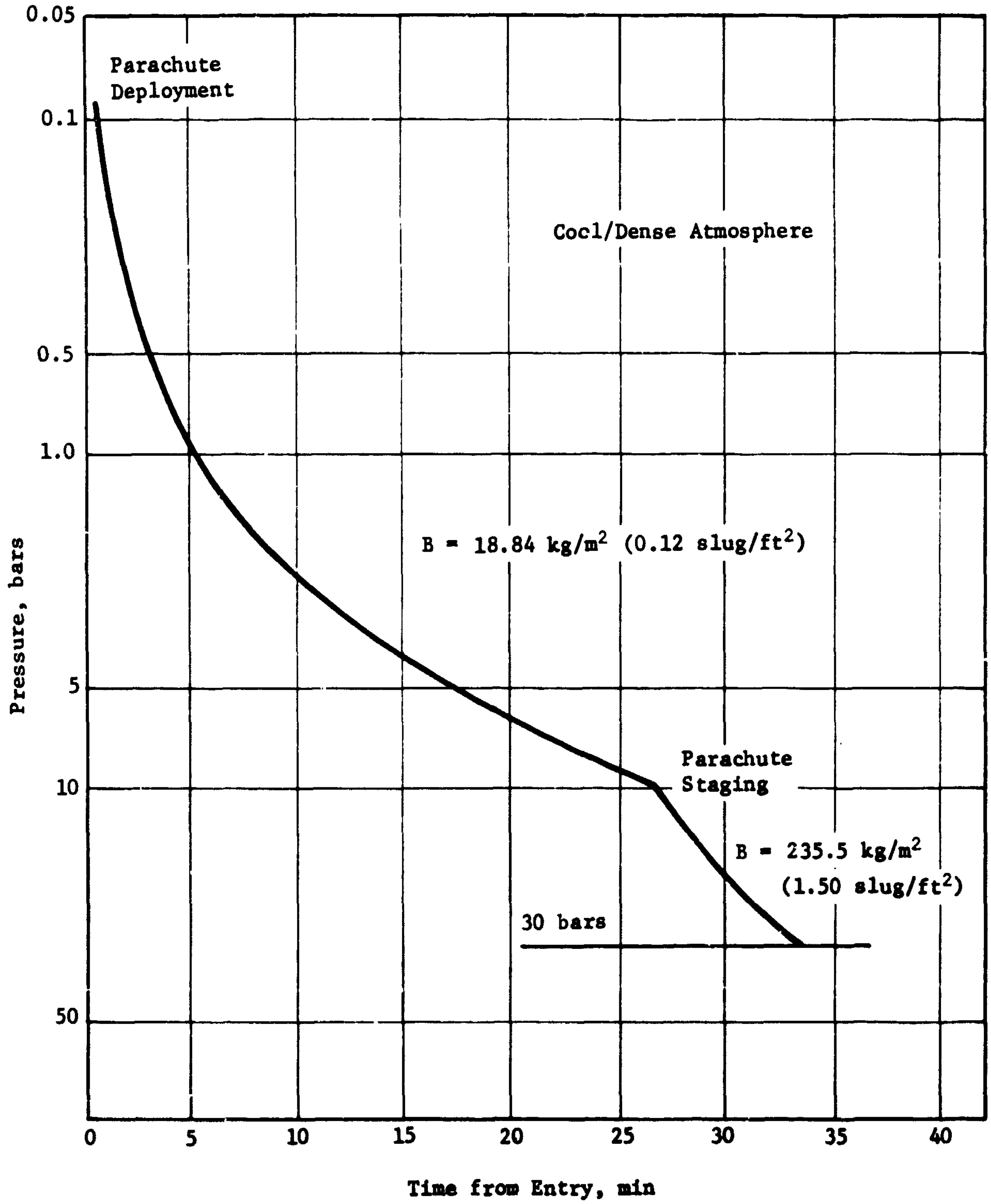

Figure II-8 Nominal Jupiter Probe Pressure Descent Probile

Descent Time - 33 min, 6 sec

Instrument Sampling Times:

Temperature and Pressure - 5 sec

Neutral Mass Spectrometer - 50 sec

Entry Accelerometers - 0.1/0.2 sec

Descent Accelerometers - 10 sec

Total bit rate - 28.0 bps

All performance criteria were satisfied.

3. System Integration

Figure II-9 shows a typical sequence of events pictorially and shows the relationship between the spacecraft and probe. A detailed sequence was generated for this and all other configurations for the purpose of determining time for acquisition, times for various power loads, etc. These sequences are discussed in Volume II.

A typical functional block diagram is shown in Figure II-10 for this configuration and all others, except for the probe-dedicated alternative Jupiter mission. For that exception, the propulsion subsystem is deleted and the ACS propulsion is very simple. This figure shows the relationship of each subsystem as well as the electrical interface with the spacecraft before and after the probe separation.

A data profile and power profile were generated for this and all other configurations. These are shown in Figures II-11 and II-12, respectively. These are similar for all configurations except the probe-dedicated alternative Jupiter probe, which has a very short separation phase during the time engineering data is not recorded; therefore, the power demand occurs at pre-entry.

A weight summary was generated for this configuration as presented in Table II-9.

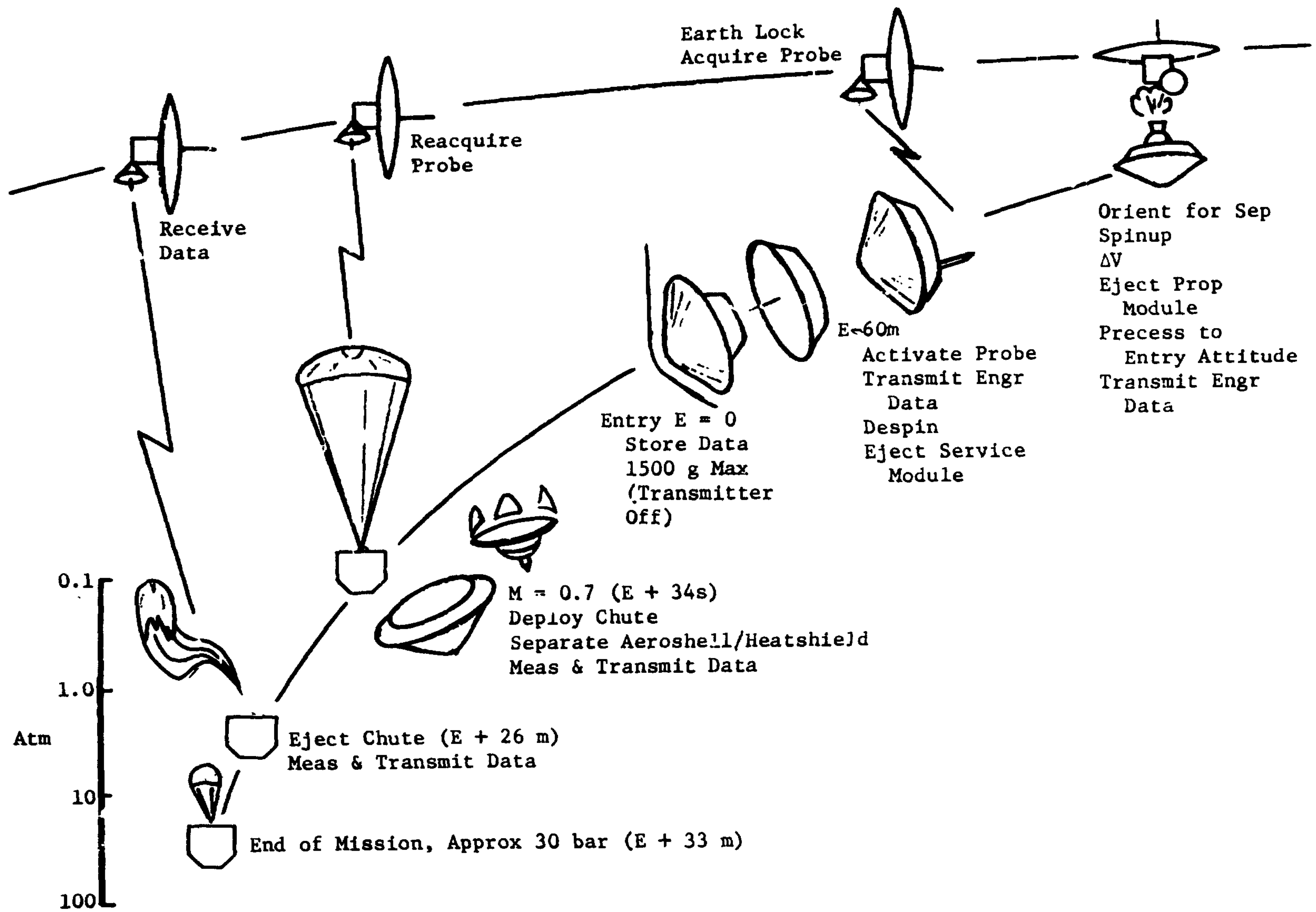

Figure II-9 Pictorial Sequence of Events for the Nominal Jupiter Probe

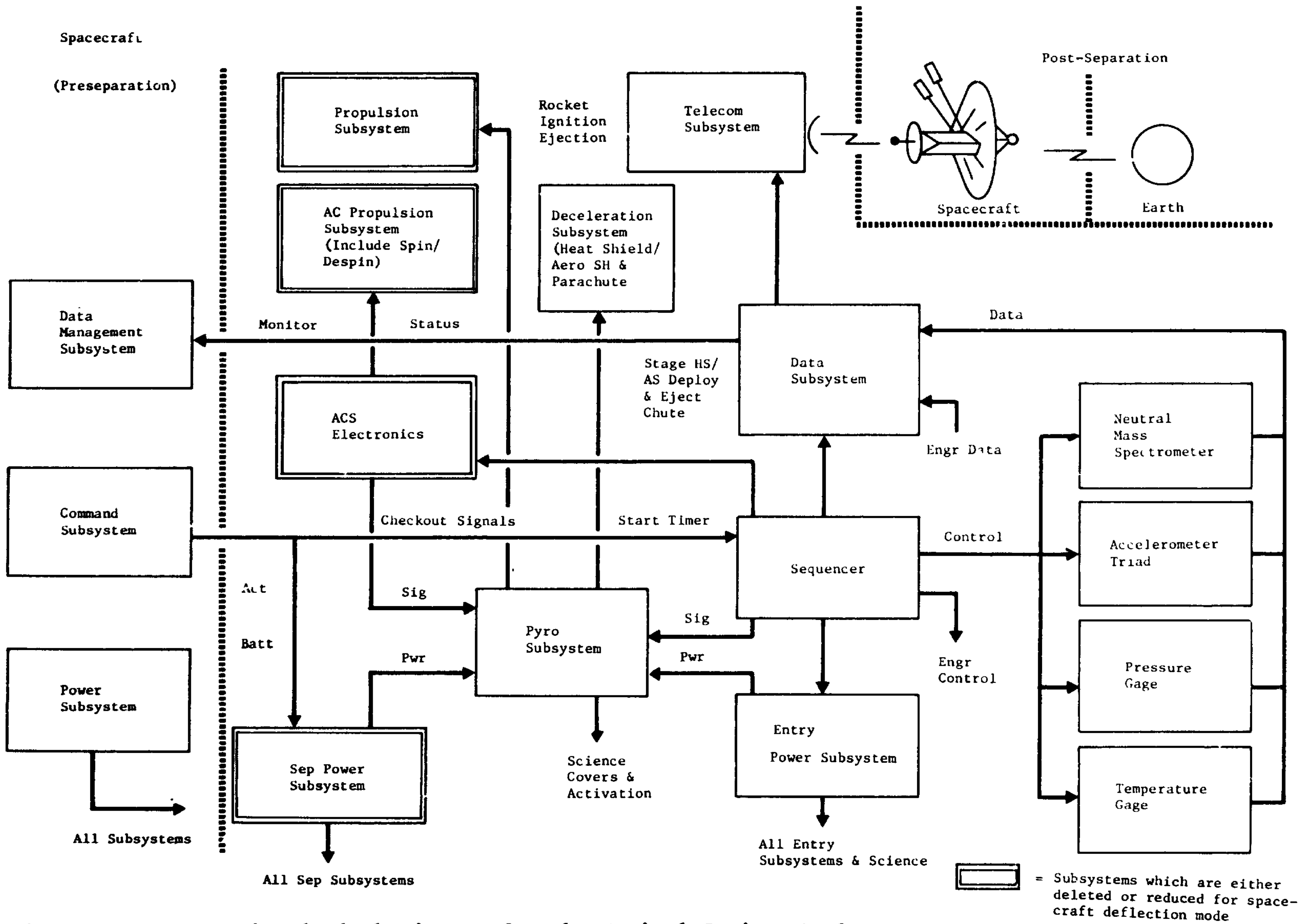

Figure II-10 Functional Block Diagram for the Nominal Jupiter Probe

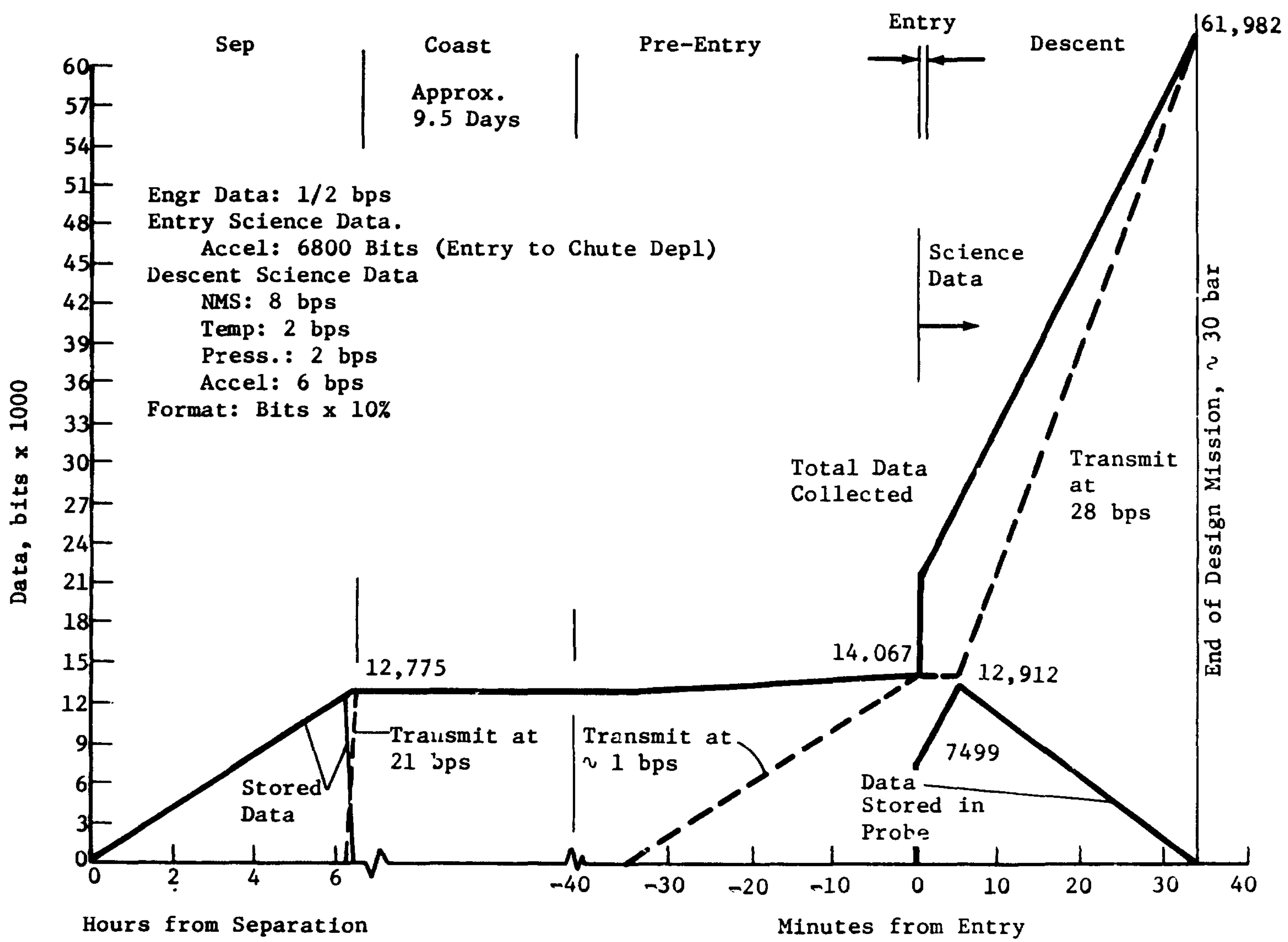

Figure II-11 Data Profile for the Nominal Jupiter Probe

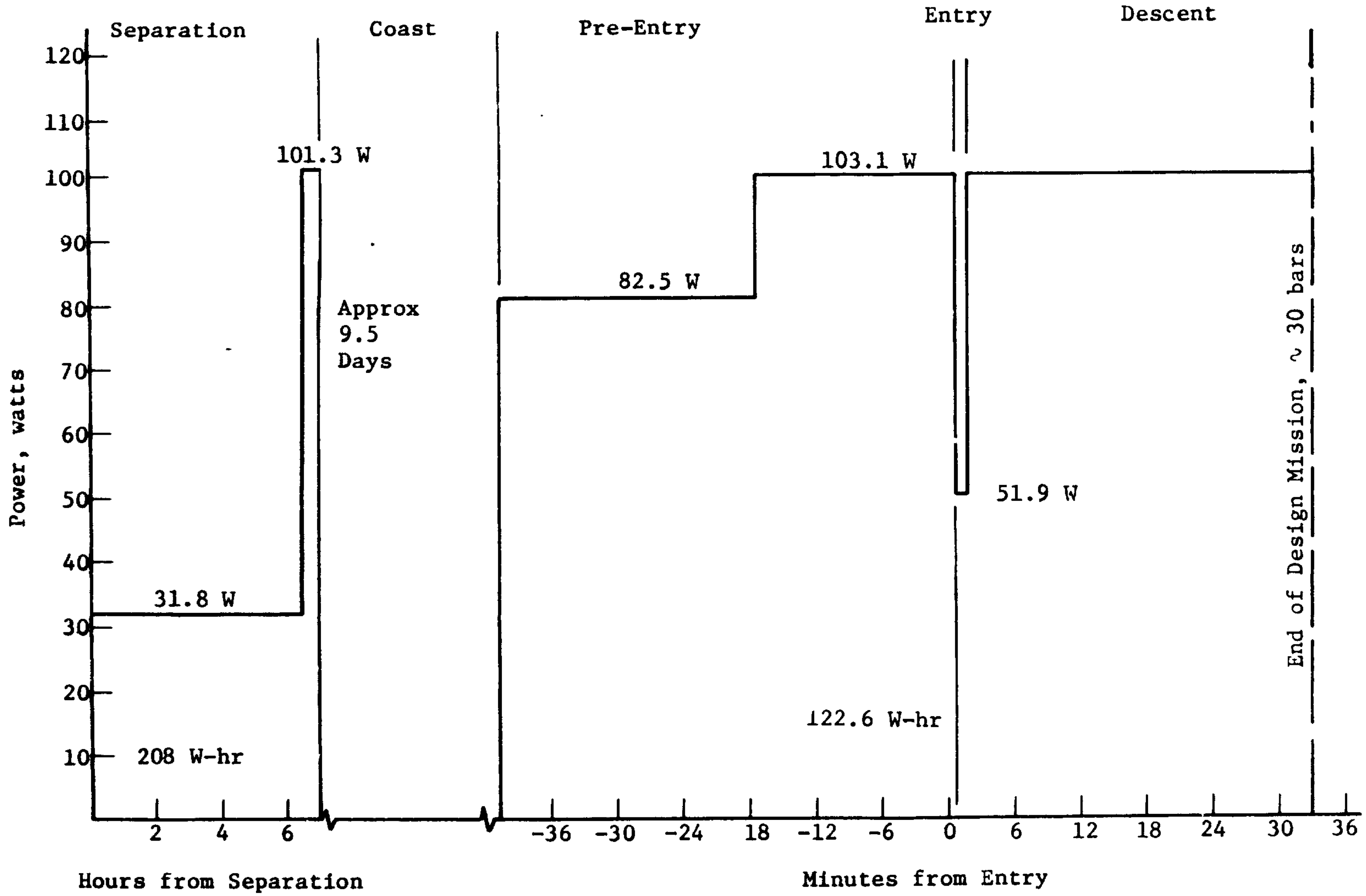

Figure II-12 System Power Prcfile for the Nominal Jupiter Probe

Table II-9 Nominal Jupiter Probe Weight Summary

Probe Breakdown	Weight, kg
Science	8.66
Power and Power Conditioning	5.91
Cabling	5.44
Data Handling	2.13
Attitude Control, dry	11.76
Communications	3.61
Pyrotechnics	6.31
Structures and Heat Shield	61.92
Mechanisms	7.71
Thermal	7.44
Propulsion, dry	3.85
Propellant	12.16
Engineering Instrumentation	0.0
15% Margin	20.54
Ejected Weight, kg	157.46
Entry Weight, kg	106.34
Descent Weight, kg	41.93

4. Telecommunications Subsystem - Definition of the telecommunications subsystem for the nominal Jupiter probe system was linked heavily with design of the probe trajectory. The mission optimized communication parameters in order to minimize the RF power required. Many changes were made in periapsis radius, lead time, and ballistic coefficient in order to arrive at a trajectory that places the spacecraft overhead at the end of the mission and minimize several RF power sensitive parameters. The objective was to have minimum communications range and probe aspect angle at mission completion.

The subsystem characteristics are summarized in Table II-10 and a functional block diagram is shown in Figure II-13.

Table II-10 Telecommunications RF Subsystem for the Nominal Jupiter Probe

CONDITIONS: Planet:Jupiter S/C: TOPS FREQUENCY: 1 GHz BIT RATE: 28 bps			
COMPONENT	CHARACTERISTIC	UNIT	VALUE
Transmitter	RF Power Out	W	25
	Overall Efficiency	%	45
	DC Power in at 28 V dc	W	55
	Total Weight	kg	2.7
		lb	6.0
RF Switch	Type		Mechanical
	Insertion Loss	dB	0.3
	Weight	kg	0.23
		lb	0.5
Entry Antenna	Type		Spiral on Cone
	Main Beam Angle	deg	55
	Beamwidth	deg	35
	Maximum Gain	dB	6.2
	Size (1 x diameter)	cm	27 x 22.5
		in.	10.6 x 8.8
	Weight	kg	0.45
		lb	1.0
Descent Antenna	Type		Turnstile in Cup
	Main Beam Angle	deg	0
	Beamwidth	deg	110
	Maximum Gain	dB	5.2
	Size (diameter x h)	cm	18.8 x 7.6
		in.	7.4 x 3.0
	Weight	kg	0.23
		lb	0.50
Spacecraft Antenna	Type		Helix
	Beamwidth	deg	45
	Maximum Gain	dB	12.3
	Size (1 x di meter)	cm	51 x 9.5
		in.	20 x 3.75
	Weight	kg	2.27
		lb	5
	Despin		No
	Position Search	sec	1
	Frequency Acquisition	deg	35
	Clock Angle, θ	deg	-94
	Cone Angle, ϕ	deg	100
Spacecraft Receiver	Noise Temperature	°K	300
	Noise Figure	dB	3.1
	DC Power in at 28 V dc	W	3.0
	Weight	kg	0.9
		lb	2.0

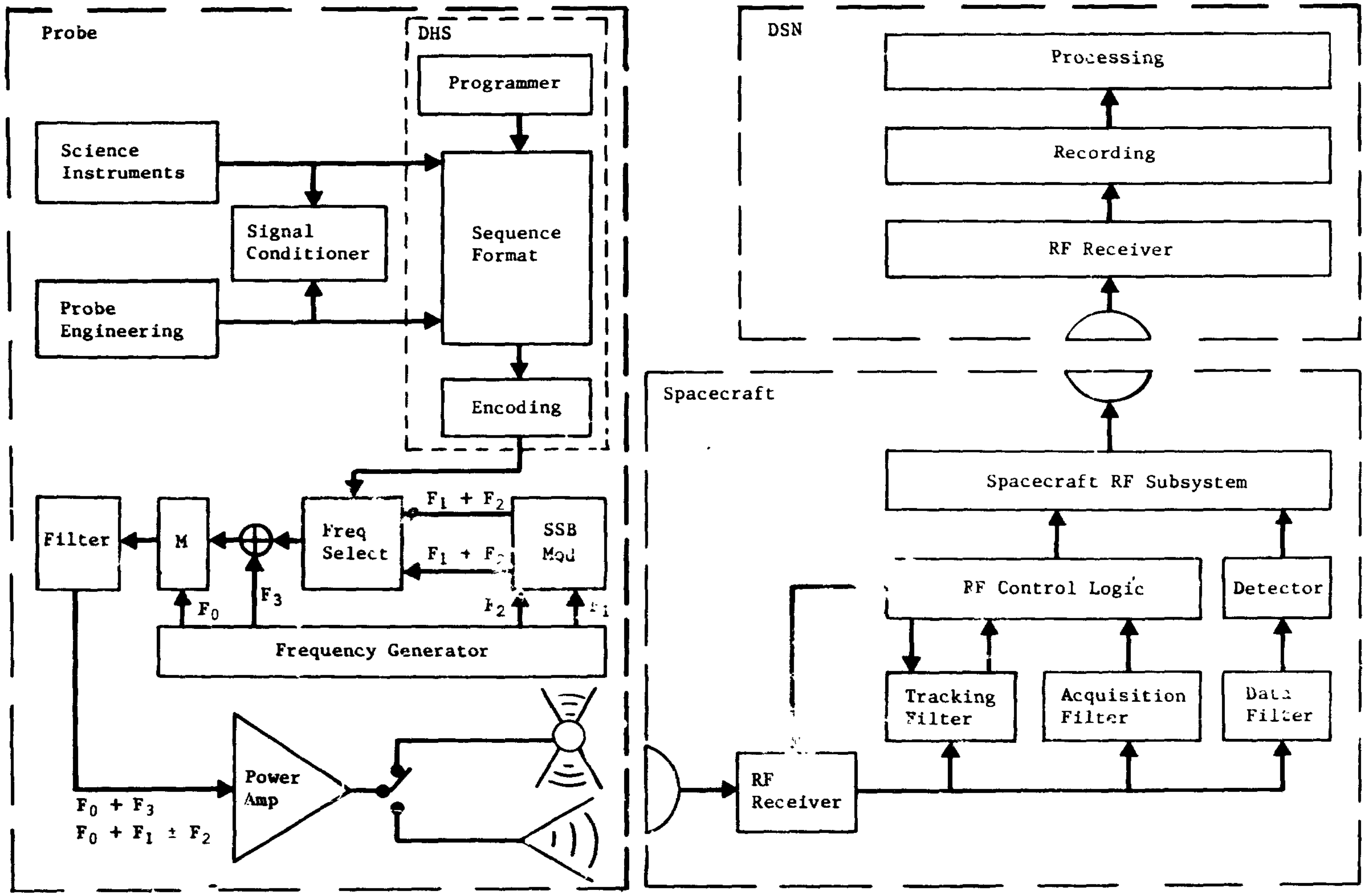

Figure II-13 Communications Functional Diagram

5. Data Handling Subsystem

The selected configuration (Fig. II-14) is a special purpose DHS that contains those functions which are necessarily centralized and must be retained in the common subsystem. These functions consist of synchronization, sequencing, and formatting. In addition to the low capacity buffer memories required for formatting, a science data storage memory is included primarily for entry deceleration data. The design size and weight are based on bipolar IC electronics, hybrids, and standard piece parts. A discussion of the design configuration details is contained in Volume II, Chapter V, Section B.5; and integrated discussion of data handling alternatives is contained in Vol III, Appendix H.

The physical characteristics were based on estimates of the number of devices required for each function. These estimates resulted in the following physical characteristics: volume 142 $in.^3$; weight 4.7 lb; and power 6.9 watts. The weight of the memory was based on an estimate from Electronic Memories (Division of Electronic Memories and Magnetics Corporation). The estimate for a 7 kb bipolar IC memory (8 kb card) is volume 6.5x4.5x0.25 in., weight 0.5 lb, power 6 watts. This has been used as a basic building block for the cost of memory capacity. The resultant total weight for the nominal Jupiter probe DHS and memory is: volume 158 $in.^3$; weight 5.7 lb; and power 18.9 watts.

6. Power and Pyrotechnic Subsystem

The subsystem (Fig. II-15) is divided to two sections: (1) the post-separation subsystem which consists of a central power conditioning unit that provides power to attitude precession logic, thrust control electronics, pyrotechnic data handling and RF subsystem; and (2) the entry and descent power subsystem which consists of power distribution (relays) and isolation power filters. Required power conditioning is implemented in the user subsystem electronics. Primary power is provided by separate remotely activated Ag-Zn batteries for post-separation and entry/descent periods. A mercury-zinc battery provides power (40 V) for capacitor bank charging for the first pyrotechnic battery event. A self-contained Hg-Zn cell provides power for the Accutron coast timer. Pyrotechnic circuitry is similar to Viking designs and estimates are derived from that program. A discussion of the power and pyrotechnic configuration may be found in Vol II, Chapter V, Section B.6 and Vol III, Appendix G. The physical characteristics of the electronics, conversion equipment and filters are based on similar subsystems and engineering estimate.

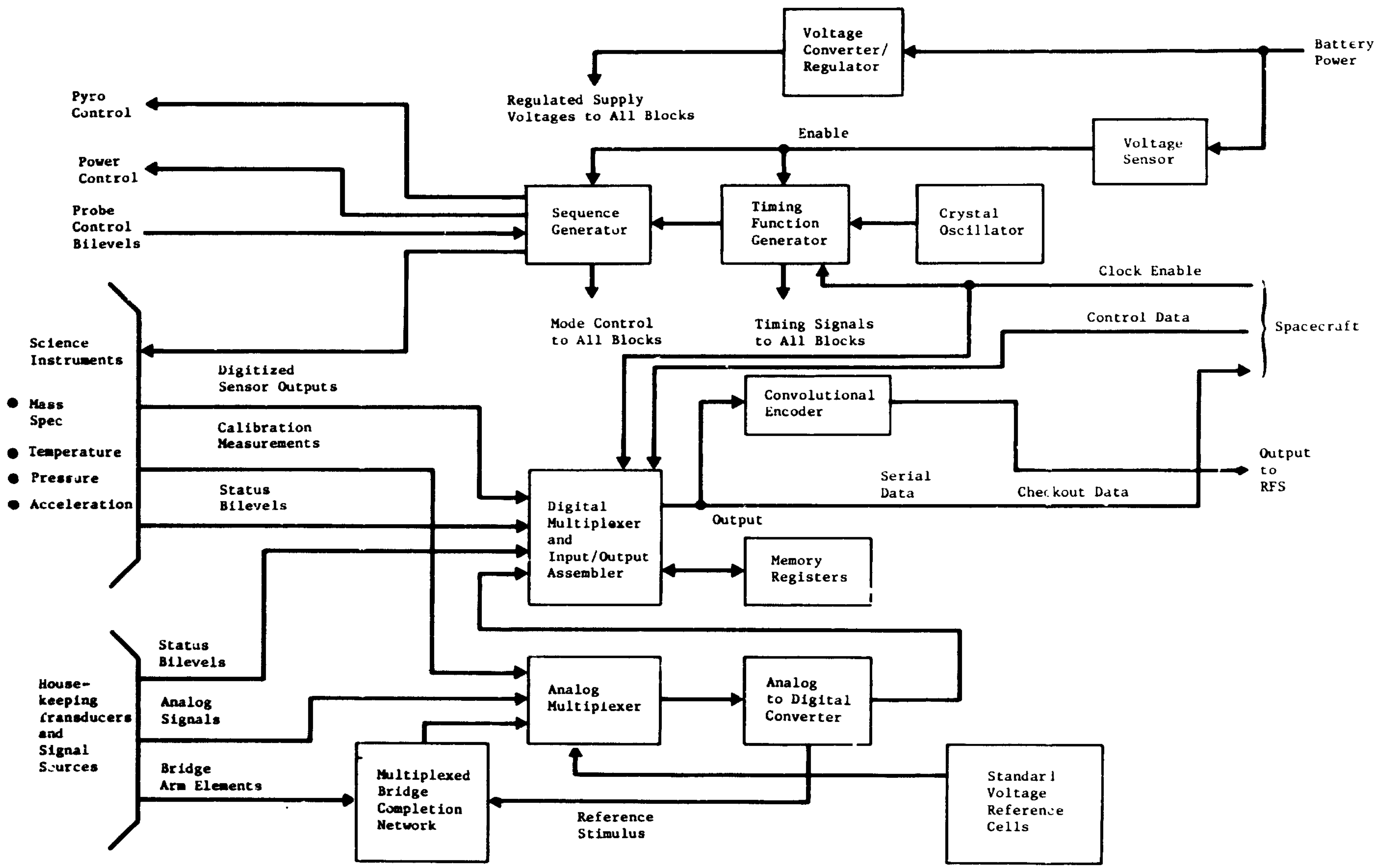

Figure II-14 Data Handling Subsystem, Special Purpose Approach

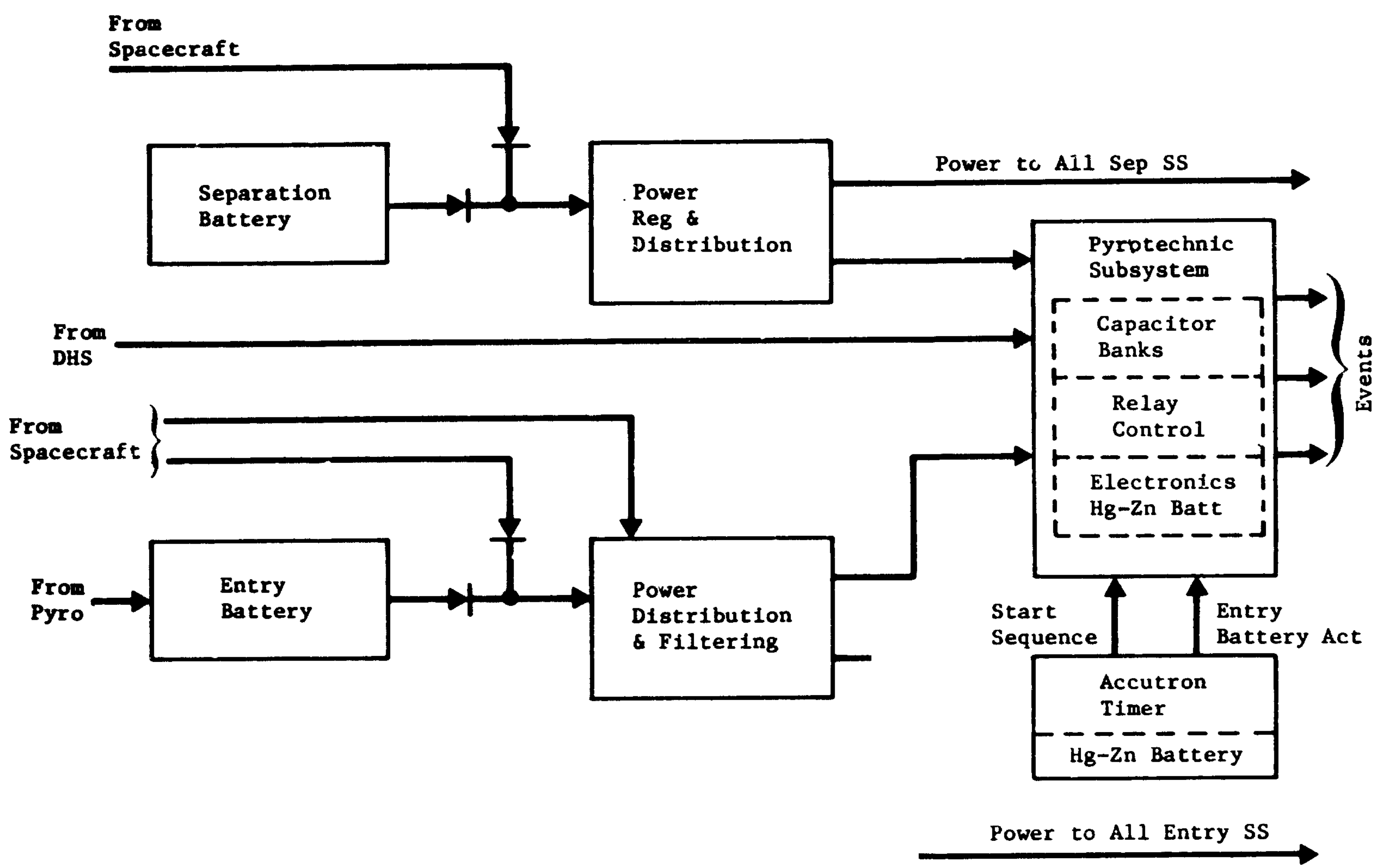

Figure II-15 Power & Pyrotechnic Subsystems

The remotely activated batteries were estimated from the weight chart in Appendix G with an assumed 13.7 in.^{3}/lb volume. Capacitor banks, pyrotechnic relay control and power distribution (relay) characteristics were based on part count and known volume and weight of the elements. The physical characteristics of these subsystems are tabulated. A more complete description of these subsystems may be found in Volume III, Appendix G.

Power Subsystem	Size, in.^{3}	Weight, lb
Post-Separation Battery	94	6.9
Entry Battery	56	4.1
Hg-Zn Battery	4x2 in. diameter	0.9
Power Conditioning	40	2.0
Power Distribution	10	1.0
Power Filters	20	2.0
Pyrotechnic Subsystem		
Electronics	75	2.0
Relays	91.8	6.6
Capacitor Banks	100	1.85

7. Attitude Control Subsystem

The attitude control subsystem (Fig. II-16) consists of sensors (solar aspect angle and planet sensor) sector and data processing logic, cold gas precession and spinup subsystem, and a nutation damper. Solar aspect angle and the angle between the Sun and the planet referred to the probe spin axis are measured. The measurements are processed to develop a precession program which is then implemented by sector logic control. A period of six hours is allowed for the maneuver to enable the nutation damper to remove excessive nutation during this period. A discussion of the configuration of the ACS is contained in Vol II, Chapter V, Section B.7, and Vol III, Appendix F.

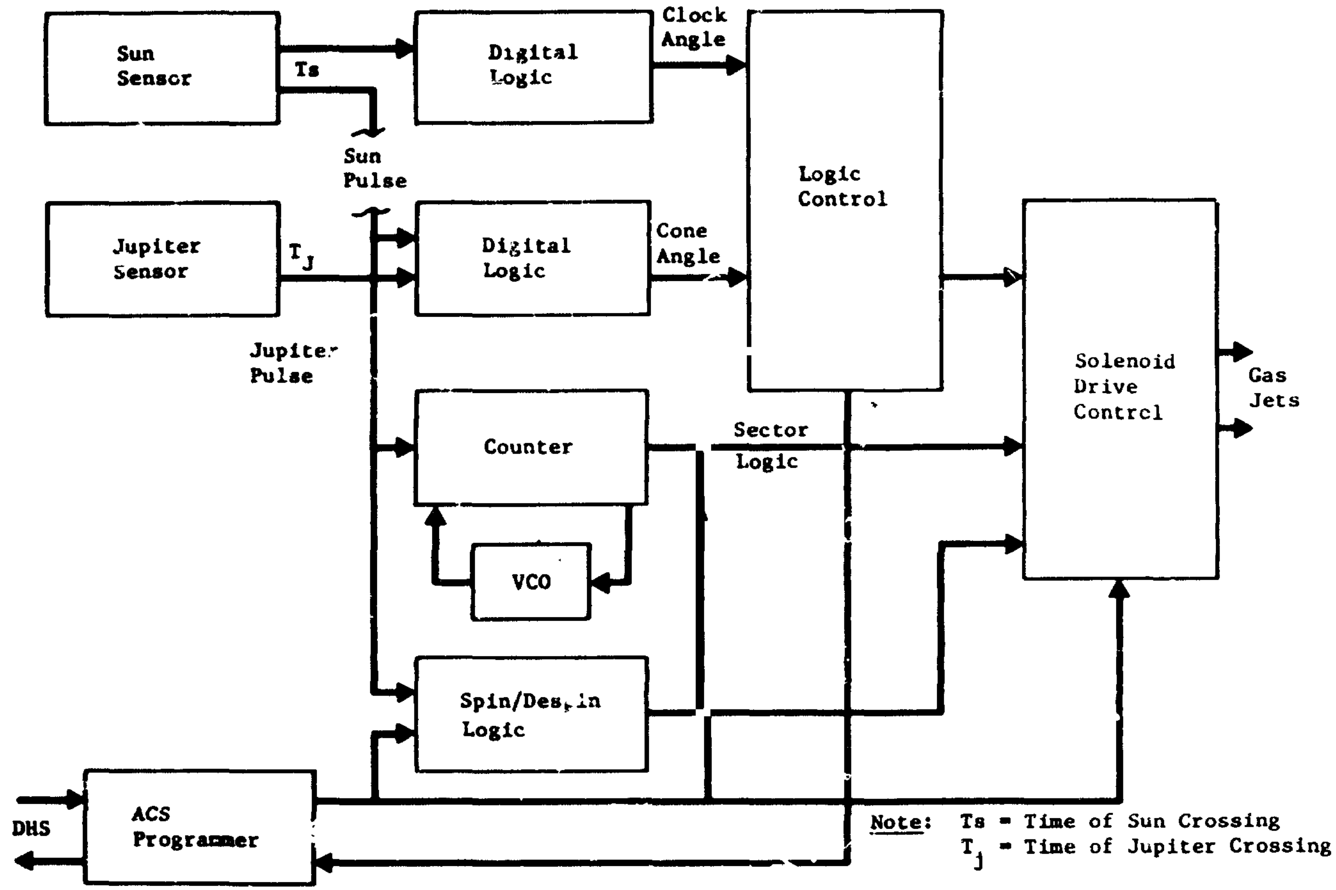

Figure II-16 ACS Block Diagram

The estimated physical characteristics of the attitude control subsystem are:

	Size, cm^3 ($in.^3$)	Weight, kg (lb)	Power, watts
Sun Sensor	228 (14)	1.59 (3.5)	2.0
Jupiter Sensor	130 (8)	0.91 (2.0)	1.0
Electronics	1630 (100)	1.36 (3.0)	2.0

3. Structures and Mechanical Subsystems

The nominal Jupiter probe consists of a descent probe, an entry module, a service module, and a deflection maneuver motor. The descent probe accommodates the scientific instrument complement and the supporting electrical and electronic components to fulfill the desired mission. These components are housed within the descent probe and supported off an equipment support deck which in turn is thermally isolated from the outer shell. The descent probe is completely encapsulated for planetary entry within a forward aeroshell/heat shield structure and an aft heat shield cover, providing protection of the descent probe against the entry heating and aerodynamic pressures. A service module containing the attitude control system is attached to the aft end of the entry module to provide attitude stabilization and attitude control of the probe from spacecraft separation until just before planetary entry. This unit is expended and ejected from the entry probe just before planetary entry. A solid propellant rocket motor attached to the aft end of the service module to provide the deflection maneuver delta velocity, completes the configuration of the Jupiter probe. The nominal Jupiter probe in its various mission phase configurations is shown in Figure II-17. The probe is 0.94 m ([illegible] in.) in diameter, 0.92 m (36.3 in.) long, weighs 157.5 kg (347.3 lbm) at spacecraft separation. The length is reduced to 0.535 m (21.1 in.) and weight is reduced to 106 kg (234 lbm) before entry. The descent probe is 0.483 m (19.0 in.) in diameter, 0.457 m (18.0 in.) long, and weighs 41.9 kg (92.6 lbm).

The structural design of the nominal Jupiter probe uses all high strength aluminum alloy construction. This is possible because of the thermal protection provided at entry by the surrounding heat shield both on the nose and on the aft end of the entry probe. (The aeroshell is assumed to be below 300°F at peak loading.) The probe is designed to withstand the entry deceleration of 1500 g encountered at entry into the Jovian atmosphere. The aeroshell of the nose cone is designed to withstand the peak dynamic pressure of approximately 1.13×10^6 N/m^2 (23500 psf), and is sized to provide a ballistic coefficient of 102 kg/m^2 (0.65 $slug/ft^2$).

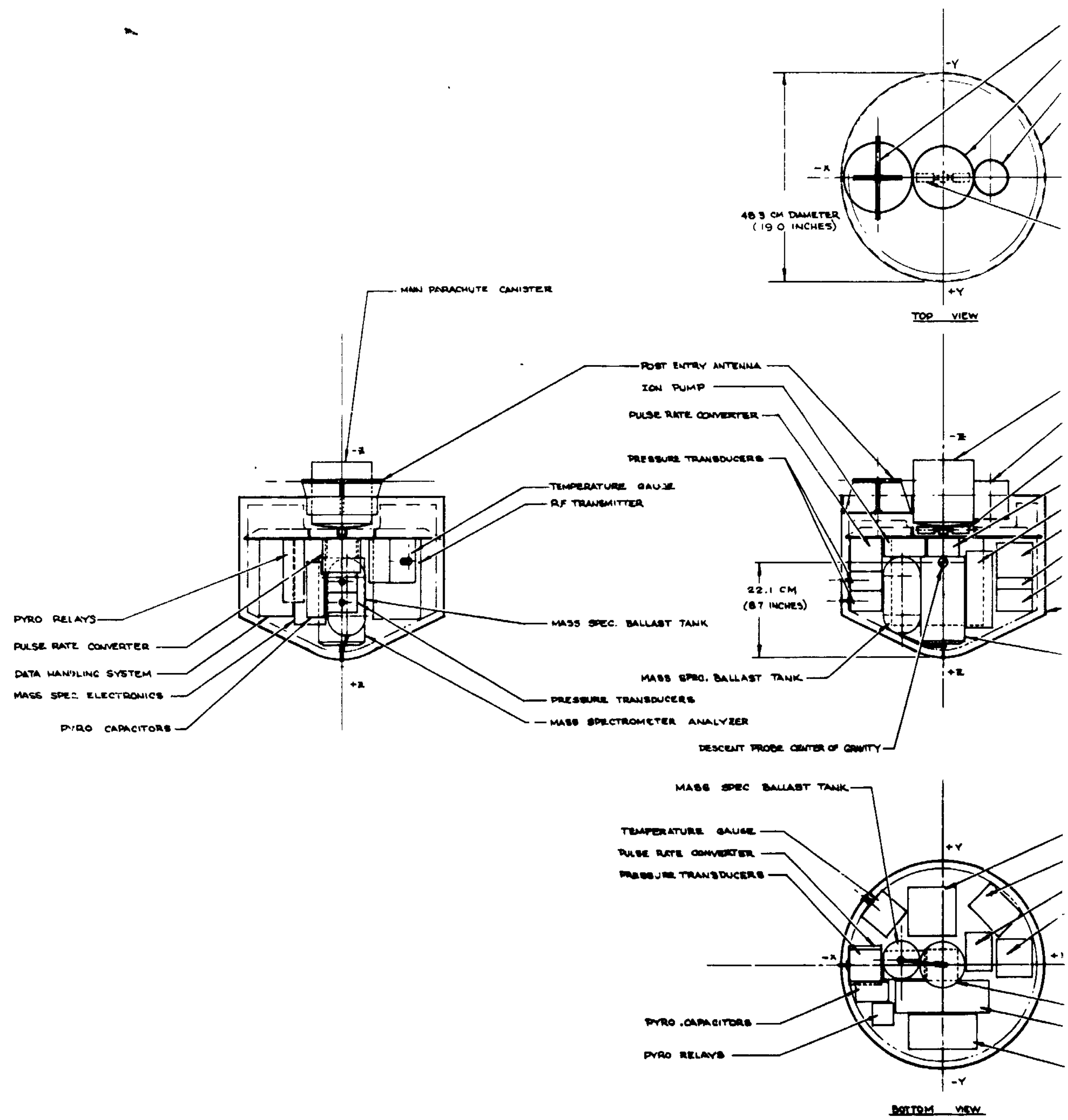

DESCENT PROBE

FOLDOUT FRAME

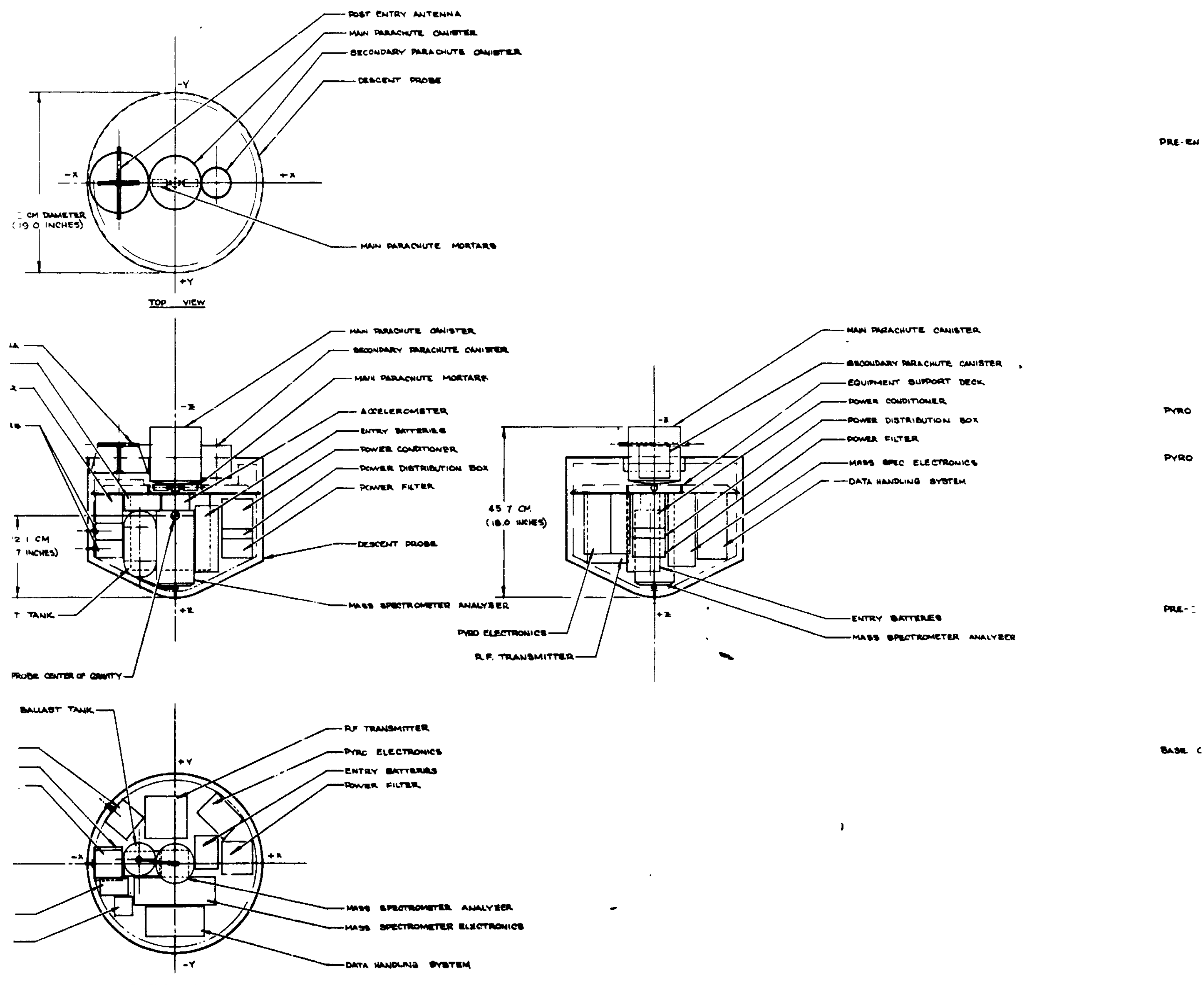

DESCENT PROBE

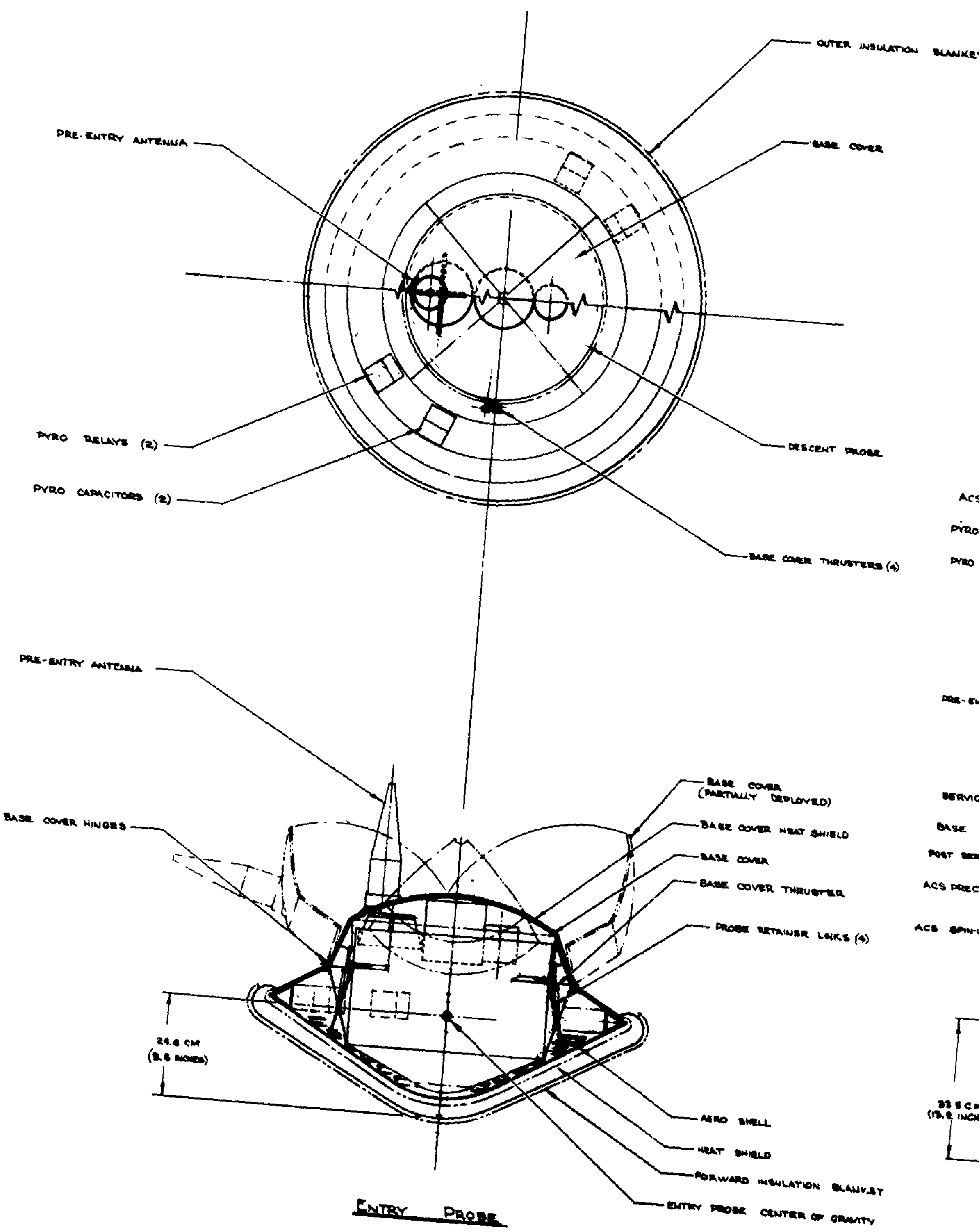

FOLDOUT FRAME 3

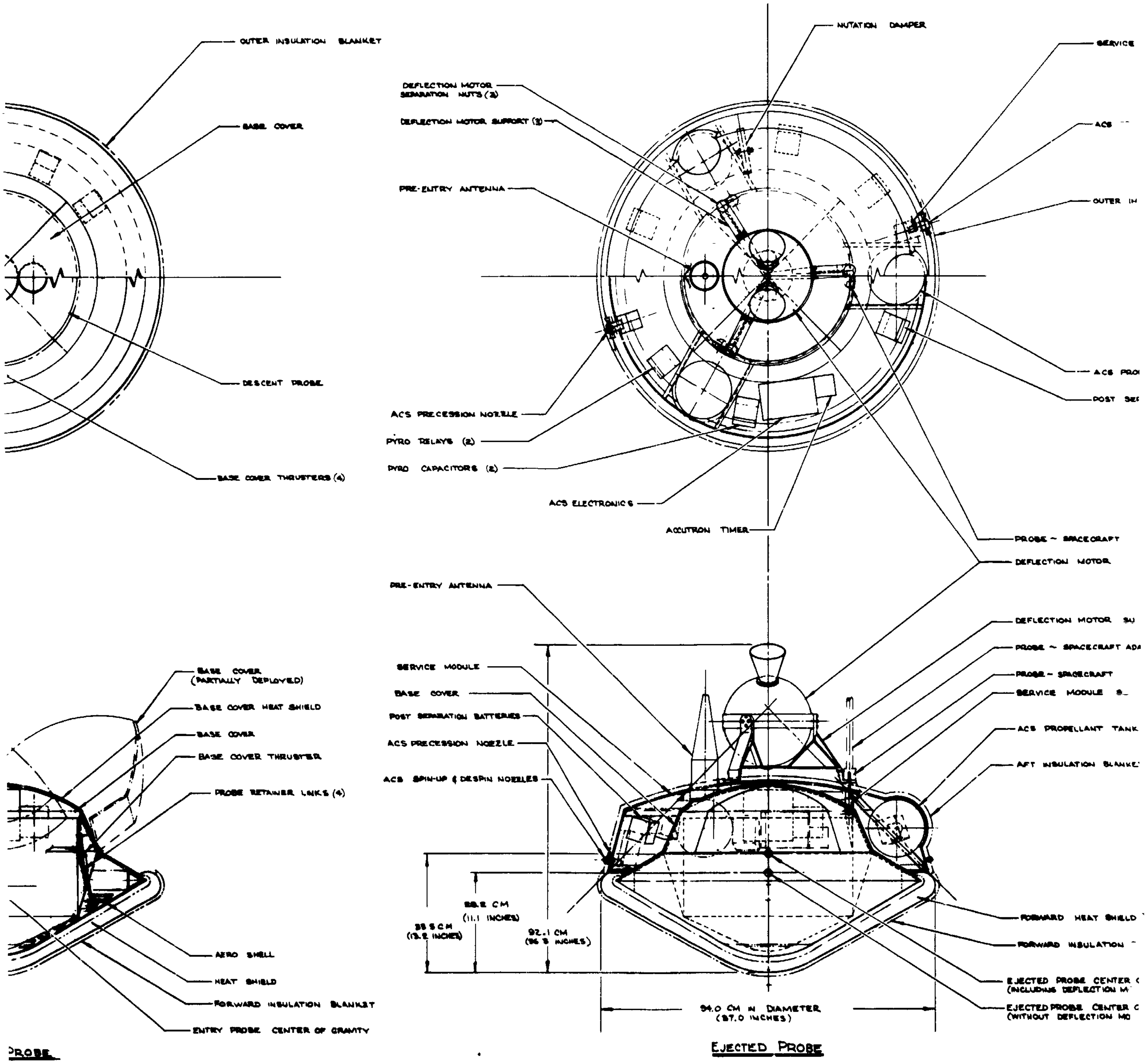

Figure II-17 Jupiter Survivable Pro

FOLDOUT FRAME 4

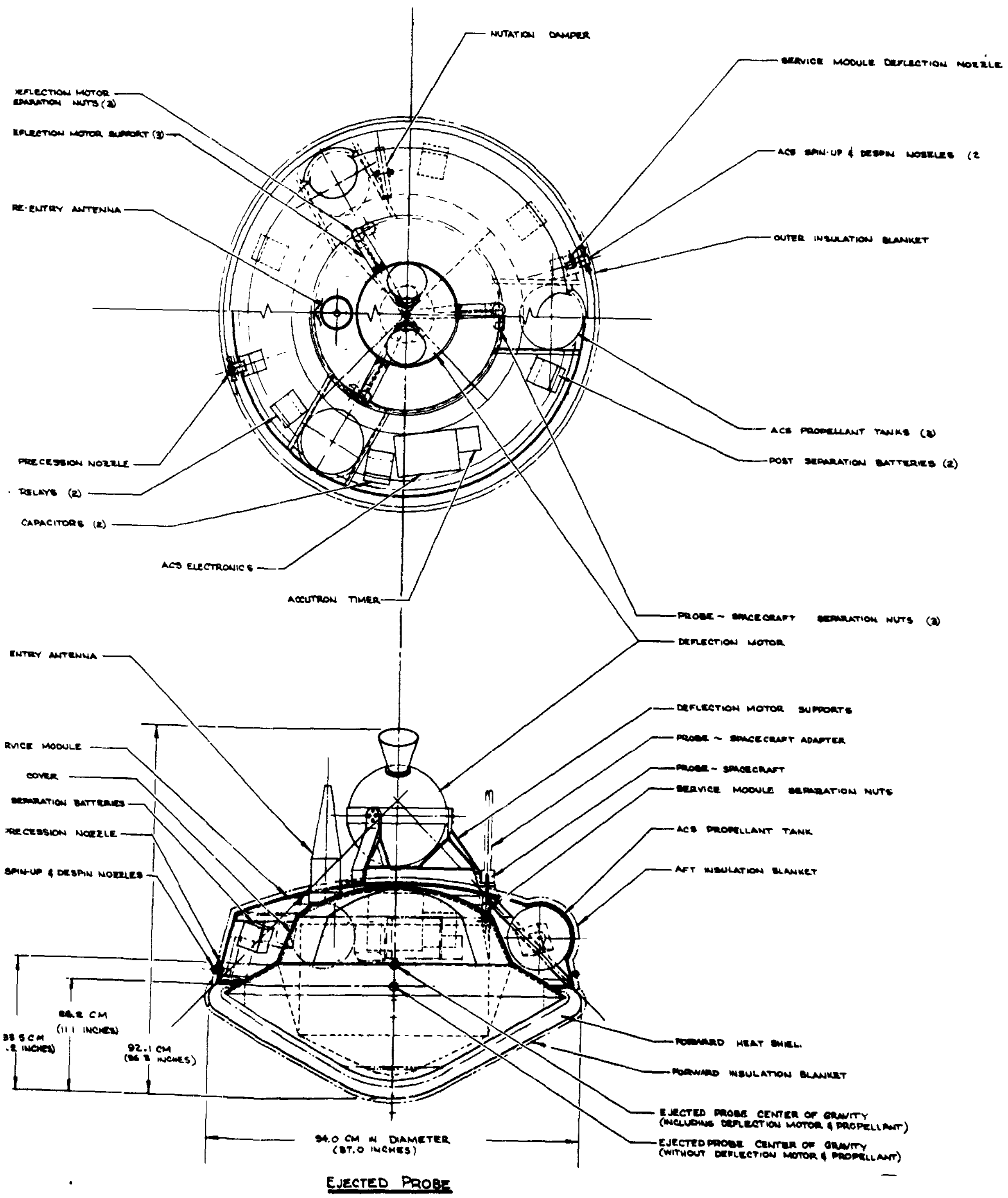

Figure II-17 Jupiter Survivable Probe - Task I Configuration II

This coefficient provides a deceleration of the probe at entry to a velocity of Mach 0.7 at a pressure altitude of approximately 100 millibars, meeting scientific requirements for staging of the descent probe and the beginning of the descent mission.

The descent probe uses two parachute stages for descent. The first parachute, deployed at 100 millibars pressure, is 2.46 m (7.5 ft) in diameter and provides a descent probe ballistic coefficient of 18.9 kg/m^2 (0.12 slug/ft^2). This ballistic coefficient satisfactorily provides adequate separation force to pull the descent probe from the aeroshell at staging and the desired initial rate of descent for the descent probe. It is mortar-deployed using a pyrotechnic energy source, and upon being jettisoned after initial descent, pulls out the secondary parachute for more rapid descent toward the end of the mission. The secondary parachute is quite small, 0.45 m (1.0 ft) in diameter, and provides a ballistic coefficient for final descent of 236 kg/m^2 (1.5 slug/ft^2). The entry heat shield uses a high density ATJ graphite ablator on the nose with a carbonaceous backface insulator. It has a mass fraction of 0.317 (heat shield weight/entry weight). The base cover heat shield uses an ESA 5500OM3 ablator to protect the base of the probe.

9. Propulsion Subsystem

The propulsion subsystem for the nominal Jupiter probe consists of a spherical, solid-propellant, rocket motor to provide the required deflection maneuver delta velocity of 221 m/sec (725 fps). It also consists of a cold gas (nitrogen) attitude control system providing a spin-despin-precess maneuver. For the attitude control of the probe after spacecraft separation, this system provides a spinup of the probe to 10.5 rad/sec (100 rpm) and then a precession maneuver through an angle of 0.87 rad (51°). The probe is despun to 0.52 rad/sec (5 rpm) before entry to provide reduced attitude stability for planetary entry.

The rocket motor to provide the deflection maneuver is a spherical solid propellant rocket motor weighing 14.5 kg (32.0 lbm) and containing 10.6 kg (23.5 lbm) of propellant. It uses two exhaust nozzles mounted at 0.78 rad (45°) with respect to each other, providing protection against impinging the carrier spacecraft with solid propellant waste products from the motor at probe separation from the spacecraft. The motor is 0.246 m (9.7 in.) in diameter. The motor is shown in Figure II-18.

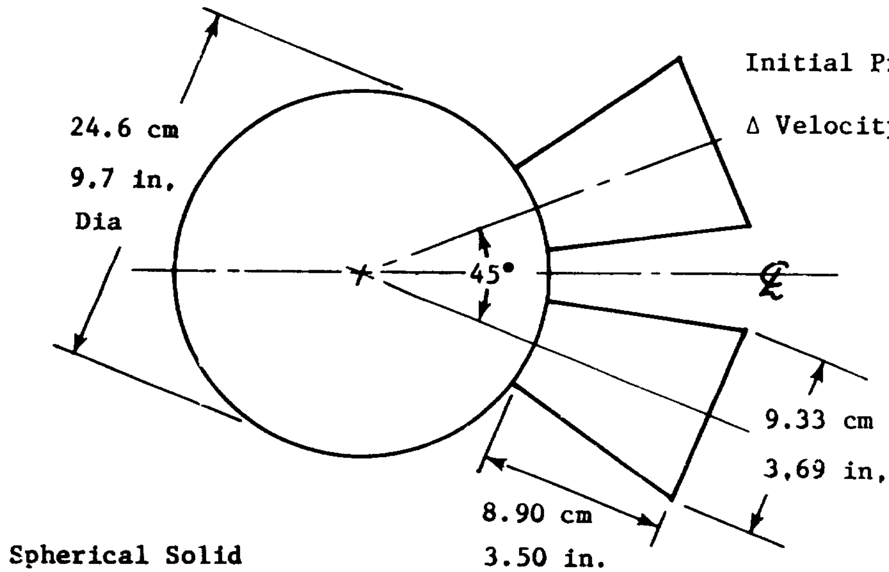

Initial Probe Weight = 138 kg/347 lbm

Δ Velocity = 221 m/sec

Propellant	10.6 kg/23.5 lbm
Mass Fraction	0.79
Loaded Weight	14.5 kg/32.0 lbm
Total Impulse	30,000 N-sec/6740 lbf-sec
Thrust	1056 N/nozzle x 2 = 2120, 1950 N net Thrust
	237 lb/nozzle x 2 = 475, 439 lbf net Thrust
	(Including Vectorial Loss)

Figure II-18 Deflection Propulsion Motor

The cold gas attitude control system consists of pairs of 4.4 N (1.0 lbf) nozzles mounted around the periphery of the entry probe to provide the required torques for the spin and despin maneuvers. A single nozzle mounted parallel to the spin axis along the probe circumference provides for the precession maneuver. This nozzle is pulsed for 0.78 rad (45°) of probe spin, once each revolution, until the precession is complete. The cold gas propellant required for the attitude control system is 1.48 kg (3.27 lbm) to perform the spin-despin-precess maneuver, and finally eject the service module. The total system weight is 6.67 kg (14.72 lbm). The schematic of the system is shown in Figure II-19.

10. Thermal Control Subsystems

Thermal control is required to maintain the probe equipment within acceptable temperature limits throughout all phases of the outer planet mission. For the nominal Jupiter probe, the thermal design concept consists of multilayer insulation, thermal coatings and radioisotope heaters for the spacecraft cruise and probe coast phases. For the entry and descent portions of the mission, the probe relies on sufficient thermal inertia and low density foam insulation protection internal to the probe shell.

The pivotal temperature from a standpoint of thermal design is the probe temperature at the end of the mission coast phase. For the nominal Jupiter probe (cool/dense atmosphere), the primary thermal problem is one of losing too much thermal energy to the atmospheric environment during descent. The probe entry temperature, therefore, must be adequate to allow sufficient leeway for probe cooling. Likewise, however, the probe equilibrium temperature during the long duration spacecraft cruise must be safely below the upper allowable battery storage limits (Chapter V, Section A.10.d in Vol II).

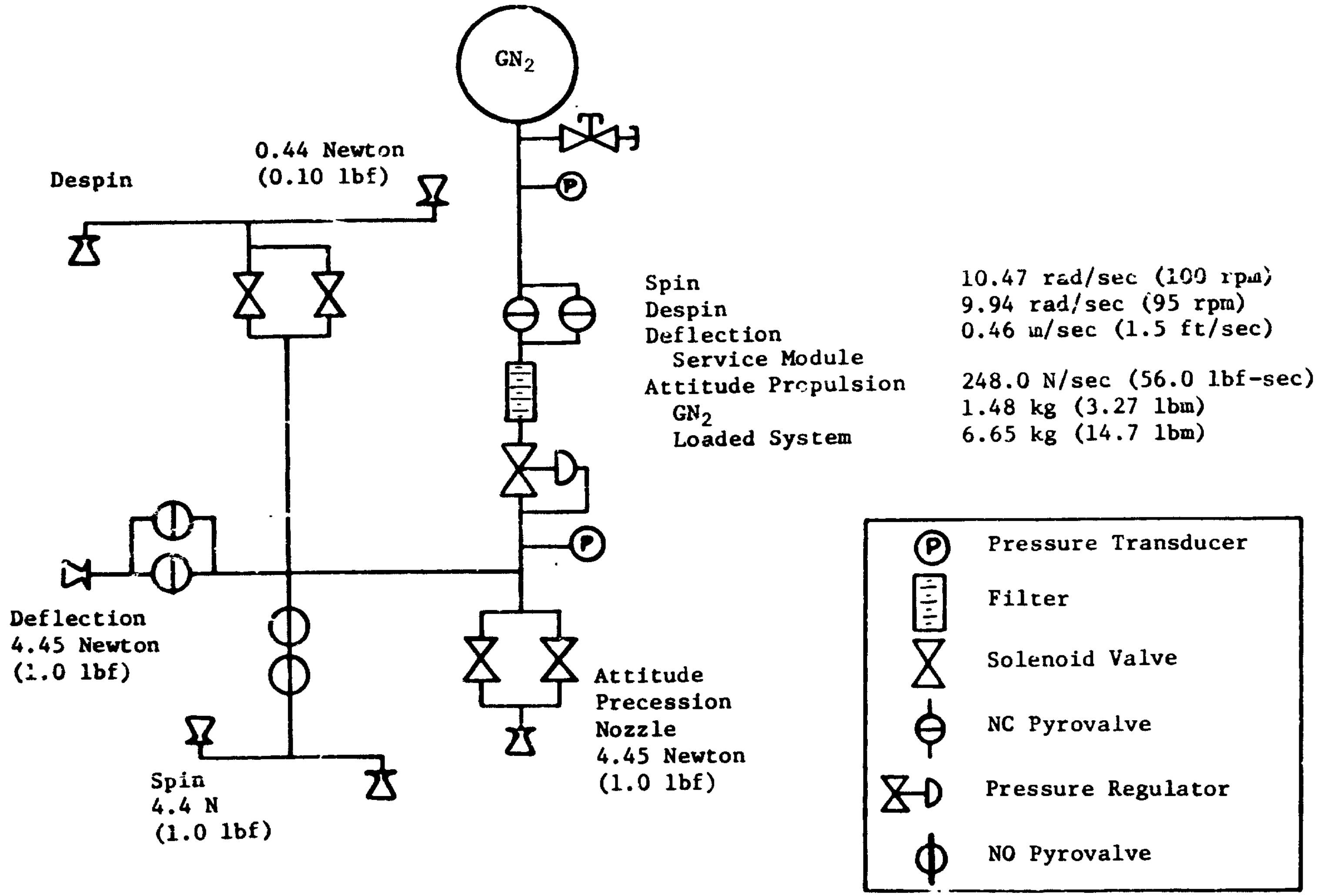

Figure II-19 Jupiter Probe Altitude Control System

A probe thermal analysis was performed for the defined nominal Jupiter probe mission. On the basis of these thermal analyses, a complete thermal history of the nominal Jupiter mission was constructed and is presented in Figure II-20. The spacecraft cruise and coast temperatures are determined based on the radioisotope heater power present and the degree of solar energy absorption during the coast phase. The probe temperatures represent the aggregate internal equipment, which includes the service module during cruise and coast. The RF transmitter is shown separately from the probe aggregate equipment when activated because of its high electrical dissipation and relatively small mass.

The results presented show that the passive thermal design selected is adequate to maintain the probe temperatures within limits. Trajectory uncertainties for entry are only 7 min for the nominal Jupiter mission and contribute to only slight initial descent probe temperature uncertainty. The biggest uncertainty in the thermal design is the performance of the multilayer insulation used to maintain the probe temperature during cruise and coast. Since the radioisotope heater output is constant, and cannot be changed during the mission, the multilayer insulation performance and repeatability will have to be accurately determined by full scale thermal tests before final design. For descent, the worst-case model atmosphere encountered was considered, and conservative foam insulation properties were assumed together with optimum heat transfer free convection inside the probe.

The probe temperature margins, predicted on the basis of probe thermal analysis for the nominal Jupiter mission are:

TEMPERATURE MARGIN	SPACECRAFT CRUISE PHASE, °K	PROBE COAST PHASE, °K	ENTRY-DESCENT PHASE, °K
Above Equipment Lower Limit	42	22	5
Below Equipment Upper Limit	8	23	17
Below Transmitter Upper Limit	NA	28	22

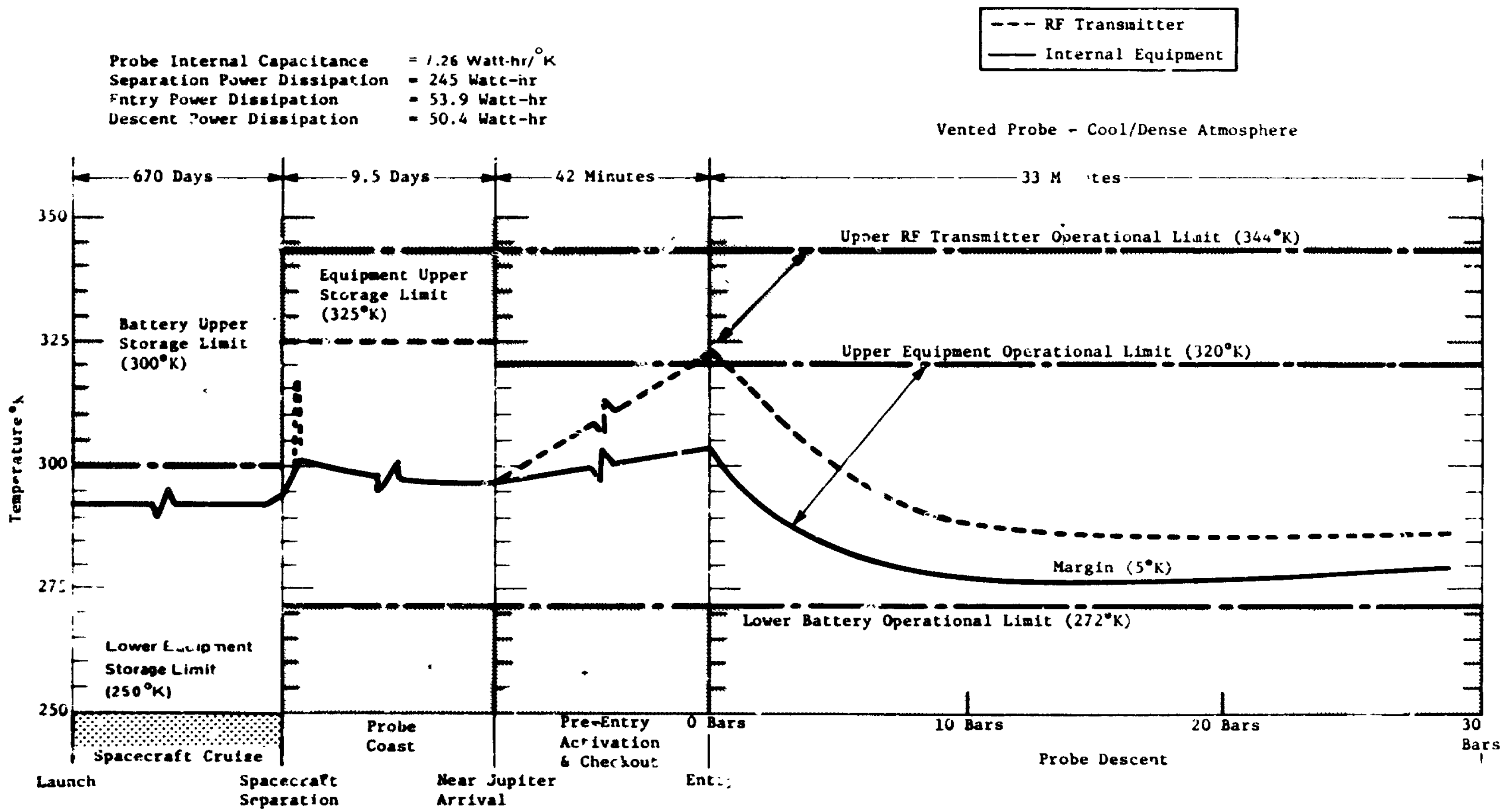

Figure II-20 Launch to Descent Thermal History of the Nominal Jupiter Probe

11. Probe to Spacecraft Integration

The integration of the planetary probe with a carrier spacecraft was performed using a Martin Marietta modified outer planet spacecraft (MOPS) as the carrier. The configuration of the spacecraft with the nominal Jupiter probe attached is shown in Figure II-21. The probe is mounted on the aft end (for launch) of the spacecraft, with the probe heat shield pointed away from the spacecraft, providing the proper probe orientation with respect to the spacecraft for later separation. The probe interfaces with the spacecraft in the following categories before separation from the spacecraft: structures and mechanical, power, thermal control, instrumentation.

The probe is attached to the spacecraft through a mechanical release joint incorporating a matched set of separation springs. The probe is held in place by means of attachments incorporating explosive nuts, which provide for release.

The interfaces of the probe with the spacecraft are discussed in Chapter V, Section B.11 of Vol II.

Probe Weight: 344 lb

Spacecraft Mod (MMC MOPS): 54 lb

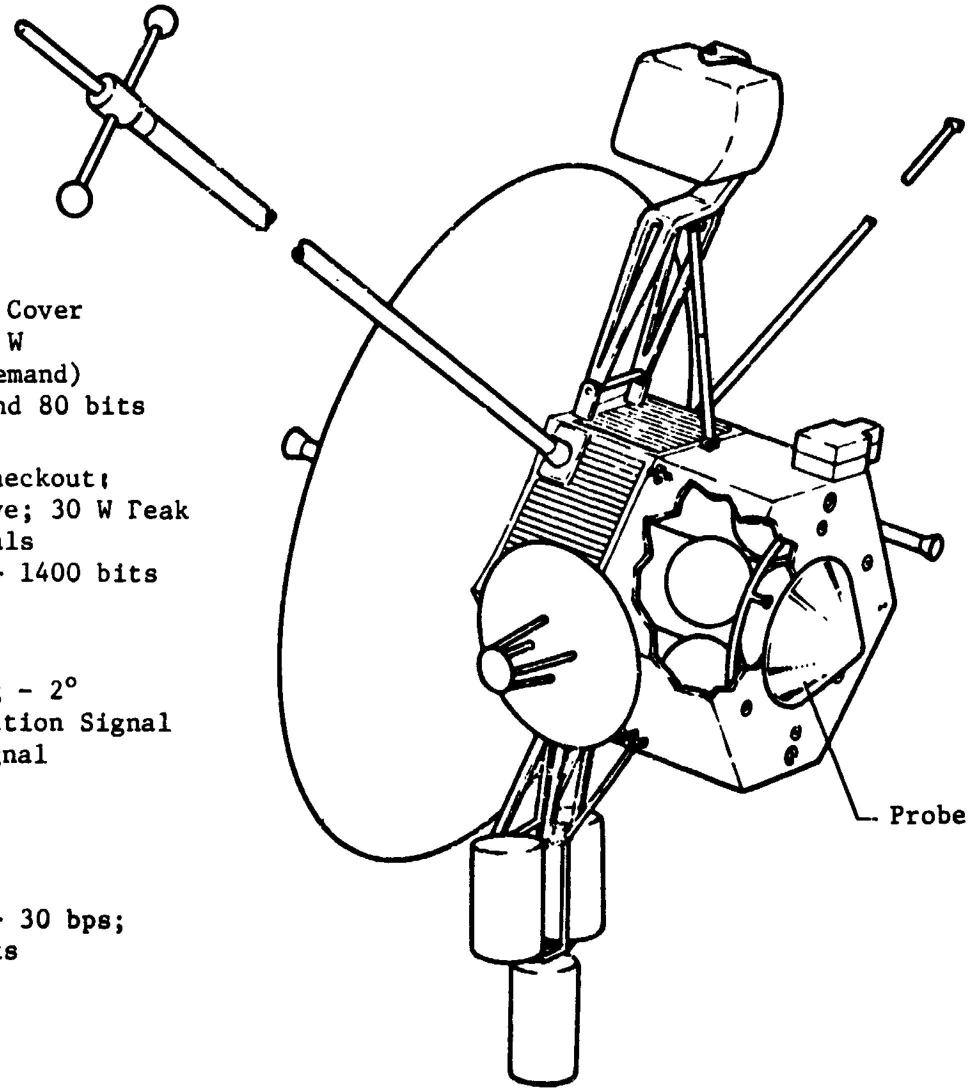

Cruise:
- Environmental Cover
- T/C Power - 5 W
- Monitor (on Demand)
  - 0.5 watts and 80 bits

Preseparation Checkout:
- Power - 8 W Ave; 30 W Peak
- Checkout Signals
- Data Monitor - 1400 bits

Separation:
- Probe Pointing - 2°
- Battery Activation Signal
- Separation Signal

Post-Separation:
- Track Probe
- Receive Data - 30 bps;
  - 60 to 80Kbits

Figure II-21 MOPS Spacecraft/Jupiter Probe Integration

D. JUPITER PROBE-DEDICATED ALTERNATIVE PROBE SYSTEM DEFINITION SUMMARY

The constraints for this alternative Jupiter probe were the result of the Jupiter parametrics discussed in Chapter II, Section C.1. In general, this configuration was intended to optimize the probe by reducing its complexity and the radiation field that it would encounter. The general constraints are:

Mission	Type I in 1979
Entry Angle	-15° (structures designed to -20°)
Entry Latitude	30°
Depth of Descent and Atmosphere	13 bars in cool/dense atmosphere and 7.5 bars in nominal atmosphere
Science	SAG exploratory payload (PAET)
Spacecraft	Mariner Family
Carrier Mode	Flyby
Periapsis Radius	2 R_J
Communication Mode	Relay
Deflection Mode	Spacecraft
Ejection Radius	30 x 10^6 km
Entry Ballistic Coefficient	0.65 slug/ft^2 (102 kg/m^2)
Descent Ballistic Coefficient	0.09 slug/ft^2 (14.1 kg/m^2)

1. Mission Definition

The probe-dedicated alternative mission is described in Figure II-22 and detailed in Table II-11. Important mission design results are summarized in this section.

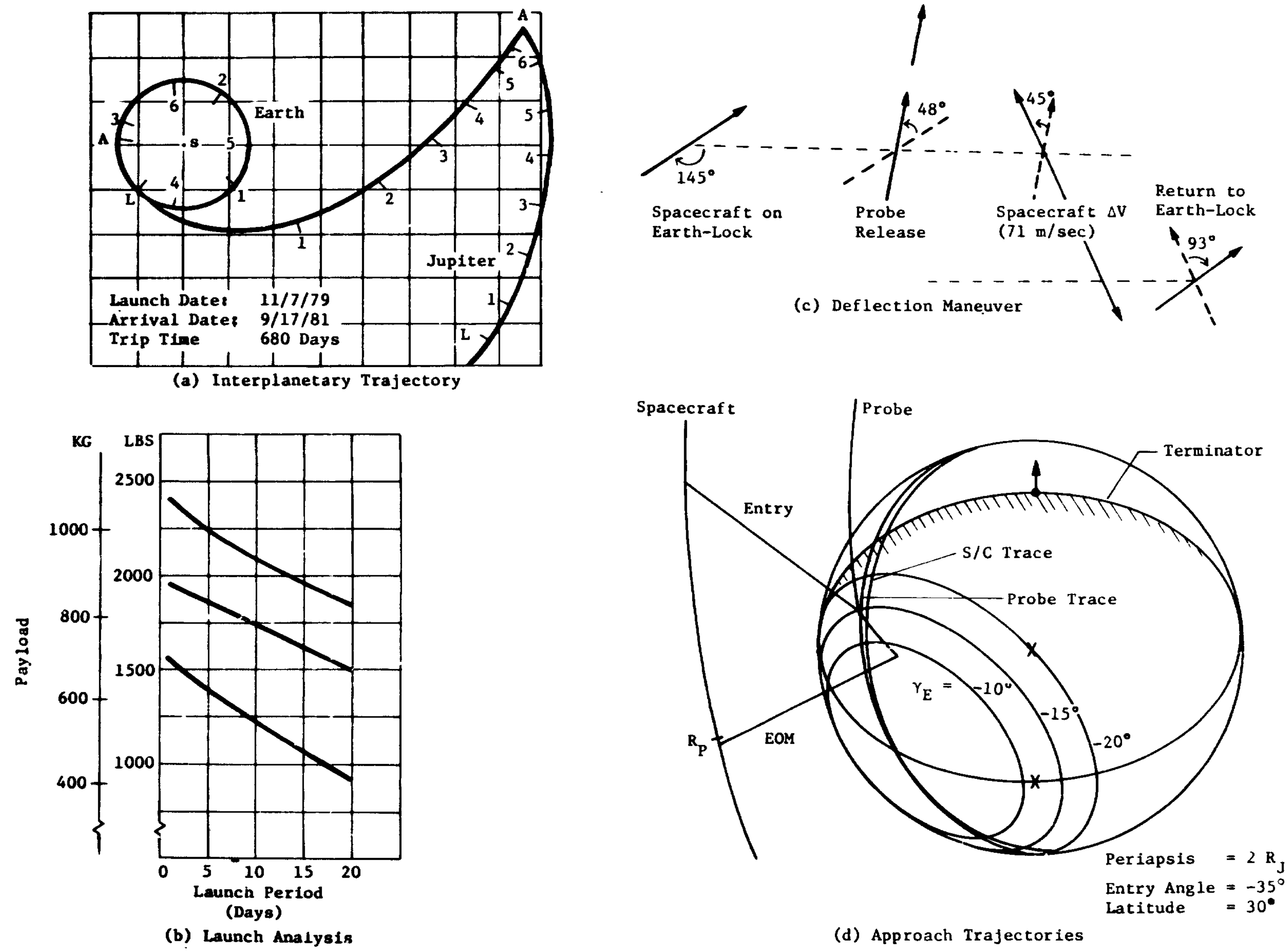

Figure II-22 Probe-Dedicated Alternative Mission Description

Table II-11 Probe-Dedicated Alternative Mission Description

a. Conic Trajectory Data

Interplanetary Trajectory	Launch Trajectory	Arrival Trajectory
Launch Date: 11/7/79 Arrival Date: 9/17/81 Flight Time: 680 days Central Angle: 155°	Nominal C_3: 93.6 km^2/sec^2 Nominal DLA: 30.5° Launch Window: 1.17 hr Parking Orbit Coast: 36 min C_3 (10 day): 97.5 km^2/sec^2 C_3 (20 day): 105 km^2/sec^2 Azimuth Range: 101.7° - 115°	VHP: 8.474 km/sec RA: 161.3° DEC: 6.81° ZAE: 145.2° ZAP: 141.4° RP: 2 R_J INC: 55°

b. Deflection Maneuver and Probe Conic

Deflection Maneuver	Probe Conic Definition
Deflection Mode: Spacecraft Deflection Radius: 30 x 10^6 km Coast Time: 34.5 days ΔV: 71 m/sec Application Angle: 108.6° Out-of-Plane Angle: 5.0° Rotation for Probe Release: +47.6° Probe Reorientation Angle: NA Spacecraft ΔV from Earth: +93.5°	Entry Angle: -15° Entry Latitude: 30.6° Entry Longitude: 109.9° Lead Time: 35.2 min Lead Angle: -12.0° Probe-Spacecraft Range (Entry): 88,287 km Probe Aspect Angle (Entry): 50.6° Probe Aspect Angle (Descent): 22° Probe Aspect Angle (EOM): 28.1°

c. Dispersion Analysis Summary

Naviation Uncertainties	Execution Errors (3σ)	Dispersions (3σ)
Type: R,$\dot{R}$/67 day-arc SMAA: 1576 km SMIA: 224 km β: 86° TOF: 122 sec	ΔV Proportionality: 1% ΔV Pointing: 2° Probe Orientation Pointing: 2°	Entry Angle: 0.3° Angle of Attack: 2.5° Down Range: 0.6° Cross Range: 0.2° Lead Angle: 4.4° Lead Time: 10 min Entry Time: 2.8 min

d. Entry and Descent Trajectory Summary

		Critical Events	
Entry Parameters	**Descent Parameters**	**Time from Entry**	**Altitudes above 1 atm**
Entry Velocity, km/sec: 60 **Entry Altitude, km: 304.6** **Entry B, slug/ft^2: 0.65** **kg/m^2: 102.1** **Entry Atmosphere:** **Cool/Dense** **Max Deceleration, g: 1650** **Max Dynamic Pressure,** **lb/ft^2: 2.1 x 10^4** **kg/m^2: 1.0 x 10^6**	**Descent Atmosphere:** **Cool/Dense** **EOM Pressure, bar: 30** **Descent B, slug/ft^2:** **slug/ft^2: 0.12** **kg/m^2: 18.84**	**g = 0.1, sec: 8.5** **Max g, sec: 18** **M = 0.7, sec: 44** **Descent Time, min:** **33.3** **EOM, min: 33.8**	**km: 189** **km: 66.8** **km: 33.4** **km: -85**

a. Interplanetary Trajectory Selection - The interplanetary trajectory is pictured in Figure II-22(a) with 100-day intervals noted. The launch date of November 7, 1979 and arrival date of September 17, 1981 (trip time of 680 days) result in a maximization of the payload weight as discussed in Volume II, Chapter IV, Section A. As indicated in the figure, the spacecraft arrives at Jupiter shortly before the view to Jupiter is obstructed by the Sun.

b. Launch Analysis - The launch analysis is provided in Figure II-22(b). Available payload is plotted against launch period for three sets of launch vehicle performance data: standard data for the Titan 5-Segment vehicle with and without Burner II plus updated data for the Burner II. For reference, the payload weight (probe, spacecraft, spacecraft modifications, and spacecraft-launch vehicle adaptor) is about 454 kg (1000 lb) for a Pioneer mission and 680 kg (1500 lb) for a Mariner mission. Thus, the Burner II option is necessary for a Mariner-type mission to obtain a 20-day launch period. The nominal launch window and parking orbit coast time are satisfactory.

c. Approach Trajectories - The probe trajectory for this mission was constrained to enter at an entry angle of -15° and an entry latitude of 30°. To satisfy this requirement, the probe trajectory must be inclined 50° to Jupiter's orbital plane. To establish an effective communication link, the spacecraft was deflected for a 55° inclination. The probe was released on the lower inclination trajectory so that during descent it would rotate through the trace of the spacecraft trajectory. The resulting trajectories are pictured in Figure II-22(d) and summarized in Tables II-11(a) and (b)

d. Deflection Maneuver - A spacecraft deflection maneuver was performed at 30 million km and 34.5 days from the planet. The ΔV required was 71 m/sec. The implementation sequence is illustrated in Figure II-22(c). The spacecraft rotates 48° off Earth lock to release the probe. It then rotates 45° further and fires a ΔV of 71 m/sec to achieve its desired flyby radius and communication geometry.

e. Dispersion Analysis - The navigation uncertainties are slightly larger in this mission than the previous mission because the deflection radius is slightly increased. Navigation uncertainties still have only a minor contribution to the final dispersions compared to the execution errors. The entry parameter dispersions are provided in Table II-11(b). These dispersions are based on the spacecraft deflection mode. For comparison, a probe deflection mode dispersion analysis was made for the identical conditions and resulted in dispersions (3σ) of entry angle 1.9°, angle of attack 2.8°, downrange 4.0°, crossrange 0.7°, lead angle 7.0°, lead time 10.0 min, and entry time 11.9 min. The communication parameter dispersions are given in the telecommunications subsection.

f. Entry and Descent - The entry latitude for the probe-dedicated mission is 30°, whereas the nominal mission has an equatorial entry. The effect of entering at a 30° latitude is to increase the g-load as well as the dynamic pressure by approximately 10%. All other critical parameters remain unchanged from the nominal mission. The nominal entry angle (chosen from science considerations) is -15°; however, to accommodate dispersions ($3\sigma \approx 5°$), a value of -20° is used to determine structural loads. The descent parameters are chosen from a combination of the cool/dense and nominal environments. The worst-case design results when the ballistic coefficient is based upon the nominal atmosphere and the resulting times and pressures determined from the cool/dense model. A summary of the entry and descent parameters is given in Table II-11(d).

2. Science

The instruments for the Jupiter alternative probe missions were to be selected from a consideration of the PAET vehicle, Viking, and discussions in the previous study. The temperature gage and accelerometer triad system is basically the same between Viking and PAET, thus no change is shown here from the nominal design. However, the pressure transducers on PAET were chosen because they are significantly smaller in size and slightly lighter in weight. The mass spectrometer on PAET used a quadrupole analyzer, which for a limited range of 1-40 amu, appears to allow packaging into a smaller volume and has a lighter weight than the magnetic sector instrument. The porous leak inlet system is the same as for the nominal mission. However, since the design pressure level is only 13 bars, a ballast volume of only 0.5 liter is required.

The alternative Jupiter probe analysis considered both the cool/dense and the nominal model atmospheres. The probe is therefore designed for worst-case atmosphere conditions. The worst-case design is the nominal parameters are:

Design pressure limit = 13 bars (C/D atmosphere)

Main Parachute Ballistic Coefficient = 0.09 slug/ft^2 (14.13 kg/m^2)

Parachute deployment pressure = 92 millibars (C/D)
or = 86 millibars (nominal)

Pressure at first measurement = 111 millibars (C/D)
or = 96 millibars (nominal)

No secondary parachute necessary

Entry time = 44 sec

Descent time = 35 min, 30 sec

Instrument sampling time [intervals]:

- Temperature and pressure = 3.5 sec
- Neutral mass spectrometer = 40 sec
- Descent accelerometers = 10 sec
- Entry accelerometers = 0.1/0.2 sec

Total bit rate = 30.4 bps

All performance criteria were satisfied. Figure II-23 shows the selected pressure descent profile for both atmospheres.

3. System Integration

The functional sequence for this probe is more abbreviated than for the other probes defined in the study. The separation phase lasts approximately 4 minutes to spin up to 5 rpm; then the probe is powered down until pre-entry. The detailed sequence is included in Volume II, Chapter V, Section C.3. The data profile and power profile are shown in Figures II-24 and II-25. From these figures it is noted that the power is nominal and the data collected is less than for the other configurations. This probe does not have a delta-velocity requirement and the ACS is a very simple definition. This "simple" probe, therefore, has a lighter weight than all the others: 127 kg (280 lb) ejected weight.

4. Telecommunications Subsystem

The Jupiter probe-dedicated-mission at 2 R_J is very similar to the nominal mission as far as the trajectory and communications geometry are concerned. The probe aspect angle is 60° at acquisition and was optimized to be a minimum during descent. The uncertainty ellipses representing probe dispersions are the most tilted, but variations in cone angle are about the same as for other missions. A 55° beamwidth spacecraft helical antenna provides sufficient gain at the points of maximum dispersion and a position search is not required. The telecommunications definition is included in Table II-12.

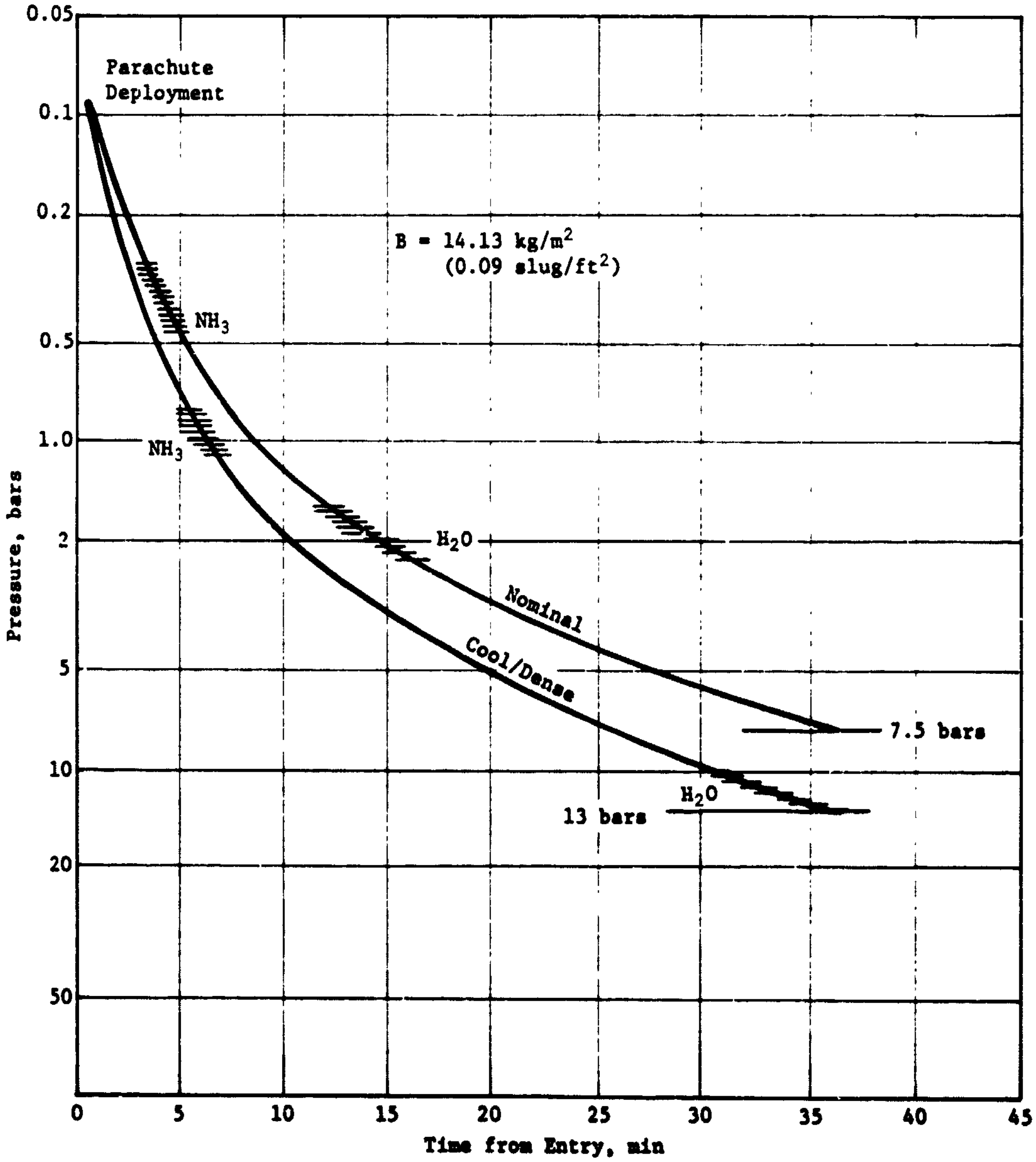

Figure II-23 Alternative Jupiter Probe Pressure Descent Profile

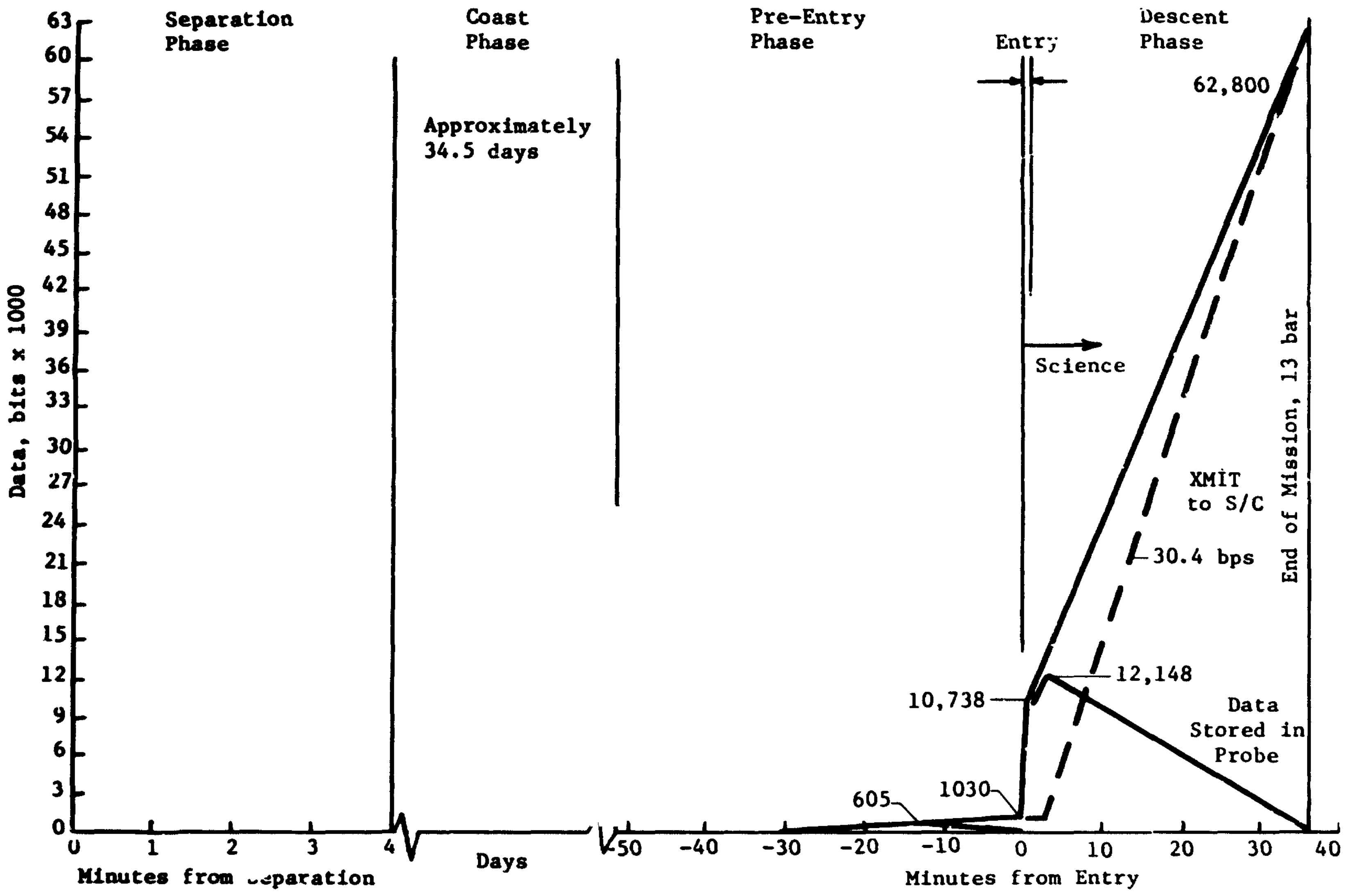

Figure II-24 Data Profile for the Probe-Dedicated Jupiter Mission

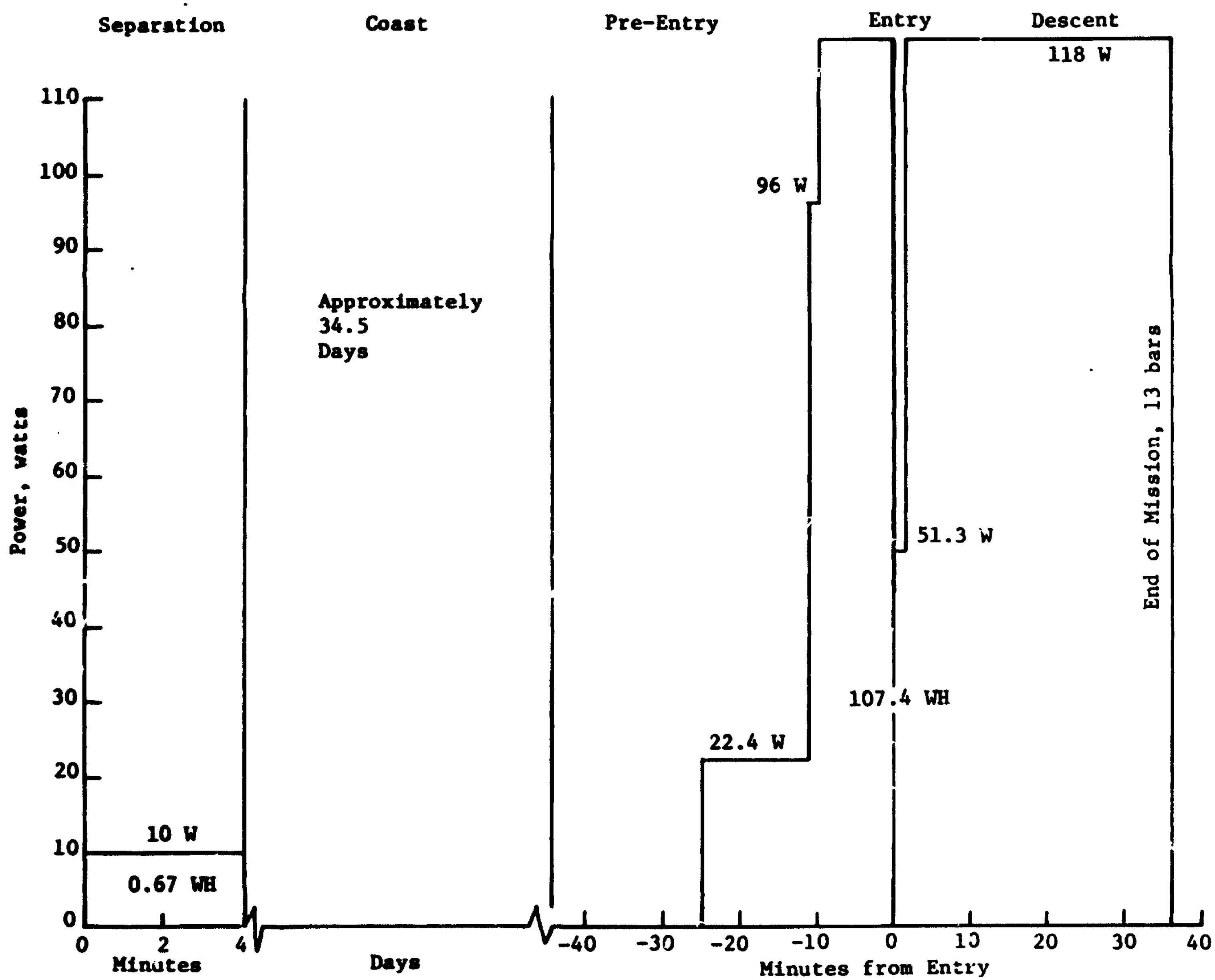

Figure II-25 Power Profile for Probe-Dedicated Jupiter Mission

Table II-12 Telecommunications RF Subsystem for the Probe-Dedicated Mission

CONDITIONS: Planet: Jupiter S/C: Mariner Frequency: 0.86 GHz
Bit Rate: 30 bps

Component	Characteristic	Unit	Value
Transmitter	RF Power Out	W	30
	Overall Efficiency	%	45
	DC Power-In at 28 V dc	W	66.7
	Total Weight	kg	2.7
	Total Weight	lb	6.0
RF Switch	Type		Mechanical
	Insertion Loss	dB	0.3
	Weight	kg	0.23
	Weight	lb	0.5
Entry Antenna	Type		Annular Slot
	Main Beam Angle	deg	60
	Beamwidth	deg	40
	Max Gain	dB	5.2
	Diameter	cm	43
		in.	17
	Weight	kg	2.1
		lb	4.7
Descent Antenna	Type		Turnstile/Cone
	Main Beam Angle	deg	0
	Beamwidth	deg	120
	Max Gain	dB	5
	Size (diameter x h)	cm	20.3 x 7.6
		in.	8 x 3
	Weight	kg	0.45
		lb	1.0
Spacecraft Antenna	Type		Helix
	Beamwidth	deg	55
	Max Gain	dB	9.6
	Size (diameter x l)	cm	29.6 x 11.1
		in.	11.7 x 4.4
	Weight	kg	1.36
		lb	3.0
	Despin		no
	Position Search		none
	Frequency Acquisition	sec	65
	Clock Angle, θ	deg	-56
	Cone Angle, ϕ	deg	67
Spacecraft Receiver	Noise Temperature	°K	300
	Noise Figure	dB	3.1
	DC Power-In at 28V dc	W	3.0
	Weight	kg	0.9
		lb	2.0

An analysis was performed to determine the effects of increased system noise temperature resulting from the flyby trajectory of the spacecraft intersecting the Jovian magnetosphere. The increase in antenna noise temperature during pre-entry maneuvers was only 59°K, and therefore was negligible.

5. Data Handling Subsystem

The configuration and functions of the data handling subsystem are essentially unchanged from the nominal Jupiter probe. Refer to Volume II Chapter V, Sections A.5., B.5. and Volume III, Appendix H. The physical and electrical characteristics are:

Size: 2580 cm^3 (158 $in.^3$); Weight: 2.6 kg (5.7 lb);
Power: 18.9 W.

6. Power and Pyrotechnics Subsystem

The post-separation power subsystem is reduced to a short active life battery bus distribution for this mission. The entry/descent configuration and functions are essentially unchanged from the nominal Jupiter probe. Refer to Volume II, Chapter V, Sections A.6., G.6., and Volume III, Appendix G. The physical characteristics are:

Size 2620 cm^3 (160 $in.^3$); Weight: 6.1 kg (13.4 lb).

7. Attitude Control Subsystem

The attitude control subsystem is reduced to an open-loop spinup (0.5 rad/sec) for this mission. A discussion of the analysis is contained in Volume II, Chapter V, Section C.7. and Volume III, Appendix F.

8. Structural and Mechanical

The probe-dedicated alternative Jupiter probe is a substantially simpler probe than the nominal Jupiter probe. For this mission, the spacecraft provides the deflection delta velocity maneuver. It leaves the probe in the proper attitude and with the proper trajectory for planetary entry at the time of separation. Thus, the probe does not need a deflection delta velocity motor nor does it need to be spun up to a spin rate of 10.5 rad/sec (100 rpm) to stabilize the probe for firing of the deflection motor and for precession. Instead, the probe needs only to be spun up to 0.52 rad/sec (5 rpm) to stabilize its attitude at separation and eliminate drift before planetary entry. The probe has no service module.

The configuration of the probe is shown in Figure II-26. The ejected probe is 1.005 m (39.6 in.) in diameter, 0.604 m (23.8 in.) long, and weights 126.99 kg (279.96 lbm). Since there is no service module, the ejected probe and entry probe are basically the same. The descent probe is 0.439 m (17.3 in.) in diameter, 0.492 m (19.4 in.) long, and weighs 42.36 kg (93.41 lbm).

A single stage of parachute descent is satisfactory for this probe, which is required to descend only to 13 bars to satisfy mission requirements. The selected descent ballistic coefficient of 14.1 kg/m^2 (0.09 $slug/ft^2$) for a descent probe weighing 42.36 kg (93.41 lbm) results in a parachute size of 2.59 m (8.5 ft) diameter.

This probe enters the planet at a latitude of 30° as compared with essentially equatorial latitude for the nominal probe. This change in entry latitude, plus the relocation of probe components from the service module (which is deleted) to the entry probe results in a fairly large heat shield and aeroshell. The heat shield mass fraction for this configuration is 0.350, resulting in a heat shield weight of 38.7 kg (85.4 lbm).

The probe basic structure is identical with the nominal Jupiter probe. The probe is designed by the structural loadings encountered during entry at an entry angle of 20°, at a latitude of 30°, with an entry ballistic coefficient of 102 kg/m^2 (0.65 $slug/ft^2$). These loadings are 1650 g peak and a maximum dynamic pressure of 1.1×10^6 N/m^2 (23,000 lbf/ft^2).

9. Propulsion Subsystem

This probe has no deflection delta velocity motor, but does have a minimal attitude stabilization system, weighing 1.5 kg (3.31 lbm). The proper entry trajectory and pointing attitude is provided by the spacecraft before probe separation for this configuration. Thus, the ACS system need only provide a probe spinup to 5 rpm to stabilize the pointing orientation during the pre-entry coast phase of flight.

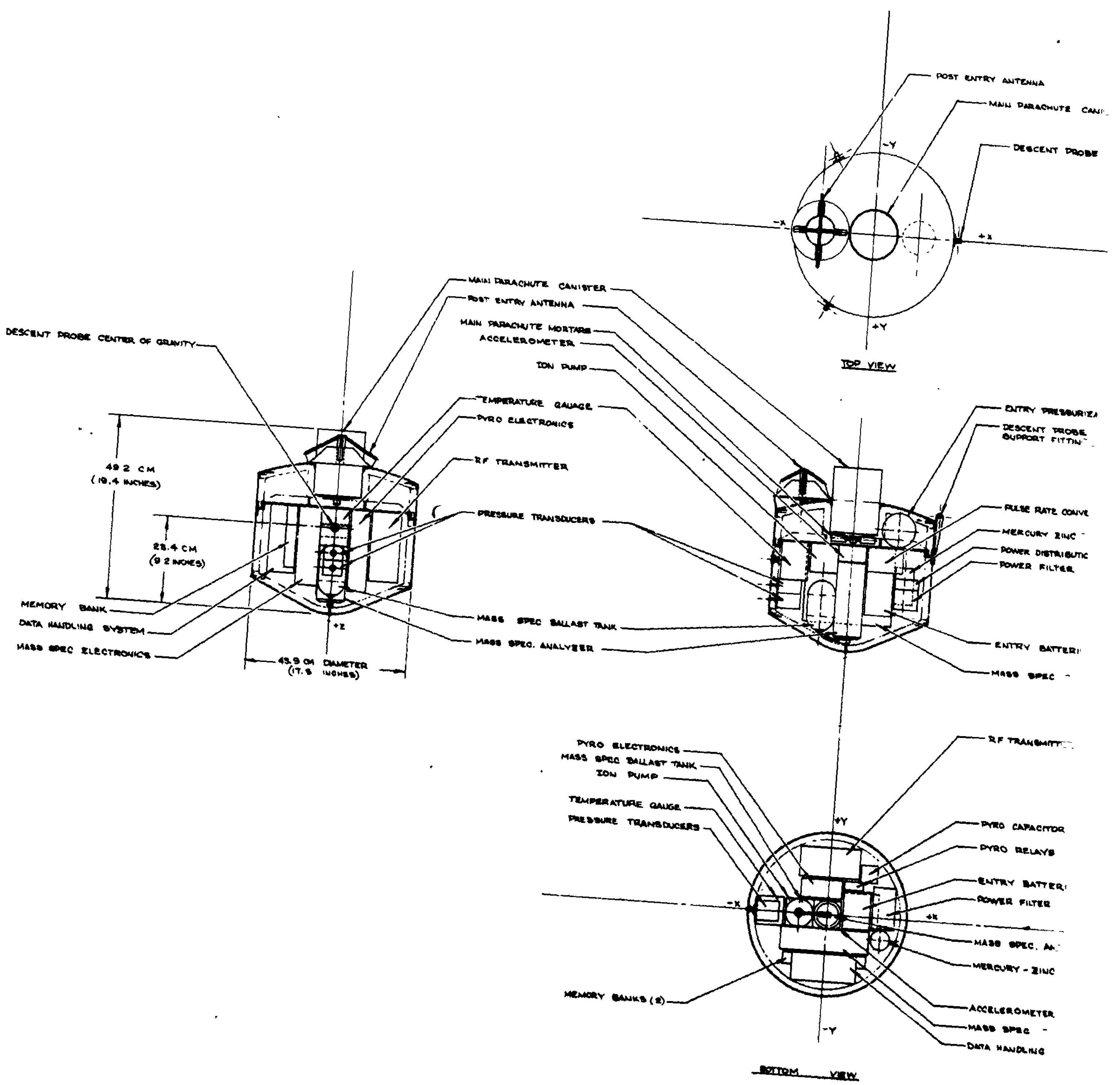
POST ENTRY ANTENNA
DESCENT PROBE
TOP VIEW
MAIN PARACHUTE CANISTER
POST ENTRY ANTENNA
MAIN PARACHUTE MORTARS
ACCELEROMETER
ION PUMP
DESCENT PROBE CENTER OF GRAVITY
TEMPERATURE GAUGE
PYRO ELECTRONICS
RF TRANSMITTER
PRESSURE TRANSDUCERS
49.2 CM
(19.4 INCHES)
23.4 CM
(9.2 INCHES)
MEMORY BANK
DATA HANDLING SYSTEM
MASS SPEC ELECTRONICS
MASS SPEC BALLAST TANK
MASS SPEC. ANALYZER
43.9 CM DIAMETER
(17.3 INCHES)
PYRO ELECTRONICS
MASS SPEC BALLAST TANK
ION PUMP
TEMPERATURE GAUGE
PRESSURE TRANSDUCERS
MEMORY BANKS (2)
PYRO CAPACITOR
PYRO RELAYS
POWER FILTER
ACCELEROMETER
BOTTOM VIEW

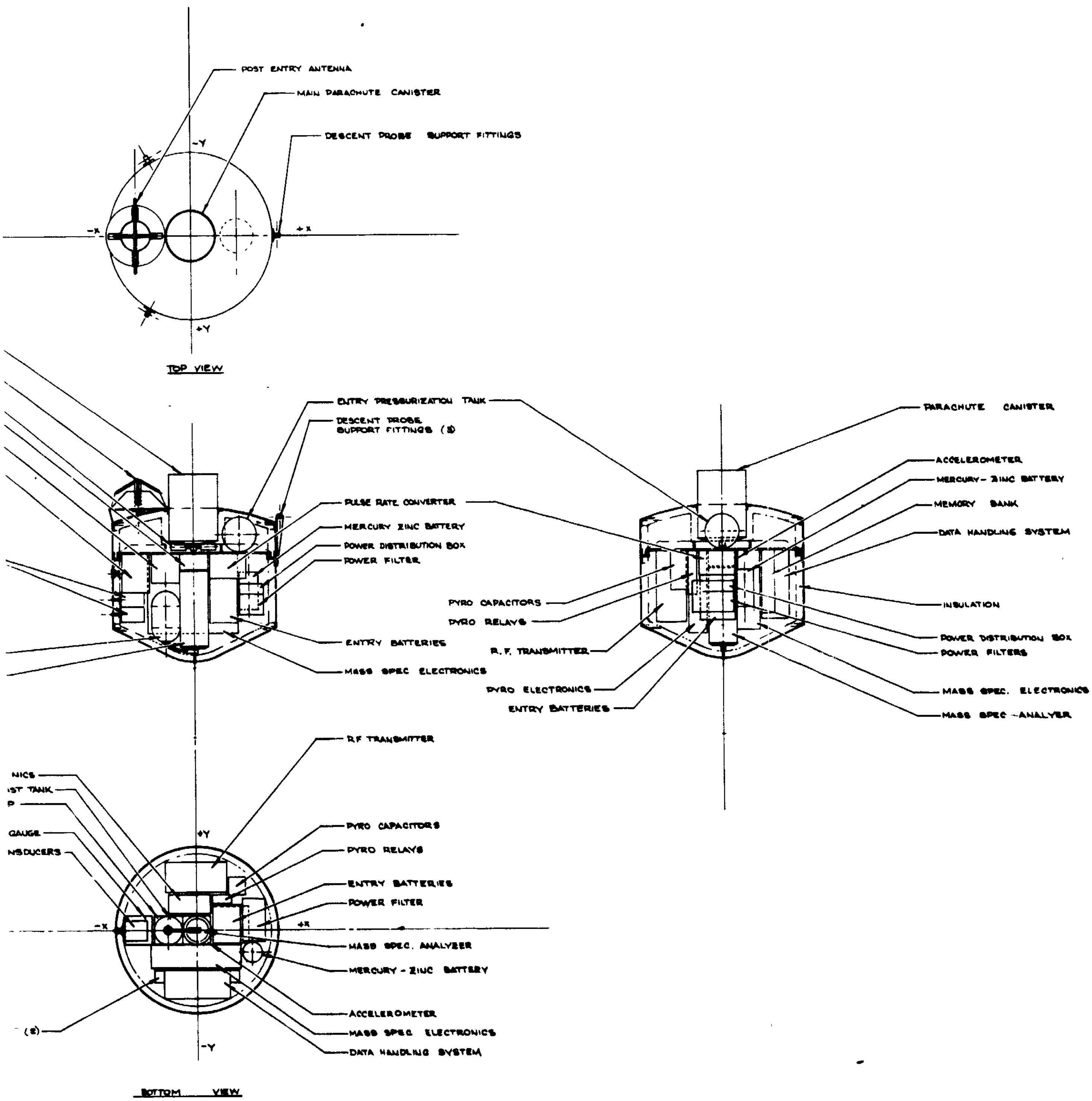
POST ENTRY ANTENNA
MAIN PARACHUTE CANISTER
DESCENT PROBE SUPPORT FITTINGS
-Y
-X
+X
+Y
TOP VIEW
ENTRY PRESSURIZATION TANK
DESCENT PROBE SUPPORT FITTINGS (3)
PULSE RATE CONVERTER
MERCURY ZINC BATTERY
POWER DISTRIBUTION BOX
POWER FILTER
ENTRY BATTERIES
MASS SPEC ELECTRONICS
PARACHUTE CANISTER
ACCELEROMETER
MERCURY- ZINC BATTERY
MEMORY BANK
DATA HANDLING SYSTEM
INSULATION
POWER DISTRIBUTION BOX
POWER FILTERS
MASS SPEC. ELECTRONICS
MASS SPEC - ANALYZER
PYRO CAPACITORS
PYRO RELAYS
R. F. TRANSMITTER
PYRO ELECTRONICS
ENTRY BATTERIES
R.F TRANSMITTER
NICS
IST TANK
P
GAUGE
NSDUCERS
PYRO CAPACITORS
PYRO RELAYS
ENTRY BATTERIES
POWER FILTER
MASS SPEC. ANALYZER
MERCURY - ZINC BATTERY
ACCELEROMETER
MASS SPEC ELECTRONICS
DATA HANDLING SYSTEM
(3)
BOTTOM VIEW

IUTE CANISTER

LEROMETER
RY-ZINC BATTERY
Y BANK
HANDLING SYSTEM

ILATION

DISTRIBUTION BOX
FILTERS

SPEC. ELECTRONICS
SPEC ANALYZER

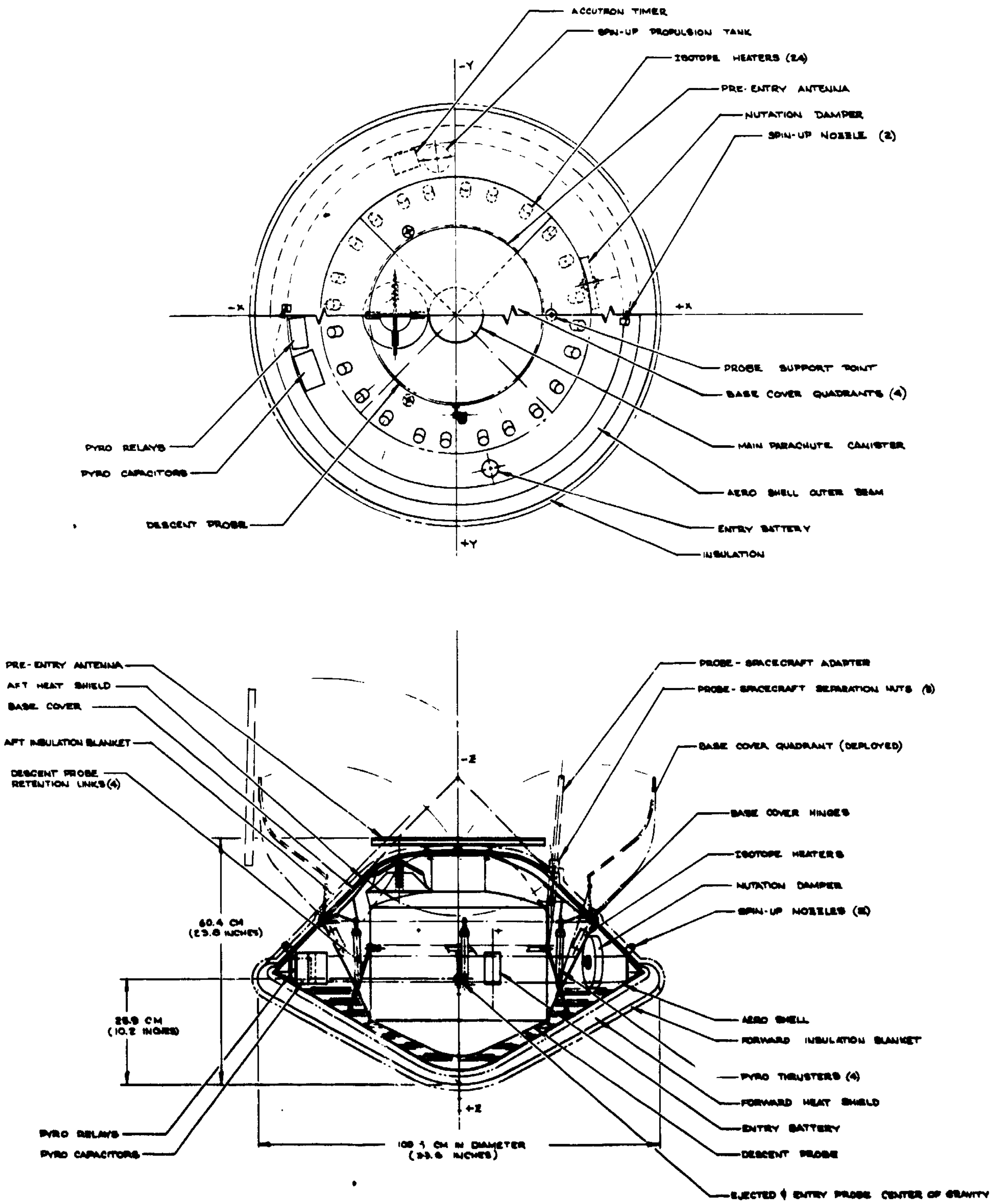

Figure II-26 Alternative Jupi

FOLDOUT FRAME 3

F

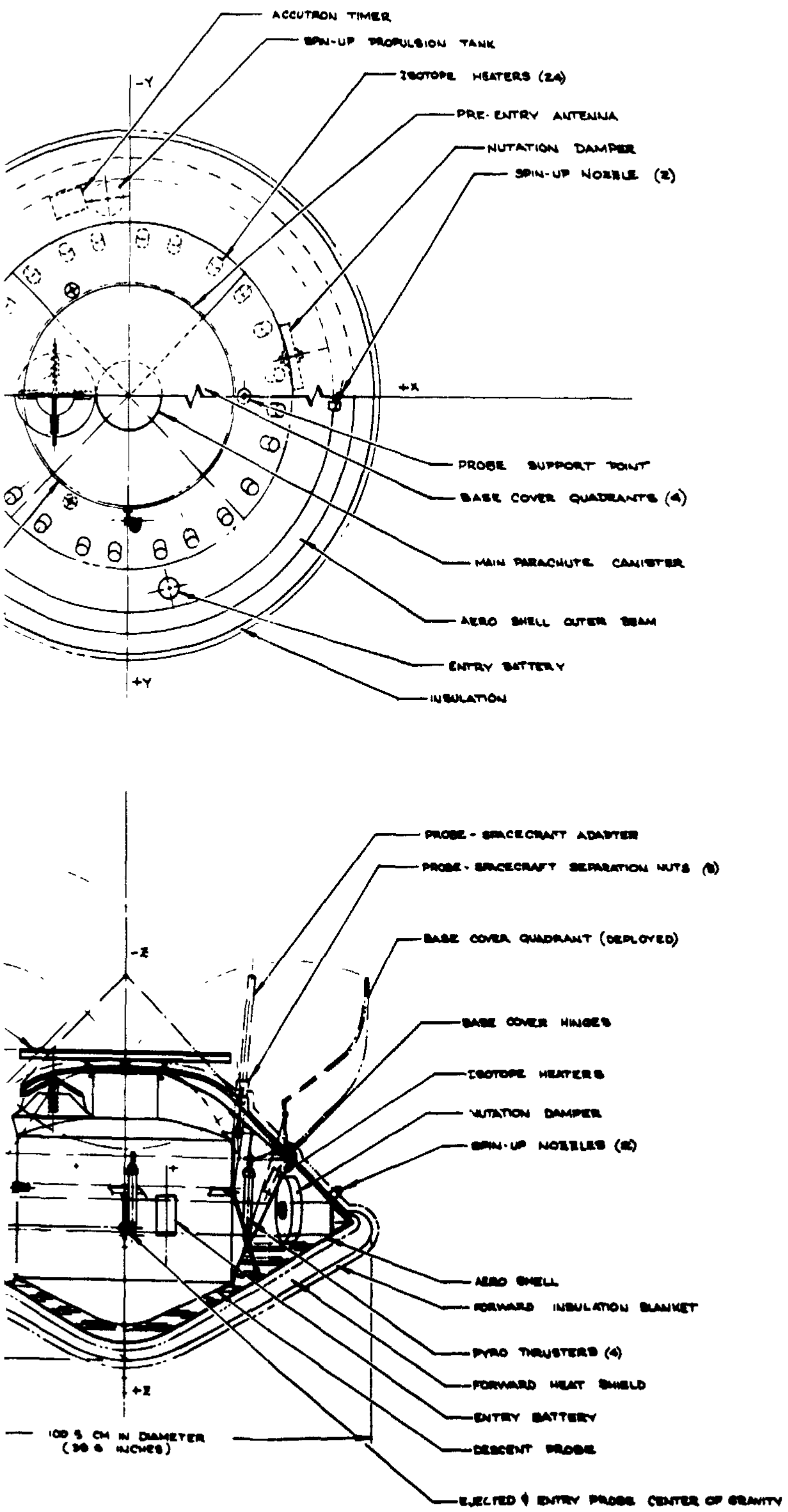

JUPITER SURVIVABLE PROBE -
OUTER PLANET ENTRY PROBE STUDY

Figure II-26 Alternative Jupiter Probe Dedicated Mission Configuration

FOLDOUT FRAME 4

10. Thermal Control Subsystem

Thermal control for the probe-dedicated mission probe is required to maintain the probe equipment within acceptable temperature limits. The thermal design concept is basically the same as the nominal Jupiter probe mission. Multilayer insulation, thermal coatings, and radioisotope heaters are used during spacecraft cruise and probe coast, and probe thermal inertia coupled with low density foam insulation is used for entry and descent. For the probe-dedicated alternative mission, the minimum temperature predicted during descent was marginal (3°K margin) and two improved probe thermal designs were therefore investigated. On the basis of those investigations, the addition of nitrogen gas environmental control was included for descent thermal control. For this design, the probe would be purged and sealed with one bar dry nitrogen gas at launch and equipped with a nitrogen gas supply bottle capable of charging the probe volume an additional 2.5 bars during descent. The delta weight and volume added by the N_2 gas supply is approximately 0.41 kg (1.1 lb) and 0.35 liters based on a storage pressure 250 bars.

As before, the pivotal temperature for thermal design was the probe temperature at the end of the mission coast phase, which determines the probe entry temperature for descent. Although the probe-dedicated mission considered either a cool/dense or nominal atmosphere encounter and descent, the primary thermal problem remains one of losing too much thermal energy to the atmosphere environment during the cool/dense descent. The probe coast and entry temperatures, therefore, were increased for this mission by using a higher α/ϵ thermal coating on the probe and absorbing a higher percentage of the solar energy during coast. Since the coast time is longer for this mission (34.5 days), the transient temperature effects following spacecraft separation were of no consequence.

Analytical results show that improved thermal design is obtained by using the N_2 gas environmental thermal control concept. The probe temperature margins predicted on the basis of thermal analysis for the probe-dedicated Jupiter mission are tabulated.

			Entry-Descent Phase	
Temperature Martin	Spacecraft Cruise Phase, °K	Probe Coast Phase, °K	Nominal Design, °K	Improved N_2 Design, °K
Above Equipment Lower Limit	37	23	3	19
Below Equipment Upper Limit	13	19	15	12
Below Transmitter Upper Limit	NA	NA	29	28

Typical probe thermal history and temperature limits are shown in the discussion for the nominal Jupiter probe.

11. Probe to Spacecraft Integration

The probe-dedicated alternative Jupiter probe integration with the spacecraft is essentially the same as that described for the nominal Jupiter probe.

E. JUPITER SPACECRAFT-RADIATION-COMPATIBLE ALTERNATIVE PROBE SYSTEM DEFINITION SUMMARY

As was done for the other alternative Jupiter probe discussed in Chapter II Section C.3, the constraints for this probe were the results of the Jupiter parametrics discussed in Chapter II, Section C.1. Compared to the other alternative Jupiter Probe, this probe provides the deflection, the encounter is essentially equatorial and the periapsis radius minimizes the radiation environment for the spacecraft. These constraints are:

Mission	Type I in 1979
Entry Angle	-15° (structures design to -20°)
Entry Latitude	5°
Periapsis Radius	6 R_J
Deflection Mode	Probe

All other constraints are the same as for the other alternative Jupiter probe.

Mission Definition

The radiation-compatible probe mission is described in Figure II-27 and detailed in Table II-13. Important mission design results are summarized in this section.

a. Interplanetary Trajectory Selection - The interplanetary trajectory is pictured in Figure II-27(a) with 100-day interval noted. The launch date of November 7, 1979 and arrival date of September 17, 1981 (trip time of 680 days) result in a maximization of the payload weight as discussed in Volume II, Chapter IV, Section A. As indicated in the figure, the spacecraft arrives at Jupiter shortly before the view to Jupiter is obstructed by the Sun.

b. Launch Analysis - The launch analysis is provided in Figure II-27(b). Available payload is plotted against launch period for three sets of launch vehicle performance data: standard data for the Titan 5-Segment vehicle with and without Burner II, plus updated data for the Burner II combination. For reference, the payload weight (probe, spacecraft, spacecraft modifications, and spacecraft launch vehicle adaptor) is about 454 kg (1000 lb) for a Pioneer mission and 680 kg (1500 lb) for a Mariner mission. Thus, the Burner II option is necessary for Mariner-type mission to obtain a 20-day launch period. The nominal launch trajectory summarized in Table II-13(a) indicates that the daily launch window and parking orbit coast time are satisfactory.

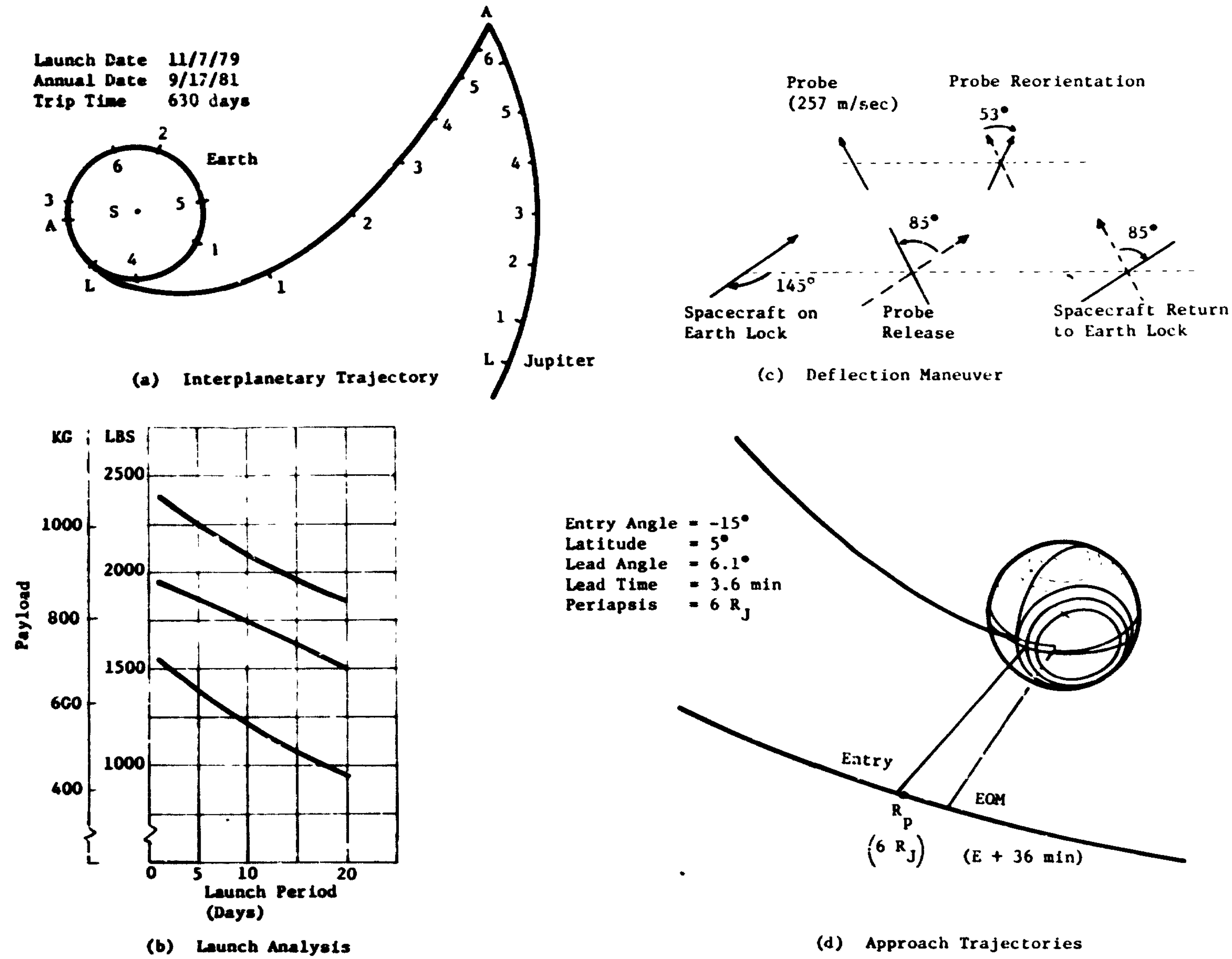

Figure II-27 Radiation-Compatible Alternative Mission Definition

Table II-13 Radiation-Compatible Alternative Mission Summary

a. Conic Trajectory Data

Interplanetary Trajectory	Launch Trajectory	Arrival Trajectory
Launch Date: 11/7/79 Arrival Date: 9/17/81 Flight Time: 680 days Central Angle: 155°	Nominal C_3: 93.6 km^2/sec^2 Nominal DLA: 30.5° Launch Window: 1.17 hr Parking Orbit Coast: 36 min C_3 (10 day): 97.5 km^2/sec^2 C_3 (20 day): 105 km^2/sec^2 Azimuth Range: 101.7° - 115°	VHP: 8.474 km/sec RA: 161.3° DEC: 6.8° ZAE: 145.2° ZAP: 141.4° RP: R. INC: 5°

b. Deflection Maneuver and Probe Conic

Deflection Maneuver	Probe Conic Definition
Deflection Mode: Probe Deflection Radius: 30 x 10^6 km Coast Time: 35.1 days ΔV: 257 m/sec Application Angle: 119° Out-of-Plane Angle: 0° Rotation for Probe Release: 85° Probe Reorientation Angle: -53° Spacecraft ΔV from Earth: NA	Entry Angle: -15° Entry Latitude: 5.10 Entry Longitude: 98.8 Lead Time: 3.55 min Lead Angle: 6.11° Probe-Spacecraft Range (Entry): 357,422 km Probe Aspect Angle (Entry): 78.4° Probe Aspect Angle (Descent): 7.3° Probe Aspect Angle (EOM): 4.7°

c. Dispersion Analysis Summary

Naviation Uncertainties	Execution Errors (3σ)	Dispersions (3σ)
Type: Range-Doppler 167-day arc SMAA: 1576 km SMIA: 224 km β: 86° TOF: 122 sec	ΔV Proportionality: 1% ΔV Pointing: 2° Probe Orientation Pointing: 2°	Entry Angle: 6.02° Angle of Attack: 5.60° Down Range: 11.46° Cross Range: 2.00° Lead Angle: 6.91° Lead Time: 37.4 min Entry Time: 38.4 min

d. Entry and Descent Trajectory Summary

		Critical Events	
Entry Parameters	Descent Parameters	Time from Entry	Altitudes above 1 atm
Entry Velocity, km/sec: 60 Entry Altitude, km: 304.6 Entry B, slug/ft^2: 0.65 kg/m^2: 102.1 Entry Atmosphere: Cool/Dense Max Deceleration, g: 1500 Max Dynamic Pressure, lb/ft^2: 2.1 x 10^4 kg/m^2: 1.0 x 10^6	Descent Atmosphere: Cool/Dense EOM Pressure, bar: 13 Descent B, slug/ft^2: 0.09 kg/m^2: 14.13	g = 0.1, sec: 8.5 Max g, sec: 18 M = 0.7, sec: 44 Descent Time, min: 35.6 EOM, min: 36.1	km: 189 km: 66.8 km: 33.4 km: -57.5

c. Approach Trajectory - The approach trajectory is pictured in Figure II-27(d) and summarized in Table II-13(b). The spacecraft flyby radius was selected to be 6 R_J to limit radiation damage to the spacecraft. Since a low inclination probe trajectory was selected (entry latitude of 5°) an in-plane deflection maneuver was used. The spacecraft initially leads the probe, but because of Jupiter's rapid rotation rate the probe quickly overtakes the spacecraft. The probe aspect angle at the start of descent is 7.3°, passes nearly through zero, and ends at 10° at the end of the mission.

d. Deflection Maneuver - A probe deflection maneuver is used in this mission at a deflection radius of 30 million km or 35.1 days from Jupiter. The deflection sequence is illustrated in Figure II-27(c). For comparison, a deflection maneuver was targeted at 50 million km. This resulted in a coast time of 61.4 days and a ΔV of 152 m/sec to establish the same conditions at entry.

e. Navigation and Dispersions - The navigation and dispersion results are pictured in Table II-13(c). Standard Doppler and range tracking is all that is assumed since navigation dispersions are not significant at Jupiter. The entry dispersions are large relative to the other missions with 3σ dispersions in entry angle of 6.0°, angle of attack 5.6°, and entry time 38.4 min. For comparison, the deflection at 50 million km resulted in dispersions of 5.8°, 5.5°, and 40.8 min, respectively.

f. Entry and Descent Trajectories - Table II-13(d) summarizes the entry and descent phases of the mission. The cool/dense atmosphere model is used for both phases for this mission. The entry phase starts at 304.6 km above the 1 atm pressure level and ends at the staging of the aeroshell 34 sec later. During this phase, the peak deceleration of 1500 g is attained. The descent phase starts after staging and lasts until the end of mission at 13 bars. The total mission time (entry and descent) is 36.1 min.

2. Science

The major differences between the two alternative probes involves spacecraft/probe functional trades and the entry and descent profile and measurement performance is identical. Thus, the description given for the other alternative Jupiter probe describes the functions for this alternative Jupiter probe design.

3. System Integration

The functional sequence is similar to that for the nominal Jupiter probe. The main difference involves the ejection of the service module. The pre-entry antenna, for this configuration, is ejected along with the service module. At this time, the transmitter is turned off and engineering data is stored until after entry. A detailed sequence is included in Volume II, Chapter V, Section D.3. The power profile and data profile are similar to those for the nominal Jupiter probe except in the areas just mentioned above for the service module ejection. The entry uncertainty of approximately 38 min causes the pre-entry activities to occur earlier than for the nominal Jupiter probe. Weights for this configuration are: ejected weight 166 kg; entry weight 110 kg; descent weight 47 kg.

4. Telecommunications Subsystem

The point design for a 6 R_J mission performed during the parametric studies of Chapter II, Section H.2 was used as a basis for the radiation-compatible mission. The trajectory is identical in R_P, R_{EJ}, γ_E, and latitude to point design 8 described in Section H.2.d. The descent depth has been raised to 13 bars in lieu of the 30 bars previously used, and the bit rate is increased to 30 bps. Probe dispersions were similar to the dispersions for that point design. As a result, a two-position sector search technique was also used for this configuration to keep the RF power requirements within reasonable limits. The characteristics for the telecommunications subsystem are presented in Table II-14.

5. Data Handling Subsystem

The configuration and functions of the DHS are unchanged from the nominal Jupiter probe. Refer to Section C.5 of this chapter.

6. Power and Pyrotechnic Subsystem

The configuration and functions of the power and pyrotechnic subsystem are unchanged from the nominal Jupiter probe. Refer to Section C.6 of this chapter.

7. Attitude Control Subsystem

The configuration and functions of the attitude control subsystem are unchanged from the nominal Jupiter probe. Refer to Section C.7 of this chapter.

Table II-14 Telecommunications RF Subsystem for the Spacecraft-Radiation-Compatible Jupiter Mission

CONDITIONS: Planet: Jupiter S/C: Mariner Frequency: 0.86 GHz Bit Rate: 30 bps

COMPONENT	CHARACTERISTIC	UNIT	VALUE
Transmitter	RF Power Out	W	55
	Overall Efficiency	%	45
	DC Power-In at 28 V dc	W	122
	Total Weight	kg	2.72
	lb	lb	6.0
RF Switch	Type		Mechanical
	Insertion Loss	dB	0.3
	Weight	kg	0.45
		lb	1.0
Entry Antenna	Type		Annular Slot
	Main Beam Angle	deg	85
	Beamwidth	deg	40
	Maximum Gain	dB	5.2
	Diameter	cm	43
		in.	17
	Weight	kg	2.1
		lb	4.7
Descent Antenna	Type		Turnstile/Cone
	Main Beam Angle	deg	0
	Beamwidth	deg	120
	Maximum Gain	dB	5.0
	Size (diameter x h)	cm	20.3 x 7.5
		in.	8 x 3
	Weight	kg	0.45
		lb	1.0
Spacecraft Antenna	Type		Parabolic Dish
	Beamwidth	deg	20
	Maximum Gain	dB	18.3
	Size	cm	128
		in.	50.5
	Weight	kg	4.54
		lb	10.0
	Despin		No
	Position Search		2
	Frequency Acquisition	sec	50
	Clock Angle, '	deg	-101
	Cone Angle, :	deg	59 and 79
Spacecraft Receiver	Noise Temperature	°K	300
	Noise Figure	dB	3.1
	DC Power-In at 28 V dc	W	3.0
	Weight	kg	0.9
		lb	2.0

8. Structures and Mechanical Subsystem

The spacecraft-radiation-compatible Jupiter probe is very similar in appearance and arrangement to that of the nominal Jupiter probe. The entry ballistic coefficient, which sizes the aeroshell/heat shield assembly, is 102 kg/m^2 (0.65 slug/ft^2). This coefficient was chosen to provide a deceleration to Mach 0.7 at a pressure altitude of approximately 100 millibars, to meet the descent-probe scientific requirements. Only a single parachute is used for descent into the Jovian atmosphere. The descent ballistic coefficient, which sizes the descent probe parachute size, is 14.1 kg/m^2 (0.09 slug/ft^2). This ballistic coefficient combined with a probe descent weight of 47.0 kg (103.6 lbm) results in a parachute size roughly the same as that for the probe-dedicated mission [roughly 2.74 m (9.0 ft)]. It is deployed by a pyrotechnic mortar after planetary entry is completed, at a pressure altitude of 100 millibars.

The configuration of the probe for the spacecraft-radiation-compatible Jupiter mission is shown in Figure II-28. The ejected configuration has a conical nose cone of 60° half angle with maximum diameter of 0.954 m (37.6 in.) and weighs 165.6 kg (365.0 lbm). The descent probe is 0.47 m (18.5 in.) in diameter and 0.463 m (18.2 in.) long. It weighs 47.0 kg (103.6 lbm).

The scientific instrument complement of the descent probe is identical to that of the probe-dedicated mission; however, mission requirements result in a different support electrical weight. The planetary entry capsule basically consists of the descent probe surrounded by the fore and aft heat shield. The forward heat shield assembly, in turn, consists of a titanium structural aeroshell capped with a graphite heat shield, and containing additional hardware needed for entry. The aft heat shield consists merely of an aft structural shell coated externally with ESA 5500M3 ablator, and a pyrotechnic system for its ejection.

The structure of the probe is governed by the entry angle of 20° at a latitude of 5°, resulting in an entry deceleration of 1500 g. The peak entry dynamic pressure is approximately 1.13 x 10^6 N/m^2 (23,500 psf), and this value converts to a local pressure normal to the nose cone of approximately 1.56 x 10^6 N/m^2 (225 psi). The descent probe and aeroshell base cover structural weight is governed by the 1500 g deceleration, while the aeroshell itself is designed by normal pressure on the nose cone. The descent probe and aeroshell base cover are designed to high strength 7075-T6 aluminum, while the aeroshell is designed of 6Aℓ-4V titanium alloy.

The nose heat shield for this probe, like the other Jupiter probe, is designed of ATJ graphite to the criteria developed by M. Tauber and M. Wakefield of NASA/Ames Research Center. This is discussed in Chapter V, Section A.8 of Volume II. The mass fraction of the heat shield including a 2 cm (0.79 in.) carbonaceous backface insulator is shown to be 0.317. This value takes into account a correction factor of 0.88, for the probe diameter of 0.94 m (37 in.), and a planetary entry latitude correction factor of 1.01. Thus, for a probe weight of 110.5 kg (243.8 lbm) at entry, the resulting heat shield weight is 29.6 kg (67.2 lbm). The heating for the base cover is estimated based on a heating pulse of 2% of the nose cone heating. For a 20° entry angle, the total heating pulse is of the order of 1620 Btu/ft^2, and a heating pulse time is approximately 8 sec. This heating pulse requires 3.2 kg/m^2 (0.65 lbm/ft^2) of ESA 5500M3 ablator to protect the base cover.

It is interesting to note that for this mission, the probe at separation and again at planetary descent is heavier than for the probe-dedicated mission. However, for planetary entry configuration, the situation is reversed; this probe is heavier, because of two factors. For this mission, the heat shield mass fraction is 0.317 compared to 0.350 for the probe-dedicated mission at 30° latitude entry. Also, the probe-dedicated mission has no service module, and carries through entry components that are jettisoned in the case of the spacecraft-radiation-compatible mission probe.

9. Propulsion Subsystem

The propulsion subsystem for the probe is the same as that for the nominal Jupiter probe except for the deflection maneuver delta velocity requirement, which requires a somewhat different size motor. This mission has a deflection maneuver of 256.5 m/sec (842 fps) as compared with 221 m/sec (725 fps) for the nominal Jupiter probe.

A spherical solid propellant rocket motor provided for the probe uses an aluminized solid propellant (described as the baseline propellant in Appendix M of Volume III) and has a dual nozzle configuration to avoid the problem of exhaust impingement on the carrier spacecraft at spacecraft separation. Using a theoretical specific impulse, I_{sp} = 287 sec, the necessary weight of propellant to provide the delta velocity is 12.4 kg (27.4 lbm) for a probe weighing 148 kg (327 lbm), not including the weight of the motor. This propellant weight must be increased to account for

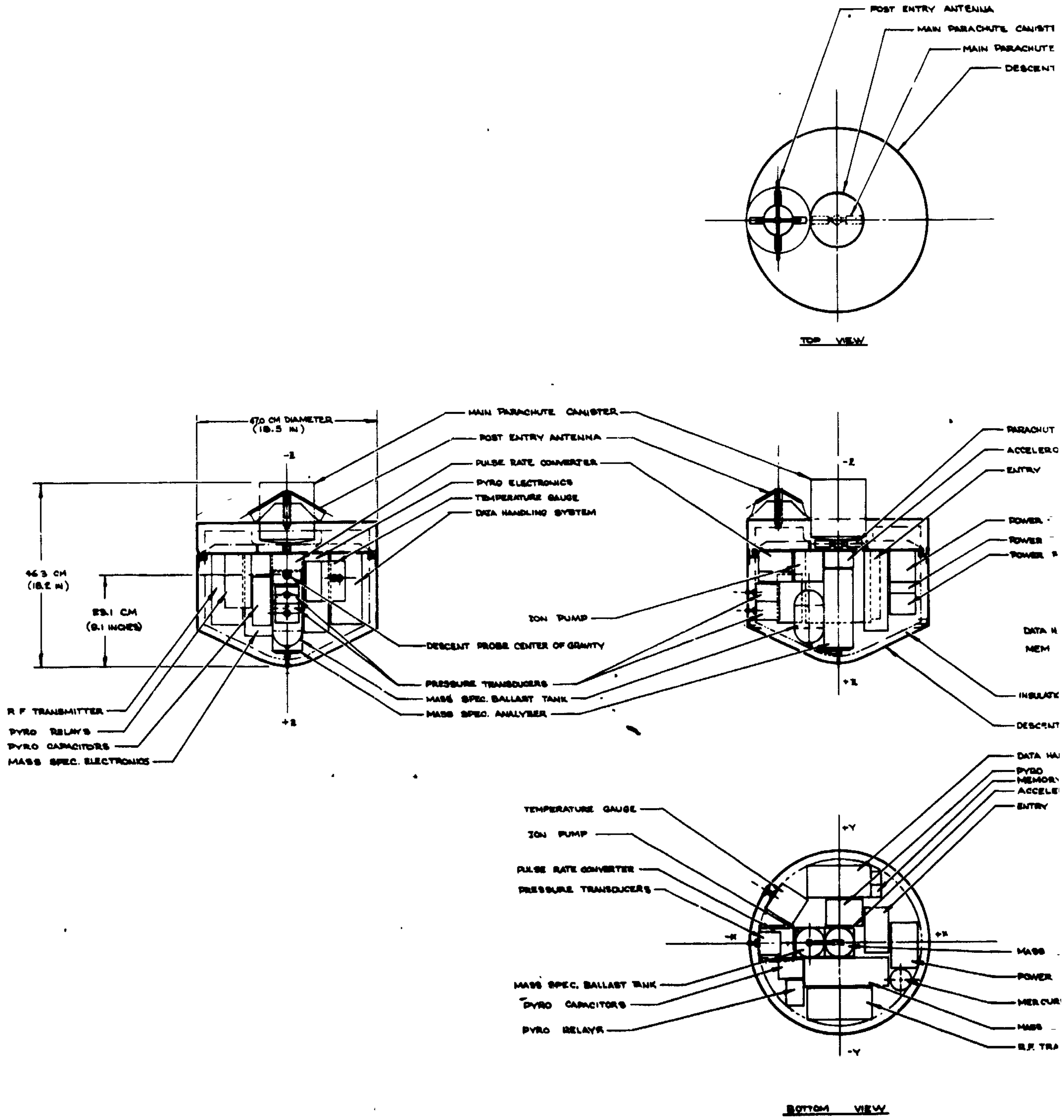

DESCENT PROBE

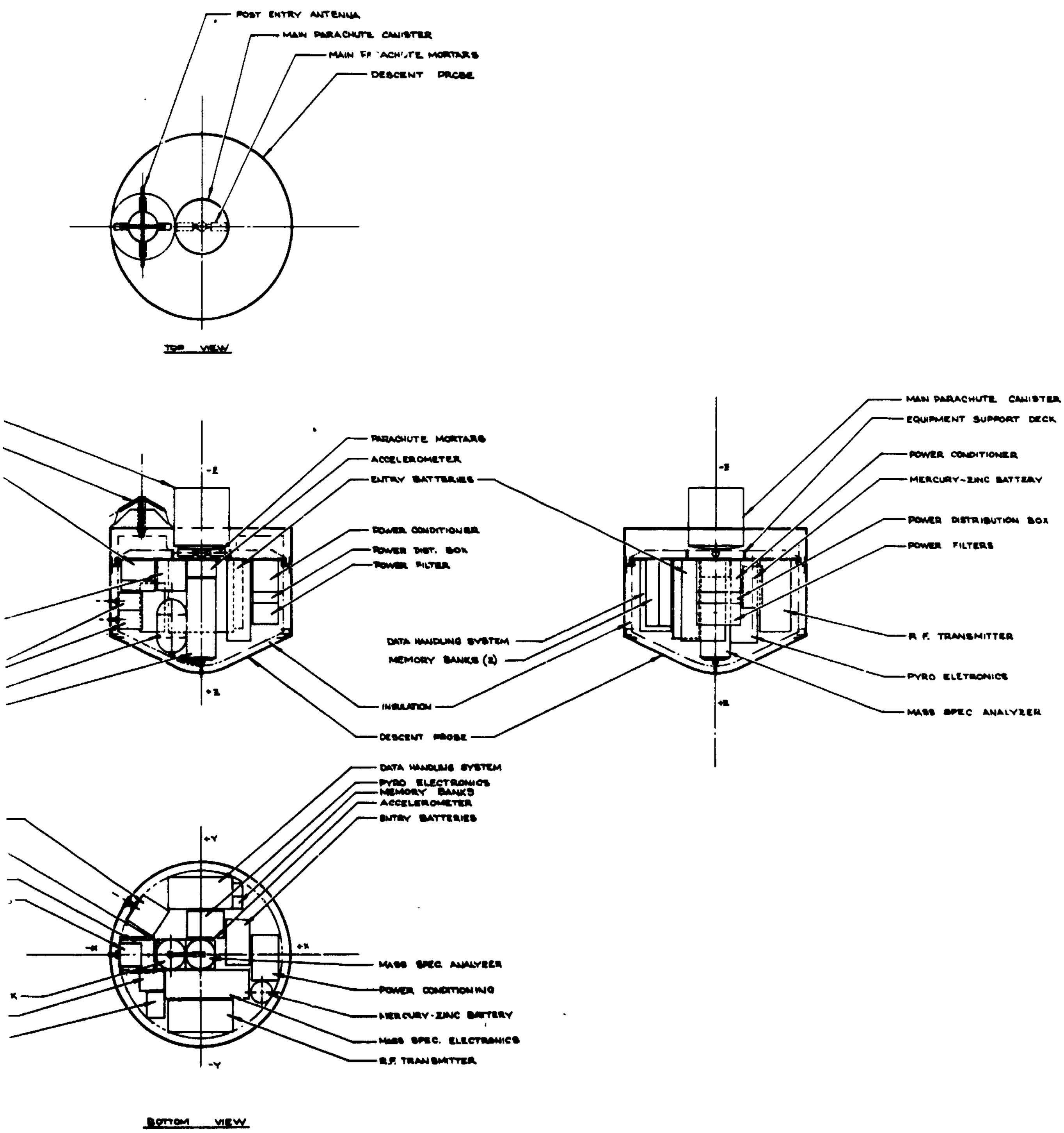

DESCENT PROBE

HUTE CANISTER
SUPPORT DECK
DITIONER
ZINC BATTERY
TRIBUTION BOX
SMITTER
RONICS
ANALYZER

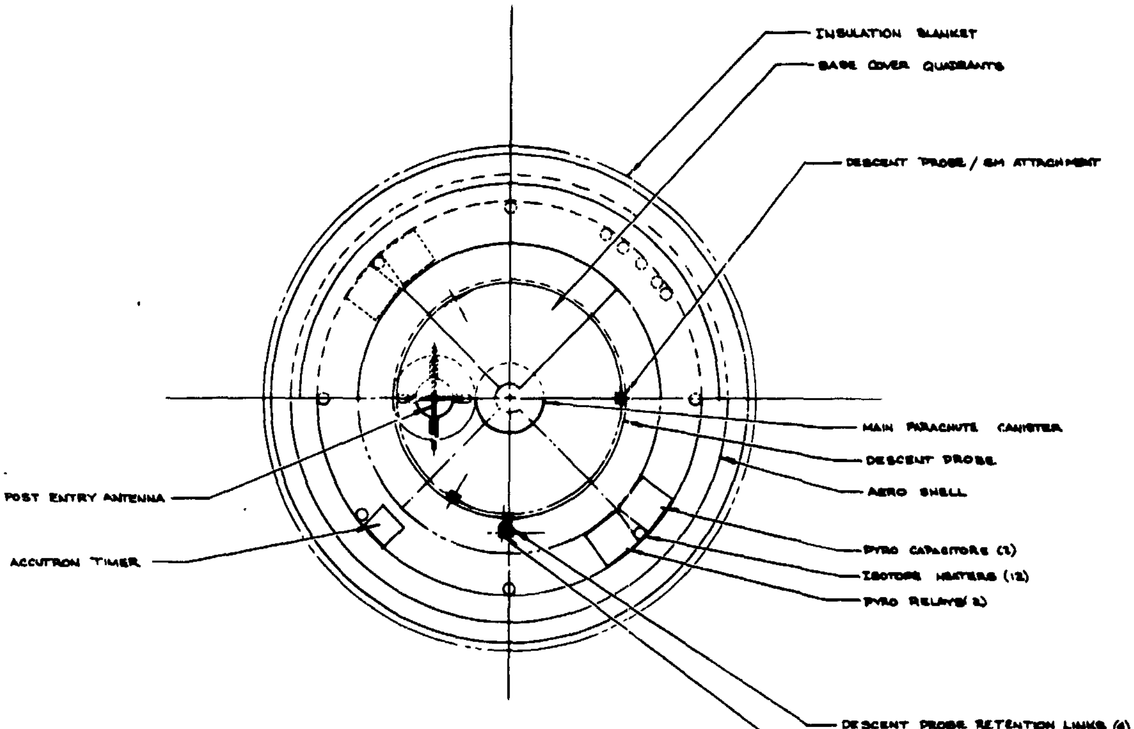

TOP VIEW

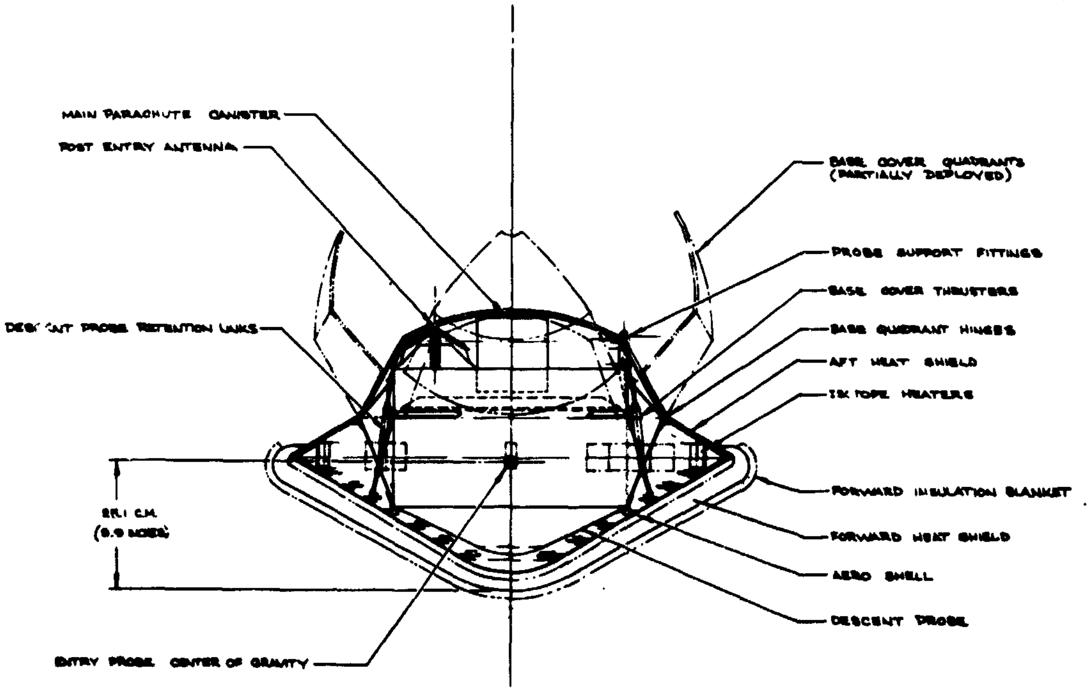

ENTRY PROBE

ACS
ACS

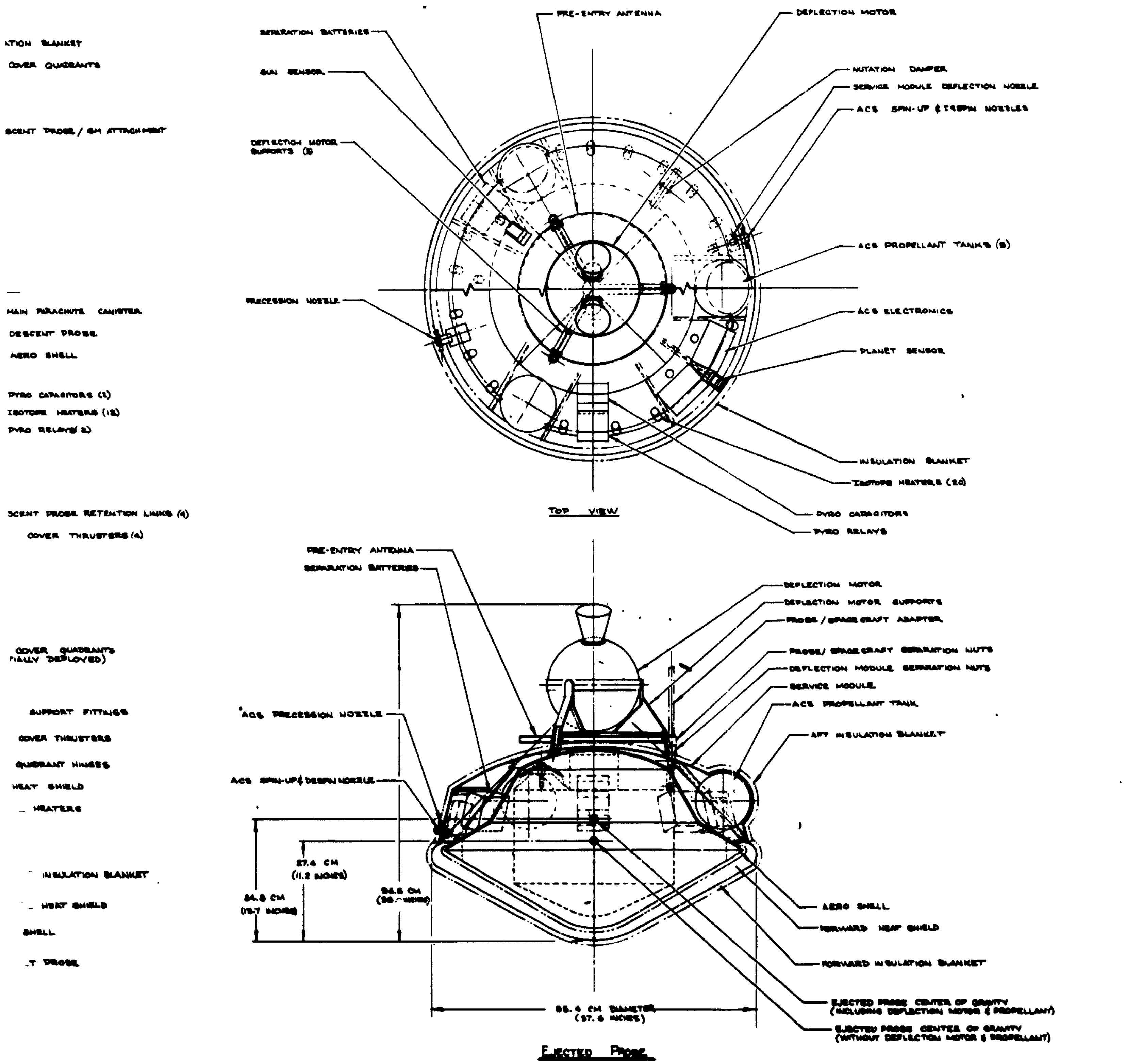

Figure II-28 Probe Definition of Spacec.

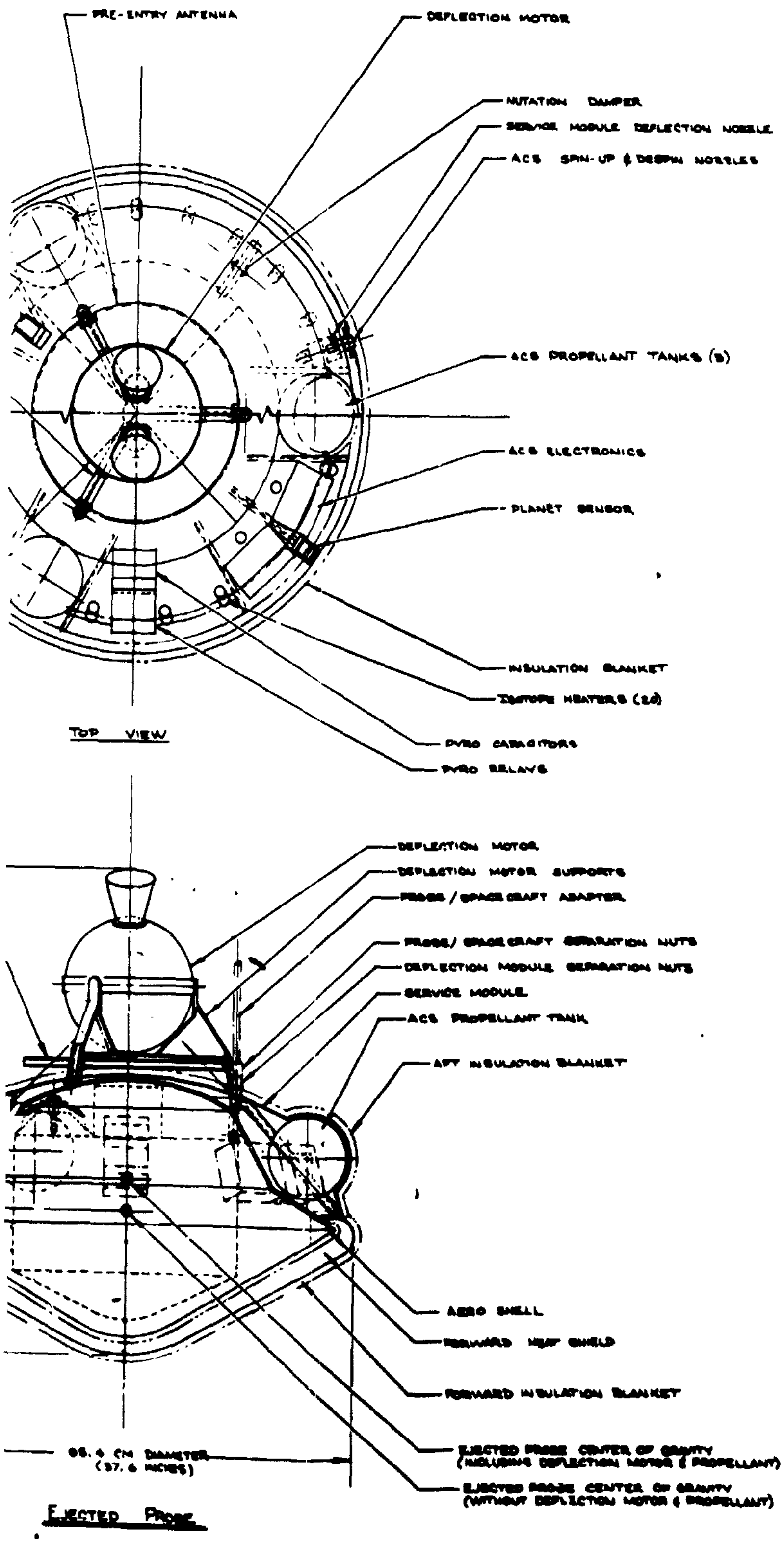

Figure II-28 Probe Definition of Spacecraft-Radiation-Compatible Jupiter Mission the vectorial loss (1 - cos 22.5°) for the dual canted nozzles. For a propellant mass of 13.4 kg (29.7 lbm), the loaded motor propellant mass fraction is 0.80, resulting in total loaded motor weight of 17.5 kg (38.6 lbm). This weight also includes a weight penalty, above and beyond the mass fraction, of 0.68 kg (1.5 lbm) to account for the extra nozzle. The configuration is the same, except for size, as that for the nominal Jupiter probe.

The probe has a service module propulsion system for the spin-despin-precess maneuver, providing a cold gas propellant supply adequate to spin to 10.45 rad/sec (100 rpm), precess through a 0.94 rad (53.5°) angle, and despin to 0.52 rad/sec (5 rpm), as well as deflect the service module at jettisoning. The service module is jettisoned just shortly before planetary entry. The moment of inertia for the radiation-compatible-mission probe is close enough to that of the nominal Jupiter probe that it is assumed to be the same. Thus, the ACS propellant supply and the ACS system is the same as that shown in Figure II-19 for the nominal Jupiter probe.

10. Thermal Control Subsystem

The thermal control required for the spacecraft radiation-compatible probe is the same as the nominal Jupiter mission and the thermal analysis shows that this design is adequate to obtain desired probe performance. The probe design requirements are not as critical since weight and transmitter power are higher because of the $6R_J$ communication distance and the relatively long pre-entry standby power requirement.

As for all missions, the pivotal design temperature is the probe temperature established at the beginning of entry. Analysis shows that with an entry temperature of 300°K, a 15°K margin on required limits can be created for both the minimum equipment temperature experienced during a cool/dense atmosphere descent encounter and the maximum equipment temperature experienced during a nominal atmosphere encounter. Trajectory uncertainties for the spacecraft radiation-compatible probe are high (± 38 min) and would have caused considerable thermal control problems if the transmitter had not been turned off following service module ejection. Since the transmitter is deactivated, probe entry temperature uncertainties are only ±3°K.

The thermal coatings used for the spacecraft-radiation-compatible probe are the same as the probe-dedicated mission. Since the probe temperatures during coast will have sufficient time to reach equilibrium, better thermal design is afforded by establishing a lower spacecraft cruise probe equilibrium temperature of 286°K.

Results for the spacecraft-radiation-compatible Jupiter mission indicated that the following probe temperature margins will be expected. Note that the entry-descent upper and lower equipment temperature margins are balanced (15°K).

Temperature Margin	Spacecraft Cruise Phase, °K	Probe Coast Phase, °K	Entry-Descent Phase, °K
Above Equipment Lower Limit	36	26	15
Below Equipment Upper Limit	14	25	15
Below Transmitter Upper Limit	NA	36	24

Typical probe thermal history and temperature limits are presented in the discussion for the nominal Jupiter probe.

11. Probe to Spacecraft Integration

The spacecraft-radiation-compatible mission probe integration with the spacecraft is essentially the same as that described for the nominal Jupiter probe.

F. SATURN PROBE SYSTEM DEFINITION SUMMARY

This probe system used the alternative Jupiter probe approach, defined in Sections D and E, but adjusted for a Saturn entry and results of the Saturn parametric analysis discussed in Section II.H.3. The general constraints are:

Mission	JPL's JS 77 High Inclination for a Titan Encounter
Entry Angle	-25° (structures designed to -30°)
Depth of Descent	7 bars
Atmosphere	Nominal
Science	SAG Exploratory payload (PAET)
Spacecraft	Mariner family
Carrier Mode	Flyby
Periapsis Radius	2.33 R_S
Communication Mode	Relay
Deflection Mode	Probe
Entry Ballistic Coefficient	0.65 slug/ft^2 (102 kg/m^2)
Ballistic Coefficient for Heat Shield Removal	0.12 slug/ft^2 (19 kg/m^2)
Descent Ballistic Coefficient	0.7 slug/ft^2 (110 kg/m^2)

1. Mission Definition

The Saturn mission upon which the system design is based is described in Figure II-29 and summarized in Table II-15. Important mission design results are discussed in this section.

a. Interplanetary Trajectory Selection - The interplanetary trajectory for this mission is based on the JST mission, a JS 77 mission including an encounter with Titan. The trajectory is pictured in Figure II-29(a) and detailed in Table II-15(a). The trajectory arrives at Jupiter 1.6 years after launch and passes by at a periapsis radius of 5.8 R_J. The flight time to Saturn is 3.4 years and the flyby radius at Saturn is 2.3 R_S. Titan is encountered 18 hours before arrival at Saturn.

b. Launch Analysis - The results of the launch analysis are given in Figure II-29(b) and Table II-15(a). The available payload weight (probe, spacecraft, spacecraft-to-launch vehicle adaptor) is plotted against launch period for three sets of performance data. The slight decrease in available payload relative to the previous Jupiter missions is due to the fact that the interplanetary trajectory was selected to satisfy the requirements of the entire JST mission and not to optimize payload weight.

c. Approach Trajectories - The approach trajectories are illustrated in Figures II-29(d) and (e) and summarized in Table II-15(a) and (b). The spacecraft flyby radius of 2.3 R_S was selected to permit the encounter with Titan but is compatible with an effective communication link. Thus, the nominal values of the probe aspect angle begin at 12.42°, reach a minimum value of 1.86°, and end at 4.05° as the faster moving spacecraft overtakes the probe. This is most clear in Figure II-29(d) where the view is from a point nearly normal to the spacecraft orbit plane. The location of Saturn's rings relative to the probe and spacecraft trajectories is indicated in Figure II-29(e).

d. Deflection Maneuver - A probe deflection maneuver was used for this mission. The deflection radius of 10.15×10^6 km was selected to give a ΔV of 170 m/sec to obtain an identical deflection motor for the Saturn and Uranus missions. The deflection sequence is illustrated in Figure II-29(c) and detailed in Table II-15(b).

e. Navigation and Dispersions - The navigation and dispersion summary is provided in Table II-15(c). The spacecraft uncertainties are based on using range/Doppler measurements over an 80-day tracking arc. The SMAA would be reduced by half by using QVLBI measurements. The navigation uncertainties have an approximately equal contribution to dispersions as execution errors. The entry dispersions are rather large but are tolerable.

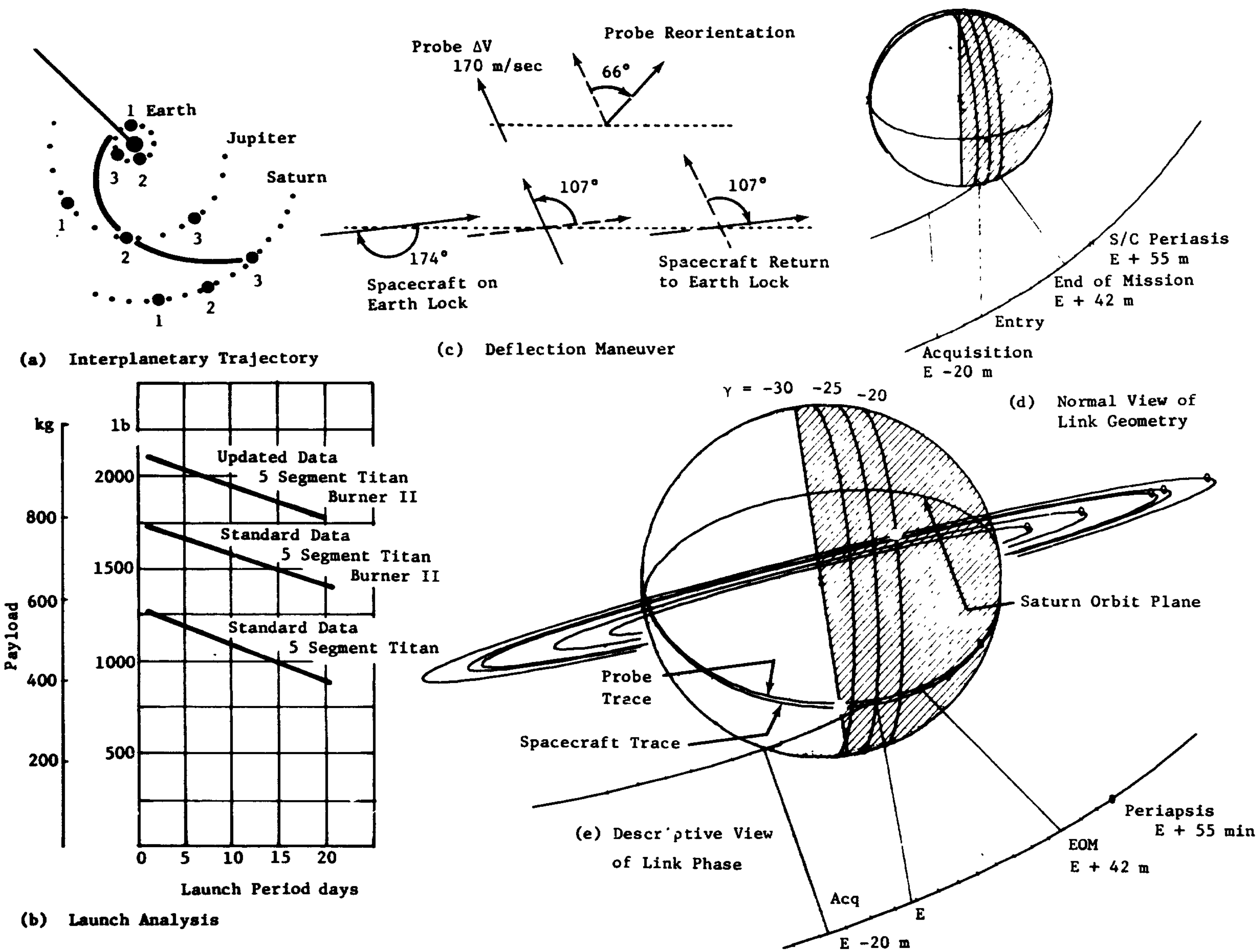

Figure II-29 Saturn Mission Description

a. Conic Trajectory Data

Interplanetary Trajectory	Launch Trajectory	Arrival Trajectory
Launch Date: 9/4/77 Arrival Date: 2/16/81 Flight Time: 1261 days Central Angle: 207.3	Nominal C_3: 99 km^2/sec^2 Nominal DLA: 27.6° Launch Window: Parking Orbit Coast: C_3 (10 day): 102 km^2/sec^2 C_3 (20 day): 107 km^2/sec^2 Azimuth Range:	VHP: 13.66 km/drv RA: 195.28° DEC: 2.54° ZAE: 173.6° ZAP: 169.7° RP: 2.31 R_S INC: 52.44°

b. Deflection Maneuver and Probe Conic

Deflection Maneuver	Probe Conic Definition
Deflection Mode: Probe D flection Radius: 10.15 x 10^6 km Coast Time: 8.02 days ΔV: 170 m/sec Application Angle: 105° Out-of-Plane Angle: 2° Rotation for Probe Release: 107° Probe Reorientation Angle: -66° Spacecraft ΔV from Earth: NA	Entry Angle: -25° Entry Latitude: -50.3° Entry Longitude: 102.2° Lead Time: 55.8 min Lead Angle: -7.63 Probe-Spacecraft Range (Entry): 96,305 km Probe Aspect Angle (Entry): 48.2° Probe Aspect Angle (Descent): 12.42° Probe Aspect Angle (EOM): 4.05°

c. Dispersion Analysis Summary

Naviation Uncertainties	Execution Errors (3σ)	Dispersions (3σ)
Type: Range-Doppler 80-day arc SMAA: 2178 km SMIA: 760 km β: 89° TOF: 40 sec	ΔV Proportionality: 1% ΔV Pointing: 2° Probe Orientation Pointing: 2°	Entry Angle: 5.04° Angle of Attack: 4.00° Down Range: 12.70° Cross Range: 1.57° Lead Angle: 5.43° Lead Time: 5.18° Entry Time: 7.59 min

d. Entry and Descent Trajectory Summary

		Critical Events	
Entry Parameters	Descent Parameters	Time from Entry	Altitudes above 1 atm
Entry Velocity, km/sec: 37.1 Entry Altitude, km: 491.4 Entry B, slug/ft^2: 0.65 Entry Atmosphere: Nominal Max Deceleration, g: 350 Max Dynamic Pressure, lb/ft^2: 7.0 x 10^3 kg/m^2: 3.3 x 10^5	Descent Atmosphere: Nominal EOM Pressure, bar: 7.0 Descent B, slug/ft^2: 0.7 kg/m^2:	g = 0.1, sec: 3.0 Max g, sec: 22.5 M = 0.7, sec: 78.5 Descent Time, min: EOM, min: 41.7	km: 444 km: 158 km: 100.

f. Entry and Descent Trajectories - Table II-15(d) summarizes the entry and descent phases on the mission. Both phases of the mission were simulated using the nominal atmosphere. The entry phase starts 491 km above the 1 atm pressure level (0 km alt = 59,800 km) and ends with the staging of the aeroshell 78.5 sec later. During this phase, a peak deceleration of 350 g is attained 19.0 sec after entry. The descent phase starts after staging of the aeroshell and continues through the end of the mission at 7.0 bars. The total descent time is 40.4 min.

2. <u>Science</u>

The instruments for the Saturn probe are identical to those for the Jupiter alternative probe. The only difference would be a modification of the range of the temperature gage and possibly entry accelerometers for the colder atmosphere and lower g-load.

The results of the descent profile parametrics are:

Design Limit Pressure = 7 bars

Parachute Ballistic Coefficient = 0.70 slug.ft^2 (109.9 kg/m^2)

Parachute Deployment Pressure = 48 millibars

Pressure at First Measurement = 57 millibars.

Entry Time = 78.5 sec

Descent Time = 40 min 25 sec

Instrument Sampling Times:

Temperature and Pressure = 4.0 sec

Neutral Mass Spectrometer = 60 sec

Entry Accelerometers = 0.2/0.4 sec

Descent Accelerometers = 8.0 sec

Total bit rate = 26.3 bps

All performance criteria was satisfied. Figure II-30 shows the selected pressure descent profile for Saturn.

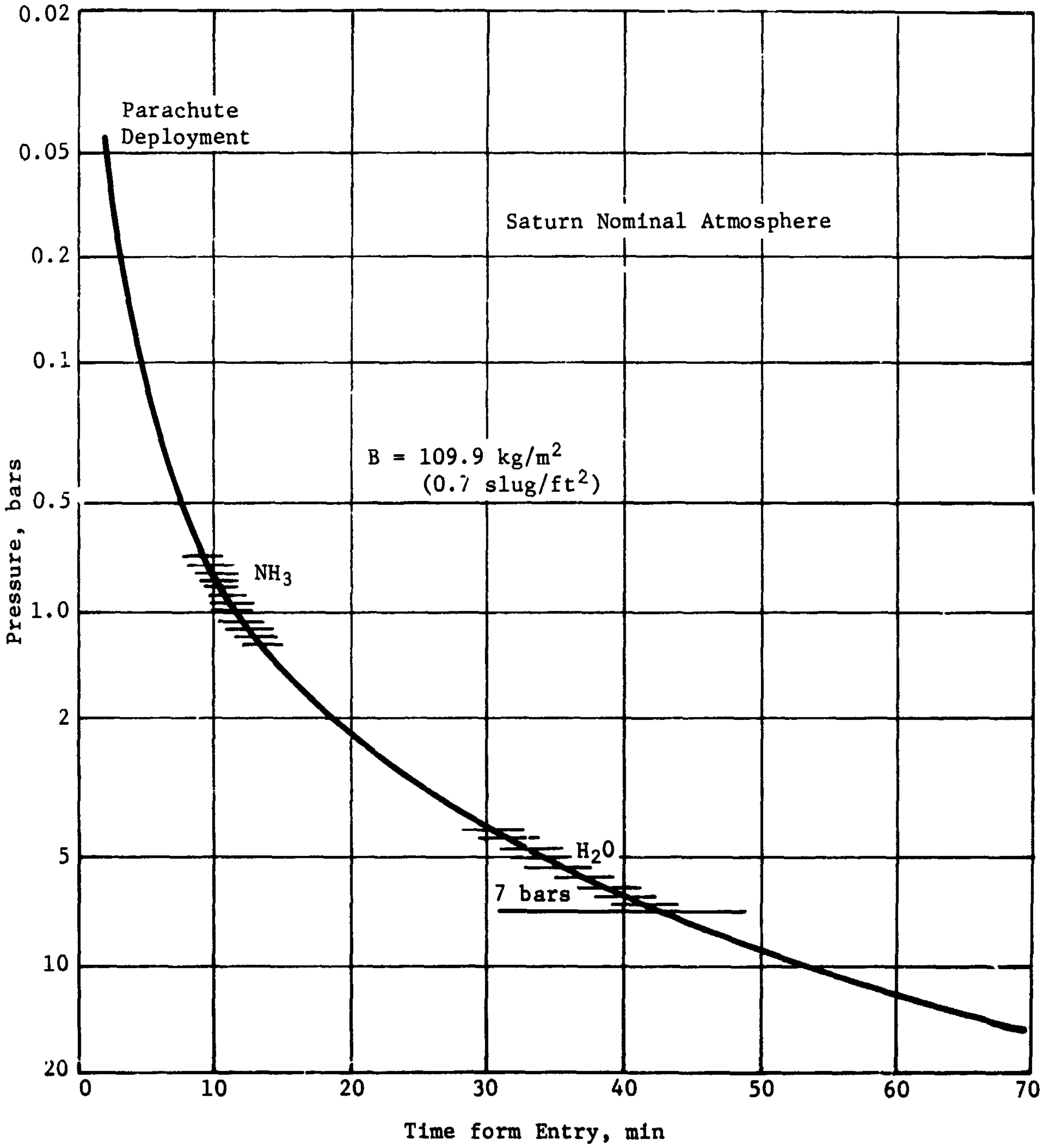

Figure II-30 Saturn Probe Pressure Descent Profile

3. System Integration

The sequence of events is similar to that for the nominal Jupiter probe in Section C.3 of this chapter except that two parachutes are used: one (primary chute) to remove the descent probe from the heat shield and the other to establish the descent rate. The primary chute is ejected after approximately 1 meter separation of the two assemblies. The data profile is similar to that for the nominal Jupiter probe except that the descent data rate is 26 bps instead of 28 bps. The power profile is similar to that for the nominal Jupiter probe except that the transmitter is turned "off" when the service module is ejected. The probe weight at ejection is 107.9 kg (237.9 lb)

4. Telecommunications Subsystem

RF power of 6.5 W is required at 0.86 GHz with a bit rate of 26 bps using binary FSK with a tracking tone. A solid-state switch may be used at this power level. The entry antenna is an annular slot which is mounted on the service module under the deflection motor. The descent antenna is a turnstile over a cone design which is mounted on the aft bulkhead of the descent probe. The spacecraft antenna is a helix with right hand circular (RHC) polarization and a 35° beamwidth. The descent antenna is also RHC polarized, but the entry slot antenna has linear polarization. Cross polarization losses occur during entry,but the link margin is high enough to overcome the loss. The spacecraft receiver is conventional solid-state design with a noise figure of 3.1 dB.

5. Data Handling Subsystem

The configuration and functions of the data handling subsystem are unchanged from the design of the nominal Jupiter probe with the exception of minor modifications of sequence and format. (See Vol II, Chapter V, Sections A.5 and B.5, and Vol III, Appendix H.)

6. Power and Pyrotechnic Subsystem

The configuration of the power and pyrotechnic subsystem is unchanged from the nominal Jupiter probe with the exception of battery size and weight. (See Vol II, Chapter V, Sections A.6 and B.6, and Vol III, Appendix G.) The physical characteristics are:

Ag-Zn Post-Separation Battery	94 $in.^3$	6.9 lb
Ag-Zn Entry Battery	39.4 $in.^3$	2.6 lb
Hg-Zn (Pyrotechnic) Battery	1x0.5x3 in.	0.9 lb

The remotely activated Ag-Zn batteries are based on power consumption for this mission.

7. Attitude Control Subsystem - Electronics

The electronics configuration and functions for this subsystem are unchanged for the nominal Jupiter probe design. (See Vol II, Chapter V, Sections A.7 and B.7, and Vol III, Appendix F.)

8. Structural and Mechanical

The Saturn probe is the smallest of the configurations evaluated. This is due to the less hostile (from a structural standpoint) entry environment. The planetary entry decelerations are lower, resulting in lower structural weights. The heat shield mass fraction is also less, and this, combined with the reduced structural weight, produces a probe design weighing substantially less than the Jupiter configurationes.

The probe is required to provide a deflection maneuver delta velocity, and to provide attitude stabilization, and attitude reorientation between the trajectory deflection maneuver and entry. Thus, the probe configuration propulsion system includes a delta velocity motor and an attitude control system.

Two configurations of the Saturn probe were evaluated. Configuration 1 uses the blunt entry nose shape recommended by the heat shield analysis results*. Configuration 2 uses the same 1.04 rad (60°) half angle nose cone as that used for the Jupiter entry probes. Each configuration used the respective heat shield mass fraction recommended by M. Tauber of NASA/ARC. The heat shield diameters are shown to be almost identical for the two configurations. This is due to the drag coefficients being very close for the two nose shapes. The hypersonic drag coefficient

---

*M. E. Tauber: *Heat Protection for Atmospheric Entry into Saturn, Uranus, and Neptune*. Preprint No. AAS 71-145, 17th Annual Meeting, American Astronautical Society, June 28, 30, 1971.

for the blunt nose is $C_D = 1.57$ while the comparable coefficient for the conical nose cone is $C_D = 1.51$.

The Configuration 1 Saturn probe is shown in Figure II-31. Generally speaking, this configuration is much like the other Jupiter probes, except for the changes necessary to accept the blunt shape of the aeroshell/heat shield assembly. This blunt nose shape of the aeroshell forces the descent probe nose to be blunted also, resulting in a slight rearrangement of internal equipment. The scientific instrument component complement is the same as that for the probe-dedicated Jupiter mission and for the spacecraft-radiation-compatible mission probes.

The second Saturn probe configuration investigated used a 1.04 rad (60°) half angle conical aeroshell/heat shield structure. Although the heat shield mass fraction is slightly larger than that for the blunt nose shape of Configuration 1, the conical aeroshell offers packaging advantages for the descent probe, and was thus investigated. The general arrangement of Configuration 2 is shown in Figure II-32. For this configuration, the aeroshell structural arrangement is similar to that of the Jupiter probes. The nose of the descent probe is allowed to project forward into the areoshell at approximately a 1.04 rad (60°) half angle cone, permitting the equipment arrangement to be less cramped and similar to that of the Jupiter probes. This packaging arrangement is a little cleaner than Configuration 1.

The Saturn probe is designed for entry at either the planet Saturn or Uranus. The entry conditions are close enough for the two planets that no appreciable structural weight penalty is involved in designing for the worst case. An entry deceleration of 380 g is encountered at Uranus as compared with 350 g at Saturn. Likewise, the planetary entry peak dynamic pressure occurs at Uranus. The peak dynamic pressure at Uranus of 35.4×10^4 N/m^2 (7400 lbf/ft^2) compares with 33.5×10^4 N/m^2 (7000 lbf/ft^2) for Saturn for the respective missions. Thus the entry probe, with the exception of the aeroshell, is designed to 380 g deceleration loads. The aeroshell is designed by the normal pressure on the nose cone, which is a function of nose cone shape, and the peak dynamic pressure at planetary entry. The dynamic pressure at Uranus, which is slightly higher than at Saturn, is used for design. Configurations 1 and 2 are identical to the spacecraft-radiation-compatible Jupiter probe in structural configuration with the exception of the aeroshell of Configuration 1. This is a thin integral rib waffle structure to minimize aeroshell thickness.

From Figure II-33 it is seen that the heat shield mass fraction for the blunt body nose shape for a Saturn entry angle of 0.52 rad (30°) is 0.145. The mass fraction for the 1.04 rad (60°) conical nose and a Saturn entry angle of 0.52 rad (30°) is higher, approximately 0.215. The former (blunt body) results in a heat shield weight of approximately 8.9 kg (19.7 lbm) for Configuration 1. Configuration 2 conical nose has a heat shield weight of approximately 14.2 kg (31.4 lbm). Therefore, the delta heat shield weight between the two configurations is 5.3 kg (11.7 lbm).

The base cover heat shield protection selected is that for the planet Saturn, which is the more severe of the two planets. The ablator material selected is ESA 3560, which is a filled silicone material reinforced with fiberglass honeycomb.

A two-stage parachute deceleration is supplied for the Saturn descent probe. This arrangement is necessary because of the high ballistic coefficient provided for descent into the atmosphere of Saturn. The selected ballistic coefficient for descent is 110 kg/m^2 (0.7 slug/ft^2). The spent aeroshell/heat shield assembly has a ballistic coefficient of 43.5 kg/m^2 (0.25 slug/ft^2) after separation, and it is readily apparent that the descent parachute will not pull the descent probe away from the aeroshell. However, once the descent probe is on the descent parachute, it will descend faster than the aeroshell assembly. The same parachute configurations are satisfactory for use on either of the two Saturn probe designs investigated.

The ballistic coefficient for the separation parachute has been arbitrarily selected as half that of the spent aeroshell, or $B = 21$ kg/m^2 (0.12 slug/ft^2). This value provides reasonable relative deceleration of the descent probe to that of the aeroshell. For a value of dynamic pressure of 1700 N/m^2 (36 lbf/ft^2), the relative deceleration is approximately 5 g--ample to provide separation.

The separation parachute is selected using the above ballistic coefficient and a descent probe mass of 37.2 kg (2.55 slugs). This results in a parachute size of 2.1 m (6.8 ft) in diameter. The descent parachute has a ballistic coefficient of 110 kg/m^2 (0.7 slug/ft^2). A descent probe weight of 37.2 kg (2.55 slugs) results in a parachute diameter of 0.67 m (2.2 ft).

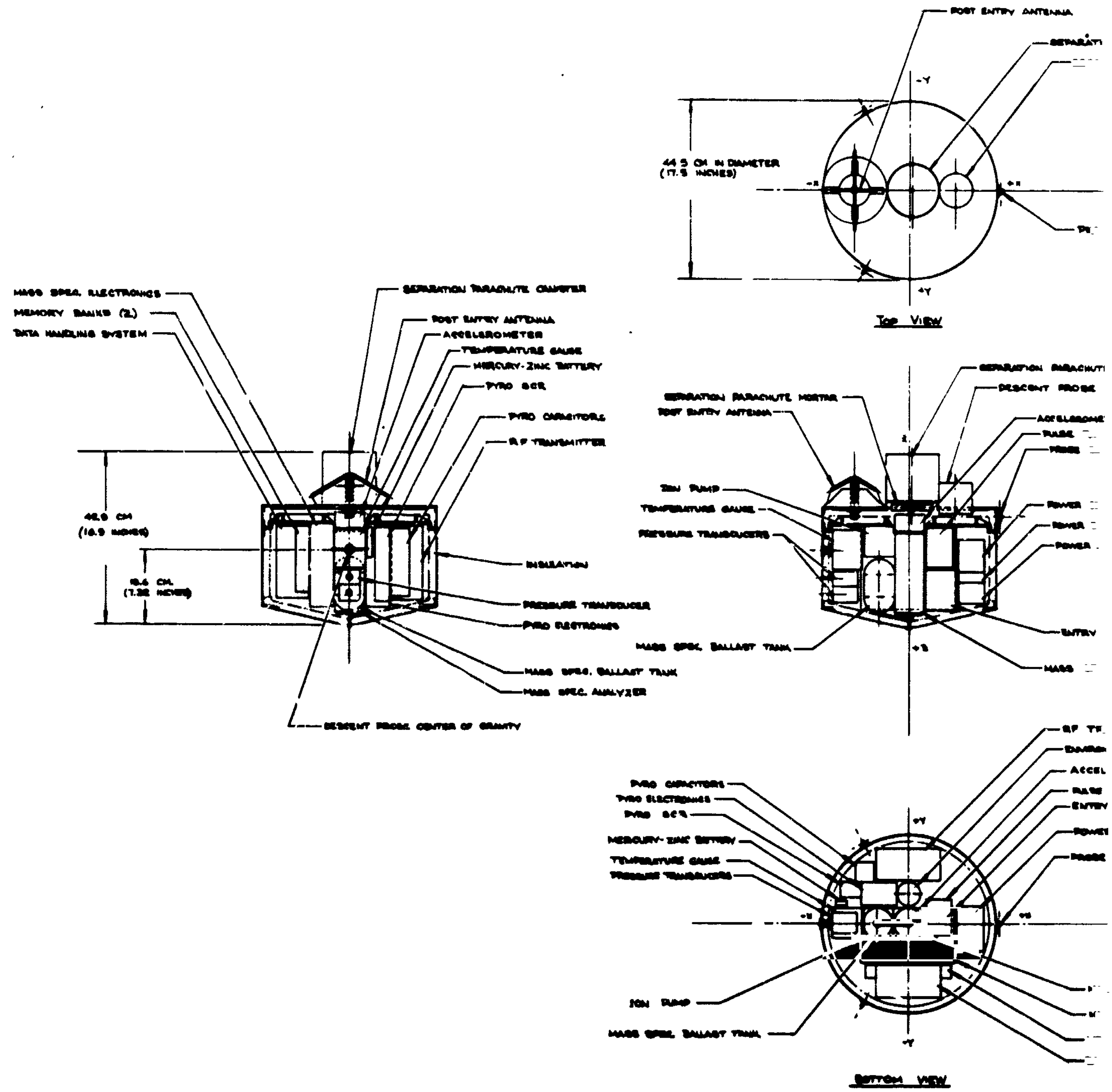

DESCENT PROBE

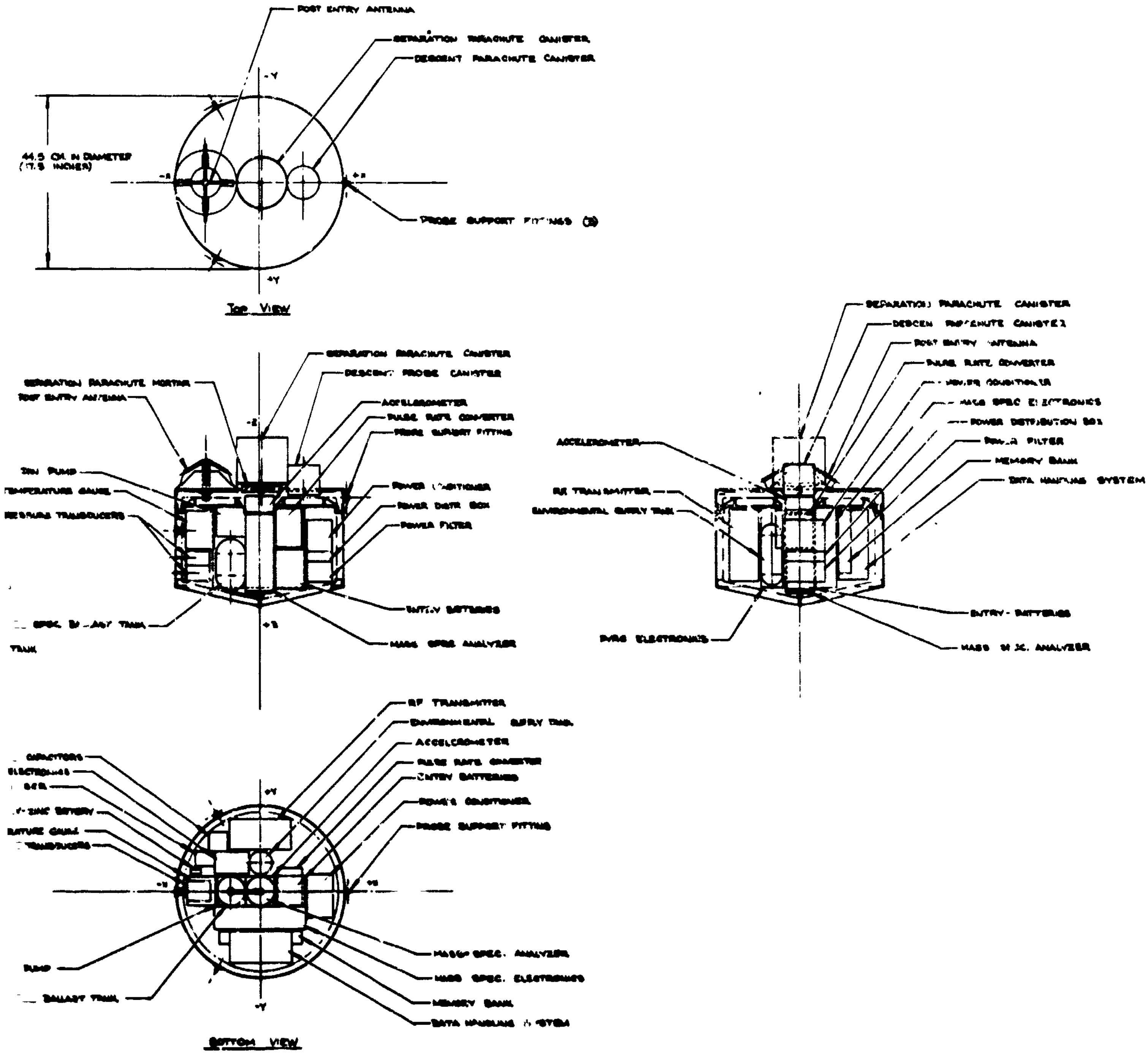

DESCENT PROBE

CANISTER
CANISTER
NNA
NVERTER
DITIONER
C ELECTRONICS
DISTRIBUTION BOX
R FILTER
MORY BANK
A HANDLING SYSTEM

BATTERIES

C. ANALYZER

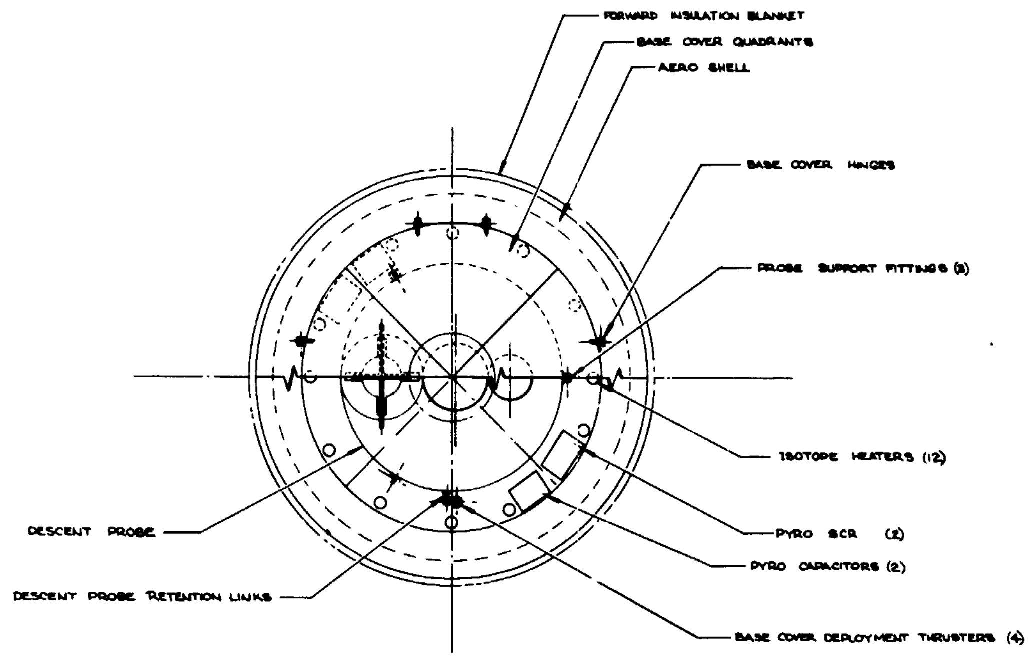

TOP VIEW

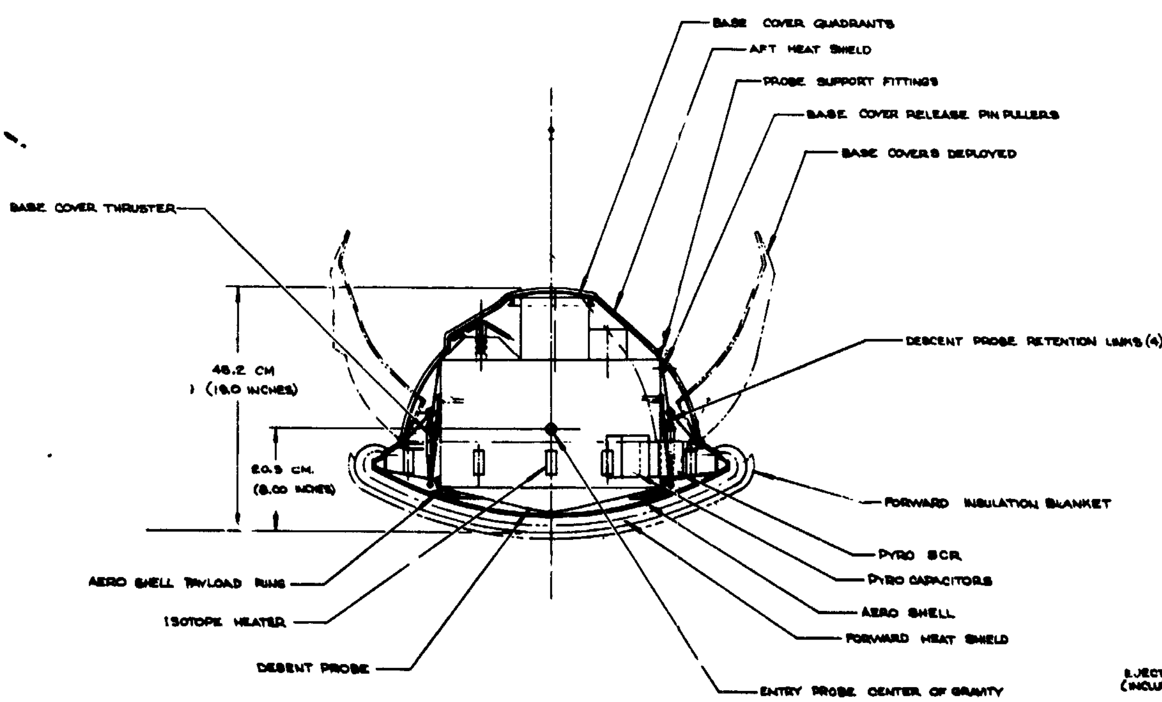

ENTRY PROBE

EJECTED PROBE (INCLUDING DEFLECT
EJECTED PROBE (WITHOUT DEFLECT

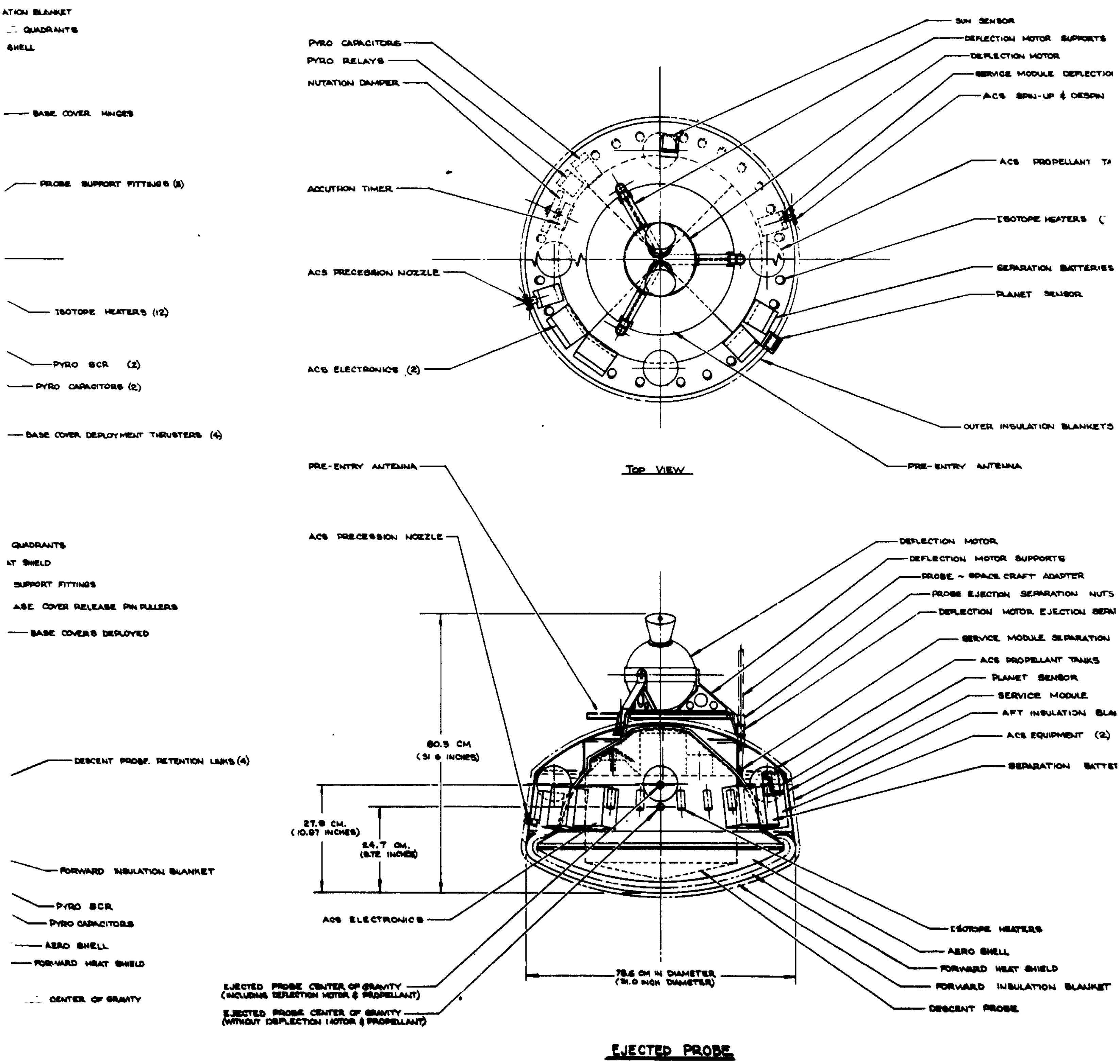

FOLDOUT FRAME 4

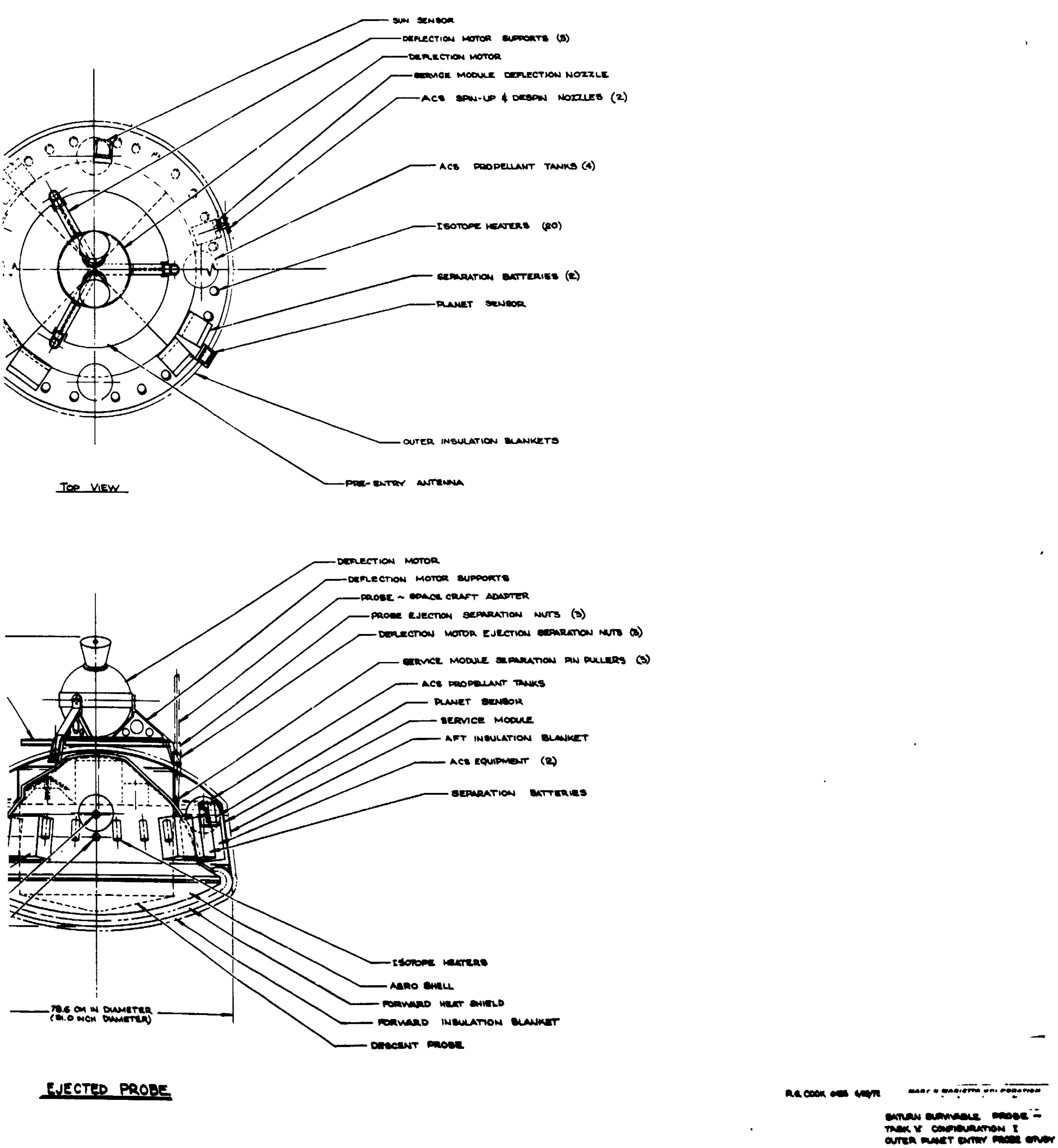

Figure II-31 Saturn Probe Configuration

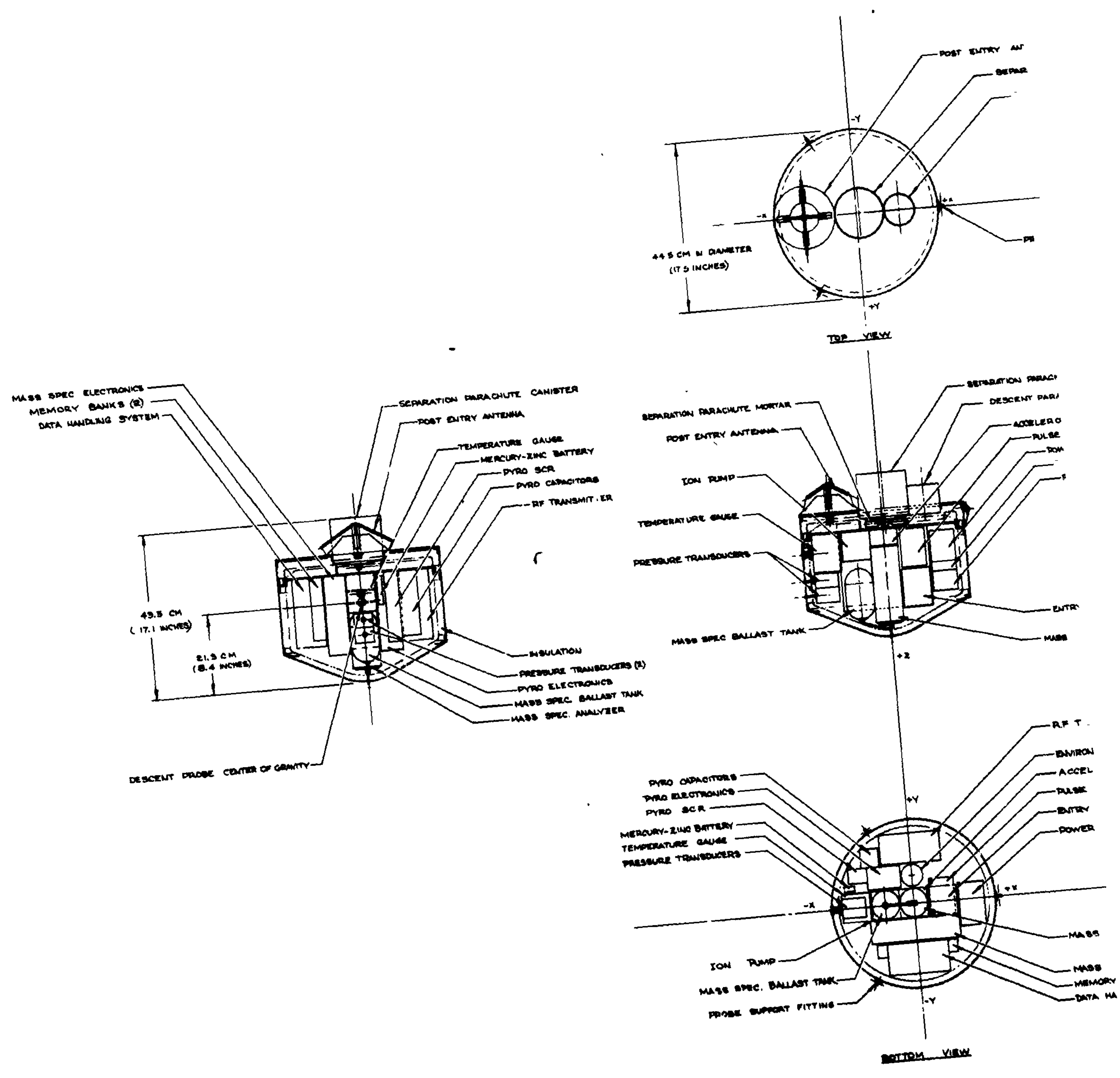

DESCENT PROBE

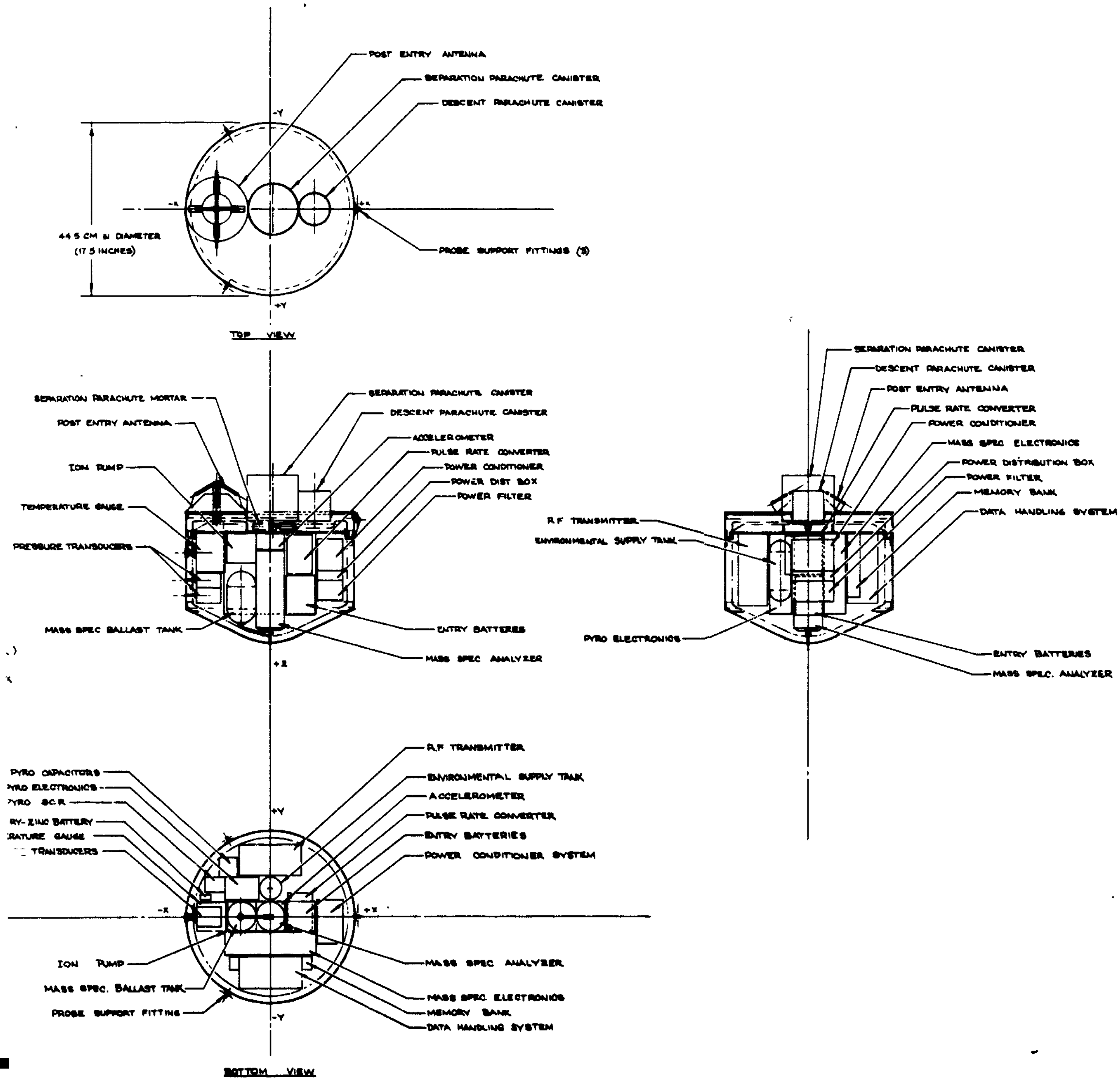

DESCENT PROBE

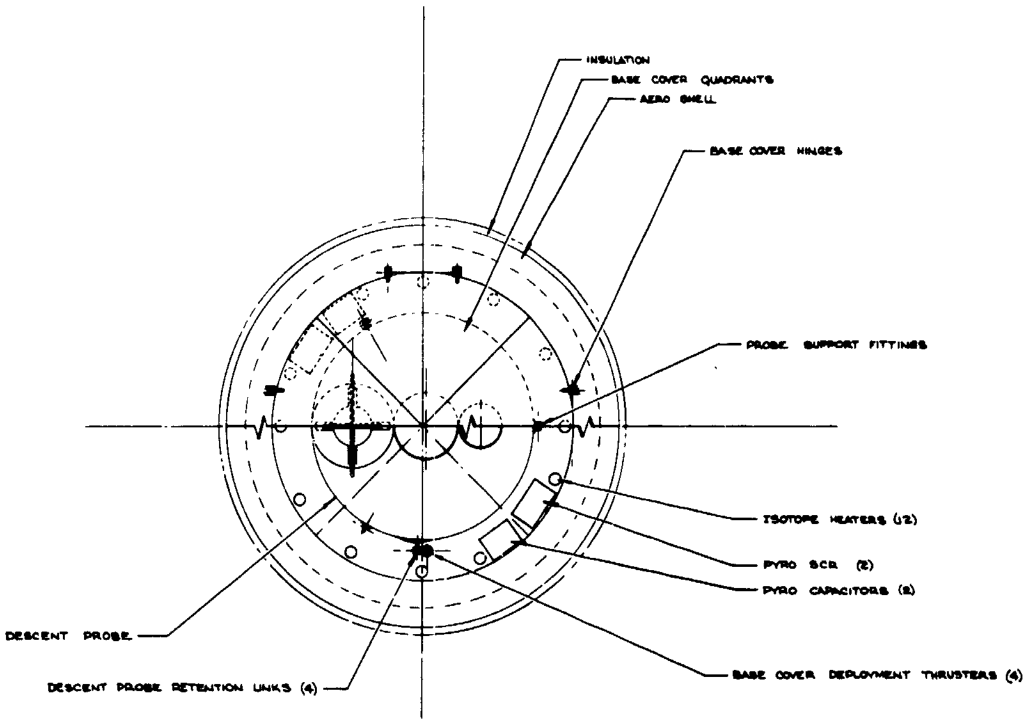

TOP VIEW

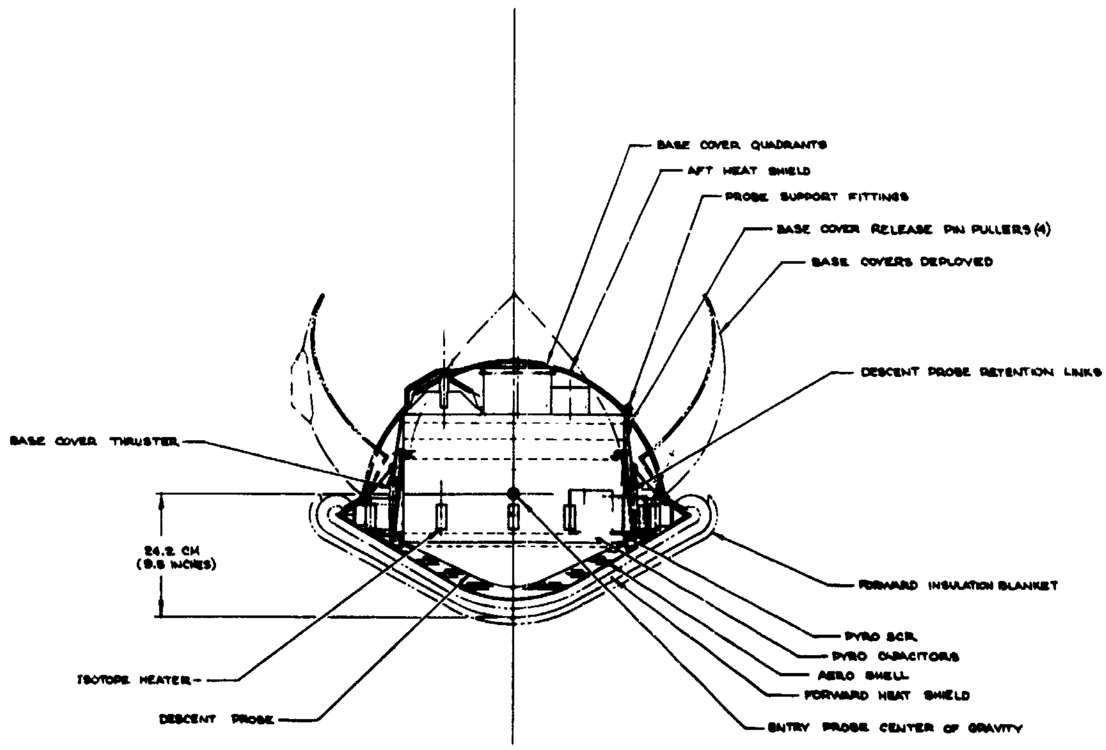

ENTRY PROBE

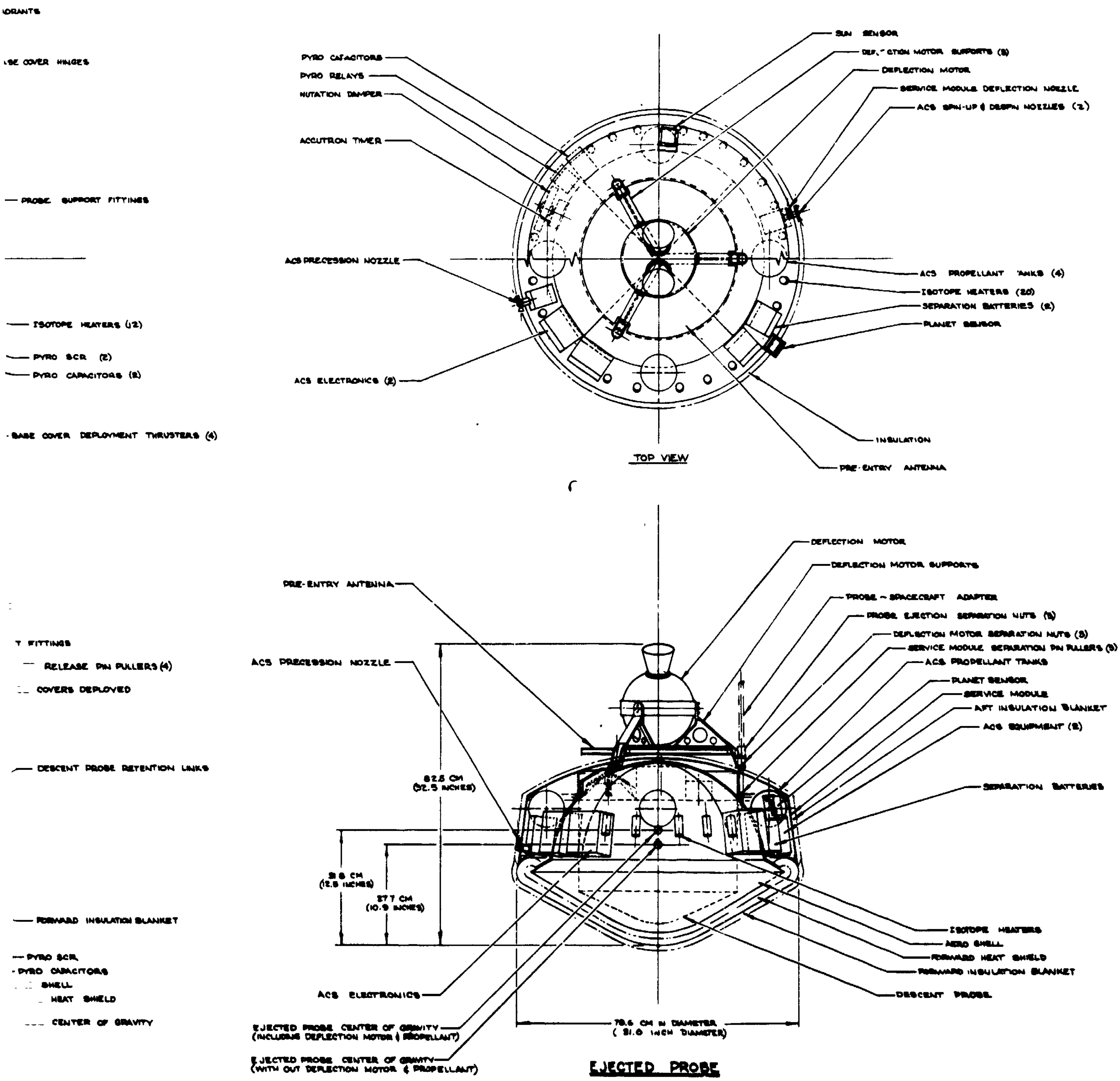

Figure II-32 A

FOLDOUT FRAME 4

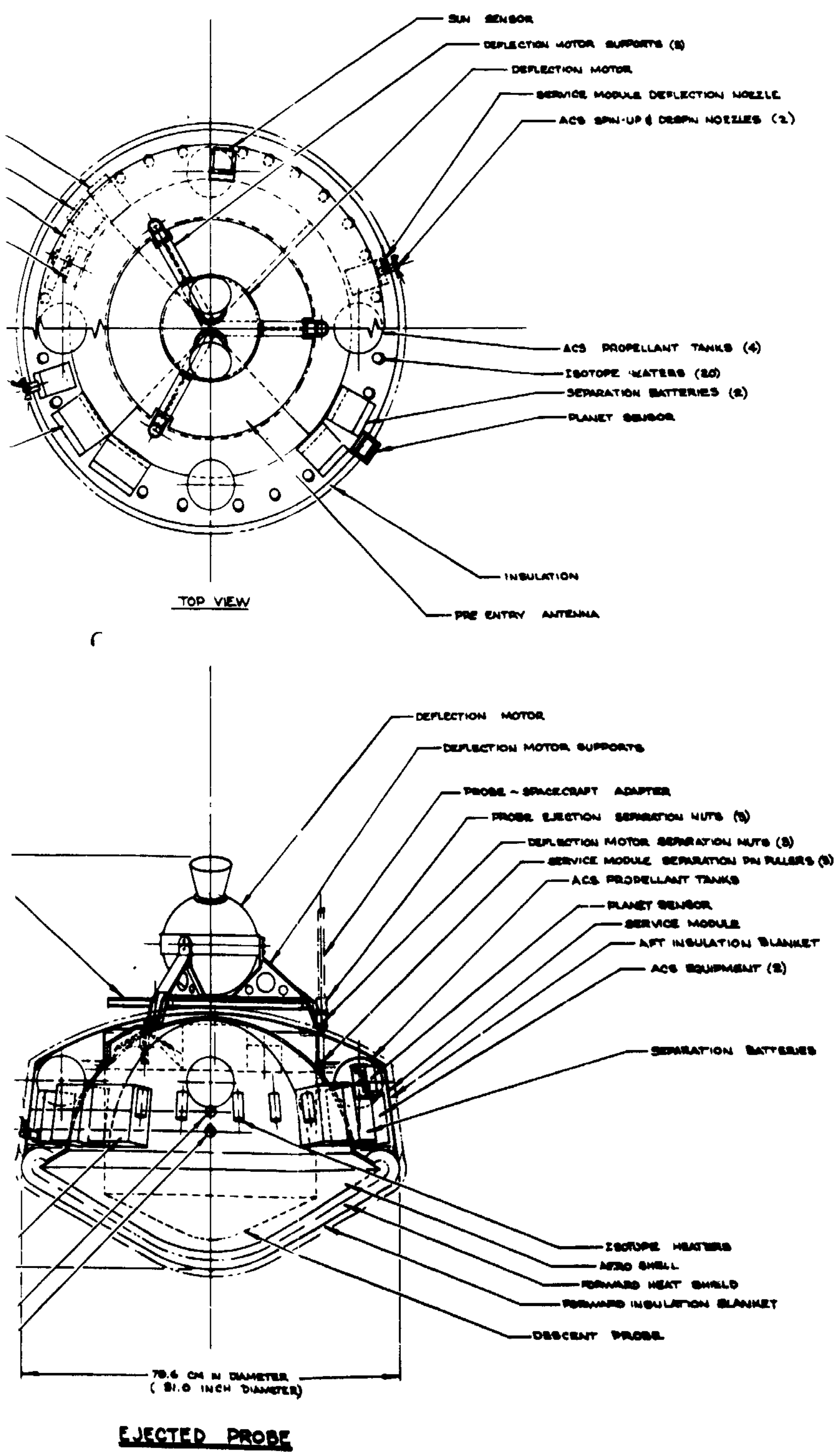

SATURN SURVIVABLE PROBE ~
TASK II CONFIGURATION II
OUTER PLANET ENTRY PROBE STUDY

Figure II-32 Alternative Saturn Probe Configuration

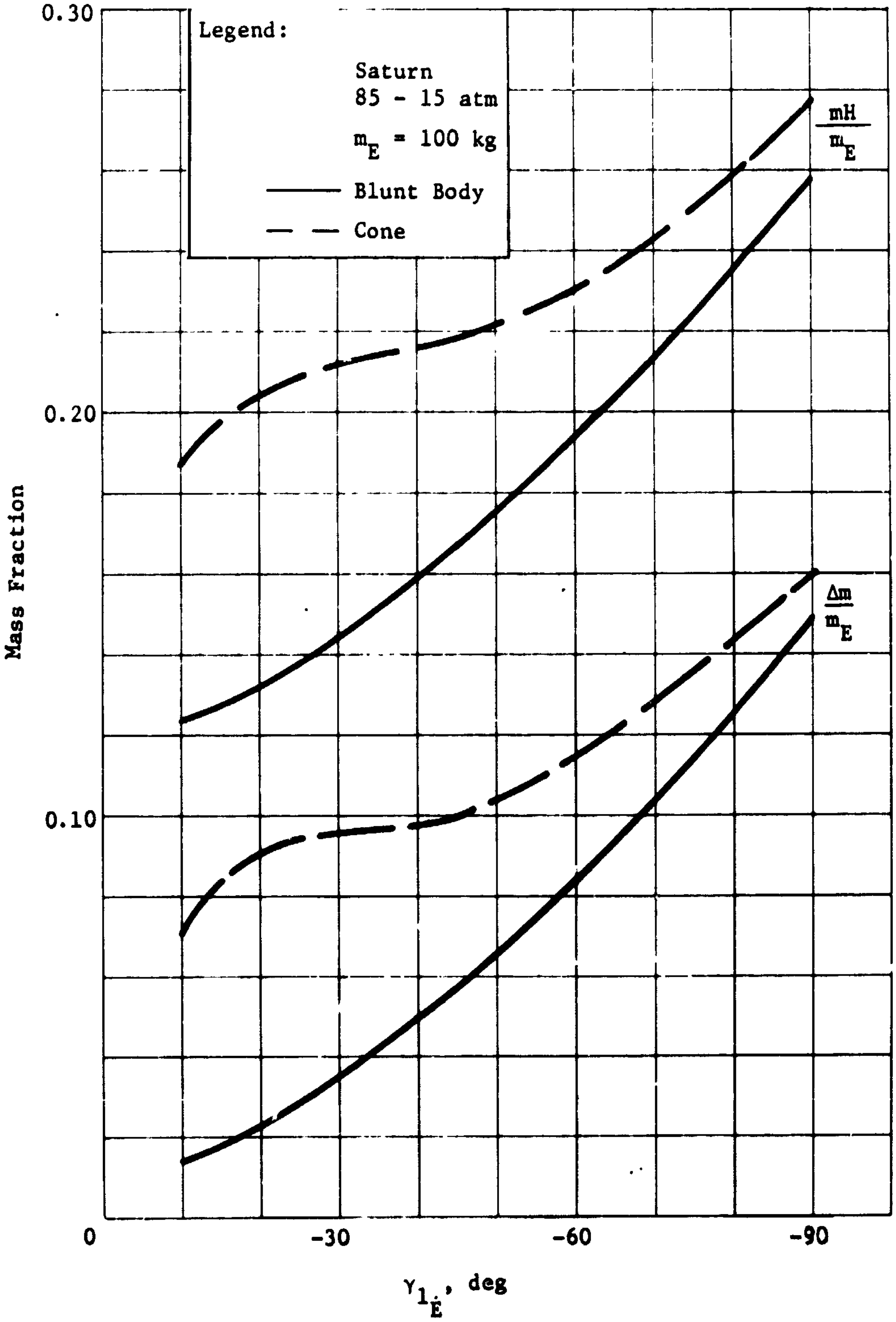

Figure II-33 Heat Shield Mass Fraction vs Entry Angle for Planet Saturn

The two probes are compared in Table II-16. As seen in the table, Configuration 1 is the lightest.

Table II-16 Configurations 1 and 2 Comparison

	CONFIGURATION 1			CONFIGURATION 2		
	SEPARATION	ENTRY	DESCENT	SEPARATION	ENTRY	DESCENT
Weight:						
kg	109	70.6	36.7	116	77.9	37.2
lbm	241	156	81.1	257	172	82
Diameter:						
cm	78.6	78.6	44.5	78.6	78.6	43.5
in.	31.0	31.0	17.5	31.0	31.0	17.1
Length:						
cm	80.3	48.2	42.9	82.5	50.8	44.5
in.	31.6	19.0	16.9	32.5	20	17.5

9. <u>Propulsion Subsystem</u>

The propulsion subsystem for the Saturn probe is identical to that for the spacecraft-radiation-compatible mission Jupiter probe except for reduced requirements. This probe is smaller and lighter than the Jupiter probe, and the required deflection maneuver is smaller, only 170 m/sec (557 fps).

The deflection motor for the Saturn probe is the smallest of those investigated for the various planetary probes. This motor is 20.3 cm (8.0 in.) in diameter and weighs 8.9 kg (19.6 lbm). It is a spherical solid propellant motor using (like the other motors designed) a dual nozzle to avoid particulate impingement on the carrier spacecraft during motor operation. The delta velocity of 170 m/sec is applicable to either the planet Saturn or Uranus, since these planets can use a common deflection delta velocity. The probe weight is also common for either planet, thus permitting the motor design to be compatible for entry in either planet.

The attitude control system for Saturn and Uranus is smaller than the other probes investigated, because of the reduced probe moment of inertia of approximately 6.6 kg/m^2 (5.0 slug/ft^2). Thus for a given spinup rate, less total impulse is required. However, the spin-despin-precess nozzles have a smaller moment arm caused by the probe smaller size. This parameter partially offsets the gain of reduced moment of inertia. The net result is a small reduction in gas weight and gas container weight for the ACS system. The total propellant gas requirement for the probe ACS maneuvers is 1.05 kg (2.33 lbm) and the gas container weight is 1.37 kg (3.02 lbm) for a total system weight of 5.7 kg (12.6 lbm).

10. Thermal Control Subsystem

A probe thermal analysis was performed for the nominal Saturn probe mission defined. These results show that passive thermal design selected is adequate to maintain the probe temperatures within limits for cruise and coast, but semi-active thermal control will be required for the more severe atmospheric descent encounter. Trajectory uncertainties for this mission were 8 minutes which is small from a thermal control standpoint. In addition, the RF transmitter power required for Saturn is small (6.5 watts RF) and consequently no transmitter thermal problems would be expected. For the descent to 7 bars, the N_2 gas environment control purge system to 2.5 bars pressure was selected for optimum design.

The probe temperature margins predicted for the Saturn probe mission are:

Temperature Margin	Spacecraft Cruise, °K	Probe Coast, °K	Entry & Descent, °K
Above Equipment Lower Limit	42	18	9
Below Equipment Upper Limit	8	25	27
Below Transmitter Upper Limit	NA	38	47

11. Spacecraft Integration

The Saturn probe has been studied for integration with the JPL Mariner Jupiter Saturn Spacecraft, Configuration 2 (JPL Drawing No. 10054478). This spacecraft configuration is shown in Figure II-34.

The integration of the Saturn probe and the Mariner spacecraft must have minimal impact on the mission and operation of the spacecraft. The probe is positioned on the spacecraft to provide for proper ejection, minimum effect on the spacecraft subsystems, and the least amount of modification of the original spacecraft concept.

The probe is mounted on the aft end of the spacecraft with its centerline angled 31° to the spacecraft centerline, away from the trajectory correction motor. The probe is supported by tubular trusses from the center cavity of the equipment bay module with the deflection motor nesting into the cavity.

The probe integration with this spacecraft is shown in Figure II-35. The probe shown in the figure is actually the alternative Saturn probe using a 1.04 rad (60°) half angle nose cone, rather than the blunt nose primary configuration. The installation would be essentially the same for either probe configuration, since there are only minor differences in the probes.

The probe is mounted so that it partially intrudes into the volume of the polygon basic body of the spacecraft. This is done to minimize the center of gravity shift of the spacecraft-plus-probe configuration as compared with that of the spacecraft-only configuration. It is mounted on the end of the spacecraft opposite the spacecraft communication antenna, so that the probe is pointed away from the Sun during most of the cruise portion of flight. This permits better thermal control of probe during the cruise portion of flight.

Changes necessary for the Mariner spacecraft to locate the probe as shown in Figure II-23 are discussed in Chapter VI, Section B.11 of Volume II.

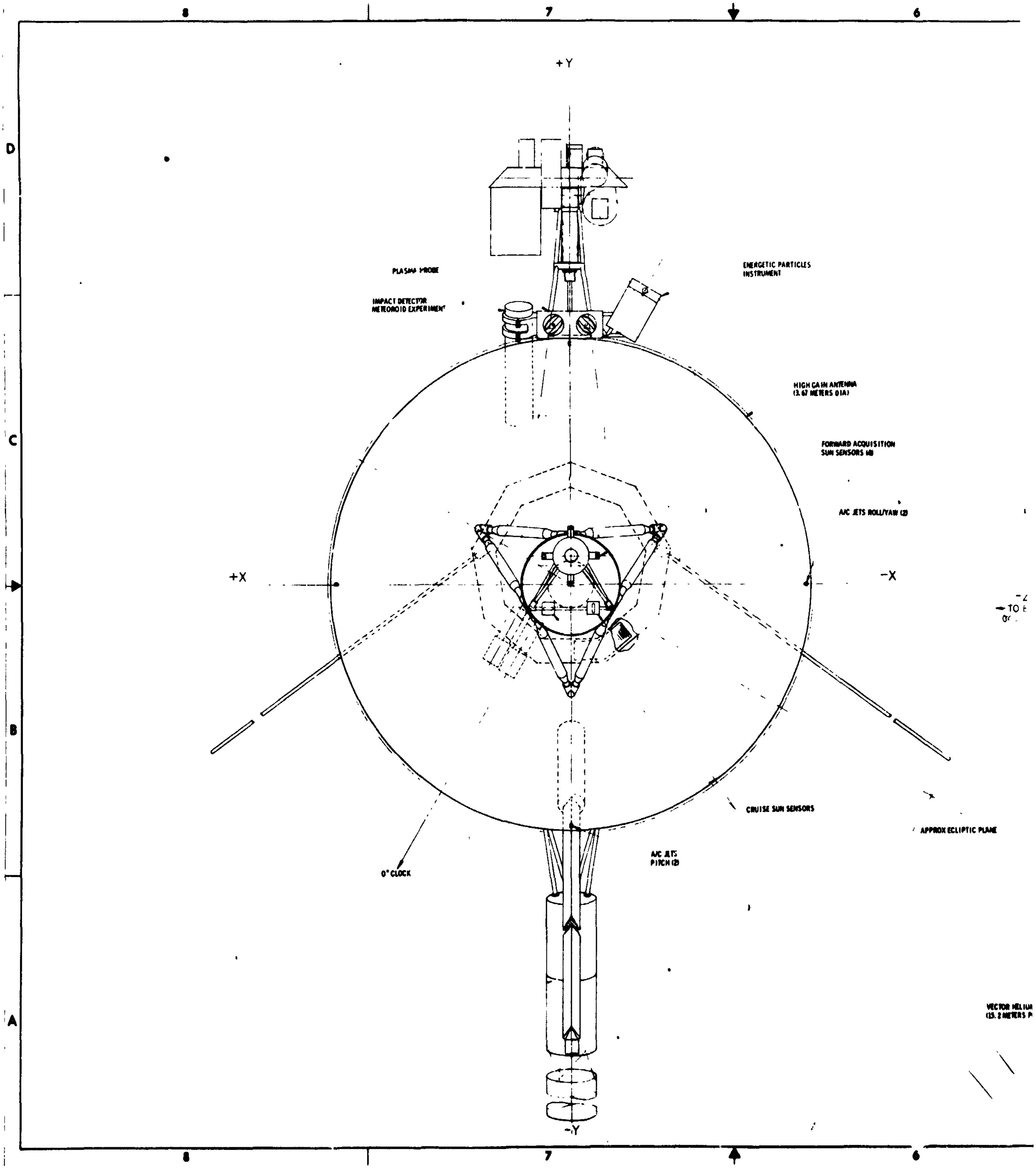

3

FOLDOUT FRAME

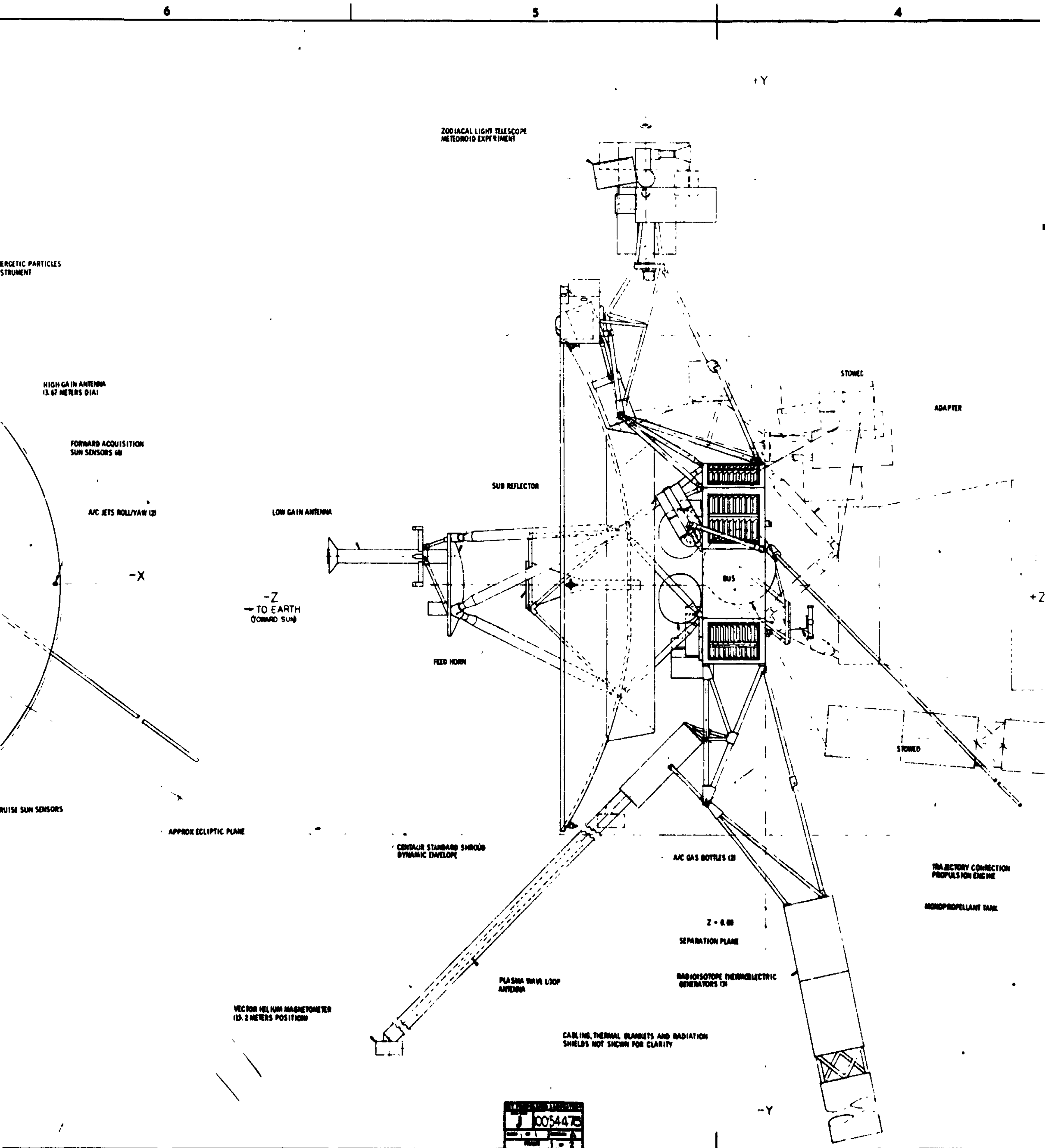

FOLDOUT FRAME 2

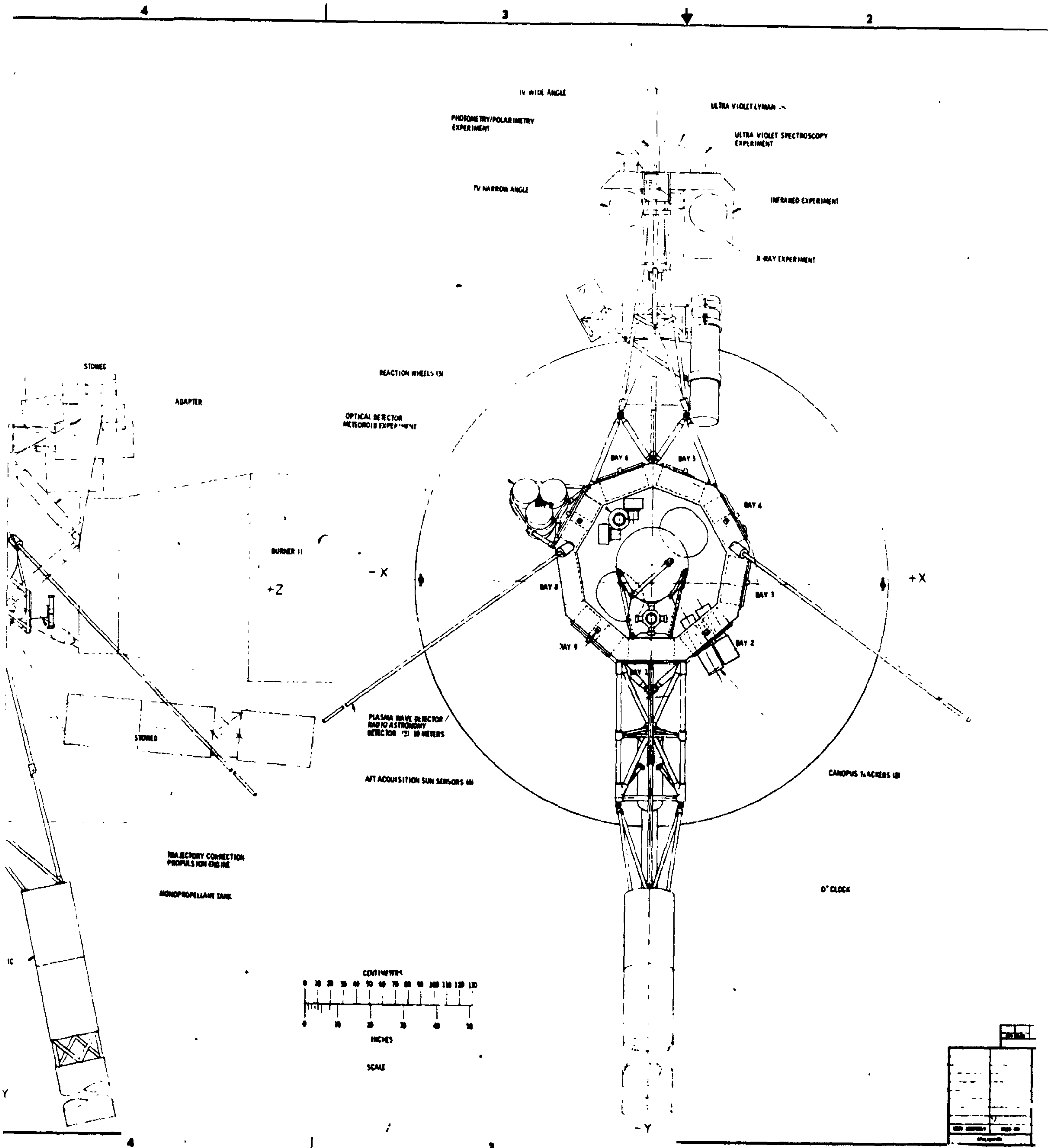

Figure II

FOLDOUT FRAME 3

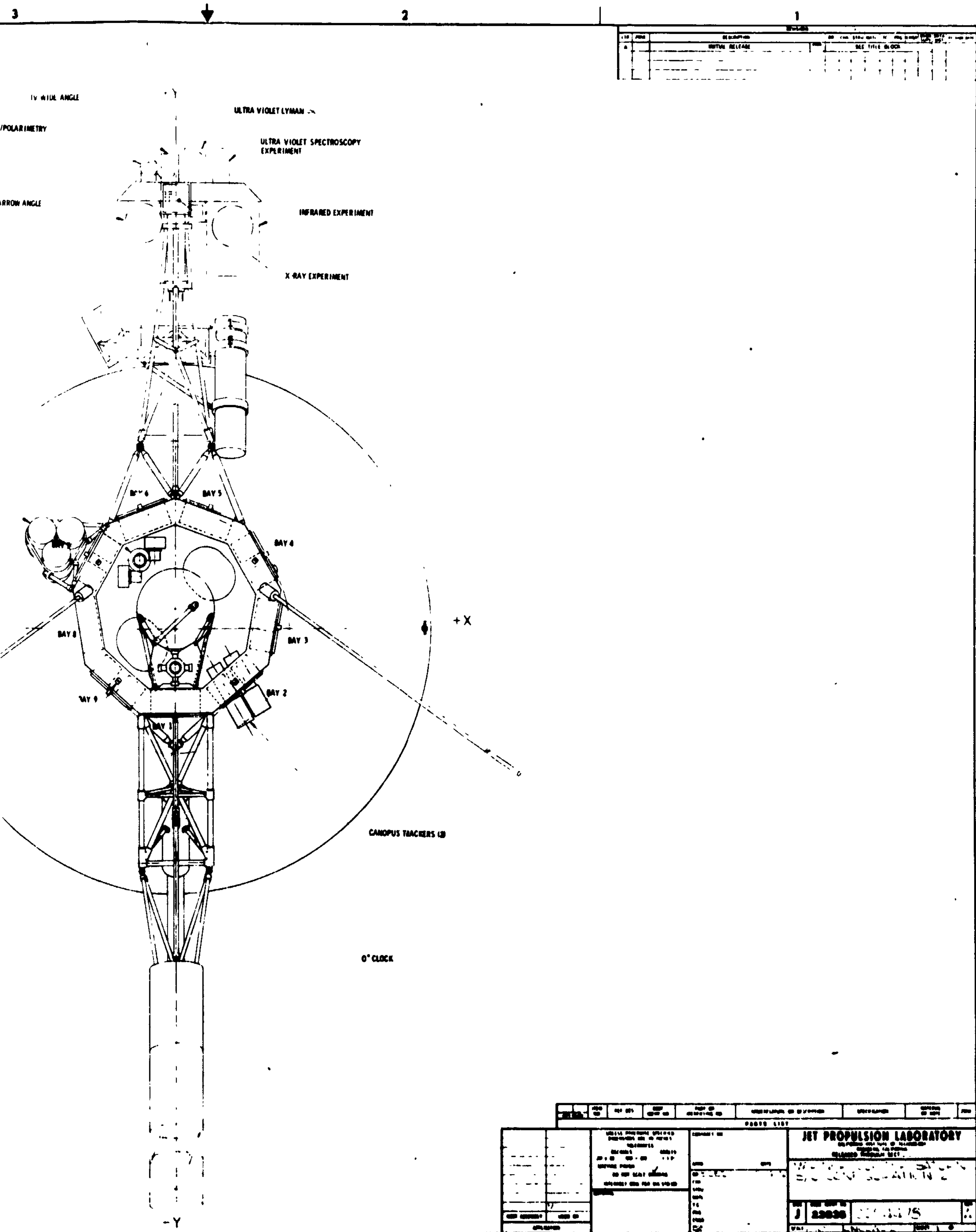

Figure II-34 Mariner Jupiter Saturn Spacecraft

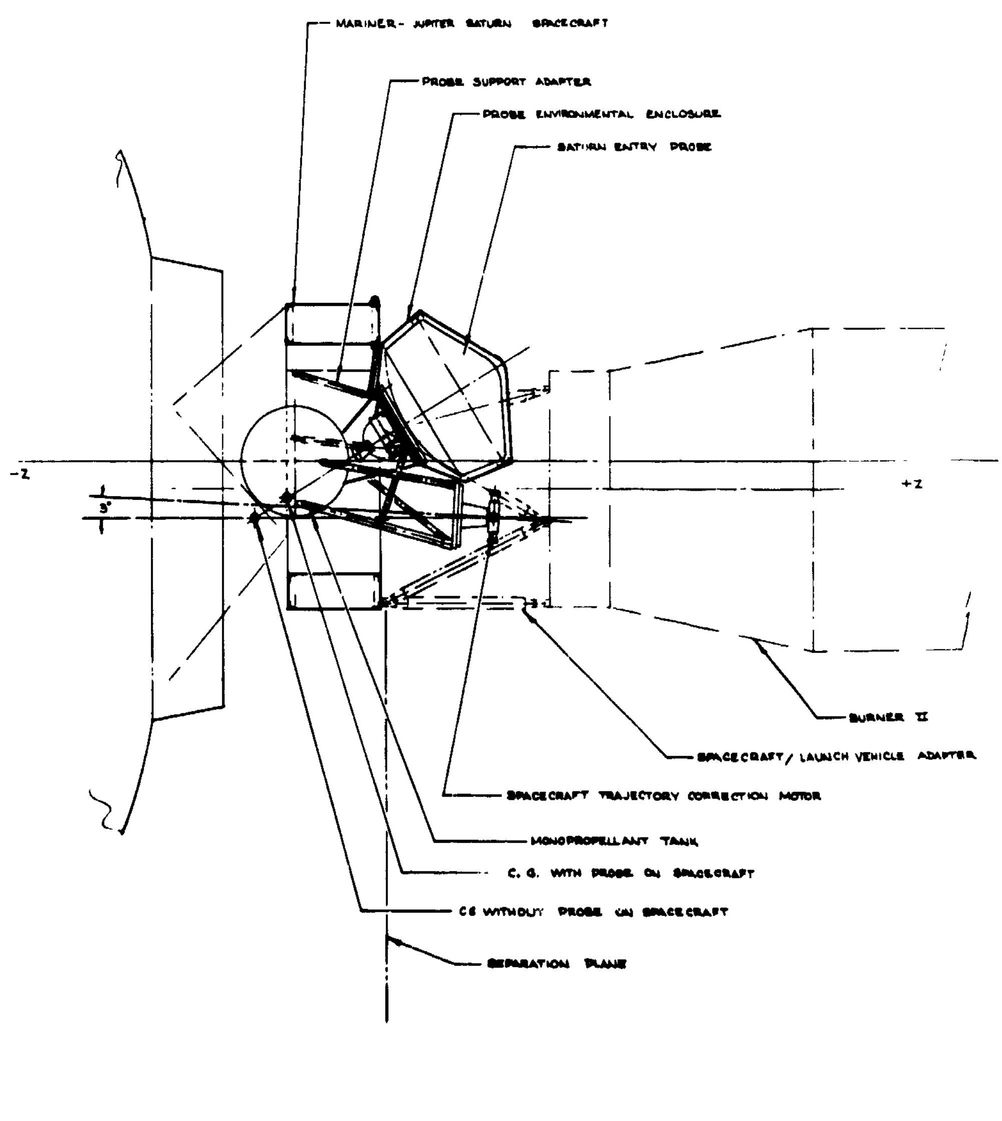

FOLDOUT FRAME

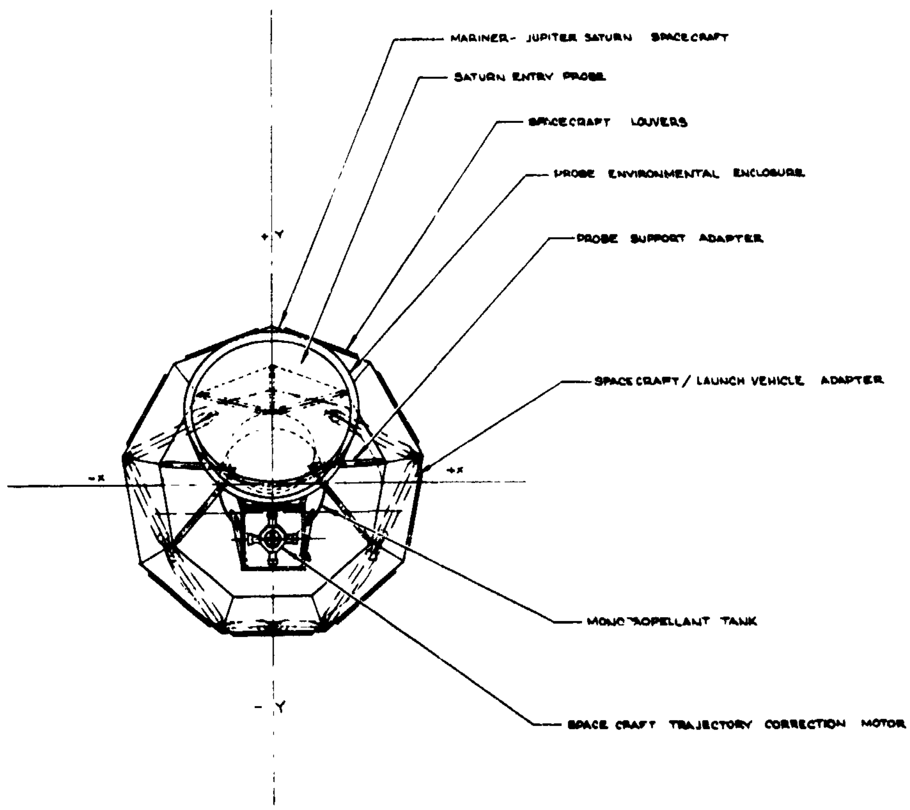

Figure II-35 Spacecraft Probe Integration Configuration

FOLDOUT FRAME 2

G. SATURN PROBE APPLICABILITY FOR URANUS SUMMARY

The object of this section is to use the Saturn probe as defined in Section II.F for atmospheric entry into Uranus and based on the parametric analysis of Section II.E.1, to identify changes only where the Saturn probe fails to meet the requirements. In such areas where the Saturn probe more than meets the requirements at Uranus, optimization is not considered. The general constraints resulted from the Uranus parametric analysis and are the following for the Uranus application:

Mission	JU-79
Entry Angle	-60° (structures designed to -65°)
Atmosphere	Nominal
Science	SAG Exploratory Payload (PAET)
Spacecraft	Mariner Family
Carrier Mode	Flyby
Periapsis Radius	2.42 R_U
Communication Mode	Relay
Deflection Mode	Probe
Entry Ballistic Coefficient	0.65 slug/ft^2 (102 kg/m^2)
Ballistic Coefficient for Heat Shield Removal	0.12 slug/ft^2 (19 kg/m^2)
Descent Ballistic Coefficient	0.7 slug/ft^2 (110 kg/m^2)

1. Mission Definition

The Uranus mission upon which the systems design is based is illustrated in Figure II-36 and summarized in Table II-17. Important characteristics of the mission design are described in this section.

a. Interplanetary Trajectory - The interplanetary trajectory for this mission is based on the JUN 79 trajectory. The flight time to Jupiter is 1.6 years with a flyby radius at Jupiter of 9.9 R_J. The total flight time to Uranus is 6.5 years. The flyby radius at Uranus was selected to be 2.42 R_U to be consistent with the JUN 79 mission. Thus, if the spacecraft continues past Uranus, it will encounter Neptune after a total flight time of 10.3 years.

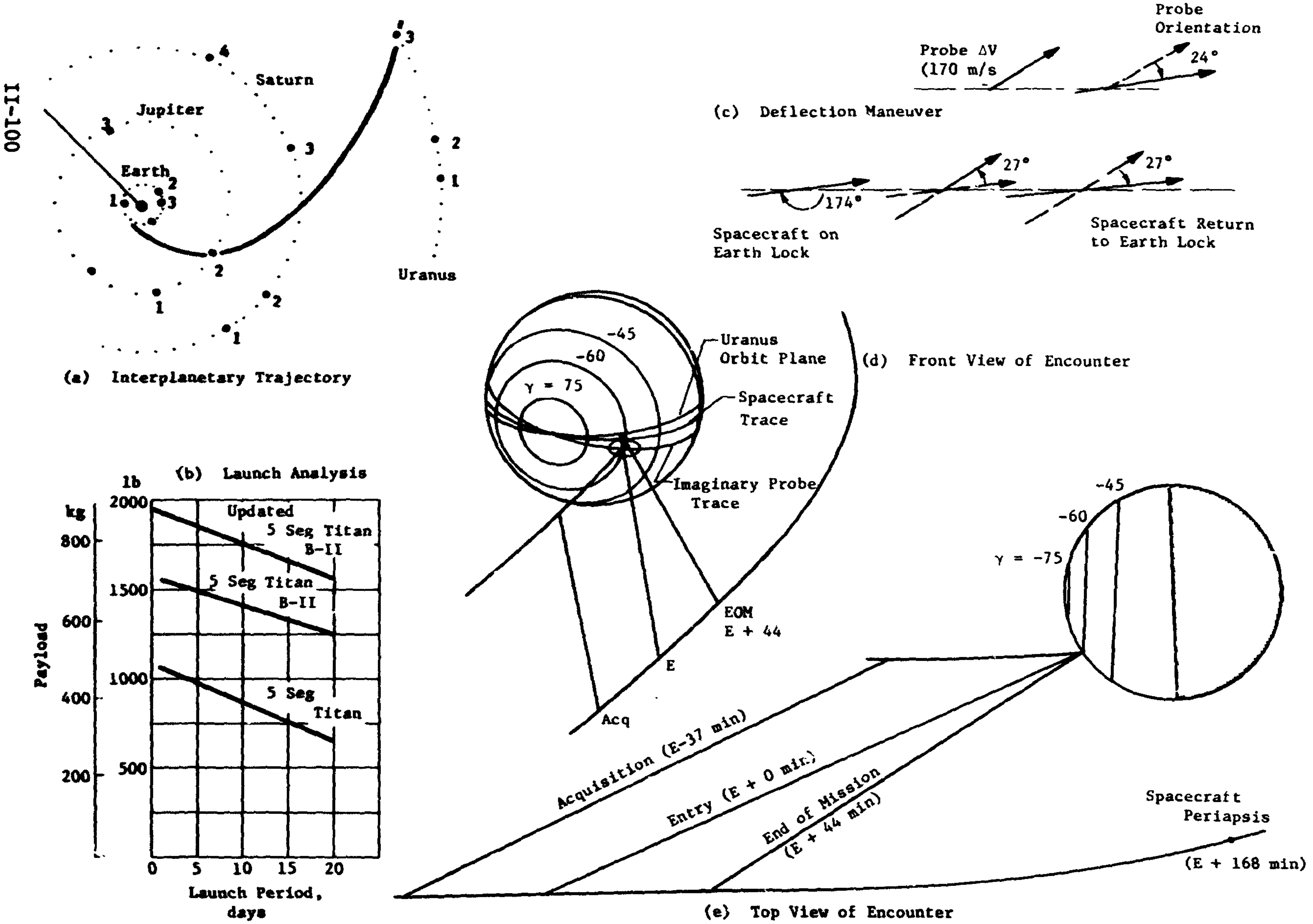

Figure II-36 Uranus Mission Description

Table II-17 Uranus Mission Summary

a. Conic Trajectory Data

Interplanetary Trajectory	Launch Trajectory	Arrival Trajectory
Launch Date: 11/6/79 Arrival Date: 5/19/86 Flight Time: 2386 days Central Angle: 212.2	Nominal C_3: 102 km^2/sec^2 Nominal DLA: 27.0° Launch Window: 4 hr Parking Orbit Coast: 40 min C_3 (10 day): 107 km^2/sec^2 C_3 (20 day): 113 km^2/sec^2 Azimuth Range: Σ_L = 10° - 110°	VHP: 13.62 km/sec RA: 255.1° DEC: -29.9° ZAE: 174.14° ZAP: 175.32° RP: 2.42° INC: 98.02°

b. Deflection Maneuver and Probe Conic

Deflection Maneuver	Probe Conic Definition
Deflection Mode: Probe Deflection Radius: 9.75 x 10^6 km Coast Time: 8.06 days ΔV: 170 m/sec Application Angle: 33° Out-of-Plane Angle: 9.1° Rotation for Probe Release: 27.3° Probe Reorientation Angle: -24.3° Spacecraft ΔV from Earth: NA	Entry Angle: -60° Entry Latitude: 53.98° Entry Longitude: 284.17° Lead Time: 168.3 min Lead Angle: -12.07° Probe-Spacecraft Range (Entry): 146,843 km Probe Aspect Angle (Entry): 18.03° Probe Aspect Angle (Descent): 13.91° Probe Aspect Angle (EOM): 7.61°

c. Dispersion Analysis Summary

Naviation Uncertainties	Execution Errors (3σ)	Dispersions (3σ)
Type: Optical/30 day Tracking arc SMAA: 1277 km SMIA: 424 km β: TOF: 440 sec	ΔV Proportionality: 1% ΔV Pointing: 2° Probe Orientation Pointing: 2°	Entry Angle: 6.08° Angle of Attack: 3.37° Down Range: 8.46° Cross Range: 8.04° Lead Angle: 6.60° Lead Time: 1.69 min Entry Time: 22.89 min

d. Entry and Descent Trajectory Summary

Entry Parameters	Descent Parameters	Critical Events: Time from Entry	Critical Events: Altitudes above 1 atm
Entry Velocity, km/sec: 25 Entry Altitude, km: 531 Entry B, $slug/ft^2$: 0.65 kg/m^2: Entry Atmosphere: Nominal Max Deceleration, g: 357 Max Dynamic Pressure, lb/ft^2: 7.4 x 10^3 kg/m^2: 3.5 x 10^5	Descent Atmosphere: Nominal EOM Pressure, bar: 7.0 Descent B, $slug/ft^2$: 0.7 kg/m^2: 109.9	g = 0.1, sec: 4.0 Max g, sec: 17.0 M = 0.7, sec: 54.3 Descent Time, min: 43.1 EOM, min: 44.0	km: 444 km: 138 km: 78.6

b. Launch Analysis - Available payload weight is plotted against launch period for three sets of launch performance data in Figure II-36(b). It should be noted that the Burner II stage is required if the Titan III/5-Segment vehicle is to be used for the launch vehicle.

c. Approach Trajectories - A front and top view of the Uranus encounter is provided in Figures II-36(d) and (e). The spacecraft trajectory was selected to be consistent with the JUN 79 mission, as explained above. The probe entry angle of -60° was selected to obtain an entry site well on the Sun-lit side of the planet. The probe was deflected so that at about the middle of descent, the spacecraft was nearly overhead the probe. This results in a link geometry quite different from the other missions.

d. Deflection Maneuver - A probe deflection maneuver was used to establish the above defined link geometry and acquire the entry side. A deflection radius of 9.75×10^6 km was used in order to obtain the same ΔV requirements (170 m/sec) as the Saturn mission. The implementation sequence is pictured in Figure II-36(c). The rotation angles are all quite small.

e. Navigation and Dispersions - This design mission is required to assume optical tracking because standard Earth-based tracking results in extreme dispersions. This is caused by the fact that Uranus' ephemeris uncertainties are about ten times more severe than those at Saturn. The navigation results provided in Table II-17(c) are consistent with including optical tracking along with standard Earth-based tracking. Even with the optical tracking, the navigation uncertainties dominate the execution errors in determining dispersions. The dispersions are now quite reasonable but the subsystems can still be designed to accommodate them.

f. Entry and Descent Trajectories - Table II-17(d) summarizes the entry and descent phases of the mission. Both phases were simulated using the nominal atmospheric model. The entry phase starts at 531 km above the 1 atm pressure level (0 km alt = 26,468 km) and ends with the staging of the aeroshell 54.5 sec later. During this phase, a peak deceleration of 357 g is attained 19.0 sec after entry. The descent phase starts after staging of the aeroshell and continues through the end of mission at 7.0 bars. The total descent time is 43.1 min.

3. Science

The instruments for the Uranus probe are identical to those for the Jupiter alternative probes. The only difference would be a modification of the range of the temperature gage, and possibly entry accelerometers for the colder environment and lower g-load, respectively.

The results of the descent profile parametrics are:

Design Limit Pressure = 7 bars

Parachute Ballistic Coefficient = 0.70 slug/ft^2 (109.9 kg/m^2)

Parachute Deployment Pressure = 33 millibars

Pressure at First Measurement = 39 millibars

Entry Time = 43 min, 4 sec

Instrument Sampling Times:

Temperature and Pressure = 4.0 sec
Neutral Mass Spectrometer = 60 sec
Descent Accelerometers = 8.0 sec
Entry Accelerometers = 0.2/0.4 sec

Total Bit Rate = 25.3 bps

All of the requirements have been satisfied, exceeding the criteria in order to keep the instrument sampling times the same as those used for Saturn. Figure II-37 shows the selected pressure descent profile for Uranus.

3. System Integration

The functional sequence for Uranus is very similar to that of Saturn except for a 23-min uncertainty at arrival. The data profile is similar to Saturn except for a 25 bps data rate during descent. The power profile approximates that for Saturn except for the effect of the entry uncertainty and for the fact that an additional descent battery is required for thermal control. Comparisons between Saturn and Uranus probes are shown in Table II-18.

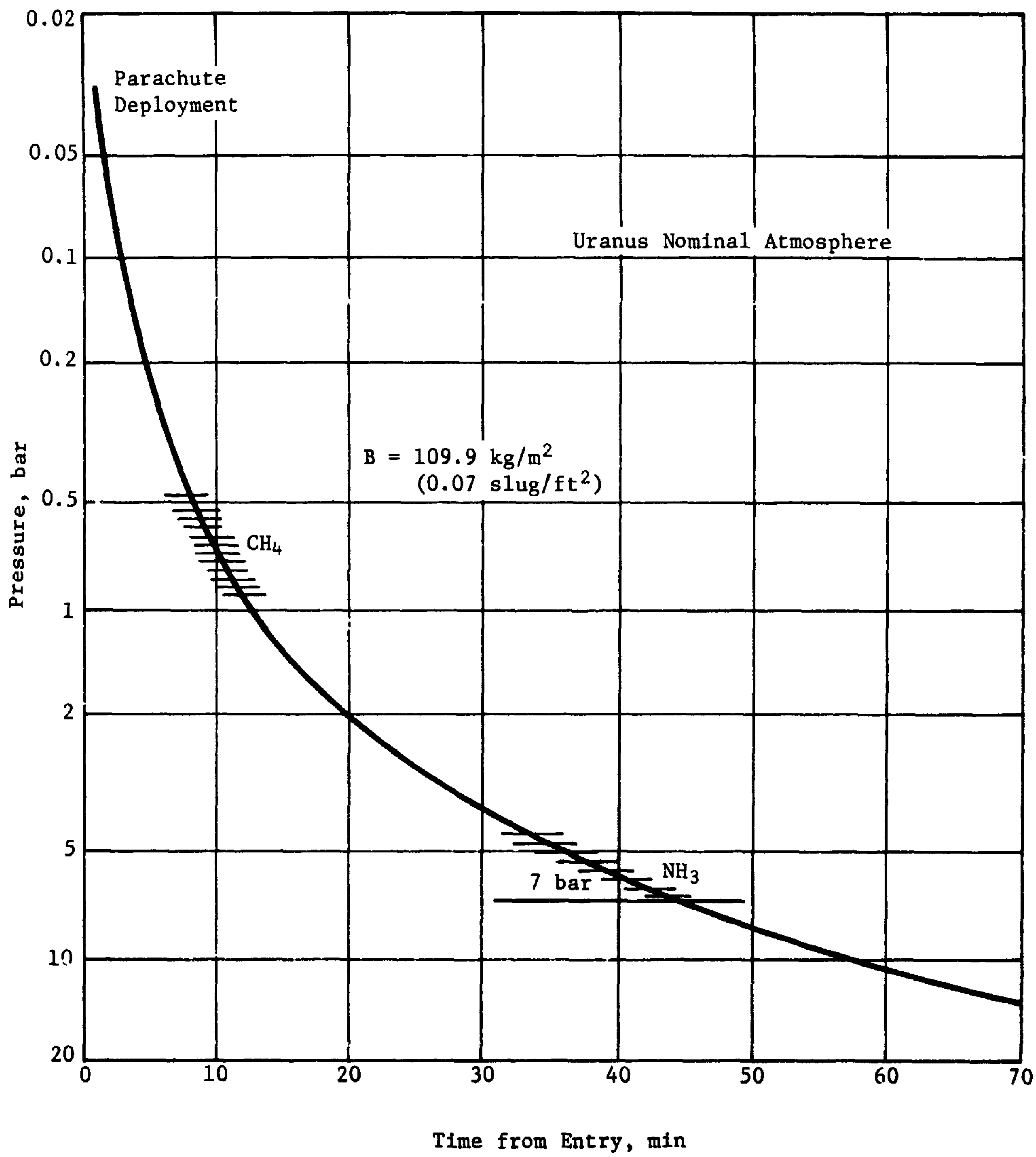

Figure II-37 Uranus Probe Pressure Descent Profile

Table II-18 Saturn/Uranus Probe Comparisons

Parameter	Saturn	Uranus
Probe, ΔV, m/sec	170	170
R_{EJ}, x 10^6 km	10.15	9.75
Entry Ballistic Coefficient, kg/m^2	102	102
Descent Ballistic Coefficient, kg/m^2	110	110
Max Deceleration, g	350 for -30° γ_E	380 for -65° γ_E
Descent Depth, bars	7	7
End of Mission, Entry +	41 m, 43.5 sec	43 m, 58.5 sec
Heat Shield Design Mass Fraction	0.215	0.126
Data Storage, bits	12,400	12,400
Descent Data Rate, bps	26.3	25.3
RF Power at 0.86 GHz for same Space- draft Antenna, W	6.5	6.4
Descent Battery, W-hr	68	93 + 12 for Thermal
Pre-Entry Antenna	Planar	Turnstile/Flared Cone
Thermal Control	Partially Sealed	Partially Sealed with an Added Descent Bat- tery
Ejected Weight, kg (lb)	108 (238)	Uranus ejected weight
Entry Weight, kg (lb)	68 (149)	is approximately 2 kg heavier than the Saturn
Descent Weight, kg (lb)	37 (82)	probe.
Heatshield Diameter, m (in.)	(31)	
Descent Probe Diameter, m (in.)	(17.5)	

4. Telecommunications Subsystem

Table II-19 depicts design details of the RF components which comprise the telecommunications subsystem for the Uranus mission. Complete details of the components are given in Volume II, Chapter V, Section A.4. 6.5 watts of RF power is required at 0.86 GHz with a bit rate of 26 bps using binary FSK with a tracking tone. The subsystem hardware design is identical to the Saturn mission except for the preentry antenna which must be changed to a 90° axial beam. Identical antennas may be employed for both preentry and descent for this mission.

5. Data Handling Subsystem

The DHS for Saturn and Uranus are essentially identical in configuration and function. The dissimilarities are slight differences in timing, sequence, and format during the entry and descent phase of the mission. These dissimilarities could be eliminated by the use of a programmable memory (core, plated wire) or by including dual banks of sequence and format control logic. The desired mission could then be selected by ground controlled programming power switching.

6. Power and Pyrotechnic Subsystem

The power and pyrotechnic subsystem for Saturn and Uranus are essentially identical in configuration. The only significant dissimilarity consists of the entry/descent (Ag-Zn) battery size and the Hg-Zn (pyrotechnics) battery size. These dissimilarities could be eliminated by using the Uranus design batteries, with negligible cost in weight.

7. Attitude Control Subsystem

The ACS subsystem for Saturn and Uranus are similar in configuration. The principal differences are (1) sensor design for low solar intensity at Uranus, and (2) ACS logic. The dissimilarity of (1) could be eliminated by the use of two Sun sensors, appropriately mounted for the two missions, and the use of a Uranus planet sensor that would perform equally well for Saturn. The changes in the logic (2) would be implemented by DHS control or the use of two sets of logic. The additional electronics would represent a minor increase in weight. The logic and sensor not in use on the selected mission would be removed from the power bus by a latching relay during preseparation checkout and would not require additional power.

Table II-19 Telecommunications RF Subsystem for the Uranus Mission

Conditions: Planet - Uranus; Spacecraft - Mariner; Frequency - 0.86 GHz; Bit Rate - 26 bps

Component	Characteristic	Unit	Value
Transmitter	RF Power Out	W	6.5
	Overall Efficiency	%	45
	DC Power in at 28 V dc	W	14.5
	Total Weight	kg	2.72
		lb	6.0
RF Switch	Type		Solid State
	Insertion Loss	dB	0.3
	Weight	kg	0.1
		lb	0.2
Entry Antenna	Type		Turnstile/Cone
	Main Beam Angle	deg	0
	Beamwidth	deg	90
	Max Gain	dB	6
	Size (dia x h)	cm	20.3 x 7.6
		in.	8 x 3
	Weight	kg	0.45
		lb	1.0
Descent Antenna	Type		Turnstile/Cone
	Main Beam Angle	deg	0
	Beamwidth	deg	90
	Max Gain	dB	6
	Size (dia x h)	cm	20.3 x 7.6
		in.	8 x 3
	Weight	kg	0.45
		lb	1.0
Spacecraft Antenna	Type		Helix
	Beamwidth	deg	35
	Max Gain	dB	13.5
	Size (l x dia)	cm	73.2 x 11.1
		in.	28.8 x 4.4
	Weight	kg	2.72
		lb	6.0
	Despin		no
	Position Search		1
	Frequency Acquisition	sec	25
	Clock Angle, θ	deg	-101
	Cone Angle, ϕ deg	deg	154.3
Spacecraft Receiver	Noise Temperature	°K	300
	Noise Figure	dB	3.1
	DC Power in at 28 V dc	W	3.0
	Weight	kg	0.9
		lb	2.0

8. Structures and Mechanics

The entry conditions selected for the planet Uranus results in a deceleration load of 380 g, as compared with 350 g for entry into the atmosphere of Saturn. This small difference is reflected in a delta weight in the equipment support deck of the probe of approximately 0.11 kg (0.25 lbm). Likewise, the delta weight for the descent probe outer structure is approximately 0.11 kg (0.25 lbm). The delta weight for the aeroshell base cover is insignificant.

The aeroshell weight is designed by the peak dynamic pressure at entry. Entry at Uranus results in a dynamic pressure of 36 x $10^4/m^2$ (7400 lbf/ft^2). The delta weight for the aeroshell is approximately 0.09 kg (0.20 lbm) to accommodate the difference in pressure acting on the nose cone. Thus, it is apparent that the total structural weight is affected by less than 0.45 kg (1.0 lbm) for entering one planet versus the other. This value is insignificant; the probe design for the joint planet entry is based on the higher loads encountered at Uranus.

Unlike the design of the structure, the severest heat shield requirements are for the planet Saturn. The 65° entry angle at Uranus requires a heat shield mass fraction of only 0.126 and would result in a heat shield weight of 7.74 kg (17.1 lbm). For the entry angle at Saturn, the heat shield mass fractions is 0.145. The heat shield weight for Saturn is therefore 8.9 kg (19.7 lbm). The penalty paid for using the Saturn heat shield to enter Uranus is therefore 1.2 kg (2.6 lbm).

9. Propulsion

The delta velocity required for the deflection maneuver is essentially identical for either Saturn or Uranus. The same motor configuration is thus used for either planet. This motor is discussed in Volume II Chapter VI, Section B.9.

The precession maneuver for the probe to enter Uranus is only 24°. The ACS propellant to perform this precession maneuver is 0.141 kg (0.311 lbm) as compared to 0.388 kg (0.856 lbm) for the precession angle for Saturn. Thus, 0.247 kg (0.545 lbm) of ACS cold gas propellant could be saved; thus a total system weight (propellant plus tank) of 0.57 kg (1.25 lbm) could be saved for a Uranus-only probe design.

10. Thermal Control Subsystem

A probe thermal analysis was performed for the nominal Uranus probe mission defined. These results show that the thermal design is critical for this mission because of the low probe entry temperature obtainable (284°K) and the very cold planetary atmosphere anticipated. To provide adequate thermal protection for this mission, both N_2 gas environmental control and thermostatically controlled electric heaters are recommended (Chapter VII, Section A.10.C in Vol II). The N_2 gas provides adequate probe temperature control until approximately 3 bars pressure (approximately 25 min after entry) after which time battery heating is required. The heater power requirement to maintain the battery at 5°K above its allowable lower operating limit would be approximately 12 W-hr of energy with 50-W peak power required at the end of the design mission.

The probe temperature margins predicted for the Uranus probe mission are:

Temperature Margin	Spacecraft Cruise, °K	Probe Coast, °K	Entry Descent, °K
Above Equipment Lower Limit	42	12	5
Below Equipment Upper Limit	8	25	30
Below Transmitter Upper Limit	--	38	52

11. Probe to Spacecraft Integration

Integration of the Uranus probe with the Mariner Jupiter Saturn Spacecraft is discussed in Volume II, Chapter VI, Section B.11 for Saturn. The only unique requirement for the Uranus probe is that optical tracking of the planet is required by the spacecraft to reduce the navigation uncertainties as discussed in Section G.1.

H. PARAMETRIC ANALYSES RESULTS

Analyses were conducted in such areas as missions, science and subsystems as a means of determining constaints for probe definitions. This chapter covers general mission parametric analyses, followed by those analyses peculiar to Jupiter, Saturn, Uranus, and Neptune.

1. Mission Analysis Parametrics

A summary of the most important mission design considerations is provided in this subsection where side-by-side comparisons of the different planets may be made. In earlier chapters of this volume, individual discussions of each planet were given with references to the figures included.

a. Launch Opportunity Comparisons - Available payload (probe, spacecraft, spacecraft modifications, and spacecraft/launch vehicle adapter) is plotted versus trip time in Figure II-38 for the 1979 launch opportunity. The result is that for a 20-day launch period satisfying the range safety constaint, the optimal trip time is slightly less than 700 days. This corresponds to missions arriving at Jupiter just before Jupiter is occulted by the Sun. The payload is based on the standard performance data for the five-segment Titan with the Burner II stage.

Figure II-39 provides a comparison of the four launch opportunities between 1978 and 1982. The payloads are based on 20-day launch periods for the reference missions noted for each opportunity in Figure IV-16 of Volume II assuming the standard performance data for the Titan IIIE/Burner II vehicle. The progressive improvement with each year is clear. Several reference weights are also indicated on the figure to aid interpretation of the results.

b. Rotation Rate Matching - In order to approximate the optimal relay link geometry described in Mission Design Considerations, Section A, it is necessary that the spacecraft angular rate be as close to the planet rotation rate as possible. Figure II-40 illustrates the results of a rotation rate matching study for each of the candidate planets. As indicated, the periapsis radii that result in effective rate matching for mission of about 30-min descent times are approximately 2.7 R_J, 2.5 R_S, 3.5 R_U, and 5.0 R_N for Jupiter, Saturn, Uranus, and Neptune, respectively. Actually the optimal periapsis radius is very mission-dependent and must be computed for the specific entry angle, descent time, and approach velocity magnitude of the mission under consideration.

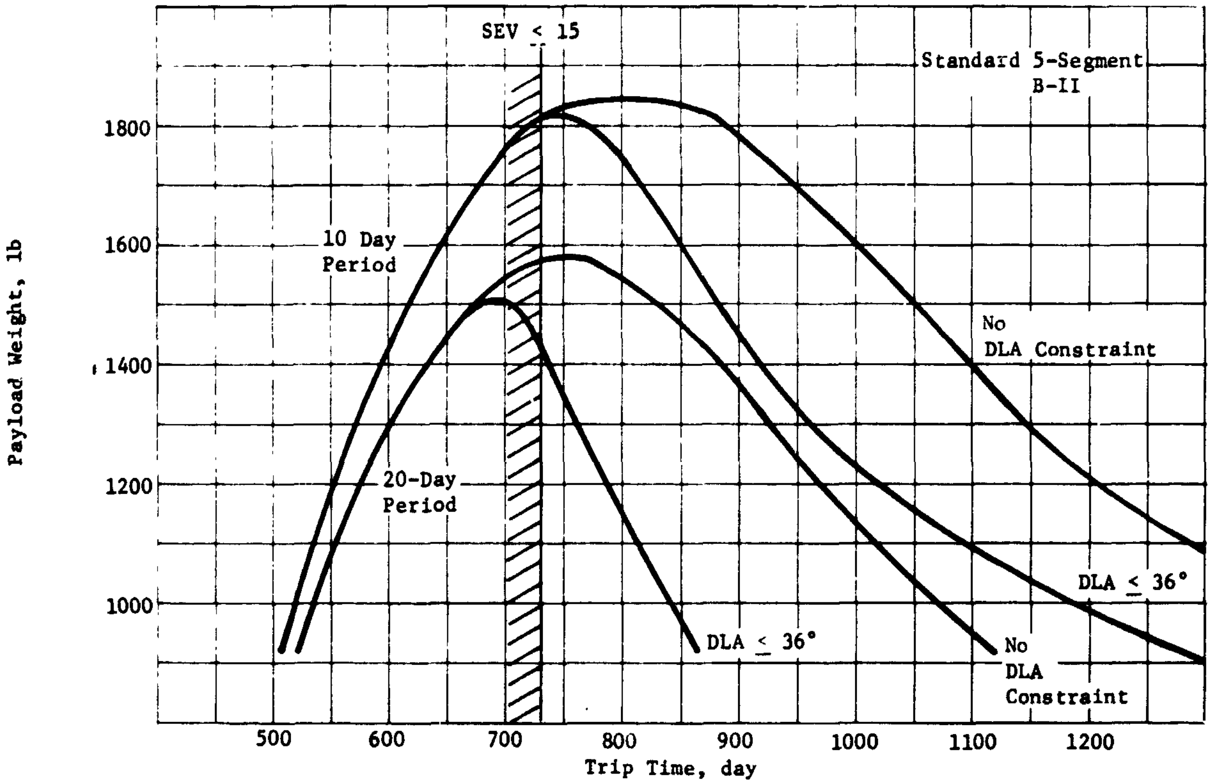

Figure II-38 Optimization of Trip Time for 1979 Launch to Jupiter

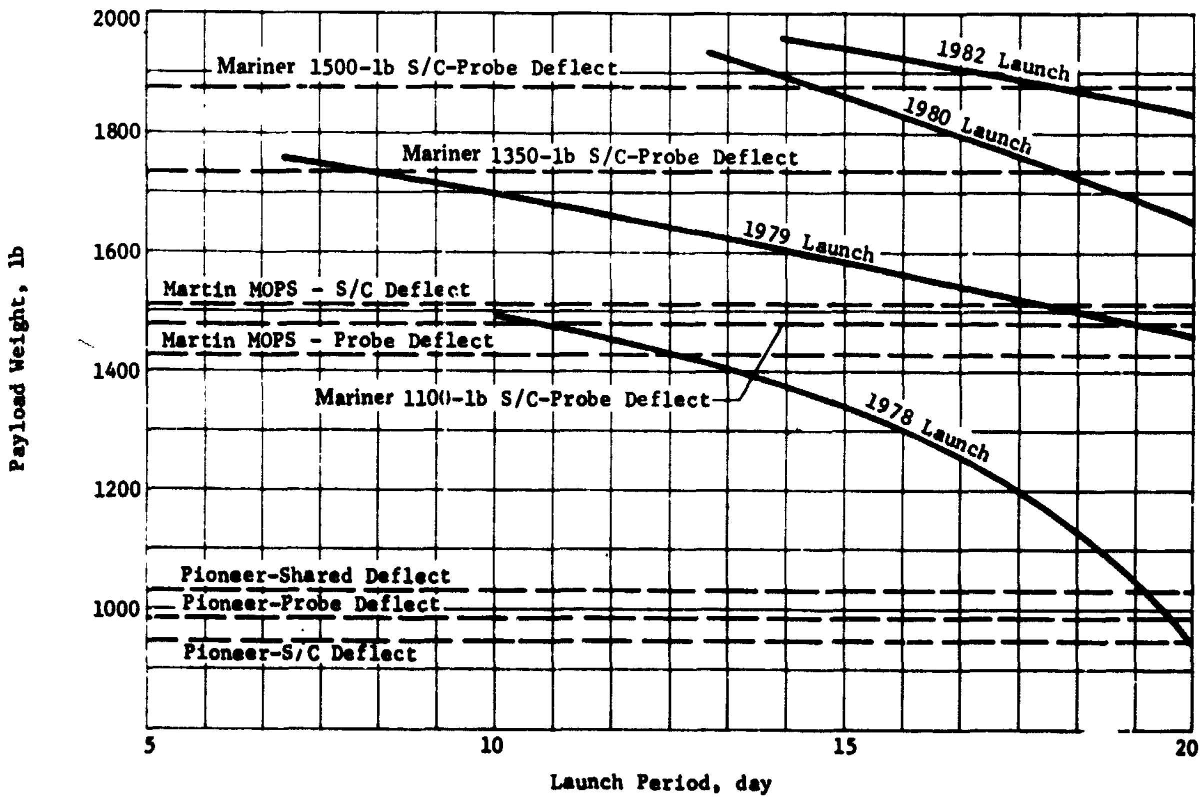

Figure II-39 Comparison of Launch Opportunities

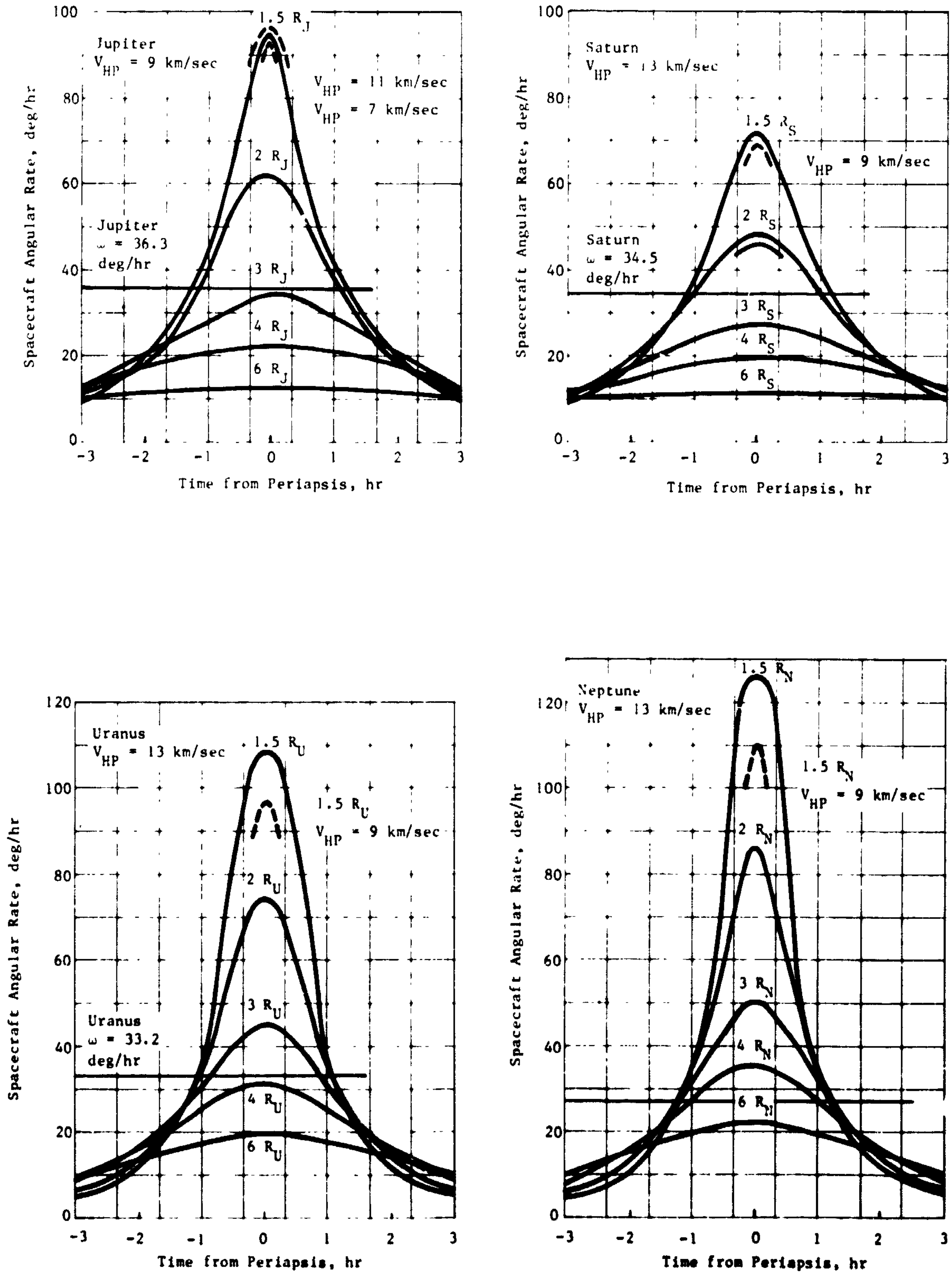

Figure II-40 Rotation Rate Matching at Planets *c. Deflection ΔV Requirements* - Deflection ΔV requirements are given for a wide range of parametrics in Figure II-41. The important trends are summarized here.

Deflection Radius - The ΔV requirements are reduced drastically as deflection radius is increased. This is apparent from the significant downward slopes of all the curves even when plotted on a logarithmic scale as in Figure II-41.

Spacecraft Periapsis - The ΔV requirements are about linearly proportional to the spacecraft periapsis; doubling the periapsis radius doubles the ΔV requirements for a fixed deflection radius.

Entry Angle - The ΔV requirements increase with entry angle as indicated for Uranus in Figure II-41. For the Jupiter nominal mission $\left(2\ R_J\right.$ periapsis, $\left.10 \times 10^6\ \text{km deflection radius}\right)$, the ΔV requirements increased from 205 to 221 to 249 m/sec, respectively, as the entry angle increased from -10° to -20° to -30°.

Approach Velocity - The ΔV requirements increase only slightly with approach velocity V_{HP}. For the Jupiter nominal mission $\left(2\ R_J \text{ periapsis, } 10 \times 10^6 \text{ km deflection radius, } -20° \text{ entry angle}\right)$, the ΔV increased from 214 to 221 to 225 m/sec as the V_{HP} was increased from 5 to 8.47 to 11 m/sec.

Deflection Mode - A comparison of the ΔV requirements for the three deflection modes is provided in Figure II-41. The ΔV requirements for the probe in probe deflection and the spacecraft in spacecraft deflection are identical. Generally for shared deflection, the probe ΔV is slightly higher than this value and the spacecraft ΔV is slightly lower.

Planetary Comparisons - The ΔV requirements are approximately proportional to the mass of the planet as indicated. Thus, reasonable deflection radius ranges appear to be 10-50 million km for Jupiter, 10-30 million km for Saturn, and 5-15 million km for Uranus and Neptune.

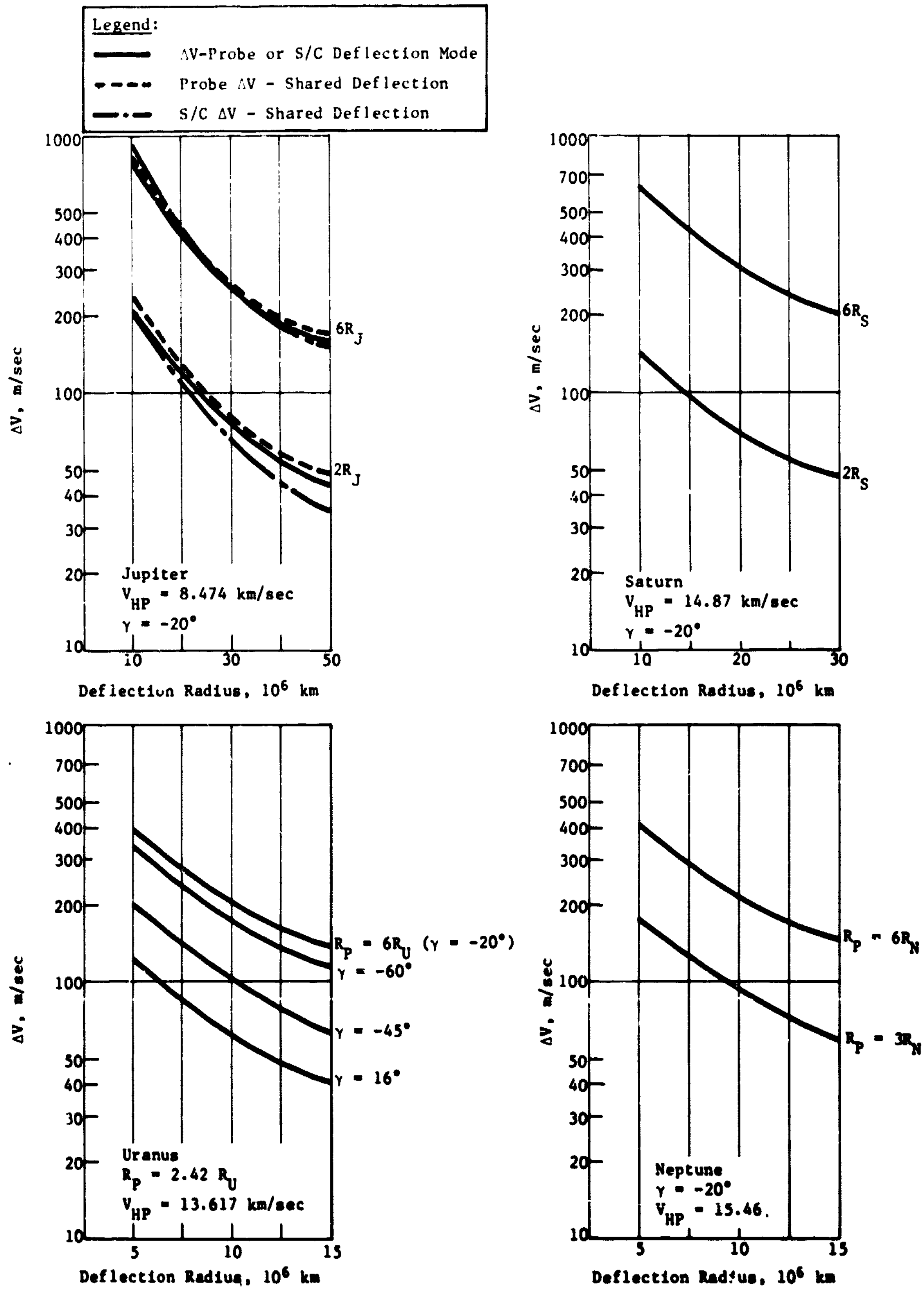

Figure II-41 Comparison of Deflection ΔV Requirements *d. Dispersion Parametrics* - The entry dispersions are produced by both errors in the spacecraft state at deflection caused by navigation uncertainties and errors in the delivered deflection ΔV caused by implementation errors. Table II-20 compares the relative contributions by these two error sources for missions at Jupiter, Uranus, and Saturn. The execution errors (3σ) in all cases are 1% proportionality, 2° pointing, and 2° orientation. The navigation uncertainties for Jupiter and Saturn assumed Doppler/range tracking only; the Uranus mission assumed optical tracking. For each mission, dispersions are given for navigation errors only, and for the combined effects of both navigation and execution errors. It is seen that at Jupiter the dispersions are totally dominated by execution errors. At Saturn, navigation and execution errors have about an equal effect. At Uranus navigation errors begin to dominate; the fact, with Earth-based tracking, 1% of the probes would miss Uranus. Even using optical tracking, the navigation errors have a significant contribution to the net dispersions. Planet independent trends in dispersions such as deflection radius effects or entry angle effects are discussed in the individual planet parametrics of this volume or in the detailed dispersion analyses contained in Chapter IV.F. of Volume II.

e. Entry Parametrics - To provide a quantitative comparison of the entry environments of the different planets, Figure II-42 is included. Here, the peak deceleration experienced by the probe for a variety of entry angles is given for each of the planets. For Jupiter, both the cool/dense and nominal models of the atmosphere are compared. The relative severity of the Jupiter atmosphere should be noted.

Table II-20 Dispersion Contributions from Orbit Determination and Execution Errors

Mission	Model	Entry Time, min	Entry Angle, deg	Angle of Attack, deg	Lead Angle, deg	Entry Site		S/C-Probe Direction		Doppler, m/sec
						DR, deg	XR, deg	CA, deg	XCA, deg	
Jupiter	No Execution	2.58	0.23	0.42	0.32	0.51	0.17	0.97	0.34	0.16
Nominal	With Execution	7.98	1.08	3.08	4.40	2.02	0.75	10.98	0.64	8.56
Saturn	No Execution	4.50	2.79	1.66	2.50	4.56	2.09	1.21	0.71	0.76
Fast JS 77	With Execution	6.58	3.41	3.75	3.25	5.60	2.30	5.16	1.28	1.02
Uranus	No Execution	22.54	4.44	1.75	3.79	6.40	2.52	0.95	0.52	0.18
JU 79	With Execution	22.89	6.08	3.37	6.60	8.46	8.04	1.40	0.98	0.25

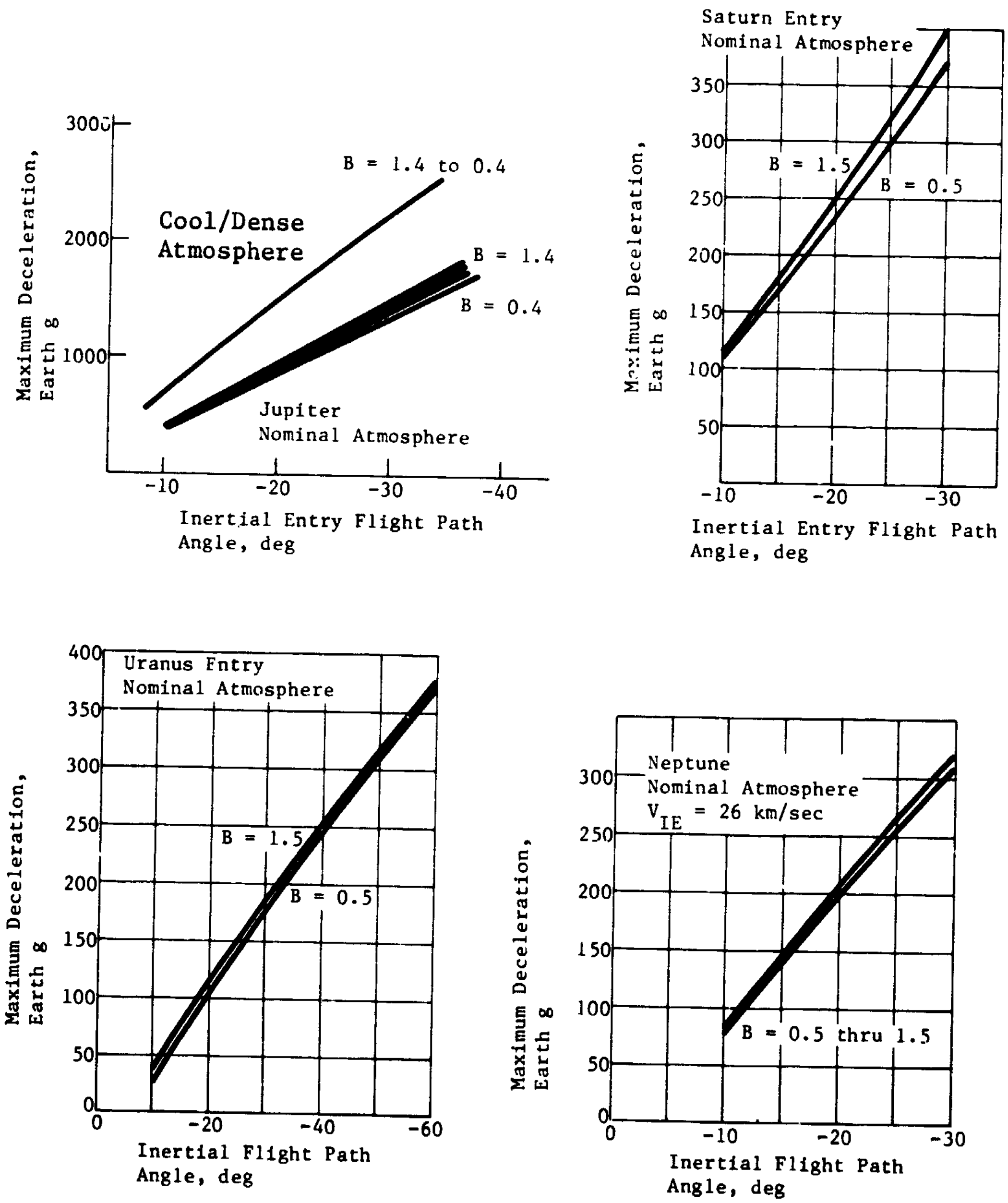

Figure II-42 Maximum Deceleration Comparisons for Jupiter, Saturn, Uranus and Neptune

2. Jupiter Parametric Analyses Summary

The Jupiter studies, as was previously shown in Figure I-1, consisted of defining a nominal Jupiter probe (Section C) using a set of nominal constraints that were determined from the previous study results and from other studies conducted by JPL. This nominal probe definition was used as a reference from which alternative constraints were varied individually to assess the sensitivity of the constraint. From this data, two sets of alternative Jupiter probe constraints were determined and two different alternative Jupiter probes defined (Sections D and E). The Jupiter parametric analyses included in this section are divided into such disciplines as mission analysis, science, followed by the subsystems analysis.

a. *Mission Analysis* - The detailed mission analysis and design studies are provided in Vol II, Chapter IV where comparisons of missions to the different planets may be made conveniently. A qualitative summary of the important results as they apply to Jupiter missions is given in this section.

The most critical consideration in selecting the interplanetary trajectory (or equivalently the launch and arrival dates) for Jupiter probe missions is payload capability. For a typical launch opportunity (1979), a flight time of slightly less than 700 days maximizes the payload capability for a fixed launch energy and period. This result is based on two constraints: the declination of the launch asymptote must be less than 36° and the Sun-Earth-vehicle angle at arrival must be greater than 15°. This results in optimal missions arriving at Jupiter before the Earth passing behind the Sun relative to Jupiter.

The payload capability improves each year in the period 1979-1982. This results not only from a progressive increase in the width of the launch energy contours each year, but also a continual reduction in the area eliminated by the DLA constraint.

For the 1979 mission opportunity, the Burner II stage is required in addition to the Titan 5-Segment launch vehicle to have a 20-day period for a Mariner class spacecraft. The Burner II stage is not required for a Pioneer class spacecraft.

For the approach selection, the relative geometry between the probe and spacecraft trajectories optimally would have the spacecraft directly overhead as the probe descends through the atmosphere. This would first require that the probe and spacecraft trajectory inclinations be chosen in concert. Generally, the probe trajectory should be a posigrade, low inclination trajectory to minimize the probe's relative velocity at entry, and thereby reduce entry effects. Then, the spacecraft should also have a posigrade, low inclination trajectory.

A second consideration involves the selection of the spacecraft periapsis radius. While in terminal descent, the probe rotates with the atmosphere at Jupiter's rotation rate of 36.6°/hr (equatorial). For the spacecraft to match this angular rate, it should have a periapsis radius of about 2.0 to 2.5 R_J for mission duration times of about half an hour.

In the navigation and guidance consideration, the uncertainty in the state of the spacecraft at deflection is essentially caused by the navigation uncertainties at the time of the last midcourse maneuver. A detailed analysis of the navigation results is given in Vol II, Chapter IV. The navigation uncertainty for the 1979 mission, using Doppler only, is characterized by a one-sigma semi-major axis (SMAA) uncertainty in the impact plane of 1600 km (30×10^6 km deflection radius). Adding ranging measurements and then QVLBI measurements reduces this to 1500 km and 1400 km, respectively. Deflecting at radii further from the planet requires tracking further from the planet which results in less effective tracking. In going from 10 to 50 million km the uncertainties are approximately doubled. Finally, the navigation characteristics vary from year to year as the geocentric declinations of Jupiter at arrival vary. The SMAAs go from 950 to 1500 to 700 to 450 as the launches proceed from 1978 through 1981/1982 with corresponding geocentric declinations at arrival of 10°, 0°, -15°, -23°, respectively.

The deflection maneuver parametrics considers the purpose of the deflection maneuver as follows:

1) to place the probe on a trajectory intersecting the selected entry site;
2) to orient the probe for zero relative angle of attack at entry;
3) to establish an effective communication link between the probe and spacecraft during the critical descent phase of the mission.

The standard means of accomplishing these objectives is probe deflection wherein the probe is separated from the spacecraft, fires a ΔV which accomplishes (1) and (3) above, and then reorients itself to the attitude required in (2) by a precession maneuver.

The ΔV requirements are such that the deflection radius (the distance from the planet when the maneuver is performed) is generally between 10 and 50 million km. For a spacecraft periapsis radius of 2 R_J and an entry angle of -20°, the ΔV requirement varies from 221 to 73 to 44 m/sec as the deflection radius increases from 10 to 30 to 50 million km, respectively. The ΔV increase by a factor of 3.5 if the spacecraft periapsis is raised to 6 R_J.

Increasing the deflection radius also increases the coast time, which results in a longer length of time during which the probe is away from the protective environment of the spacecraft, and during which dispersions may grow. The coast time is approximately a linear function of deflection radius varying from 9.5 to 34.6 to 61.4 days as the deflection radius is increased from 10 to 30 to 50 million km.

The uncertainty in the spacecraft state at deflection caused by errors and the error in the delivered ΔV caused by execution errors, result in dispersions that must be accounted for in the design of the probe mission. Dispersions in entry site and entry flight path angle affect science return and interpretation. Dispersions in angle of attack at entry affect science as well as structural, thermal, and aerodynamic design. Dispersions in entry time affect mission sequencing. Dispersions in the relative geometry of the probe and spacecraft determines requirements on the communication link.

For Jupiter missions dispersions are dominated by execution errors and the navigation uncertainties have little impact. Approximately 95% of the total dispersions associated with any of the parameters discussed above are contributed by execution errors.

The dispersions are, of course, a function of the level of execution errors. The proportionality error of 1% (3σ) is dominated by the less well-defined pointing error in the delivered ΔV, which is assumed to be about 2° (3σ). Using entry angle as a typical example, 3σ dispersions of 0.2°, 0.9°, 1.1°, and 1.3° result from assuming ΔV pointing errors (3σ) of 0°, 1.5°, 2.0°, and 3.0°, respectively, while holding the navigation uncertainties and proportionality errors (1%) constant (for the nominal mission).

The dispersions are also proportional to the length of the coast arc between deflection and entry, and to the magnitude of the deflection ΔV. Therefore, there is a complicated trade in increasing the deflection radius which lowers the deflection ΔV and increases the coast time.

Two alternative deflection modes have been identified in addition to the probe deflection mode discussed above. These are--

1) Shared Deflection (Planar) - The probe is released in the attitude required for zero relative angle of attack. The ΔV magnitude is then chosen so that when fired in the axial direction, the probe impacts the entry site. The spacecraft is then corrected to establish the desired communication geometry.

2) Spacecraft Deflection - The initial spacecraft trajectory is targeted to impact the desired entry site. The probe is released in the attitude required for zero relative angle of attack. The spacecraft then rotates to a new direction and fires a ΔV which deflects it for the desired flyby radius and communication geometry.

The deflection ΔV requirements for the probe and spacecraft deflection modes are essentially identical as they are mirror images of each other. The two ΔV required by the shared deflection are approximately of the same magnitude as the probe or spacecraft deflection mode ΔV. Thus, for the nominal mission, the ΔV required for the probe (in probe deflection) or spacecraft (in spacecraft deflection) is 221 m/sec, while the probe ΔV is 246 m/sec and the spacecraft ΔV is 236 m/sec in the shared deflection mode.

According to dispersion comparisons of the three modes, the spacecraft deflection is best and shared deflection is worst. Entry dispersions (entry angle, entry site, etc) are smallest for the spacecraft deflection as no deflection ΔV execution errors are added to the probe trajectory. The communication parameter dispersions for shared deflection are largest because execution errors have been added to both the probe and spacecraft in that mode. Any time a ΔV maneuver is performed, resulting dispersions are approximately proportional to the size of the maneuver.

The critical entry parametric studies deal with the selection of the entry ballistic coefficient which permits deceleration to less than Mach 0.7 above 100 mb for the staging of the aeroshell and the study of the behavior of the peak decelerations and maximum dynamic pressures with a variety of entry conditions.

A ballistic coefficient of 102.1 kg/m^2 (0.65 slug/ft^2) results in velocities below Mach 0.7 at 100 mb in the cool/dense model and 90 mb in the nominal atmosphere for an entry angle of -20°. To meet the staging requirements at an entry angle of -30° for the cool/dense atmosphere requires a ballistic coefficient of 78.5 kg/m^2.

The peak g experienced at entry angles of -10°, -20°, and -30° are 675, 1500, and 2250 g, respectively, in the cool/dense atmosphere, and 450, 920, and 1450 g, respectively, in the nominal atmosphere (equatorial entry). Thus, the cool/dense model has g levels roughly 50% higher than the nominal atmosphere. Entering at higher latitudes increases the peak g as the relative velocity is increased. Thus, entering at latitudes of 0°, 30°, and 90° latitude results in peak g of 1500, 1650, and 1800 g, respectively, for an entry angle of -20° in the cool/dense atmosphere. The peak g level is essentially independent of the ballistic coefficient. However, increasing the ballistic coefficient delays the time at which the peak g is achieved.

The maximum dynamic pressures are functions of ballistic coefficient. Entering with a ballistic coefficient of 157 kg/m^2 at entry angles of -10°, -20°, and -30° results in max q of 10, 22, and 40 x 10^3 psf, respectively, in the cool/dense atmosphere and 6.6, 14.7, and 26.6 x 10^3 psf, respectively, in the nominal atmosphere. The dynamic pressure increases linearly with ballistic coefficient.

b. Science - The major parametrics performed in the science area were to establish a descent profile that would satisfy the objectives of the mission by making the necessary measurements within the criteria. The parameters involved are: (1) the main parachute ballistic coefficient, (2) the drogue or secondary parachute ballistic coefficient, if one is necessary, (3) the pressure at parachute staging, if required, (4) the design limit pressure, and (5) the sampling times for each instrument. The total descent time is also considered because of the limited time the flyby spacecraft is available to establish relay communications link. Also, for Jupiter, the model atmosphere for descent is bounded by two distinct models: the nominal and cool/dense, and these parameters are considered separately in each.

The cool/dense model atmosphere was investigated first. The range of the ballistic coefficients considered were from 7.85 kg/m^2 (0.05 $slug/ft^2$) to 39.25 kg/m^2 (0.25 $slug/ft^2$) for the main parachute (B_1) and from 157.0 kg/m^2 (1.0 $slug/ft^2$) to 378.8 kg/m^2 (2.4 $slug/ft^2$) for the secondary parachute (B_2) with staging pressures from 3 to 15 bars. The size and weight of the main parachute system establishes the lower limit for B_1 while the descent time and velocity and resultant measurement performance constrin the larger values.

The results of this parametric analysis are summarized herein. To descend to 30 bars of pressure, a double parachute system is required. The first parachute must allow the descent probe to fall at a slow enough velocity to enable the measurements to meet the criteria at cloud tops. The second (smaller) parachute is necessary to allow the probe to descend faster at higher densities so that it reaches 30 bars in a reasonable time, compatible with communications. The value of the second parachute ballistic coefficient, within the range studied, had very little effect on the descent profile. However, the pressure at staging must be 8 bars or greater, depending upon the exact selected value of B_1, in order for the instrument measurement performance to meet the criteria immediately after staging.

The gradient of pressure with respect to distance in the nominal atmosphere is smaller, thus the clouds exist higher in altitude and lower in pressure, and the pressure gradient across them is less. This has two distinct effects. One is that since the clouds are higher, the probe will not have to penetrate as deeply to satisfy the mission objectives. In fact, descent to 10 bars in the nominal is roughly equivalent in relation to objectives as descent to 30 bars in the cool/dense. This eliminates the necessity for a dual parachute descent, as for all ballistic coefficients studied, the times to 10 bars are less than 54 minutes. Secondly, the pressure gradient being less means that to obtain equivalent measurement performance in the nominal as in the cool/dense, the velocity with respect to pressure must be less. Therefore, the time to descend to a given pressure level is longer, for a given ballistic coefficient. This is summarized by Figure II-43.

The range of main parachute ballistic coefficients studied for the nominal atmosphere was the same as for the cool/dense. Results show that for optimum performance, the value of B for the nominal should be smaller than that for the cool/dense, and it can be noted that for a given value of B, the instrument sampling times must be shorter to satisfy performance requirements. Furthermore, since the nominal atmosphere is the worst-case for measurement performance, a probe designed to meet the criteria in the nominal will also satisfy it in the cool/dense, and any combination in between.

The model atmosphere also has an effect on data rate. For the same ballistic coefficient and terminal descent pressure, the science data rate can be approximately the same regardless of the descent time, but if both entry phases are in the same atmosphere, the descent in the cool/dense model will require a higher bit rate.

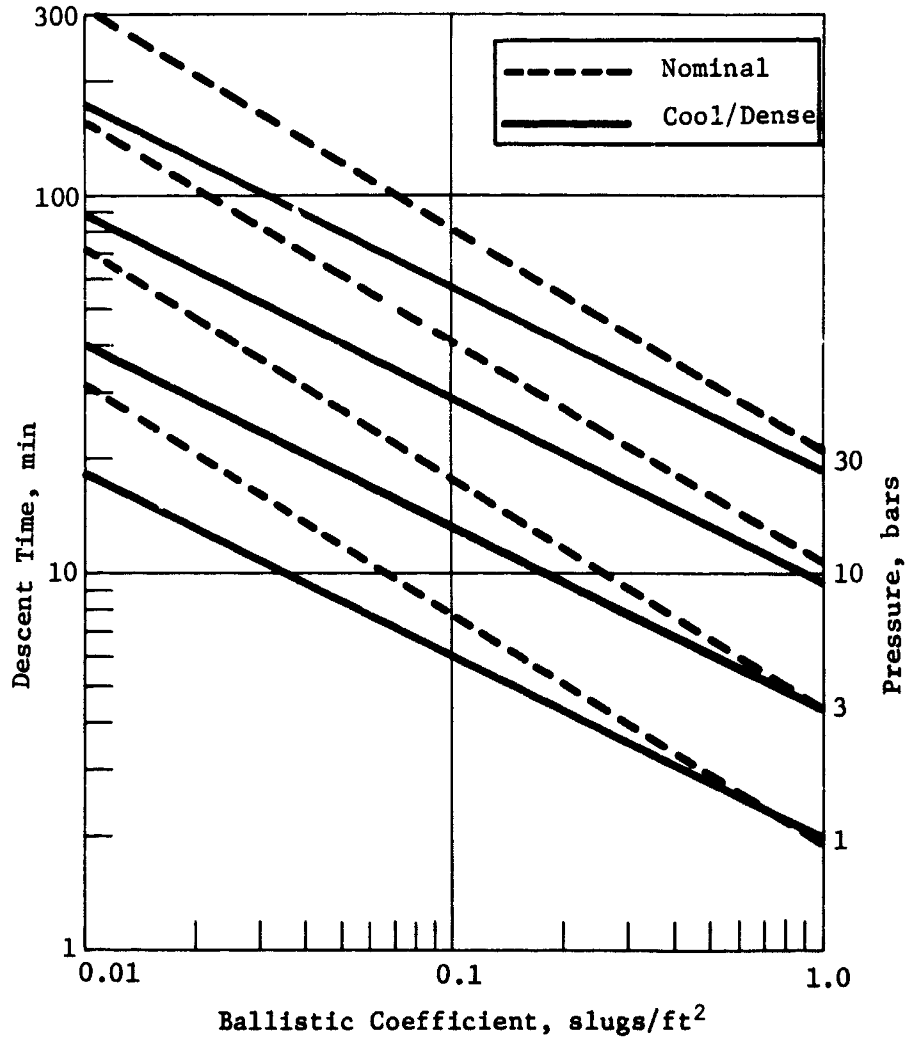

Figure II-43 Descent Times to Various Pressures in Both Jupiter Model Atmospheres

The entry flight path angle affects the entry phase directly by changing the time to reach Mach 0.7 and the descent phase indirectly by changing the altitude at which Mach 0.7 is reached, thus varying the starting point in the atmosphere for descent. The combined effect can cause the total mission time to vary up to about 2 min. However, variation in entry time has a strong effect on total bit rate since entry accelerometers are measuring up to 200 bps.

c. System Integration - Guidelines for the program parametric analyses point designs are shown in Table II-21. The reference configuration is the nominal Jupiter probe.

Table II-21 Constraints for Program Parametric Point Designs

	Configuration											
Constraint	Ref	1	2	3	4	5	6	7	8	9	10	11
R_P (R_J)	2	2	2	2	2	2	2	2	6	2	2	2
R_{EJ} (x 10^6 km)	10	10	10	10	10	10	10	10	30	10	10	10
γ_E (- deg)	20	10	30	42.6	20	20	20	20	20	20	20	2[illegible]
Latitude (deg)	5	5	5	90	5	5	5	5	5	5	5	5
Atm E	CD	CD	CD	CD	CD	NOM	CD	CD	CD	CD	CD	CD
Atm D	CD	CD	CD	CD	NOM	NOM	CD	CD	CD	CD	CD	CD
Deflection Mode	P	P	P	P	P	P	P	P	P	S/C	S/C	S
S/C	MOPS	MOPS	MOPS	MOPS	MOPS	MOPS	PION	MOPS	MOPS	PION	MOPS	PION
Descent (bar)	30	30	30	30	10	10	30	30	30	30	30	30

Legend: CD-Cool/Dense; NOM-Nominal; P-Probe; E-Entry; D-Descent.

d. Telecommunication Subsystem - The parametric analyses were intended to determine the effects of variations in trajectory parameters on the design of the probe. Major trajectory parameters, such as periapsis radius and entry angle, affect RF power requirements significantly.

Considerable effort was expended in determining if an optimum operating frequency exists since several losses are directly proportional to frequency and others are inversely proportional to frequency. The analysis is discussed in detail in Volume III, Appendix B. Results of the frequency selection indicate that an optimum frequency does not exist, but, in general, the lower frequencies are affected less by the RF link variables. For this reason, the original operating frequency at S-band (2.3 GHz) was abandoned in favor of a frequency near 1 GHz.

Signal attenuation in the cool/dense atmosphere for 1 GHz varies from 2.2 dB at 30 bars to 0.2 dB at 10 bars, and for 0.86 GHz, it varies from 1.5 dB at 30 bars to approximately 0 at 10 bars. The nominal atmosphere has significantly less loss. A further discussion of the losses is included in Vol II, Chapter V, Section A.4 and Vol III, Appendix A.

Several types of antennas are required for the various missions depending on beamwidth and frequency. Antenna designs are discussed in detail in Vol III, Appendix D. The spacecraft antenna for narrow beamwidths (<20°) uses a parabolic dish antenna of conventional design. For missions that require high gain, a dish antenna provides a compact design. Circular polarization is required since the probe is spin stabilized. Missions that require a spacecraft antenna with a wide beamwidth and low gain use a helical antenna. Probe pre-entry antennas must have a butterfly pattern because of a large probe aspect angle before entry. For the parametric designs at 1 GHz, a spiral design on a cone was selected. The probe descent antenna uses a turnstile design over a flared cone to provide circular polarization, a large axial pattern, and a compact design.

The probe transmitter uses solid-state design with an overall efficiency of 45%. The transmitter is switched from the entry antenna to the descent antenna during planet entry. An RF coaxial switch reliably performs this function. For power levels up to 20 W, a solid-state switch may be used. Above 20 W, a mechanical switch is required. This is a routine performance for space vehicles; RF switches are the most reliable way to transfer power from one antenna to another.

Requirements for the spacecraft receiver are not critical and a solid-state design, using transistors or tunnel diodes, may be used. Average noise figures for the receiver front end are 3 dB at 1 GHz.

Several point designs were investigated to determine the design of the telecommunications subsystem. Results are shown in Table II-22. Point design number 8 was the most difficult because of the relatively large cone angle and space loss. The resulting definition used a two-position acquisition search in order to keep the RF power within reasonable limits.

Table II-22 Telecommunication Subsystem Parameters for the Parametric Point Designs

PARAMETER	UNIT	POINT DESIGN CONFIGURATION					
		NOMINAL	1	2	3	5	8
Periapsis Radius, R_P	R_J	2	2	2	2	2	6
Ejection Radius, R_{RJ}	10^7km	1	1	1	1	1	3
Entry Path Angle, γ_E	-deg	20	10	30	42.6	20	20
Atmosphere		C/D	C/D	C/D	C/D	NOM	C/D
Descent Depth	bar	30	30	30	30	10	30
Entry Antenna B/W	deg	35	40	20	20	35	30
Entry Antenna Gain	dB	13.5	12.3	16.4	16.4	13.5	14.8
Descent Antenna B/W	deg	120	120	125	120	120	120
Descent Antenna Gain	dB	5	5	4.7	5	5	5
Spacecraft Antenna B/W	deg	45	70	[illegible]0	30	45	20/15
Spacecraft Antenna Gain	dB	11.3	7.[illegible]	12.3	15	11.3	1[illegible].3/21
Total RF Power	W	22.8	37.9	17.6	29	12.4	81/36

INVARIENT PARAMETERS:

Frequency = 1 GHz

Bit Rate = 28 bps

System Temperature = 1280 °K

E_b/N_o = 8.9 dB

S/N Ratio = 10 dB

Tone Bandwidth = 15 Hz

LEGEND FOR JUPITER ATMOSPHERES:

C/D = Cool/Dense

NOM = Nominal

B/W = Beamwidth

A direct link analysis was made to compare with the 6 R_J periapsis point design (No. 8). For this analysis, the probe was assumed to have optimum pointing to the deep space network. Results are shown in Table II-23.

Table II-23 Direct Link RF Power Results

Frequency, GHz	RF Power, W at Depth	
	10 bar	30 bar
2.3	37.5	400
1.0	19.5	31

e. Data Handling Subsystem - A study was performed to evaluate the applicability of a centralized computer controlled DHS as opposed to a decentralized approach in which the majority of data processing functions are located in the various subsystem electronics. Factors that were considered in this evaluation were (a) flexibility of design, (b) potential change of requirements, (c) common failure modes, (d) design/build cycle economy, (e) adaptive requirements, and (f) data processing complexity required by the mission. These considerations resulted in a selection of a special purpose DHS design approach. Data processing will be performed primarily in the instrument electronics. In general, modifications required of the data processing requirements will not affect the DHS/instrument interface. Furthermore, it should be possible to update the data processing circuitry in the instrument electronics more rapidly than the causal instrument modifications. The DHS will provide the relatively simple functions required for probe data management and the design/build schedule will not be subject to expensive delays caused by changes in instrument requirements. A more detailed description of these tradeoffs may be found in Vol II, Chapter V, Section A.5, and an integrated discussion of the DHS is contained in Vol III, Appendix H.

f. Power and Pyrotechnics - Preliminary studies of power sources considered solar cells, RTGs, and batteries for probe bus power and coast timer power. The choice of probe bus power source rapidly evolved to batteries. An evaluation of primary and secondary batteries for a nominal Jupiter probe resulted in a selection of remotely activated Ag-Zn batteries. Solar cells appear to be a possibility to supply power for the coast timer and the initial pyrotechnic pre-entry event; however, a Hg-Zn battery was selected on the basis of size, weight, and subsystem consistency. The entry and descent power system distribute raw battery power through isolation power filters. Subsystems provide individual power conditioning where required. This reduces the probability of common mode failures in the high radiation Jupiter environment. The pyrotechnic subsystem uses capacitor bank discharge circuitry similar to Viking and Mariner approaches. A discussion of the alternative approaches for the power and pyrotechnic subsystem may be found in Vol II, Chapter V, Section A.6 and Vol III, Appendix G.

g. *Attitude Control Subsystem* - Attitude control configurations that were considered used stored programs, stored momentum, offset thrusters, single and three-axis control, and open and closed loop. A three-axis closed-loop maneuver control of a spin-stabilized vehicle was selected. A detailed design study may indicate that an open-loop single-axis maneuver using Sun-stimulated vector logic control would be adequate. However, uncertainty in the expected entry angle of attack resulted in an allowable design error of 3° which necessitated a closed-loop system. The configuration uses a solar aspect sensor, planet sensor, cold gas precession, and spinup jets. A discussion of the configuration selection may be found in Vol II, Chapter V, Section A.7 and a more complete analysis in Vol III, Appendix F.

h. *Structures Subsystem* - The structure of the Jupiter probes was evaluated parametrically to determine the factors affecting the design and weight of the probe. The basic components of the probe are affected by the environment they encounter during the spaceflight and planetary entry mission. For reference discussion, the components of interest of the probe are as shown in Figure II-44. These components consist of the entry probe body assembly (including heat shield and aeroshell), base cover (not shown), descent probe, service module, and deflection propulsion motor. All of the above components are exposed to the mechanical loading of spacecraft launch phase. The loads encountered during the phase consist of relatively steady-state accelerations combined with vibration and acoustic inputs. The peak acceleration value has arbitrarily been chosen as 10 g for the launch phase. The scope of the program did not permit evaluating the effects of vibration and acoustic inputs at launch; however, these environments generally affect only the design of details such as attachment bracketry, etc. For the Jupiter mission, the planetary entry loads are so high that it was felt realistic to ignore the vibration and acoustic inputs.

Integrates Science Instruments Provides Proper Thermal Environment Aero Stability with Dual Ballistic Coefficient Design Load Factor*	Entry Heating Protection Aero Stability Open to Release Descent Probe Design Load Factor*	Thermal Spin/Despin Attitude Propusion Sun & Planet Sensors Power Design Load Factor 10g	Velocity Change Design Load Factor 10g

*See Figure V-22

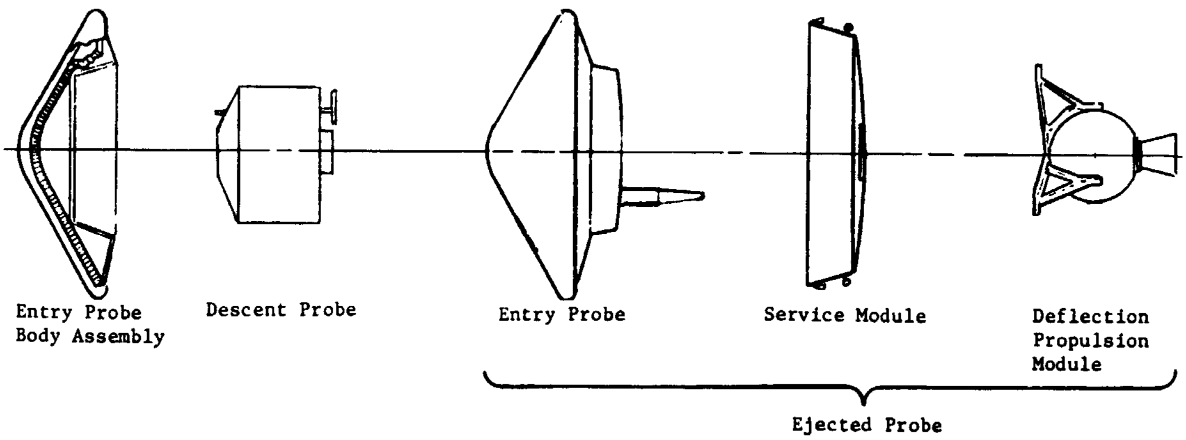

Figure II-44 Probe Major Assemblies

All of the planetary probes experience the high loadings of planetary entry except for the deflection motor and the service module containing the attitude control system. The deflection motor is expended and jettisoned shortly after separation of the probe from the spacecraft. The service module is jettisoned before planetary entry. Thus, these two components are designed for their self-generated loads plus launch pad liftoff acceleration.

The remainder of the probe is designed by entry deceleration loads and entry dynamic pressure. The aeroshell itself is essentially a pressure vessel exposed to high external aerodynamic pressure on the forward face. It is this pressure load that governs the design and configuration. The aft base cover and the descent probe are designed totally by inertia loads of planetary deceleration. Parametric curves showing structural weight of the aeroshell versus diameter and pressure load have been generated for construction materials of aluminum and titanium. Likewise, parametric data has been generated for the structural components of the descent probe. These data are presented in Chapter V, Section A.8 of Vol II, and Appendix O of Vol III.

Entry into the Jovian atmosphere produces very high heating on the nose of the Jupiter probe. The heating pulse of 25 kw/cm^2 resulted from entry angles from this study. The heat shield protection provided for the nose of Jupiter probes is based on work performed by M. Tauber and R. Wakefield of NASA-Ames Research Center. This data was prepared in parametric form for point design probes of different sizes, entry ballistic coefficients, and planetary entry angles. These data are presented in Chapter V, Section A.8 of Vol II. For practical entry probes, the heat shield mass fraction (heat shield weight/entry weight) for the probe nose is of the order of 0.31 to 0.35. The heat shield material is ATJ graphite.

Base heating on the probe is of the order of 2% of that on the nose. Parametric data for the base cover heat shield versus entry conditions has been generated versus entry angle. This data is presented in Vol II. The heat shield ablator weight for ESA 5500M3 ablator is of the order of 2.5 kg/m^2 (0.5 lbm/ft^2).

Conventional parachute decelerators are used to separate the descent probe from the aeroshell/heat shield assembly after entry, and to provide the required descent ballistic coefficient meeting science requirements of the mission. A disc-gap-band configuration parachute is used for separation of the descent probe and for slow descent in the upper atmosphere of Jupiter. A circular disc parachute is used for a secondary descent parachute configuration where higher descent rates are desired in the lower atmosphere. The main parachute is typically of a diameter of 2 to 2.5 m (7 to 8 ft) in diameter, while the secondary parachute is typically 0.3 to 0.5 m (1 to 1.5 ft). Parametric data on parachute size and weight for both main and secondary parachutes has been generated for varying descent probe weights and ballistic coefficients. These data are presented in Vol II.

i. Propulsion Subsystem - The propulsion subsystem for the Jupiter probe must provide the deflection maneuver delta velocity and must provide attitude stabilization and control of the probe after separation of the probe from the carrier spacecraft. The attitude control system must spin the probe to the proper angular velocity to stabilize the probe during firing of the delta velocity motor. It must further precess the longitudinal axis of the probe from the direction required for application of the delta velocity to that required for planetary entry. The system must finally despin the probe to a lesser spin rate for planetary entry. For purposes of design, the spin velocity was selected to be 10.4 rad/sec (100 rpm). The residual spin after despin is 0.52 rad/sec (5 rpm).

Comparisons were made of candidate propulsion systems accomplishing the delta velocity and attitude control propulsion functions. These candidates included a cold gas system, solid propellant, monopropellant, and bipropellant. The selected system (and lightest weight system) proved to be a spherical solid propellant delta velocity motor combined with a cold gas attitude control system. The comparison of this selection with a monopropellant system performing both delta velocity and attitude control is shown in Table II-24.

Table II-24 Jupiter Probe Propulsion System Parameter Comparisons

Parameter	Trajectory Correction and Attitude Control		
	Solid	Cold Gas	Monohydrazine
Specific Impulse, sec	287	72	230
Mass Fraction	0.76	0.18	0.55
Propellant Weight, lbm	27.0	2.5	34
System Weight, lbm	35.5	14	62
0-g Effects	None	None	PMD Required
Reliability	0.997	0.997	0.995
Total Impulse Control	Fixed	Variable	Variable

This effort also included developing parametric design data for spherical solid propellant rocket motors. All of the above selection and design data is presented in Chapter V, Section A.9 of Vol II, and Appendix M, Vol III.

j. Thermal Control Subsystems - Thermal control for outer planet probes must be provided to ensure that all probe systems will be maintained within acceptable temperature limits throughout all phases of the mission. For the purposes of analyzing the thermal control subsystem, the entry probe study missions were divided into three phases: spacecraft cruise, probe coast, and entry and descent.

The cruise phase is that long-term phase of spaceflight from liftoff and Earth orbit departure until within approximately 10 to 30 million km of the planet to be entered. During this phase, the probe is attached to the spacecraft and housed under an environmental cover, shadowed from direct solar impingement except for brief midcourse maneuvers, and in a power-off storage mode. The probe coast commences with separation of the probe from the spacecraft and ends just before planetary entry. During this time, the probe is in a brief power-up mode for separation and checkout, and then deactivated for the duration of the coast phase. The probe is directly exposed to solar radiation during this phase. The entry phase begins about one hour before actually entering the planet atmosphere with the activation of the probe and powering up for probe checkout. The probe systems then become operational at entry and function throughout the science-return descent portion of the mission.

To analyze the probe thermal performance requirements, the criticality of the probe components to temperature variations for long-term storage and for operation was established. The temperature limits then established the thermal control requirements for the long-term cruise and coast phases and the short-term operational phase of entry and descent. It was found from the thermal analysis that the most critical probe temperatures from a thermal design standpoint are the temperatures at the end of probe coast, the maximum internal equipment temperature experienced at the end of descent in a Jupiter nominal atmosphere, and the minimum internal equipment temperature experienced during descent in a Jupiter cool/dense atmospheric encounter.

Tradeoff studies were performed to determine the type and quantity of insulation required for the descent probe to provide the best thermal-control versus insulation-weight parameter. It was concluded that a low density foam insulation of 1.9 cm (0.75 in.) thickness provided the best descent probe insulation configuration. In the course of the thermal control evaluation for Jupiter, the various planetary atmospheres were compared for temperature trends of the atmospheres as they affect the descent probe. These temperature comparisons are shown in Figure II-45. It can be seen that the variations in temperature encountered by the probe are large and could result in different control requirements for different planets.

An evaluation of instantaneous heat leak from the descent probe while descending through the Jupiter atmosphere, was also performed to determine the severity of the thermal control problems. This data, shown in Figure II-46, depicts the heat outflow rate from the probe versus descent pressure altitude. It is important to note the high initial heat outflow from the probe and the general shape of the curve. These data were used to develop thermal control concepts for protection of individual entry probe designs.

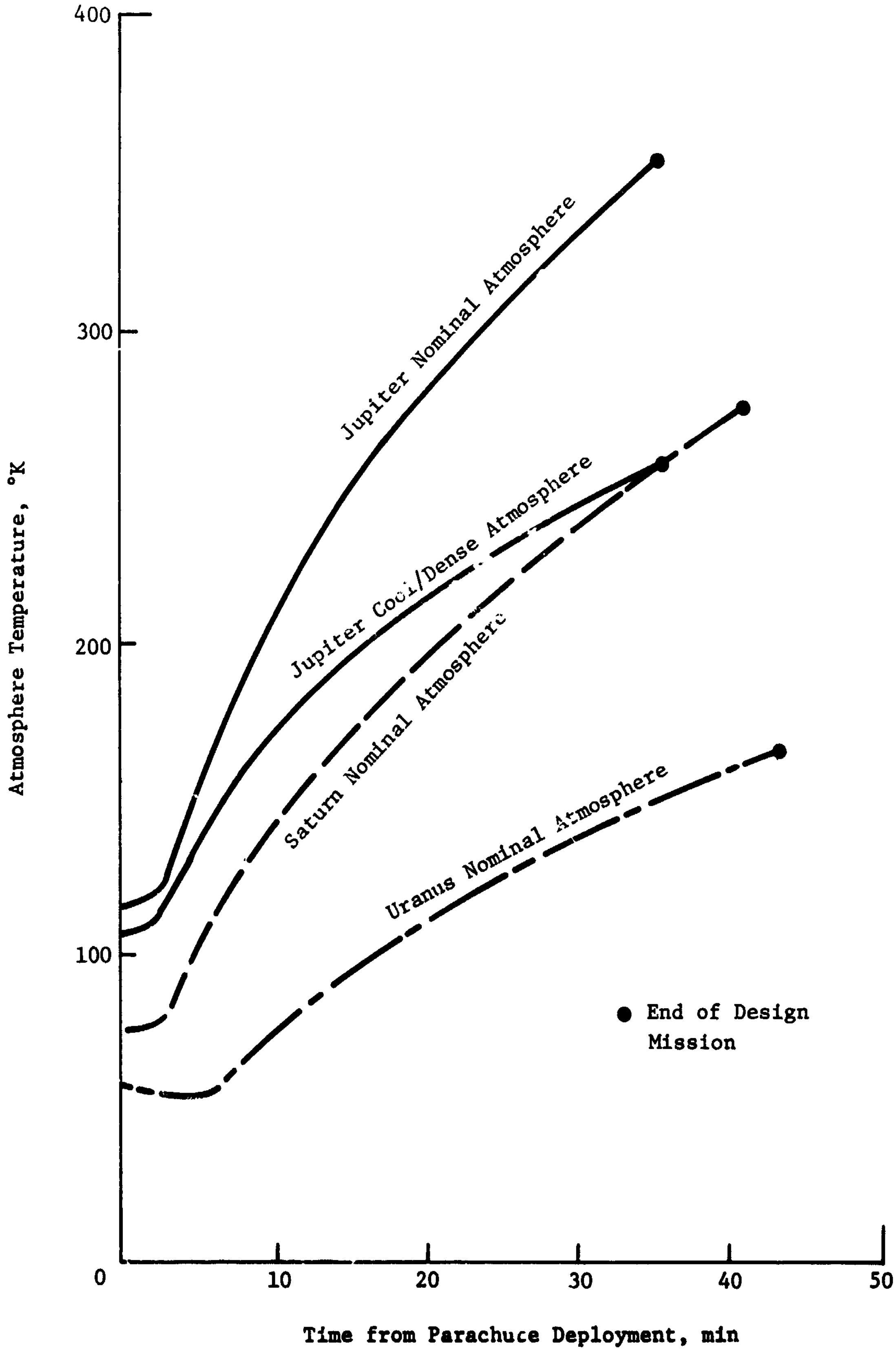

Figure II-45 Comparison of Thermal Descent Severity for Planetary Missions Investigated

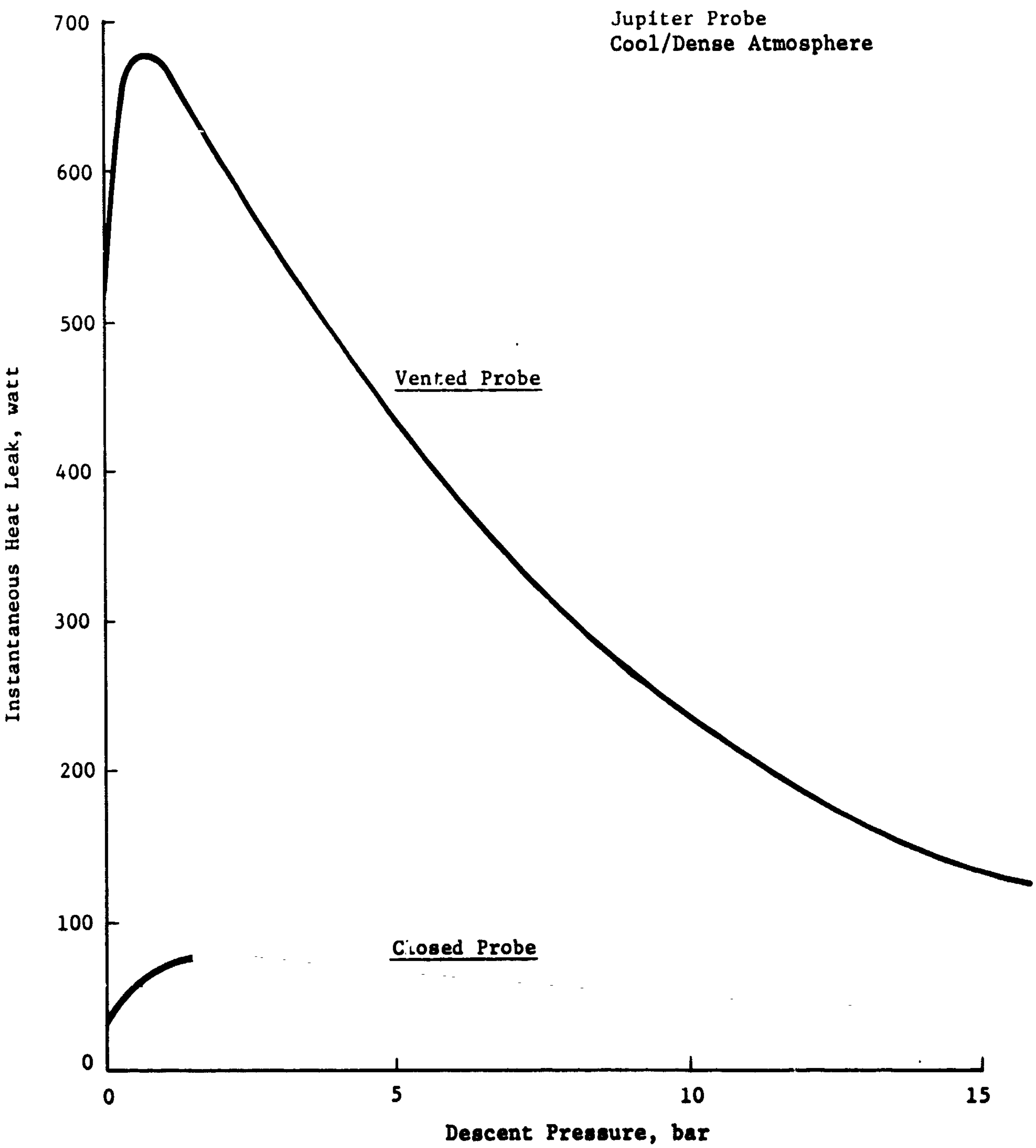

Figure II-46 Instantaneous Probe Heat Leak

Studies were also performed on the required thermal protection during the cruise and coast phases to establish values of outer probe insulation, outer surface absorbance and emittance values, and internal heat needed to keep the long-term storage temperatures of probe components within acceptable limits. These studies are reported in the thermal design sections of Vol II for parametric and point probe designs.

k. Subsystem Sensitivity to Radiation - The trapped radiation environment as a function of latitude is shown in Figure II-47 based upon the workshop model and the post-workshop model. Solid-state devices are more susceptible to damage than are most other materials. Component and material selection along with circuit designs will aid in hardening against the environment. As data is obtained from the Pioneer flight to update the models, the final design must be tested to those expected levels.

l. Probe to S/C Integration - Two candidate spacecraft were used during the parametric analysis as shown previously in Figure I-1 and Table II-21. The point design combinations including the spacecraft, probe, and spacecraft modifications have launch weights that range from 430.46 kg for the Pioneer spacecraft and a spacecraft deflection mode to 854.57 kg for the MOPS and probe deflection mode. The Pioneer is spin-stabilized compared to the MOPS, which is three-axis-stabilized. Detailed comparisons are included in Vol II, Chapter V, Section A.12.

m. Summary of Jupiter Parametric Analyses - A summary of the Jupiter parametric analyses results is:

Mission Time to Jupiter	680 days
Optimal Flyby Radius at Jupiter	2.7 R_J
Three-Sigma Dispersions (max)	
Entry Time	7.98 min
Entry Angle	1.08°
Angle of Attack	3.08°
Lead Time	4.40°
Entry Ballistic Coefficient	<156 kg/m^2
Depth of Descent for Science Objectives	13 bars in a Cool/Dense Atmosphere
Descent Ballistic Coefficient for Science Objectives	14.1 kg/m^2
Descent Time	Approximately 36 min

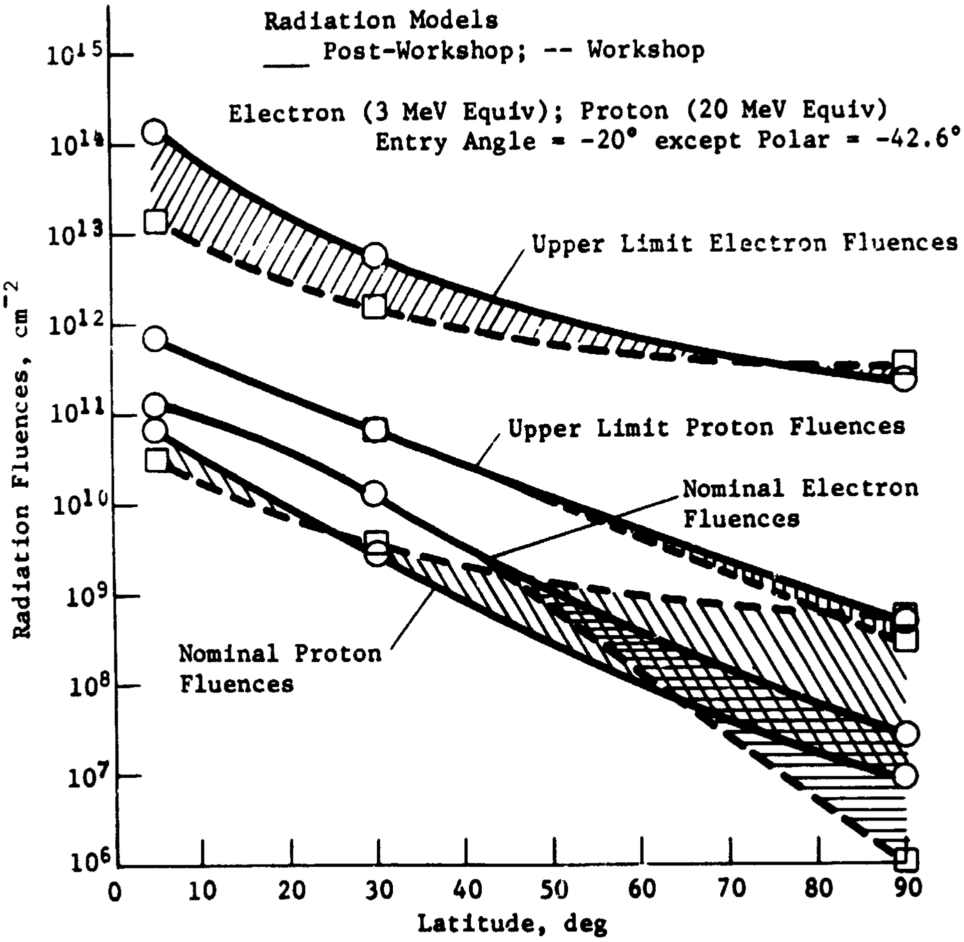

Figure II-47 Radiation Sensitivity to Latitude

3. Saturn Parametric Analysis

At the beginning of the contract, the multiple planet studies involved Saturn, Uranus, and Neptune. Five different missions for each planet were evaluated to identify the encounter parameters and two representative missions were selected for further applications. The initial five Saturn missions were; JSP 78, SUN 81-82, *SUN 82-83, SUN 84, and *JS 77. The two selected for in-depth analysis are identified by an asterick. The initial objectives were to identify the changes to the Jupiter probe functional requirements for Saturn atmospheric entry. Similar effort was included for the planets Uranus and Neptune. Jupiter probe changes for these three planet applications were then to be used to define a joint usage Uranus/Neptune probe. At the midterm oral presentation, the emphasis was revised to define a Saturn probe and to assess its applicability for Uranus atmospheric entry. Some of the parametric effort was begun for the five missions and results are reported in this chapter.

The revised combined objectives of the Saturn studies and those for Uranus then are to define a Saturn probe and identify changes required for Uranus application. The Saturn parametric and general analysis also considered the major impact for use at Uranus.

The analysis for this section is centered primarily in the mission and science areas, and consider the five missions denoted above with emphasis on SUN 82-83 and JS 77 as well as the high inclination JS 77 mission for a Titan encounter.

a. Mission Analysis - The detailed mission analysis parametric data is provided in Vol II, Chapter IV. This section summarizes the important design considerations for probe missions to Saturn.

The interplanetary trajectories considered for Saturn missions were either Jupiter flybys (JS 77, JSP 78) or solar electric propulsion trajectories (SUN 81, 82, 83). The interplanetary trajectories for these candidate missions are given in Vol II, Chapter IV, Section F. The trip times from Earth to Saturn are marginally possible at best for payload weights discussed in this study for the 1978-82 time period.

As at Jupiter, the optimal probe-spacecraft geometry would have the probe entering on the equator with the spacecraft flyby in the same plane. The optimal flyby radius at Saturn is about 2.5 R_S

(Fig. II-40). With this flyby, it is possible to keep the spacecraft approximately over the probe during the probe descent. For the JS 77 mission, involving a Titan encounter, the flyby radius is 2.33 R_J with a highly inclined orbit.

The approach orbit determination at Saturn is less effective than at Jupiter because the Saturn ephemeris uncertainties are approximately twice those of Jupiter. The navigation is further degraded at Saturn on the JS 77 mission because the geocentric declination of Saturn during the encounter period is very near zero. Thus, with Doppler and range measurements, the uncertainty ellipse (1σ) is characterized by a semi-major axis (SMAA) of 2200 km; adding QVLBI measurements reduces the SMAA to 1100 km; adding optical tracking reduces the value to 500 km.

The deflection maneuver trends indicated for Jupiter also apply at Saturn. Reasonable deflection radii at Saturn are from 10 to 30 million km. Thus, for a spacecraft periapsis radius of 2 R_S the ΔV requirements decrease from 140 to 70 to 47 m/sec as the deflection radius is increased from 10 to 20 to 30 million km, respectively. For a spacecraft flyby radius of 6 R_S, the corresponding ΔV become 620 to 300 to 200, respectively.

For Saturn missions, the vavigation uncertainties become significant relative to the deflection maneuver execution errors in terms of dispersions. This is in contrast to the situation at Jupiter where execution errors dominated the dispersions. Thus, at Saturn, the three sigma uncertainties in entry time, entry angle, angle of attack, and lead angle are 4.50/6.58 min, 2.79°/3.41°, 1.66°/3.75°, and 2.50°/3.25°, respectively, where the numerator is the uncertainty contributed by navigation uncertainties (80 days tracking or Doppler-range) alone, and the denominator is the total uncertainty resulting from both navigation uncertainties and deflection execution errors.

The selection of an entry ballistic coefficient that results in satisfactory staging conditions (deceleration to M = 0.7 above 100 mb) for entry angles of from -10° to -30° was investigated. Any ballistic coefficient less than 156.0 kg/m^2 (1.0 slug/ft^2) was identified as adequate.

The peak g experienced at entry angles of -10°, -20°, and -30° are 105, 240, and 355, respectively, in the nominal atmosphere. Entering at higher latitudes increases the peak g-loading as the relative velocity is increased. A polar entry increases the g-loading by approximately 30%. Parametric analysis has shown that the g-loading is essentially independent of ballistic coefficient.

The maximum aerodynamic g-loading is a function of ballistic coefficient of 1.0 slug/ft^2 at entry angles of -10°, -20°, and -30° results in max g of 2000, 7000, and 11000 psf, respectively, in the nominal atmosphere. The dynamic pressure increases linearly with ballistic coefficient.

b. *Science* - The parametrics for Saturn and Uranus are both given in this section because of the commonality of much of the data. The analyses performed for these two planets benefited greatly from those performed for Jupiter, and thus are more limited in scope. The major parametrics performed for both Saturn and Uranus were to establish descent profiles in both atmospheres, using as many common parameters as possible, which would satisfy the objectives of the mission by making the necessary measurements within the criteria. The parameters involved are the parachute ballistic coefficient the sampling times for each of the instruments, and the total descent time. The design limit pressure, initially a variable, was selected to be 7 bars by the analysis. The descent time becomes a constraining factor for Uranus because the probe, upon entering, rotates upward with the planet, away from the spacecraft, and the time available for good communications is shortened.

The statement of work specified consideration of the nominal model atmospheres of both planets. The first descent computer run made was at 15.7 kg/m^2 (0.10 slug/ft^2) which was near the optimal value for Jupiter descent. However, the descent time to 10 bars in Saturn's atmosphere was 134 minutes, which presents intolerable communications and thermal control problems. Also, the amount of data collected was several times that which was necessary for satisfactory mission performance. The range of ballistic coefficients that resulted in satisfactory descent times was that from 78.5 kg/m^2 (0.50 slug/ft^2) to 157 kg/m^2 (1.0 slug/ft^2). The range of values for reasonable descent times at Uranus was about the same as that for Saturn. A summary of descent times versus ballistic coefficient is given in Figure II-48.

Selection of a particular descent profile involves investigation of the variation of the measurement performance of a given instrument with both ballistic coefficient and instrument sampling

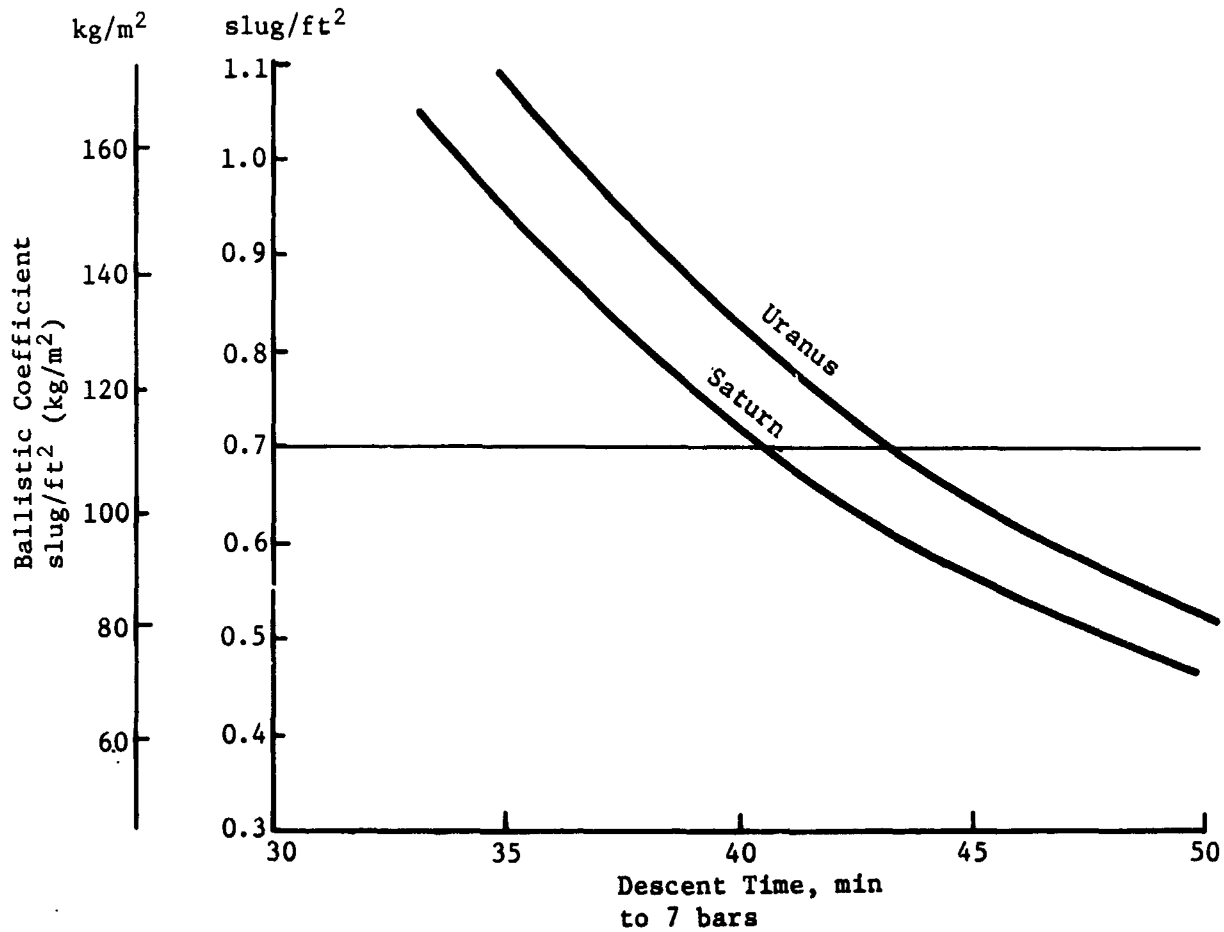

Figure II-48 Descent Time for Saturn and Uranus vs Ballistic Coefficient times. It was thus discovered that although the ballistic coefficient for Saturn had to be increased by a factor of at least 6 over that for Jupiter to give similar descent times, the instrument sampling times did not vary greatly to satisfy performance. However, for Uranus, the measurement data is greatly increased, but the sampling times were left the same as for Saturn for commonality and the performance requirements are satisfied.

c. System Integration - The constraints that control the Saturn parametric effort for the revised multiple planet objectives are:

1) Mission - Define a Saturn mission using JPL's high inclination trajectory for a Titan encounter so that the spacecraft and probe do not penetrate Saturn's rings.

3) Deflection Mode - probe

4) Atmosphere - nominal Saturn

5) Science Payload - SAG Exploratory payload (PAET)

d. Telecommunications Subsystem - General results of the parametric study performed for Jupiter were used to define the telecommunications subsystem for Saturn. The operating frequency was established for Jupiter at 0.86 GHz and applies to the Saturn mission. Binary FSK modulation is used with the same characteristics as for the Jupiter missions.

Microwave attenuation of the nominal Saturn atmosphere at 7 bars and 1 GHz is 0.5 dB and is very close to the loss at the same conditions in the Jovian cool/dense atmosphere. Saturn atmospheric loss is slightly lower than the loss for Jupiter as the pressure is increased. Therefore, atmospheric loss for Saturn to depths up to 10 bars are very close to the atmospheric loss encountered in the Jovian cool/dense atmosphere.

The system noise temperature was determined for Saturn based on information provided with the study by JPL. The upper-limit thermal disk brightness temperature was used in determining the antenna noise temperature. The increase in brightness temperature with increasing wavelength is entirely due to thermal radiation from the atmosphere of Saturn.

Radioastronomy measurements have not verified the existence of a magnetosphere around Saturn. An atmospheric thermal source can be responsible for all of the characteristics of the UHF radiation, with the exception of linear polarization reported by Rose *et al.* in 1963, which has not been confirmed by subsequent observations. Comparative discussions with respect to Jupiter indicate the possibility that Saturn could possess a trapped radiation belt that should be considered by probe mission designs. The belt would be similar to Jupiter's but weaker in strength. The rings of Saturn interfere with the formation of a belt interior to 2.3 R_S (the radius of the outer ring). Haffner discusses the magnetosphere of Saturn and assumes a Van Allen belt with typical dipole characteristics. The size of the belt is not known but should be between 3 and 4 R_S when compared with Earth and Jupiter. The high inclination trajectory at 2.3 R_S will miss the rings but would be within the magnetosphere. The synchrotron brightness temperature of Saturn, as provided in the JPL monograph is independent of path length since a magnetosphere model is not defined as in the case of Jupiter. It is only a function of frequency. The spacecraft antenna noise temperature is the sum of disk and synchrotron temperatures. The noise temperature of the receiving system is the sum of the antenna temperature and the receiver front-end noise temperature. The system noise temperature rises sharply below 1 GHz because of synchrotron and thermal disk noise. It is fairly constant at approximately 750°K between 1.6 and 3 GHz, rising slightly near 3 GHz from increased noise figure of the receiver. Variations in the system noise temperature are similar to the Jupiter dedicated probe mission and will be 0.2 dB or less from acquisition to mission completion. The planet disk is in the background of the spacecraft antenna at acquisition and distance in the magnetosphere is 1.75 R_S. The path length decreases to 1.2 R_S at mission completion.

Adjustments in spacecraft lead time were made in order to optimize probe-to-spacecraft range and probe aspect angle. Maximum range occurs at entry and decreases by 0.3 R_S at mission completion. Periapsis occurs after the mission is over (7-bar level reached) at one hour after entry. Definition of the subsystem is presented in Section F.4 and Table II-18 with design given in Section H.2.d.

e. Data Handling Subsystem - The data handling subsystem is essentially identical to that for the nominal Jupiter probe subsystem. Minor modifications of the time sequence and data format will occur but do not influence the parametric or analytic approach. For discussion of these alternatives, see Vol II, Chapter V, A.5 and Vol III, Appendix H.

f. Power and Pyrotechnic Subsystem - The power and pyrotechnic subsystem analysis is essentially identical to that for the nominal Jupiter probe subsystem. Minor modifications of battery weight and size will occur. For discussion of the parametric and analytic considerations, see Vol II, Chapter V, Section A.6 and Vol III, Appendix G.

g. Attitude Control Subsystem - The attitude control subsystem analysis is essentially identical to that for the nominal Jupiter probe subsystem. The most significant parameter that is modified is the Sun/probe/Saturn range which affects the sensor capability. Review of state of art sensor capability indicates that present solar aspect sensors have sufficient sensitive range to provide adequate performance at Saturn distance solar density (MSC-04568 *Evaluation Test Report for Precision Digital Solar Aspect Sensor*, June 1971). The planet sensor may require additional optics. For a discussion of the attitude control subsystem parametrics and analysis, refer to Vol II, Chapter V, Section A.7 and Vol III, Appendix F.

h. Structures and Mechanical - The parametric structural studies performed for the Jupiter probe, and reported in Section F.8, are applicable to the Saturn probe provided that the proper parameters are observed. The aeroshell weights data, however apply only to a conical nose shape, and not to the blunt nose configuration.

The aft cover of the entry probe was evaluated parametrically for weight of ablator heat shield required versus planet entry angle. This data is reported in Section F.8.

Two configurations of the Saturn entry probe were evaluated for comparison of effects of heat shield shape. This data also is reported in Vol II, Chapter VI, Section B.8.

j. Thermal Control Subsystems - For Saturn, thermal control must be provided. Like Jupiter, the primary thermal problem is one of losing too much thermal energy during the atmospheric descent phase of the mission and exceeding the allowable primary battery lower limit described for the nominal Jupiter probe. The selection of and approach to the thermal control subsystem is the same as the Jupiter probes design and consists of:

Cruise/Coast Phase Thermal Control

1) Radioisotope Heaters

2) Multilayer Insulation

3) Environmental Cover

4) Thermal Coatings

5) Deflection Motor Blanket and Heater

Entry/Descent Phase Thermal Control

1) Graphite Ablator and Aeroshell Insulator

2) Low Density Internal Foam Insulation

3) Nitrogen Gas Environmental Control

The pivotal temperature is the probe temperature at the end of the mission coast phase. This temperature must be high so that the probe will have sufficient thermal inertia to survive the critical heat losses during descent. For the Jupiter probe, radioisotope heaters maintain the probe temperature during cruise and thermal coatings were selected for solar heating of the probe by approximately 15°K following spacecraft separation. With the Saturn probe, however, the solar flux has reduced to 15 w/m^2 and thermal coatings are now just sufficient to maintain the probe at the cruise equilibrium temperature. Better thermal protection, therefore, must be provided during descent since the obtainable entry temperature will be lower than previous Jupiter analysis.

k. Summary of Saturn Parametric Analysis - A summary of the Saturn parametric analysis results in:

Mission Times to Saturn	3¼ years
Optimal Flyby Radius at Saturn	2.5 R_S
Flyby Radius for JST	2.33 R_S

One Sigma Navigation Uncertainty x/QVLBI	1100 km
Three Sigma Dispersions (max):	
Entry Time	6.58 min
Entry Angle	3.41°
Angle of Attack	3.75°
Lead Angle	3.25°
Entry Ballistic Coefficient	< 156 kg/m^2
Depth of Descent for Science Objectives	7 bar
Descent Ballistic Coefficient for Science Objectives	19 kg/m^2
Descent Time	Approximately 40 min

4. Uranus Parametric Analyses

The Uranus parametric analysis is centered around the mission and science areas. The five missions that were considered at the beginning of the contract (JUN 79, JUN 80, SUN 81-82, SUN 82-83, and SUN 84) are discussed in this section as well as the JU 79 mission that influenced the Saturn probe definition in Section F.

a. *Mission Analysis* - The detailed mission analysis parametric data is provided in Volume II, Chapter IV where side-by-side comparisons of mission design studies for the different planets may be made. This section summarizes the important results for Uranus probe missions.

The interplanetary trajectories to be considered for Uranus were specified as either Jupiter swingbys (JUN 79, 80) or Saturn swingbys using solar electric propulsion (SUN 81, 82, 83). The interplanetary trajectories for these missions are summarized in Chapter IV, Section G. The trip times to Uranus are about 6.5 years for the JUN 79, 6.9 years for the JUN 80, 7.2 years for the SUN 81 and 82, and 7.5 years for the SUN 83.

The selection of the approach trajectories at Uranus is complicated by the fact that the approach velocity is generally about normal to the planet equator, thereby making equatorial flybys impossible (see Volume II, Figure IV-32). Therefore, if the spacecraft flyby is in the ecliptic plane, the probe should be deflected below the spacecraft trace so that the probe rotates with the planet it will pass through the spacecraft trace. Generally, an effective relay link geometry then has the spacecraft on the same radius ray as the probe halfway through the probe descent.

The ephemeris uncertainties at Uranus are characterized by values about ten times worse than those at Saturn. This results in severe navigational problems during the approach orbit determination. The impact plane uncertainty ellipse (1σ) has a semi-major axis (SMAA) of 9400 km using range/Doppler measurements. This led to impractical entry dispersions. Therefore, optical navigation was included during the approach orbit determination, resulting in a SMAA of 1300 km.

The general deflection trends indicated for Jupiter also apply to Uranus. Because of the relatively small mass of Uranus, the deflection may be made closer to Uranus than at Jupiter or Saturn. Thus, deflection ΔV magnitudes of 180, 90, and 60 m/sec are required for deflection radii of 5, 10, and 15 million km for a 3 R_N flyby radius. These numbers are increased to 410, 205, and 145 m/sec, respectively, for a 6 R_N periapsis radius.

The navigation uncertainties are so large at Uranus that they dominate the entry dispersions instead of the execution errors. Thus, at Uranus, the three-sigma dispersions is entry time, entry angle, angle of attack, and lead angle are 22.54/22.89 min, 4.44°/6.08°, 1.75°/3.37° and 3.79°/6.60°, respectively, where the numerator is the uncertainty contributed by navigation uncertainties alone (assuming optical navigation), and the denominator is the net uncertainty contributed by both navigation uncertainties and deflection maneuver execution errors. If Earth-based tracking only is used, one probe out of 100 will miss the planet (-60° nominal entry angle), pointing up the necessity for using optical tracking. Because of the large dispersions at Uranus, it is important to enter at steeper entry angles than at Jupiter or Saturn. If the nominal entry angle were -15° and Earth-based tracking were used, 41 probes out of 100 cases would miss the planet.

The selection of an entry ballistic coefficient which results in satisfactory staging conditions (deceleration to M = 0.7 above 100 mb) for entry angles of from -10° to -60° was investigated. Any ballistic coefficient less than 156.0 kg/m^2 (1.0 slug/ft^2) was identified as adequate.

The peak g experienced at entry angles of -20°, -40°, and -60° are 100, 250, and 370, respectively, in the nominal atmosphere. The encounter at Uranus is such that entry with rotation is not possible.

The maximum aerodynamic g-loading is a function of the ballistic coefficients. Entering with a ballistic coefficient of 1.0 slug/ft^2 at entry angles of -20°, -40°, and -60° results in max q of 3500, 8000, and 11,500 psf, respectively, in the nominal atmosphere. The dynamic pressure increases linearly with ballistic coefficient.

b. Science - The science parametrics for Uranus are given along with those for Saturn in previous Subsection 3.b. These include descent profile parametrics and entry accelerometer performance analysis.

c. System Integration - The JU 79 trajectory and the nominal Uranus atmosphere are the controlling constraints for these parametrics. All other constraints are the same as for the Saturn studies.

d. Telecommunications Subsystem - The telecommunications subsystem design for the Saturn mission was used for the Uranus mission to determine feasibility and any required changes. The design goal was to have a subsystem design that can be used for a mission to Saturn or Uranus with a minimum of hardware changes.

Microwave attenuation of the nominal Uranus atmosphere is greater for Uranus than Saturn for depths greater than 10 bars. Atmosphere loss is approximately equal for 10 bars and, for the design end-of-mission depth of 7 bars, Saturn has a slightly greater loss. The atmosphere losses are very similar at 0.86 GHz to the design depth of 7 bars.

Maximum communications range occurs at entry and decreases by 0.5 R_J at mission completion. Periapsis occurs 168 min after entry, which is long after the mission is completed. Major differences in the link parameters from the Saturn mission are space loss, system noise temperature, and the fact that worst-case RF power requirements occur at entry for Uranus instead of typically at the end of mission. End-of-mission power requirements are only 3.5 watts. Using the Saturn probe and spacecraft antennas with lower gains did not create severe power requirements, and the only hardware change necessary is the entry antenna for Uranus that must be changed to an axial beam antenna with a beamwidth of 90°. This results in both entry and descent antennas having the same gain and beamwidth requirements; two identical antennas may be employed.

Definition of the telecommunications subsystem is provided in Section G.5 with comparisons to the Saturn probe given in Table II-18.

e. Data Handling Subsystem - The analysis of the data handling subsystem is essentially unchanged from the nominal Jupiter probe. Functional requirements remain the same with the exception of minor modifications to sequence and format to conform with the mission profile. For a discussion of DHS selection and configuration, refer to Volume II, Chapter V, Sections A.5 and B.5, and Vol III, Appendix H.

f. Power and Pyrotechnic Subsystem - The power and pyrotechnic subsystem configuration remains unchanged from the nominal Jupiter probe (Volume II, Chapter V, Sections A.6 and A.7, and Vol III, Appendix G) with the exception of the battery size and weight.

g. Attitude Control Subsystem - The configuration of the attitude control subsystem is unchanged from the nominal Jupiter probe definition. Two detail modifications will be required: (1) the sensors will require additional optics due to the extreme solar range; (2) the geometry for this mission places the Sun 4° off the spin axis of the probe in the entry orientation. The sequence of attitude maneuver will consist of (1) preprogrammed series of pulses to place the spin axis near the Sun line; (2) closed loop precession to complete alignment of the spin axis with the Sun-probe vector; (3) open loop preprogrammed precession to obtain the 4° offset from the Sun-probe vector. The final maneuver will use the planet sensor to control the sector logic and will contain errors due to nutation effects and total impulse prediction. However, percentage errors would be allowable for the small angular precession required. The attitude control subsystem is discussed in more detail in Volume II, Chapter V, Sections A.7 and B.7, and Vol III, Appendix F.

h. Structures and Mechanical - The parametric data reported for Saturn probes as reported for Saturn are applicable to the Uranus probe.

i. Propulsion - The propulsion parametric data reported for the Jupiter probes and for Saturn are applicable to Uranus.

j. Thermal Control Subsystems - The Uranus probe is basically identical to the Saturn probe definition. For Uranus, thermal control must be provided and for this planet, the heat losses experienced during atmospheric descent become very critical. The planetary model atmospheres presented previously in Figure II-45 show that the atmosphere temperatures expected will be significantly below those studied for Jupiter and Saturn. The thermal control subsystem for Uranus includes the following:

Cruise/Coast Phase Thermal Control

1) Radioisotope Heaters
2) Multilayer Insulation
3) Environmental Cover
4) Thermal Coatings
5) Deflection Motor Blanket and Heater

Entry/Descent Phase Thermal Control

1) Graphite Ablator and Aeroshell Insulator
2) Low Density Internal Foam Insulation
3) Nitrogen Gas Environment Control
4) Battery Thermal Control Heaters

For cruise and coast, the thermal design is the same as Saturn with 18 watts of radioisotope heaters being required. After spacecraft separation, however, the solar energy is significantly less than Saturn, and the probe coast temperature will decrease 8°K. The solar flux at Uranus was assumed to be 3.7 w/m^2.

For the thermal design, the 2.5-bar nitrogen gas system was analyzed versus a completely vented probe. For both designs, the probe temperature exceeded the lower allowable limit for battery operation and for the completely vented probe, the probe temperature also exceeded the lower limit desired for electronic equipment operation.

For the Uranus probe, therefore, semi-active descent thermal control including both nitrogen gas environmental control and battery thermal control by thermostatically controlled electrical heating have been recommended.

k. *Uranus Parametric Analysis Summary* - The Uranus parametric analysis summary was presented along with the Saturn analysis of Volume II, Chapter VI, Section A, especially in the science area. Analyses results unique to Uranus are:

Mission	6.5 years for JUN 79 to 7.5 years for SUN 83
Approach	Ecliptic with probe deflected below the spacecraft
One Sigma Navigation Undertainty with Optical Tracking	1300 km

Three Sigma Dispersions (Max):

Entry Time	22.89 min
Entry Angle	6.08°
Angle of Attack	3.37°
Lead Angle	6.60°
Entry Ballistic Coefficient	<156 kg/m^2
Depth of Descent for Science Objectives	7 bar
Descent Ballistic Coefficient for Science Objectives	1.9 kg/m^2
Descent Time	Approximately 40 min

4

5. Neptune Parametric Analyses Results

As was previously stated, the initial Neptune study objectives were revised. The present objectives de-emphasize the Neptune studies; however, parametric analyses using the five initial missions were initiated especially in the mission and science areas. The missions discussed in this chapter are JUN 79, JUN 80, SUN 81-82, SUN 82-83, and SUN 84.

a. *Mission Analysis Parametrics* - The detailed mission analysis parametrics are given in Volume II, Chapter IV where parallel discussions of the different planets are provided. This section briefly summarizes the results at Neptune. The mission analysis effort at Neptune was limited to a study of the deterministic characteristics of Neptune missions. A typical Neptune mission is illustrated in Figure II-49. The interplanetary trajectories to Neptune considered in this study included the JUN 79 and 80 swingbys and the SUN 81, 82 and 83 solar electric propulsion/swingby missions. The total flight times to Neptune are 10.3 and 11.4 years for the JUN missions and 11.1, 11.6, and 12.6 for the SUN missions respectively. The interplanetary trajectories are pictured in Volume II, Chapter IV, Section G.

The launch analysis is identical to that given in Section G.1 for the Uranus phase of the same interplanetary trajectory. The optimal relay link geometry at Neptune would have a probe entry site on the equator and a low inclination spacecraft flyby trajectory. The spacecraft periapsis radius should be about 5 R_N for effective rotation rate matching.

Reasonable deflection radii appear to be in the range 5 to 15 million km from the planet. For an entry angle of -20°, the ΔV requirements go from 190 to 90 to 60 m/sec as the deflection radius increases from 5 to 10 to 15 million km for a spacecraft periapsis radius of 3 R_N. The ΔV requirements become 410, 210 and 150 m/sec, respectively, as the periapsis is increased to 6 R_N.

No specific navigation studies were made at Neptune; however it is possible to make general observations from extrapolations of existing data. The ephemeris uncertainties at Neptune are characterized by a position uncertainty of about 3000 km. This is to be compared with values at Saturn of 1000 km and 10,000 km at Uranus. Therefore, it is to be expected that navigation uncertainties would play a major role in generating dispersions. Steep entry angles and possibly optical tracking would, therefore, be advisable for Neptune missions.

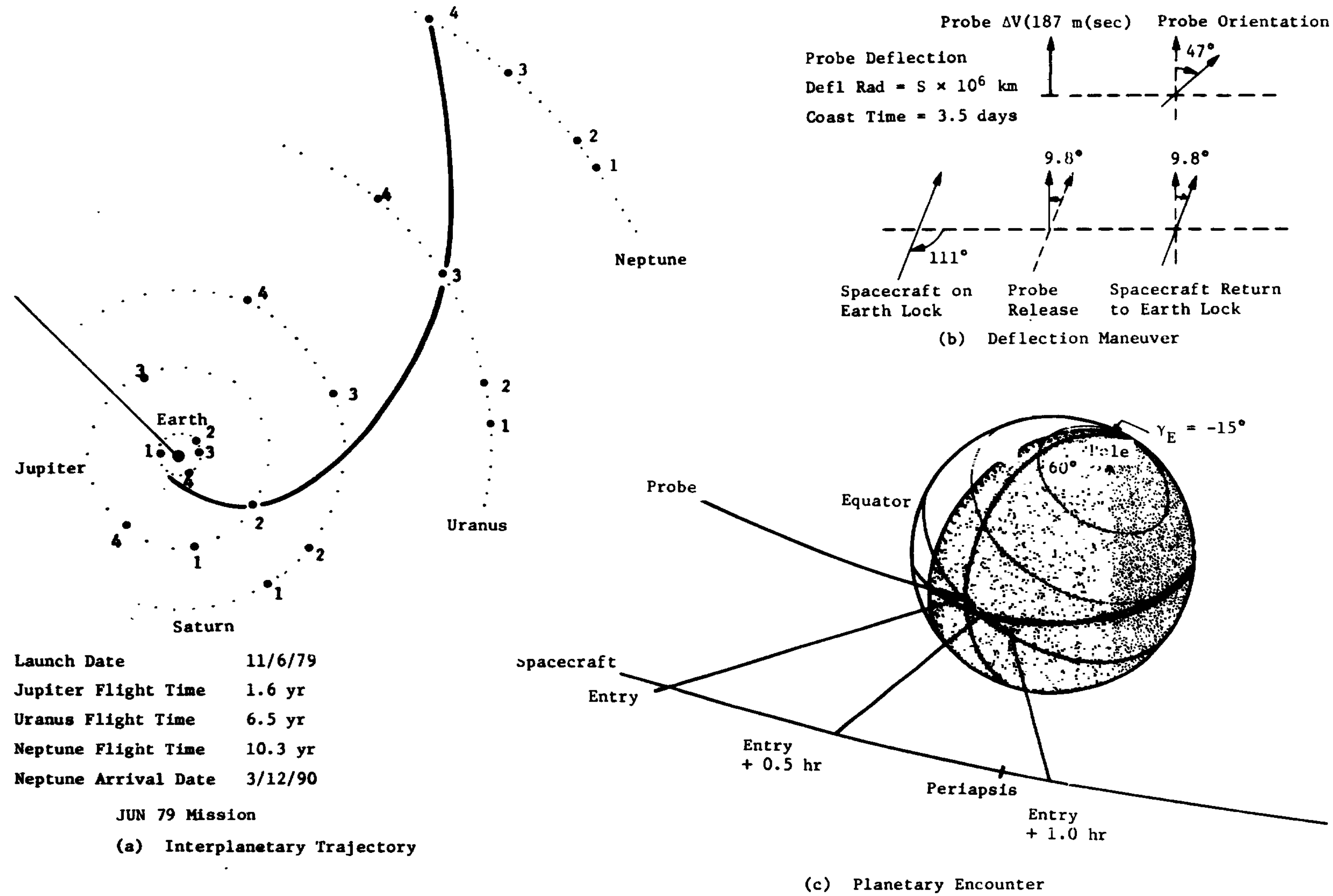

Launch Date	11/6/79
Jupiter Flight Time	1.6 yr
Uranus Flight Time	6.5 yr
Neptune Flight Time	10.3 yr
Neptune Arrival Date	3/12/90

JUN 79 Mission

(a) Interplanetary Trajectory

(b) Deflection Maneuver

(c) Planetary Encounter

Figure II-49 Neptune Mission (JUN 79)

Generally the entry trajectories at Neptune are similar to those at Saturn or Uranus. The selection of an entry ballistic coefficient less than 156.0 kg/m^2 (1.0 slug/ft^2) results in satisfactory staging conditions (deceleration to M = 0.7 above 100 mb) for entry angles from -10° to -40°. Volume II, Figure IV-18 illustrates the relevant trades.

The peak decelerations for Neptune missions are about 200 g for γ = -20° and 300 g for γ = -30° (see Vol II, Fig. IV-24). The maximum dynamic pressure varies from 3000 to 10,000 psf as the entry increases from -10° to -30° for a ballistic coefficient of 156.0 kg/m^2 (1.0 slug/ft^2).

b. *Science* - For Neptune, the instruments can be identical with those for the other planets with a possible modification in the ranges of the temperature gage and entry accelerometers. Parametrics were not generated for Neptune descent either in ballistic coefficient or instrument sampling times. However, with the goal of using the same probe for Saturn, Uranus. and Neptune entries, Figure II-50 shows a pressure descent profile for a ballistic coefficient of 109.9 kg/m^2 (0.7 slug/ft^2). The parachute is deployed at 20 millibars and the design limit pressure is 20 bars. The descent time from parachute deployment to end of mission is only 48.4 min despite having started higher in pressure and having to go to greater depths of penetration than for the other planets. This approximate agreement with the descent times of the other planets allows for greater commonality of design. Using the same instrument sampling times as for Saturn and Uranus, the descent measurement performance for this descent profile satisfies the criteria.

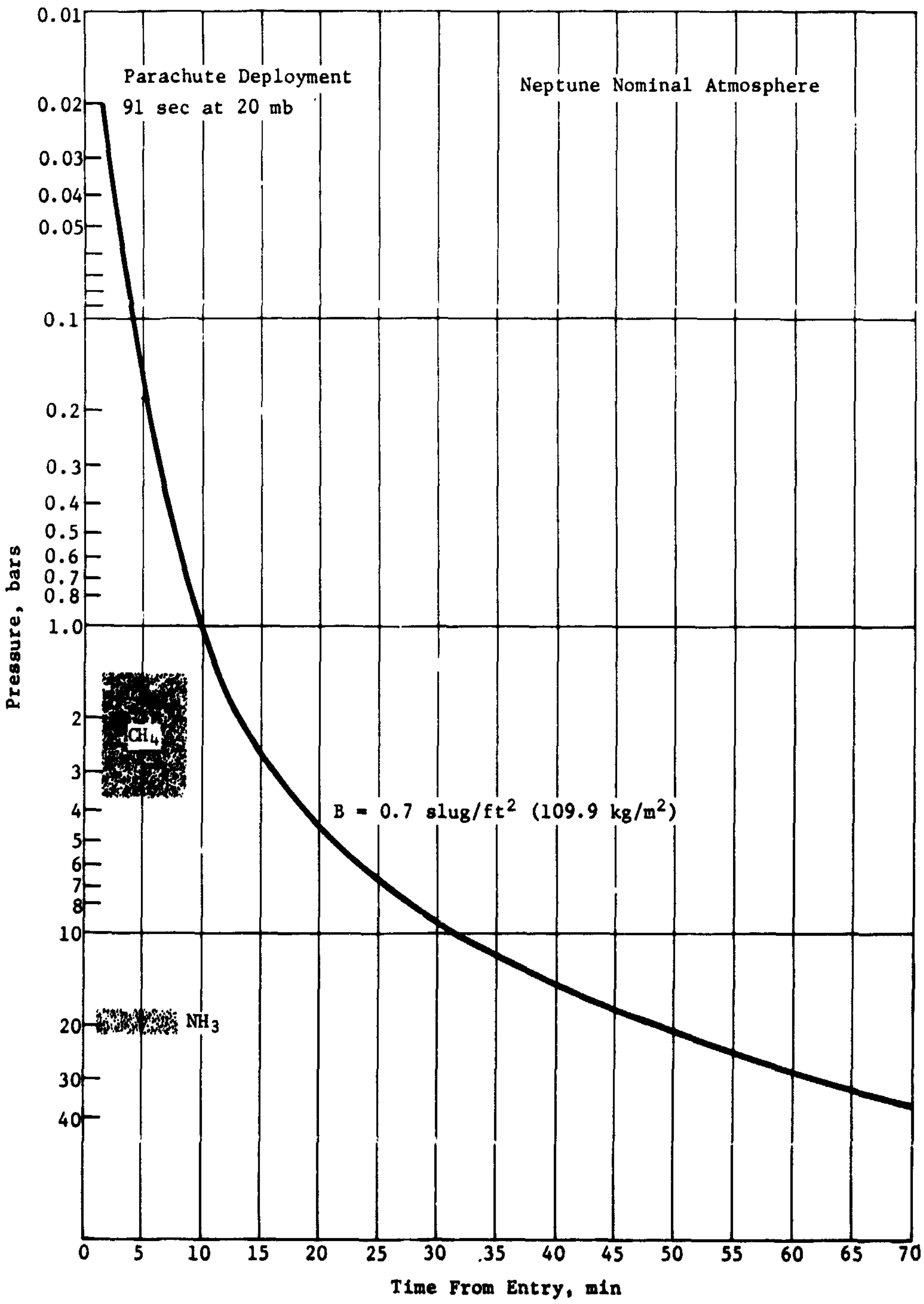

Figure II-50 Neptune Pressure Descent Profile

I. PROGRAM EVALUATION

This section discusses the feasibility of a probe system in terms of hardware availability and also identifies the commonality of constraints and hardware for Jupiter, Saturn and Uranus missions, and for Neptune missions to a limited extent.

1. Feasibility Summary

After defining the nominal Jupiter probe (see Section C.2), various Air Force, NASA and other programs were researched to determine components that were available for probe implementation. Results of this effort are contained herein.

A component search for developed hardware suitable for use in the outer planet probes reveals ready availability of certain components directly applicable to the probes. In other instances, the technology exists but components developed to that technology do not quite fit the requirements of the probe. Commercial components exist that could probably accomplish the program requirements with some added development and or qualification. Listed in Section IX A of Volume II are the results of a review providing examples of feasible hardware for the first two categories.

In the electrical and electronic areas, hardware is either available or is being designed for applications in the near future for all components used, except for the demodulation and data acquisition area. Tables II-25 and II-26 are typical examples of data collected.

In the mechanical engineering area, certain subsystems were not included in the industry search because they are unique and must be designed and developed for the program. Examples are the structure, parachute subsystems, insulation blankets, certain mechanical components and propulsion subsystem plumbing. Table II-27 shows typical mechanical data obtained.

Science sensors, available from the Viking and PAET programs, can be modified for probe applications.

Table II-25 Critical Component Availability

Transmitter (Solid State)	0.26 GHz 170 W SMS		WDL Philco/Ford
	0.46 GHz 40 W SMS		
	0.86 GHz 80 W ATS F/G		
	1.55 GHz 40 W ATS F/G		
	2.55 GHz 18 W ATS F/G		
Attitude Sensors	Digital		Adcole
	Analog		Honeywell
Battery	Ag-Zn Primary	(Silo Applications)	Yardney
	Remote Actuator		Eagle Picher
Electronics	Digital		General Piece Part Availability
Pyrotechnics	Capacitor Bank Discharge (Mariner/Viking)		

Table II-26 Attitude Control System Availability

COMPONENT	SOURCE*	APPLICATIONS*
Sensors	Adcole Honeywell	Tiros, Itos, OAO
Sector Logic	Ball Brothers CDC	ATS-3, OSO-H, IMP-F, ATS F/G
Electronics	(Many)	Space Qualified Parts
Nutation Damper	RCA TRW	Tiros, Vela, LES
Pneumatics	GE MMC	Mariner '71, Viking Orbiter '75

*Not limited to these sources or applications.

Table II-27 Deflection Propulsion Solid Propellant Motor

FUNCTIONAL REQUIREMENTS	POTENTIAL SUPPLIERS	CANDIDATE(S)
Total Impulse, 7,750 lbf sec ±0.7% Thrust, 500 lbf Two Canted Nozzles Minimum Weight Space Storage for 800 days	Hercules Thiokol Aerojet Atlantic Research UTC	New design required, but state of the art exists to provide a motor with an I_{sp} of 287 and a mass fraction = 0.76. A motor is required intermediate between the Thiokol TE-M-541, I_t = 3,075 lbf sec I_{sp} = 287 lbf sec/lbm Mass Fraction = 0.81 and the Thiokol TE-M-516, I_t = 21,000 lbf sec I_{sp} = 288 lbf sec/lbm Mass Fraction = 0.86

2. Commonality Summary

There is maximum amount of commonality between the Saturn and Uranus probes as discussed in Section G. The following presents additional commonality among the Jupiter, Saturn, and Uranus probes:

Entry Ballistic Coefficient	102 kg/m^2 (0.65 slug/ft^2)
Initial Descent Coefficient	14 to 19 kg/m^2
Data Rate	30 bps max
Data Storage (except for probe-dedicated mission)	12.4 K bits
Frequency	0.86 GHz
DHS	Identical with a programmable sequence
Thermal Control Subsystem	Isotope heaters, insulation, and thermal coatings

ACS Propulsion (except for probe-dedicated mission)	Identical except for quantity of gas
ACS Electronics	Similar
Descent Time	36 to 48 min

J. REFERENCES

1. *Preliminary SAG Payload and Mission Recommendations for Jupiter Entry Probes.* JPL Section Document 131-15, 20 September 1971.

2. S. J. Ducsai, Program Manager: *Jupiter Atmospheric Entry Mission Study.* Final Report, Vol II, III, MMC Report No. 71-1, JPL Contract 952811, April 1971.

3. *Science Criteria for Jupiter Entry Missions.* JPL Section Report 131-07, December 31, 1969.

4. *A 1971 Assessment of the Feasibility of a Jupiter Atmospheric Entry Mission.* JPL Advanced Technical Studies Office, September 1971.

5. Murry Meldrum, Bell Aerospace Company, Telecon.

6. *Bell Aerospace Inertial Instruments.* Bell Aerospace Company, Buffalo, N.Y.

7. *Absolute Pressure Transducer.* Viking Specification Document PD7400069, November 1969.

8. *Temperature Transducers.* Viking Specification Document, PD7400086, September 1971.

III. CONCLUSIONS AND RECOMMENDATIONS

The study showed that scientific probes, along with their candidate carrier spacecraft and launch vehicles, are technically feasible for missions in the 1978-79 time frame and later. In addition, the study identified areas that require some further development activities in areas such as heat shield, radiation damage to hardware, and demodulation and data acquisition techniques.

NASA-ARC has done extensive development in the heat shield area in the past and has established a good reference for further development and testing.

Various companies throughout industry have researched the radiation effects on components. This data, along with a better definition of the Jupiter radiation environment expected from the Pioneer G flight, should provide an excellent reference for future development.

Demodulation and data acquisition techniques require further study to establish firm criteria on which to base receiver data signal-to-noise ratios.

Additional test and evaluations are required for long-life components. Especially for Saturn and Uranus, applications where the mission times range from 1260 days to 3180 days, component performance is expected to deteriorate.

The inlet system for the mass spectrometer requires further evaluations to ensure compatiblity with the masses of the primary constituents that exist in two different groups: 1-4 amu and 15-18 amu. The leak rates through the sintered plug might be appreciably different for each group and cause distortion in the measurements. Also there could be an ammonia/water condensation problem in the leak pores causing blockage.

It is recommended that additional development and test be done in the areas denoted above. In addition, it is recommended that emphasis be placed upon Saturn, and Uranus probe missions because the Jupiter entry environment requires significant heat shield and radiation development.